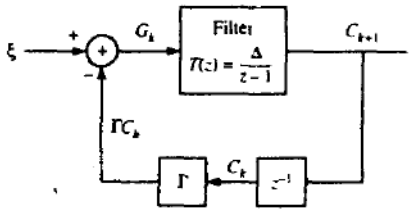

FIGURE 11-1-3 Closed-loop control system representation of recursive equation in (11-1-20).

where $\mathbf{I}$ is the identity matrix, $\mathbf{\Gamma}$ is the autocorrelation matrix of the received signal, $\mathbf{C}_k$ is the $(2K+1)$-dimensional vector of equalizer tap gains, and $\boldsymbol{\xi}$ is the vector of cross-correlations given by (10-2-45). The recursive relation in (11-1-20) can be represented as a closed-loop control system as shown in Fig. 11-1-3. Unfortunately, the set of $2K+1$ first-order difference equations in (11-1-20) are coupled through the autocorrelation matrix $\mathbf{\Gamma}$. In order to solve these equations and, thus, establish the convergence properties of the recursive algorithm, it is mathematically convenient to decouple the equations by performing a linear transformation. The appropriate transformation is obtained by noting that the matrix $\mathbf{\Gamma}$ is Hermitian and, hence, can be represented as

$$\mathbf{\Gamma} = \mathbf{U}\mathbf{\Lambda}\mathbf{U}'^{*} \tag{11-1-21}$$

where $\mathbf{U}$ is the normalized modal matrix of $\mathbf{\Gamma}$ and $\mathbf{\Lambda}$ is a diagonal matrix with diagonal elements equal to the eigenvalues of $\mathbf{\Gamma}$.

When (11-1-21) is substituted into (11-1-20) and if we define the transformed (orthogonalized) vectors $\mathbf{C}_k^o = \mathbf{U}'^{*}\mathbf{C}_k$ and $\boldsymbol{\xi}^o = \mathbf{U}'^{*}\boldsymbol{\xi}$, we obtain

$$\mathbf{C}_{k+1}^o = (\mathbf{I} - \Delta\mathbf{\Lambda})\mathbf{C}_k^o + \Delta\boldsymbol{\xi}^o \tag{11-1-22}$$

This set of first order difference equations is now decoupled. Their convergence is determined from the homogeneous equation

$$\mathbf{C}_{k+1}^o = (\mathbf{I} - \Delta\mathbf{\Lambda})\mathbf{C}_k^o \tag{11-1-23}$$

We see that the recursive relation will converge provided that all the poles lie inside the unit circle, i.e.,

$$|1 - \Delta\lambda_k| < 1, \qquad k = -K, \ldots, -1, 0, 1, \ldots, K \tag{11-1-24}$$

where $\{\lambda_k\}$ is the set of $2K+1$ (possibly nondistinct) eigenvalues of $\mathbf{\Gamma}$. Since $\mathbf{\Gamma}$ is an autocorrelation matrix, it is positive-definite and, hence, $\lambda_k > 0$ for all k. Consequently convergence of the recursive relation in (11-1-22) is ensured if Δ satisfies the inequality

$$0 < \Delta < \frac{2}{\lambda_{\max}} \tag{11-1-25}$$

where $\lambda_{\max}$ is the largest eigenvalue of $\mathbf{\Gamma}$.

Since the largest eigenvalue of a positive-definite matrix is less than the sum

of all the eigenvalues of the matrix and, furthermore, since the sum of the eigenvalues of a matrix is equal to its trace, we have the following simple upper bound on λ_{max}:

$$\lambda_{max} < \sum_{k=-K}^{K} \lambda_k = \text{tr}\,\Gamma = (2K+1)\Gamma_{kk}$$
$$= (2K+1)(x_0 + N_0) \tag{11-1-26}$$

From (11-1-23) and (11-1-24) we observe that rapid convergence occurs when $|1 - \Delta\lambda_k|$ is small, i.e., when the pole positions are far from the unit circle. But we cannot achieve this desirable condition and still satisfy (11-1-25) if there is a large difference between the largest and smallest eigenvalues of Γ. In other words, even if we select Δ to be near the upper bound given in (11-1-25), the convergence rate of the recursive MSE algorithm is determined by the smallest eigenvalue λ_{min}. Consequently, the ratio $\lambda_{max}/\lambda_{min}$ ultimately determines the convergence rate. If $\lambda_{max}/\lambda_{min}$ is small, Δ can be selected so as to achieve rapid convergence. However, if the ratio $\lambda_{max}/\lambda_{min}$ is large, as is the case when the channel frequency response has deep spectral nulls, the convergence rate of the algorithm will be slow.

11-1-4 Excess MSE Due to Noisy Gradient Estimates

The recursive algorithm in (11-1-11) for adjusting the coefficients of the linear equalizer employs unbiased noisy estimates of the gradient vector. The noise in these estimates causes random fluctuations in the coefficients about their optimal values and, thus, leads to an increase in the MSE at the output of the equalizer. That is, the final MSE is $J_{min} + J_\Delta$, where J_Δ is the variance of the measurement noise. The term J_Δ due to the estimation noise has been termed *excess means-square error* by Widrow (1966).

The total MSE at the output of the equalizer for any set of coefficients $\mathbf{C}$ can be expressed as

$$J = J_{min} + (\mathbf{C} - \mathbf{C}_{opt})'^{*}\Gamma(\mathbf{C} - \mathbf{C}_{opt}) \tag{11-1-27}$$

where $\mathbf{C}_{opt}$ represents the optimum coefficients, which satisfy (11-1-6). This expression for the MSE can be simplified by performing the linear orthogonal transformation used above to establish convergence. The result of this transformation applied to (11-1-27) is

$$J = J_{min} + \sum_{k=-K}^{K} \lambda_k E\,|c_k^o - c_{k\,opt}^o|^2 \tag{11-1-28}$$

where the $\{c_k^o\}$ are the set of transformed equalizer coefficients. The excess MSE is the expected value of the second term in (11-1-28), i.e.,

$$J_\Delta = \sum_{k=-K}^{K} \lambda_k E\,|c_k^o - c_{k\,opt}^o|^2 \tag{11-1-29}$$

It has been shown by Widrow (1970, 1975) that the excess MSE is

$$J_\Delta = \Delta^2 J_{\min} \sum_{k=-K}^{K} \frac{\lambda_k^2}{1-(1-\Delta\lambda_k)^2} \tag{11-1-30}$$

The expression in (11-1-30) can be simplified when Δ is selected such that $\Delta\lambda_k \ll 1$ for all k. Then

$$\begin{aligned} J_\Delta &\approx \tfrac{1}{2}\Delta J_{\min} \sum_{k=-K}^{K} \lambda_k \\ &\approx \tfrac{1}{2}\Delta J_{\min} \operatorname{tr} \Gamma \\ &\approx \tfrac{1}{2}\Delta(2K+1)J_{\min}(x_0+N_0) \end{aligned} \tag{11-1-31}$$

Note that $x_0 + N_0$ represents the received signal plus noise power.

It is desirable to have $J_\Delta < J_{\min}$. That is, Δ should be selected such that

$$\frac{J_\Delta}{J_{\min}} \approx \tfrac{1}{2}\Delta(2K+1)(x_0+N_0) < 1$$

or, equivalently,

$$\Delta < \frac{2}{(2K+1)(x_0+N_0)} \cdot \tag{11-1-32}$$

For example, if Δ is selected as

$$\Delta = \frac{0.2}{(2K+1)(x_0+N_0)} \tag{11-1-33}$$

the degradation in the output SNR of the equalizer due to the excess MSE is less than 1 dB.

The analysis given above on the excess mean square error is based on the assumption that the mean value of the equalizer coefficients has converged to the optimum value $\mathbf{C}_{\text{opt}}$. Under this condition, the step size Δ should satisfy the bound in (11-1-32). On the other hand, we have determined that convergence of the mean coefficient vector requires that $\Delta < 2/\lambda_{\max}$. While a choice of Δ near the upper bound $2/\lambda_{\max}$ may lead to initial convergence of the deterministic (known) steepest-descent gradient algorithm, such a large value of Δ will usually result in instability of the LMS stochastic gradient algorithm.

The initial convergence or transient behavior of the LMS algorithm has been investigated by several researchers. Their results clearly indicate that the step size must be reduced in direct proportion to the length of the equalizer as specified by (11-1-32). Hence, the upper bound given by (11-1-32) is also necessary to ensure the initial convergence of the LMS algorithm. The papers by Gitlin and Weinstein (1979) and Ungerboeck (1972) contain analyses of the transient behavior and the convergence properties of the LMS algorithm.

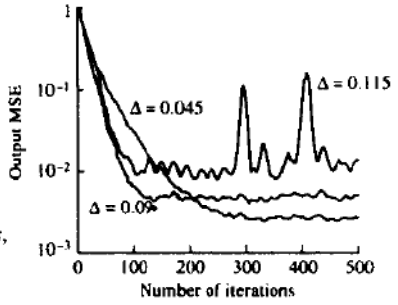

FIGURE 11-1-4 Initial convergence characteristics of the LMS algorithm with different step sizes. [*From* Digital Signal Processing, *by J. G. Proakis and D. G. Manolakis, 1988, Macmillan Publishing Company. Reprinted with permission of the publisher.*]

The following example serves to reinforce the important points made above regarding the initial convergence of the LMS algorithm.

Example 11-1-1

The LMS algorithm was used to adaptively equalize a communication channel for which the autocorrelation matrix Γ has an eigenvalue spread of $\lambda_{max}/\lambda_{min} = 11$. The number of taps selected for the equalizer was $2K + 1 = 11$. The input signal plus noise power $x_0 + N_0$ was normalized to unity. Hence, the upper bound on Δ given by (11-1-32) is 0.18. Figure 11-1-4 illustrates the initial convergence characteristics of the LMS algorithm for $\Delta = 0.045$, 0.09, and 0.115, by averaging the (estimated) MSE in 200 simulations. We observe that by selecting $\Delta = 0.09$ (one-half of the upper bound) we obtain relatively fast initial convergence. If we divide Δ by a factor of 2 to $\Delta = 0.045$, the convergence rate is reduced but the excess mean square error is also reduced, so that the LMS algorithm performs better in steady state (in a time-invariant signal environment). Finally, we note that a choice of $\Delta = 0.115$, which is still far below the upper bound, causes large undesirable fluctuations in the output MSE of the algorithm.

In a digital implementation of the LMS algorithm, the choice of the step-size parameter becomes even more critical. In an attempt to reduce the excess mean square error, it is possible to reduce the step-size parameter to the point where the total mean square error actually increases. This condition occurs when the estimated gradient components of the vector $\varepsilon_k \mathbf{V}_k^*$ after multiplication by the small step-size parameter Δ are smaller than one-half of the least significant bit in the fixed-point representation of the equalizer coefficients. In such a case, adaptation ceases. Consequently, it is important for the step size to be large enough to bring the equalizer coefficients in the vicinity of $\mathbf{C}_{opt}$. If it is desired to decrease the step size significantly, it is necessary to increase the precision in the equalizer coefficients. Typically, 16

bits of precision may be used for the coefficients, with about 10–12 of the most significant bits used for arithmetic operations in the equalization of the data. The remaining least significant bits are required to provide the necessary precision for the adaptation process. Thus, the scaled, estimated gradient components $\Delta\varepsilon\mathbf{V}_k^*$ usually affect only the least-significant bits in any one iteration. In effect, the added precision also allows for the noise to be averaged out, since many incremental changes in the least-significant bits are required before any change occurs in the upper more significant bits used in arithmetic operations for equalizing the data. For an analysis of roundoff errors in a digital implementation of the LMS algorithm, the reader is referred to the papers by Gitlin and Weinstein (1979), Gitlin *et al.* (1982), and Caraiscos and Liu (1984).

As a final point, we should indicate that the LMS algorithm is appropriate for tracking slowly time-invariant signal statistics. In such a case, the minimum MSE and the optimum coefficient vector will be time-variant. In other words, $J_{\min}(n)$ is a function of time and the $(2K+1)$-dimensional error surface is moving with the time index n. The LMS algorithm attempts to follow the moving minimum $J_{\min}(n)$ in the $(2K+1)$-dimensional space, but it is always lagging behind due to its use of (estimated) gradient vectors. As a consequence, the LMS algorithm incurs another form of error, called the *lag error*, whose mean square value decreases with an increase in the step size Δ. The total MSE error can now be expressed as

$$J_{\text{total}} = J_{\min}(n) + J_\Delta + J_l$$

where J_l denotes the mean square error due to the lag.

In any given nonstationary adaptive equalization problem, if we plot the errors J_Δ and J_l as a function of Δ, we expect these errors to behave as illustrated in Fig. 11-1-5. We observe that J_Δ increases with an increase in Δ while J_l decreases with an increase in Δ. The total error will exhibit a minimum, which will determine the optimum choice of the step-size parameter.

When the statistical time variations of the signal occur rapidly, the lag error

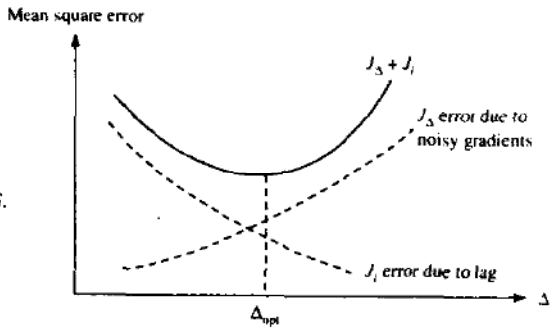

FIGURE 11-1-5 Excess mean square error J_Δ and lag error J_l as a function of the step size. [*From* Digital Signal Processing, *by J. G. Proakis and D. G. Manolakis, 1988. Macmillan Publishing Company. Reprinted with permission of the publisher.*]

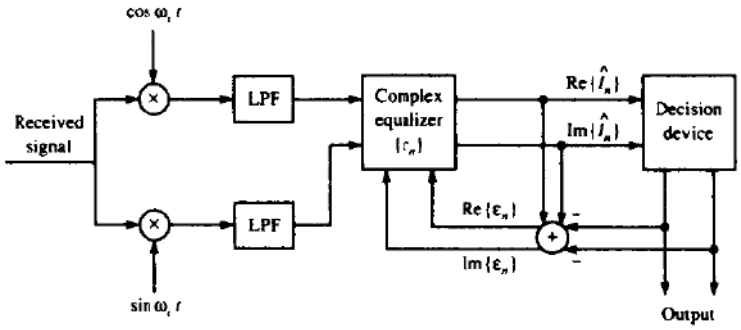

FIGURE 11-1-6 QAM signal demodulation.

will dominate the performance of the adaptive equalizer. In such a case, $J_t \gg J_{\min} + J_\Delta$, even when the largest possible value of Δ is used. When this condition occurs, the LMS algorithm is inappropriate for the application and one must rely on the more complex recursive least-squares algorithms described in Section 11-4 to obtain faster convergence and tracking.

11-1-5 Baseband and Passband Linear Equalizers

Our treatment of adaptive linear equalizers has been in terms of equivalent lowpass signals. However, in a practical implementation, the linear adaptive equalizer shown in Fig. 11-1-2 can be realized either at baseband or at bandpass. For example Fig. 11-1-6 illustrates the demodulation of QAM (or multiphase PSK) by first translating the signal to baseband and equalizing the baseband signal with an equalizer having complex-valued coefficients. In effect, the complex equalizer with complex-valued (in-phase and quadrature components) input is equivalent to four parallel equalizers with real-valued tap coefficients as shown in Fig. 11-1-7.

As an alternative, we may equalize the signal at passband. This is

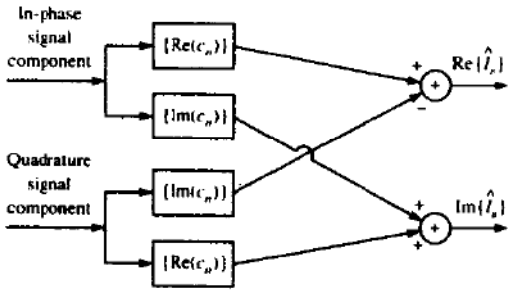

FIGURE 11-1-7 Complex-valued baseband equalizer for QAM signals.

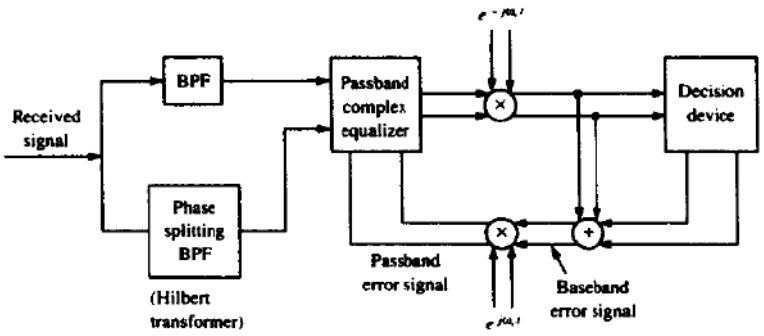

FIGURE 11-1-8 QAM or PSK signal equalization at passband.

accomplished as shown in Fig. 11-1-8 for a two-dimensional signal constellation such as QAM and PSK. The received signal is filtered and, in parallel, it is passed through a Hilbert transformer, called a *phase-splitting filter*. Thus, we have the equivalent of in-phase and quadrature components at passband, which are fed to a passband complex equalizer. Following the equalization, the signal is down-converted to a baseband and detected. The error signal generated for the purpose of adjusting the equalizer coefficients is formed at baseband and frequency-translated to passband as illustrated in Fig. 11-1-8.

11-2 ADAPTIVE DECISION-FEEDBACK EQUALIZER

As in the case of the linear adaptive equalizer, the coefficients of the feedforward filter and the feedback filter in a decision-feedback equalizer may be adjusted recursively, instead of inverting a matrix as implied by (10-3-3). Based on the minimization of the MSE at the output of the DFE, the steepest-descent algorithm takes the form

$$\mathbf{C}_{k+1} = \mathbf{C}_k + \Delta E(\varepsilon_k \mathbf{V}_k^*) \tag{11-2-1}$$

where $\mathbf{C}_k$ is the vector of equalizer coefficients in the kth signal interval, $E(\varepsilon_k \mathbf{V}_k^*)$ is the cross-correlation of the error signal $\varepsilon_k = I_k - \hat{I}_k$ with $\mathbf{V}_k$ and $\mathbf{V}_k = [v_{k+K_1} \cdots v_k \; I_{k-1} \cdots I_{k-K_2}]^t$, representing the signal values in the feedforward and feedback filters at time $t = kT$. The MSE is minimized when the cross-correlation vector $E(\varepsilon_k \mathbf{V}_k^*) = \mathbf{0}$ as $k \to \infty$.

Since the exact cross-correlation vector is unknown at any time instant, we use as an estimate the vector $\varepsilon_k \mathbf{V}_k^*$ and average out the noise in the estimate through the recursive equation

$$\hat{\mathbf{C}}_{k+1} = \hat{\mathbf{C}}_k + \Delta \varepsilon_k \mathbf{V}_k^* \tag{11-2-2}$$

This is the LMS algorithm for the DFE.

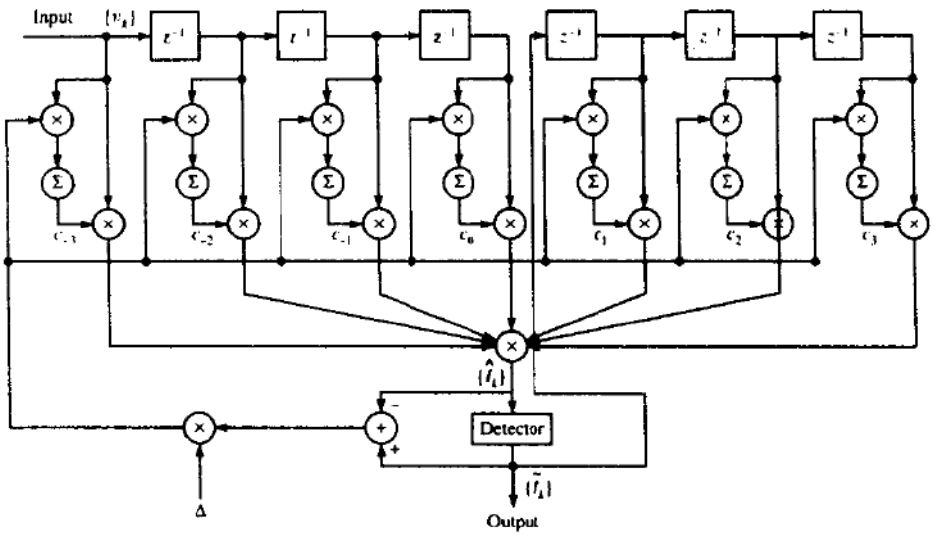

FIGURE 11-2-1 Decision-feedback equalizer.

As in the case of a linear equalizer, we may use a training sequence to adjust the coefficients of the DFE initially. Upon convergence to the (near-) optimum coefficients (minimum MSE), we may switch to a decision-directed mode where the decisions at the output of the detector are used in forming the error signal ε_k and fed to the feedback filter. This is the adaptive mode of the DFE, which is illustrated in Fig 11-2-1. In this case, the recursive equation for adjusting the equalizer coefficient is

$$\tilde{\mathbf{C}}_{k+1} = \tilde{\mathbf{C}}_k + \Delta \tilde{\varepsilon}_k \mathbf{V}_k^* \tag{11-2-3}$$

where $\tilde{\varepsilon}_k = \tilde{I}_k - \hat{I}_k$ and $\mathbf{V}_k = [v_{k+K_1} \cdots v_k \ \tilde{I}_{k-1} \cdots \tilde{I}_{k-K_2}]'$.

The performance characteristics of the LMS algorithm for the DFE are basically the same as the development given in Sections 11-1-3 and 11-1-4 for the linear adaptive equalizer.

11-2-1 Adaptive Equalization of Trellis-Coded Signals

Bandwidth efficient trellis-coded modulation that was described in Section 8-3 is frequently used in digital communications over telephone channels to reduce the required SNR per bit for achieving a specified error rate. Channel distortion of the trellis-coded signal forces us to use adaptive equalization in order to reduce the intersymbol interference. The output of the equalizer is then fed to the Viterbi decoder, which performs soft-decision decoding of the trellis-coded signal.

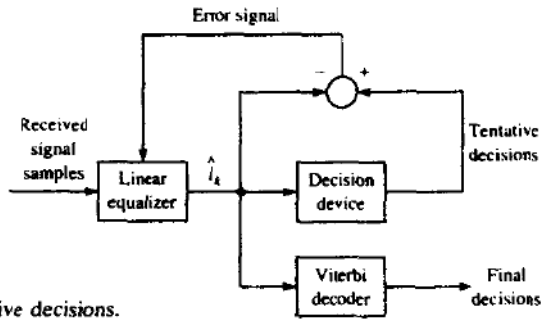

FIGURE 11-2-2 Adjustment of equalizer based on tentative decisions.

The question that arises regarding such a receiver is how do we adapt the equalizer in a data transmission mode? One possibility is to have the equalizer make its own decisions at its output solely for the purpose of generating an error signal for adjusting its tap coefficients, as shown in the block diagram in Fig. 11-2-2. The problem with this approach is that such decisions are generally unreliable, since the pre-decoding coded symbol SNR is relatively low. A high error rate would cause a significant degradation in the operation of the equalizer, which would ultimately affect the reliability of the decisions at the output of the decoder. The more desirable alternative is to use the post-decoding decisions from the Viterbi decoder, which are much more reliable, to continuously adapt the equalizer. This approach is certainly preferable and viable when a linear equalizer is used prior to the Viterbi decoder. The decoding delay inherent in the Viterbi decoder can be overcome by introducing an identical delay in the tap weight adjustment of the equalizer coefficients as shown in Fig. 11-2-3. The major price that must be paid for the added delay is that the step-size parameter in the LMS algorithm must be reduced, as described by Long *et al.* (1987, 1989), in order to achieve stability in the algorithm.

In channels with one or more in-band spectral nulls, the linear equalizer is

FIGURE 11-2-3 Adjustment of equalizer based on decisions from the Viterbi decoder.

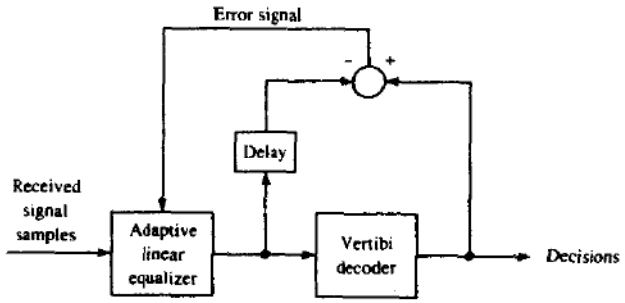

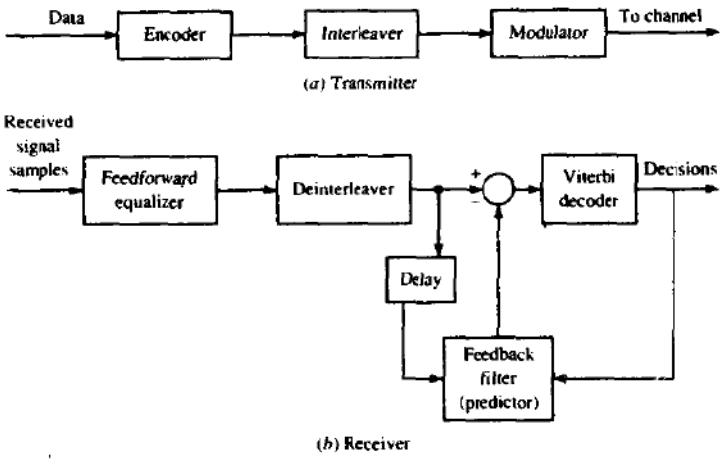

FIGURE 11-2-4 Use of predictive DFE with interleaving and trellis-coded modulation.

no longer adequate for compensating the channel intersymbol interference. Instead, we should like to use a DFE. But the DFE requires reliable decisions in its feedback filter in order to cancel out the intersymbol interference from previously detected symbols. Tentative decisions prior to decoding would be highly unreliable and, hence, inappropriate. Unfortunately, the conventional DFE cannot be cascaded with the Viterbi algorithm in which post-decoding decisions from the decoder are fed back to the DFE.

One alternative is to use the predictive DFE described in Section 10-3-3. In order to accommodate for the decoding delay as it affects the linear predictor, we introduce a periodic interleaver/deinterleaver pair that has the same delay as the Viterbi decoder and, thus, makes it possible to generate the appropriate error signal to the predictor as illustrated in the block diagram of Fig. 11-2-4. The novel way in which a predictive DFE can be combined with Viterbi decoding to equalize trellis-coded signals is described and analyzed by Eyuboglu (1988). This same idea has been carried over to the equalization of fading multipath channels by Zhou *et al.* (1988, 1990), but the structure of the DFE was modified to use recursive least-squares lattice-type filters, which provide faster adaptation to the time variations encountered in the channel.

11-3 AN ADAPTIVE CHANNEL ESTIMATOR FOR ML SEQUENCE DETECTION

The ML sequence detection criterion implemented via the Viterbi algorithm as embodied in the metric computation given by (10-1-23) and the probabilistic symbol-by-symbol detection algorithm described in Section 5-1-5 require knowledge of the equivalent discrete-time channel coefficients $\{f_k\}$. To accommodate a channel that is unknown or slowly time-varying, one may include a

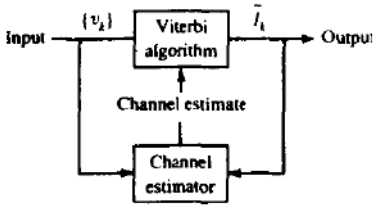

FIGURE 11-3-1 Block diagram of method for estimating the channel characteristics for the Viterbi algorithm.

channel estimator connected in parallel with the detection algorithm, as shown in Fig. 11-3-1. The channel estimator, which is shown in Fig. 11-3-2 is identical in structure to the linear transversal equalizer discussed previously in Section 11-1. In fact, the channel estimator is a replica of the equivalent discrete-time channel filter that models the intersymbol interference. The estimated tap coefficients, denoted by $\{\hat{f}_k\}$, are adjusted recursively to minimize the MSE between the actual received sequence and the output of the estimator. For example, the steepest-descent algorithm in a decision-directed mode of operation is

$$\hat{\mathbf{f}}_{k+1} = \hat{\mathbf{f}}_k + \Delta \varepsilon_k \tilde{\mathbf{I}}_k^* \tag{11-3-1}$$

where $\hat{\mathbf{f}}_k$ is the vector of tap gain coefficients at the kth iteration, Δ is the step size, $\varepsilon_k = v_k - \hat{v}_k$ is the error signal, and $\tilde{\mathbf{I}}_k$ denotes the vector of detected information symbols in the channel estimator at the kth iteration.

We now show that when the MSE between v_k and $\hat{v}_k$ is minimized, the resulting values of the tap gain coefficients of the channel estimator are the values of the discrete-time channel model. For mathematical tractability, we assume that the detected information sequence $\{\tilde{I}_k\}$ is correct, i.e., $\{\tilde{I}_k\}$ is

FIGURE 11-3-2 Adaptive transversal filter for estimating the channel dispersion.

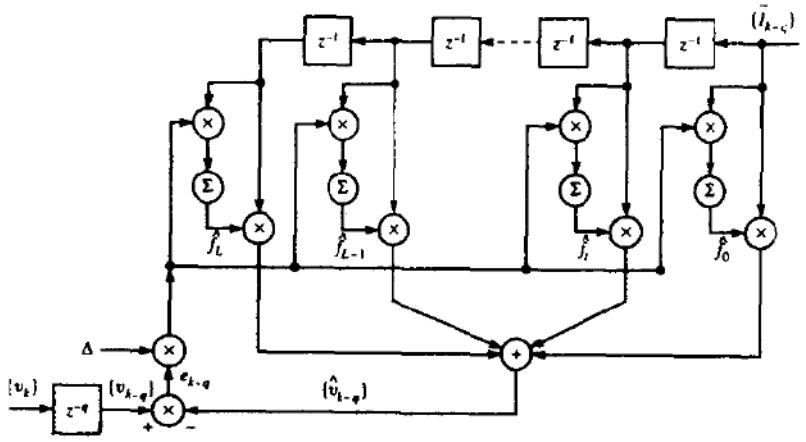

identical to the transmitted sequence $\{I_k\}$. This is a reasonable assumption when the system is operating at a low probability of error. Thus, the MSE between the received signal v_k and the estimate $\hat{v}_k$ is

$$J(\hat{\mathbf{f}}) = E\left(\left|v_k - \sum_{j=0}^{N-1} \hat{f}_j I_{k-j}\right|^2\right) \tag{11-3-2}$$

The tap coefficients $\{\hat{f}_k\}$ that minimize $J(\hat{\mathbf{f}})$ in (11-3-2) satisfy the set of N linear equations

$$\sum_{j=0}^{N-1} \hat{f}_j \phi_{kj} = d_k, \qquad k = 0, 1, \ldots, N-1 \tag{11-3-3}$$

where

$$\phi_{kj} = E(I_k I_j^*), \qquad d_k = \sum_{j=0}^{N-1} f_j \phi_j \tag{11-3-4}$$

From (11-3-3) and (11-3-4), we conclude that, as long as the information sequence $\{I_k\}$ is uncorrelated, the optimum coefficients are exactly equal to the respective values of the equivalent discrete-time channel. It is also apparent that when the number of taps N in the channel estimator is greater than or equal to $L+1$, the optimum tap gain coefficients $\{\hat{f}_k\}$ are equal to the respective values of the $\{f_k\}$, even when the information sequence is correlated. Subject to the above conditions, the minimum MSE is simply equal to the noise variance N_0.

In the above discussion, the estimated information sequence at the output of the Viterbi algorithm or the probabilistic symbol-by-symbol algorithm was used in making adjustments of the channel estimator. For startup operation, one may send a short training sequence to perform the initial adjustment of the tap coefficients, as is usually done in the case of the linear transversal equalizer. In an adaptive mode of operation, the receiver simply uses its own decisions to form an error signal.

11-4 RECURSIVE LEAST-SQUARES ALGORITHMS FOR ADAPTIVE EQUALIZATION

The LMS algorithm that we described in Sections 11-1 and 11-2 for adaptively adjusting the tap coefficients of a linear equalizer or a DFE is basically a (stochastic) steepest-descent algorithm in which the true gradient vector is approximated by an estimate obtained directly from the data.

The major advantage of the steepest-descent algorithm lies in its computational simplicity. However, the price paid for the simplicity is slow convergence, especially when the channel characteristics result in an autocorrelation matrix Γ whose eigenvalues have a large spread, i.e., $\lambda_{max}/\lambda_{min} \gg 1$. Viewed in another way, the gradient algorithm has only a single adjustable parameter for

controlling the convergence rate, namely, the parameter Δ. Consequently the slow convergence is due to this fundamental limitation.

In order to obtain faster convergence, it is necessary to devise more complex algorithms involving additional parameters. In particular, if the matrix Γ is $N \times N$ and has eigenvalues $\lambda_1, \lambda_2, \ldots, \lambda_N$, we may use an algorithm that contains N parameters—one for each of the eigenvalues. The optimum selection of these parameters to achieve rapid convergence is a topic of this section.

In deriving faster converging algorithms, we shall adopt a least-squares approach. Thus, we shall deal directly with the received data in minimizing the quadratic performance index, whereas previously we minimized the expected value of the squared error. Put simply, this means that the performance index is expressed in terms of a time average instead of a statistical average.

It is convenient to express the recursive least-squares algorithms in matrix form. Hence, we shall define a number of vectors and matrices that are needed in this development. In so doing, we shall change the notation slightly. Specifically, the estimate of the information symbol at time t, where t is an integer, from a linear equalizer is now expressed as

$$\tilde{I}(t) = \sum_{j=-K}^{K} c_j(t-1) v_{t-j}$$

By changing the index j on $c_j(t-1)$ to run from $j=0$ to $j=N-1$ and simultaneously defining

$$y(t) = v_{t+K}$$

the estimate $\tilde{I}(t)$ becomes

$$\begin{aligned} \tilde{I}(t) &= \sum_{j=0}^{N-1} c_j(t-1) y(t-j) \\ &= \mathbf{C}_N(t-1)\mathbf{Y}_N(t) \end{aligned} \tag{11-4-1}$$

where $\mathbf{C}_N(t-1)$ and $\mathbf{Y}_N(t)$ are, respectively, the column vectors of the equalizer coefficients $c_j(t-1)$, $j=0, 1, \ldots, N-1$, and the input signals $y(t-j)$, $j=0, 1, 2, \ldots, N-1$.

Similarly, in the decision-feedback equalizer, we have tap coefficients $c_j(t)$, $j=0, 1, \ldots, N-1$, where the first K_1+1 are the coefficients of the feedforward filter and the remaining $K_2 = N - K_1 - 1$ are the coefficients of the feedback filter. The data in the estimate $\hat{I}(t)$ is $v_{t+K_1}, \ldots, v_{t+1}, \tilde{I}_{t-1}, \ldots, \tilde{I}_{t-K_2}$, where $\tilde{I}_{t-j}$, $1 \leq j \leq K_2$, denote the decisions on previously detected symbols. In this development, we neglect the effect of decision errors in the algorithms. Hence, we assume that $\tilde{I}_{t-j} = I_{t-j}$, $1 \leq j \leq K_2$. For notational convenience, we also define

$$y(t-j) = \begin{cases} v_{t+K_1-j} & (0 \leq j \leq K_1) \\ I_{t+K_1-j} & (K_1 < j \leq N-1) \end{cases} \tag{11-4-2}$$

Thus,

$$\begin{aligned}\mathbf{Y}_N(t) &= [y(t) \quad y(t-1) \quad \ldots \quad y(t-N+1)]' \\ &= [v_{t+K_1} \quad \ldots \quad v_{t+1} \quad v_t \quad I_{t-1} \quad \ldots \quad I_{t-K_2}]' \end{aligned} \tag{11-4-3}$$

11-4-1 Recursive Least-Squares (Kalman) Algorithm

The recursive least-squares (RLS) estimation of $\hat{I}(t)$ may be formulated as follows. Suppose we have observed the vectors $\mathbf{Y}_N(n)$, $n = 0, 1, \ldots, t$, and we wish to determine the coefficient vector $\mathbf{C}_N(t)$ of the equalizer (linear or decision-feedback) that minimizes the time-average weighted squared error

$$\mathscr{E}_N^{LS} = \sum_{n=0}^{t} w^{t-n} |e_N(n, t)|^2 \tag{11-4-4}$$

where the error is defined as

$$e_N(n, t) = I(n) - \mathbf{C}_N'(t)\mathbf{Y}_N(n) \tag{11-4-5}$$

and w represents a weighting factor $0 < w < 1$. Thus we introduce exponential weighting into past data, which is appropriate when the channel characteristics are time-variant. Minimization of $\mathscr{E}_N^{LS}$ with respect to the coefficient vector $\mathbf{C}_N(t)$ yields the set of linear equations

$$\mathbf{R}_N(t)\mathbf{C}_N(t) = \mathbf{D}_N(t) \tag{11-4-6}$$

where $\mathbf{R}_N(t)$ is the signal correlation matrix defined as

$$\mathbf{R}_N(t) = \sum_{n=0}^{t} w^{t-n}\mathbf{Y}_N^*(n)\mathbf{Y}_N'(n) \tag{11-4-7}$$

and $\mathbf{D}_N(t)$ is the cross-correlation vector

$$\mathbf{D}_N(t) = \sum_{n=0}^{t} w^{t-n} I(n)\mathbf{Y}_N^*(n) \tag{11-4-8}$$

The solution of (11-4-6) is

$$\mathbf{C}_N(t) = \mathbf{R}_N^{-1}(t)\mathbf{D}_N(t) \tag{11-4-9}$$

The matrix $\mathbf{R}_N(t)$ is akin to the statistical autocorrelation matrix Γ_N, while the vector $\mathbf{D}_N(t)$ is akin to the cross-correlation vector ξ_N, defined previously. We emphasize, however, that $\mathbf{R}_N(t)$ is not a Toeplitz matrix. We also should mention that, for small values of t, $\mathbf{R}_N(t)$ may be ill conditioned; hence, it is customary to initially add the matrix $\delta\mathbf{I}_N$ to $\mathbf{R}_N(t)$, where δ is a small positive

constant and $\mathbf{I}_N$ is the identity matrix. With exponential weighting into the past, the effect of adding $\delta\mathbf{I}_N$ dissipates with time.

Now suppose we have the solution (11-4-9) for time $t-1$, i.e., $\mathbf{C}_N(t-1)$, and we wish to compute $\mathbf{C}_N(t)$. It is inefficient and, hence, impractical to solve the set of N linear equations for each new signal component that is received. To avoid this, we proceed as follows. First, $\mathbf{R}_N(t)$ may be computed recursively as

$$\mathbf{R}_N(t) = w\mathbf{R}_N(t-1) + \mathbf{Y}_N^*(t)\mathbf{Y}_N'(t) \tag{11-4-10}$$

We call (11-4-10) the *time-update equation* for $\mathbf{R}_N(t)$.

Since the inverse of $\mathbf{R}_N(t)$ is needed in (11-4-9), we use the matrix-inverse identity

$$\mathbf{R}_N^{-1}(t) = \frac{1}{w}\left[\mathbf{R}_N^{-1}(t-1) - \frac{\mathbf{R}_N^{-1}(t-1)\mathbf{Y}_N^*(t)\mathbf{Y}_N'(t)\mathbf{R}_N^{-1}(t-1)}{w + \mathbf{Y}_N'(t)\mathbf{R}_N^{-1}(t-1)\mathbf{Y}_N^*(t)}\right] \tag{11-4-11}$$

Thus $\mathbf{R}_N^{-1}(t)$ may be computed recursively according to (11-4-11).

For convenience, we define $\mathbf{P}_N(t) = \mathbf{R}_N^{-1}(t)$. It is also convenient to define an N-dimensional vector, called the *Kalman gain vector*, as

$$\mathbf{K}_N(t) = \frac{1}{w + \mu_N(t)}\mathbf{P}_N(t-1)\mathbf{Y}_N^*(t) \tag{11-4-12}$$

where $\mu_N(t)$ is a scalar defined as

$$\mu_N(t) = \mathbf{Y}_N'(t)\mathbf{P}_N(t-1)\mathbf{Y}_N^*(t) \tag{11-4-13}$$

With these definitions, (11-4-11) becomes

$$\mathbf{P}_N(t) = \frac{1}{w}\left[\mathbf{P}_N(t-1) - \mathbf{K}_N(t)\mathbf{Y}_N'(t)\mathbf{P}_N(t-1)\right] \tag{11-4-14}$$

Suppose we postmultiply both sides of (11-4-14) by $\mathbf{Y}_N^*(t)$. Then

$$\begin{aligned}\mathbf{P}_N(t)\mathbf{Y}_N^*(t) &= \frac{1}{w}\left[\mathbf{P}_N(t-1)\mathbf{Y}_N^*(t) - \mathbf{K}_N(t)\mathbf{Y}_N'(t)\mathbf{P}_N(t-1)\mathbf{Y}_N^*(t)\right] \\ &= \frac{1}{w}\left\{[w + \mu_N(t)]\mathbf{K}_N(t) - \mathbf{K}_N(t)\mu_N(t)\right\} \\ &= \mathbf{K}_N(t)\end{aligned} \tag{11-4-15}$$

Therefore, the Kalman gain vector may also be defined as $\mathbf{P}_N(t)\mathbf{Y}_N(t)$.

Now we use the matrix inversion identity to derive an equation for obtaining $\mathbf{C}_N(t)$ from $\mathbf{C}_N(t-1)$. Since

$$\mathbf{C}_N(t) = \mathbf{P}_N(t)\mathbf{D}_N(t)$$

and

$$\mathbf{D}_N(t) = w\mathbf{D}_N(t-1) + I(t)\mathbf{Y}_N^*(t) \tag{11-4-16}$$

we have

$$\begin{aligned}\mathbf{C}_N(t) &= \frac{1}{w}[\mathbf{P}_N(t-1) - \mathbf{K}_N(t)\mathbf{Y}'_N(t)\mathbf{P}_N(t-1)][w\mathbf{D}_N(t-1) + I(t)\mathbf{Y}^*_N(t)] \\ &= \mathbf{P}_N(t-1)\mathbf{D}_N(t-1) + \frac{1}{w}I(t)\mathbf{P}_N(t-1)\mathbf{Y}^*_N(t) \\ &\quad - \mathbf{K}_N(t)\mathbf{Y}'_N(t)\mathbf{P}_N(t-1)\mathbf{D}_N(t-1) \\ &\quad - \frac{1}{w}I(t)\mathbf{K}_N(t)\mathbf{Y}'_N(t)\mathbf{P}_N(t-1)\mathbf{Y}^*_N(t) \\ &= \mathbf{C}_N(t-1) + \mathbf{K}_N(t)[I(t) - \mathbf{Y}'_N(t)\mathbf{C}_N(t-1)] \end{aligned} \tag{11-4-17}$$

Note that $\mathbf{Y}'_N(t)\mathbf{C}_N(t-1)$ is the output of the equalizer at time t, i.e.,

$$\hat{I}(t) = \mathbf{Y}'_N(t)\mathbf{C}_N(t-1) \tag{11-4-18}$$

and

$$e_N(t, t-1) = I(t) - \hat{I}(t) \equiv e_N(t) \tag{11-4-19}$$

is the error between the desired symbol and the estimate. Hence, $\mathbf{C}_N(t)$ is updated recursively according to the relation

$$\mathbf{C}_N(t) = \mathbf{C}_N(t-1) + \mathbf{K}_N(t)e_N(t) \tag{11-4-20}$$

The residual MSE resulting from this optimization is

$$\mathscr{E}^{LS}_{N\min} = \sum_{n=0}^{t} w^{t-n}|I(n)|^2 - \mathbf{C}'_N(t)\mathbf{D}^*_N(t) \tag{11-4-21}$$

To summarize, suppose we have $\mathbf{C}_N(t-1)$ and $\mathbf{P}_N(t-1)$. When a new signal component is received, we have $\mathbf{Y}_N(t)$. Then the recursive computation for the time update of $\mathbf{C}_N(t)$ and $\mathbf{P}_N(t)$ proceeds as follows:

- compute output:

$$\hat{I}(t) = \mathbf{Y}'_N(t)\mathbf{C}_N(t-1)$$

- compute error:

$$e_N(t) = I(t) - \hat{I}(t)$$

- compute Kalman gain vector:

$$\mathbf{K}_N(t) = \frac{\mathbf{P}_N(t-1)\mathbf{Y}'_N(t)}{w + \mathbf{Y}'_N(t)\mathbf{P}_N(t-1)\mathbf{Y}^*_N(t)}$$

- update inverse of the correlation matrix:

$$\mathbf{P}_N(t) = \frac{1}{w}[\mathbf{P}_N(t-1) - \mathbf{K}_N(t)\mathbf{Y}'_N(t)\mathbf{P}_N(t-1)]$$

- update coefficients:

$$\begin{aligned}\mathbf{C}_N(t) &= \mathbf{C}_N(t-1) + \mathbf{K}_N(t)e_N(t) \\ &= \mathbf{C}_N(t-1) + \mathbf{P}_N(t)\mathbf{Y}^*(t)e_N(t)\end{aligned} \tag{11-4-22}$$

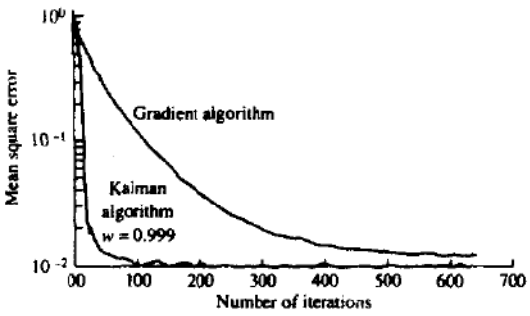

FIGURE 11-4-1 Comparison of convergence rate for the Kalman and gradient algorithms.

The algorithm described by (11-4-22) is called the *RLS direct form* or *Kalman algorithm*. It is appropriate when the equalizer has a transversal (direct-form) structure.

Note that the equalizer coefficients change with time by an amount equal to the error $e_N(t)$ multiplied by the Kalman gain vector $\mathbf{K}_N(t)$. Since $\mathbf{K}_N(t)$ is N-dimensional, each tap coefficient in effect is controlled by one of the elements of $\mathbf{K}_N(t)$. Consequently rapid convergence is obtained. In contrast, the steepest-descent algorithm, expressed in our present notation, is

$$\mathbf{C}_N(t) = \mathbf{C}_N(t-1) + \Delta \mathbf{Y}_N^*(t) e_N(t) \tag{11-4-23}$$

and the only variable parameter is the step size Δ.

Figure 11-4-1 illustrates the initial convergence rate of these two algorithms for a channel with fixed parameters $f_0 = 0.26$, $f_1 = 0.93$, $f_2 = 0.26$, and a linear equalizer with 11 taps. The eigenvalue ratio for this channel is $\lambda_{max}/\lambda_{min} = 11$. All the equalizer coefficients were initialized to zero. The steepest-descent algorithm was implemented with $\Delta = 0.020$. The superiority of the Kalman algorithm is clearly evident. This is especially important in tracking a time-variant channel. For example, the time variations in the characteristics of an (ionospheric) high-frequency (HF) radio channel are too rapid to be equalized by the gradient algorithm, but the Kalman algorithm adapts sufficiently rapidly to track such variations.

In spite of its superior tracking performance, the Kalman algorithm described above have two disadvantages. One is its complexity. The second is its sensitivity to roundoff noise that accumulates due to the recursive computations. The latter may cause instabilities in the algorithm.

The number of computations or operations (multiplications, divisions, and subtractions) in computing the variables in (11-4-22) is proportional to N^2. Most of these operations are involved in the updating of $\mathbf{P}_N(t)$. This part of the computation is also susceptible to roundoff noise. To remedy that problem, algorithms have been developed that avoid the computation of $\mathbf{P}_N(t)$ according to (11-4-14). The basis of these algorithms lies in the decomposition of $\mathbf{P}_N(t)$ in the form

$$\mathbf{P}_N(t) = \mathbf{S}_N(t) \mathbf{\Lambda}_N(t) \mathbf{S}_N'(t) \tag{11-4-24}$$

where $\mathbf{S}_N(t)$ is a lower-triangular matrix whose diagonal elements are unity, and $\mathbf{\Lambda}_N(t)$ is a diagonal matrix. Such a decomposition is called a *square-root factorization* (see Bierman, 1977). This factorization is described in Appendix D. In a square-root algorithm, $\mathbf{P}_N(t)$ is not updated as in (11-4-14) nor is it computed. Instead, the time updating is performed on $\mathbf{S}_N(t)$ and $\mathbf{\Lambda}_N(t)$.

Square-root algorithms are frequently used in control systems applications in which Kalman filtering is involved. In digital communications, the square-root Kalman algorithm has been implemented in a decision-feedback-equalized PSK modem designed to transmit at high speed over HF radio channels with a nominal 3 kHz bandwidth. This algorithm is described in the paper by Hsu (1982). It has a computational complexity of $1.5N^2 + 6.5N$ (complex-valued multiplications and divisions per output symbol). It is also numerically stable and exhibits good numerical properties. For a detailed discussion of square-root algorithms in sequential estimation, the reader is referred to the book by Bierman (1977).

It is also possible to derive RLS algorithms with computational complexities that grow linearly with the number N of equalizer coefficients. Such algorithms are generally called *fast RLS algorithms* and have been described in the papers by Carayannis *et al.* (1983), Cioffi and Kailath (1984), and Slock and Kailath (1988).

11-4-2 Linear Prediction and the Lattice Filter

In Chapter 3, we considered the linear prediction of a signal, in the context of speech encoding. In this section, we shall establish the connection between linear prediction and a lattice filter.

The linear prediction problem may be stated as follows: given a set of data $y(t-1), y(t-2), \ldots, y(t-p)$, predict the value of the next data point $y(t)$. The predictor of order p is

$$\hat{y}(t) = \sum_{k=1}^{p} a_{pk}\, y(t-k) \tag{11-4-25}$$

Minimization of the MSE, defined as

$$\begin{aligned} \mathscr{E}_p &= E[y(t) - \hat{y}(t)]^2 \\ &= E\left[y(t) - \sum_{k=1}^{p} a_{pk}\, y(t-k)\right]^2 \end{aligned} \tag{11-4-26}$$

with respect to the predictor coefficients $\{a_{pk}\}$ yields the set of linear equations

$$\sum_{k=1}^{p} a_{pk}\, \phi(k-l) = \phi(l), \qquad l = 1, 2, \ldots, p \tag{11-4-27}$$

where

$$\phi(l) = E[y(t)y(t+l)]$$

These are called the *normal equations* or the *Yule–Walker equations.*

The matrix $\mathbf{\Phi}$ with elements $\phi(k-l)$ is a Toeplitz matrix, and, hence, the Levinson–Durbin algorithm described in Appendix A provides an efficient means for solving the linear equations recursively, starting with a first-order predictor and proceeding recursively to the solution of the coefficients for the predictor of order p. The recursive relations for the Levinson–Durbin algorithm are

$$\begin{aligned} a_{11} &= \frac{\phi(1)}{\phi(0)}, \qquad \mathscr{E}_0 = \phi(0) \\ a_{mm} &= \frac{\phi(m) - \mathbf{A}_m' \boldsymbol{\phi}_{m-1}^r}{\mathscr{E}_{m-1}} \\ a_{mk} &= a_{m-1\,k} - a_{mm} a_{m-1\,m-k} \\ \mathscr{E}_m &= \mathscr{E}_{m-1}(1 - a_{mm}^2) \end{aligned} \tag{11-4-28}$$

for $m = 1, 2, \ldots, p$, where the vectors $\mathbf{A}_{m-1}$ and $\boldsymbol{\phi}_{m-1}^r$ are defined as

$$\begin{aligned} \mathbf{A}_{m-1} &= [a_{m-1\,1} \quad a_{m-1\,2} \quad \cdots \quad a_{m-1\,m-1}]' \\ \boldsymbol{\phi}_{m-1}^r &= [\phi(m-1) \quad \phi(m-2) \quad \ldots \quad \phi(1)]' \end{aligned}$$

The linear prediction filter of order m may be realized as a transversal filter with transfer function

$$A_m(z) = 1 - \sum_{k=1}^{m} a_m z^{-k} \tag{11-4-29}$$

Its input is the data $\{y(t)\}$ and its output is the error $e(t) = y(t) - \hat{y}(t)$. The prediction filter can also be realized in the form of a lattice, as we now demonstrate.

Our starting point is the use of the Levinson–Durbin algorithm for the predictor coefficients a_{mk} in (11-4-29). This substitution yields

$$\begin{aligned} A_m(z) &= 1 - \sum_{k=1}^{m-1} (a_{m-1\,k} - a_{mm} a_{m-1\,m-k}) z^{-k} - a_{mm} z^{-m} \\ &= 1 - \sum_{k=1}^{m-1} a_{m-1\,k} z^{-k} - a_{mm} z^{-m} \left(1 - \sum_{k=1}^{m-1} a_{m-1\,k} z^{k}\right) \\ &= A_{m-1}(z) - a_{mm} z^{-m} A_{m-1}(z^{-1}) \end{aligned} \tag{11-4-30}$$

Thus we have the transfer function of the mth-order predictor in terms of the transfer function of the $(m-1)$th-order predictor.

Now suppose we define a filter with transfer function $G_m(z)$ as

$$G_m(z) = z^{-m} A_m(z^{-1}) \tag{11-4-31}$$

Then (11-4-30) may be expressed as

$$A_m(z) = A_{m-1}(z) - a_{mm} z^{-1} G_{m-1}(z) \tag{11-4-32}$$

Note that $G_{m-1}(z)$ represents a transversal filter with tap coefficients $(-a_{m-1\,m-1}, -a_{m-1\,m-2}, \ldots, -a_{m-1\,1}, 1)$, while the coefficients of $A_{m-1}(z)$ are exactly the same except that they are given in reverse order.

More insight into the relationship between $A_m(z)$ and $G_m(z)$ can be obtained by computing the output of these two filters to an input sequence $y(t)$. Using z-transform relations, we have

$$A_m(z)Y(z) = A_{m-1}(z)Y(z) - a_{mm}z^{-1}G_{m-1}(z)Y(z) \tag{11-4-33}$$

We define the outputs of the filters as

$$\begin{aligned} F_m(z) &= A_m(z)Y(z) \\ B_m(z) &= G_m(z)Y(z) \end{aligned} \tag{11-4-34}$$

Then (11-4-33) becomes

$$F_m(z) = F_{m-1}(z) - a_{mm}z^{-1}B_{m-1}(z) \tag{11-4-35}$$

In the time domain, the relation in (11-4-35) becomes

$$f_m(t) = f_{m-1}(t) - a_{mm}b_{m-1}(t-1), \quad m \geq 1 \tag{11-4-36}$$

where

$$f_m(t) = y(t) - \sum_{k=1}^{m-1} a_{mk}\,y(t-k) \tag{11-4-37}$$

$$b_m(t) = y(t-m) - \sum_{k=1}^{m-1} a_{mk}\,y(t-m+k) \tag{11-4-38}$$

To elaborate, $f_m(t)$ in (11-4-37) represents the error of an mth-order forward predictor, while $b_m(t)$ represents the error of an mth-order backward predictor.

The relation in (11-4-36) is one of two that specifies a lattice filter. The second relation is obtained from $G_m(z)$ as follows:

$$\begin{aligned} G_m(z) &= z^{-m}A_m(z^{-1}) \\ &= z^{-m}[A_{m-1}(z^{-1}) - a_{mm}z^{m}A_{m-1}(z)] \\ &= z^{-1}G_{m-1}(z) - a_{mm}A_{m-1}(z) \end{aligned} \tag{11-4-39}$$

Now, if we multiply both sides of (11-4-39) by $Y(z)$ and express the result in terms of $F_m(z)$ and $B_m(z)$ using the definitions in (11-4-34), we obtain

$$B_m(z) = z^{-1}B_{m-1}(z) - a_{mm}F_{m-1}(z) \tag{11-4-40}$$

By transforming (11-4-40) into the time domain, we obtain the second relation that corresponds to the lattice filter, namely,

$$b_m(t) = b_{m-1}(t-1) - a_{mm}f_{m-1}(t), \quad m \geq 1 \tag{11-4-41}$$

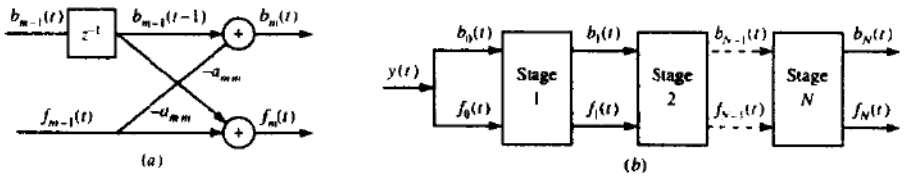

FIGURE 11-4-2 A lattice filter.

The initial condition is

$$f_0(t) = b_0(t) = y(t) \tag{11-4-42}$$

The lattice filter described by the recursive relations in (11-4-36) and (11-4-41) is illustrated in Fig. 11-4-2. Each stage is characterized by its own multiplication factor $\{a_{ii}\}$, $i = 1, 2, \ldots, m$, which is defined in the Levinson–Durbin algorithm. The forward and backward errors $f_m(t)$ and $b_m(t)$ are usually called the *residuals*. The mean square value of these residuals is

$$\mathscr{E}_m = E[f_m^2(t)] = E[b_m^2(t)] \tag{11-4-43}$$

$\mathscr{E}_m$ is given recursively, as indicated in the Levinson–Durbin algorithm, by

$$\begin{aligned} \mathscr{E}_m &= \mathscr{E}_{m-1}(1 - a_{mm}^2) \\ &= \mathscr{E}_0 \prod_{i=1}^{m} (1 - a_{ii}^2) \end{aligned} \tag{11-4-44}$$

where $\mathscr{E}_0 = \phi(0)$.

The residuals $\{f_m(t)\}$ and $\{b_m(t)\}$ satisfy a number of interesting properties, as described by Makhoul (1978). Most important of these are the orthogonality properties

$$\begin{aligned} E[b_m(t)b_n(t)] &= \mathscr{E}_m \delta_{mn} \\ E[f_m(t+m)f_n(t+n)] &= \mathscr{E}_m \delta_{mn} \end{aligned} \tag{11-4-45}$$

Furthermore, the cross-correlation between $f_m(t)$ and $b_n(t)$ is

$$E[f_m(t)b_n(t)] = \begin{cases} a_{nn}\mathscr{E}_m & (m \geq n) \\ 0 & (m < n) \end{cases} \qquad m, n \geq 0 \tag{11-4-46}$$

As a consequence of the orthogonality properties of the residuals, the different sections of the lattice exhibit a form of independence that allows us to add or delete one or more of the last stages without affecting the parameters of the remaining stages. Since the residual mean square error $\mathscr{E}_m$ decreases monotonically with the number of sections, $\mathscr{E}_m$ can be used as a performance index in determining where the lattice should be terminated.

From the above discussion, we observe that a linear prediction filter can be implemented either as a linear transversal filter or as a lattice filter. The lattice filter is order-recursive, and, as a consequence, the number of sections it contains can be easily increased or decreased without affecting the parameters

of the remaining sections. In contrast, the coefficients of a transversal filter obtained on the basis of the RLS criterion are interdependent. This means that an increase or a decrease in the size of the filter results in a change in all coefficients. Consequently, the Kalman algorithm described in Section 11-4-1 is recursive in time but not in order.

Based on least-squares optimization, RLS lattice algorithms have been developed whose computational complexity grow linearly with the number N of filter coefficients (lattice stages). Hence, the lattice equalizer structure is computationally competitive with the direct-form fast RLS equalizer algorithms. RLS lattice algorithms are described in the papers by Morf *et al.* (1973), Satorius and Alexander (1979), Satorius and Pack (1981), Ling and Proakis (1984), and Ling *et al.* (1986).

RLS lattice algorithms have the distinct feature of being numerically robust to round-off error inherent in digital implementations of the algorithm. A treatment of their numerical properties may be found in the papers by Ling *et al.* (1984, 1986).

11-5 SELF-RECOVERING (BLIND) EQUALIZATION

In the conventional zero-forcing or minimum MSE equalizers, we assumed that a known training sequence is transmitted to the receiver for the purpose of initially adjusting the equalizer coefficients. However, there are some applications, such as multipoint communication networks, where it is desirable for the receiver to synchronize to the received signal and to adjust the equalizer without having a known training sequence available. Equalization techniques based on initial adjustment of the coefficients without the benefit of a training sequence are said to be *self-recovering* or *blind*.

Beginning with the paper by Sato (1975), three different classes of adaptive blind equalization algorithms have been developed over the past two decades. One class of algorithms is based on steepest descent for adaptation of the equalizer. A second class of algorithms is based on the use of second- and higher-order (generally, fourth-order) statistics of the received signal to estimate the channel characteristics and to design the equalizer. More recently, a third class of blind equalization algorithms based on the maximum-likelihood criterion have been investigated. In this section, we briefly describe these approaches and give several relevant references to the literature.

11-5-1 Blind Equalization Based on Maximum-Likelihood Criterion

It is convenient to use the equivalent, discrete-time channel model described in Section 10-1-2. Recall that the output of this channel model with ISI is

$$v_n = \sum_{k=0}^{L} f_k I_{n-k} + \eta_n \tag{11-5-1}$$

where $\{f_k\}$ are the equivalent discrete-time channel coefficients, $\{I_n\}$ represents the information sequence, and $\{\eta_n\}$ is a white gaussian noise sequence.

For a block of N received data points, the (joint) probability density function of the received data vector $\mathbf{v} = [v_1\ v_2\ \ldots\ v_N]^t$ conditioned on knowing the impulse response vector $\mathbf{f} = [f_0\ f_1\ \ldots\ f_L]^t$ and the data vector $\mathbf{I} = [I_1\ I_2\ \ldots\ I_N]^t$ is

$$p(\mathbf{v} \mid \mathbf{f}, \mathbf{I}) = \frac{1}{(2\pi\sigma^2)^N} \exp\left(-\frac{1}{2\sigma^2} \sum_{n=1}^{N} \left| v_n - \sum_{k=0}^{L} f_k I_{n-k} \right|^2\right) \tag{11-5-2}$$

The joint maximum-likelihood estimates of $\mathbf{f}$ and $\mathbf{I}$ are the values of these vectors that maximize the joint probability density function $p(\mathbf{v} \mid \mathbf{f}, \mathbf{I})$ or, equivalently, the values of $\mathbf{f}$ and $\mathbf{I}$ that minimize the term in the exponent. Hence, the ML solution is simply the minimum over $\mathbf{f}$ and $\mathbf{I}$ of the metric

$$\begin{aligned} DM(\mathbf{I}, \mathbf{f}) &= \sum_{n=1}^{N} \left| v_n - \sum_{k=0}^{L} f_k I_{n-k} \right|^2 \\ &= \|\mathbf{v} - \mathbf{A}\mathbf{f}\|^2 \end{aligned} \tag{11-5-3}$$

where the matrix $\mathbf{A}$ is called the *data matrix* and is defined as

$$\mathbf{A} = \begin{bmatrix} I_1 & 0 & 0 & \ldots & 0 \\ I_2 & I_1 & 0 & \ldots & 0 \\ I_3 & I_2 & I_1 & \ldots & 0 \\ \vdots & \vdots & \vdots & & \vdots \\ I_N & I_{N-1} & I_{N-2} & \ldots & I_{N-L} \end{bmatrix} \tag{11-5-4}$$

We make several observations. First of all, we note that when the data vector $\mathbf{I}$ (or the data matrix $\mathbf{A}$) is known, as is the case when a training sequence is available at the receiver, the ML channel impulse response estimate obtained by minimizing (11-5-3) over $\mathbf{f}$ is

$$\mathbf{f}_{ML}(\mathbf{I}) = (\mathbf{A}^t\mathbf{A})^{-1}\mathbf{A}^t\mathbf{v} \tag{11-5-5}$$

On the other hand, when the channel impulse response $\mathbf{f}$ is known, the optimum ML detector for the data sequence $\mathbf{I}$ performs a trellis search (or tree search) by utilizing the Viterbi algorithm for the ISI channel.

When neither $\mathbf{I}$ nor $\mathbf{f}$ are known, the minimization of the performance index $DM(\mathbf{I}, \mathbf{f})$ may be performed jointly over $\mathbf{I}$ and $\mathbf{f}$. Alternatively, $\mathbf{f}$ may be estimated from the probability density function $p(\mathbf{v} \mid \mathbf{f})$, which may be obtained by averaging $p(\mathbf{v}, \mathbf{f} \mid \mathbf{I})$ over all possible data sequences. That is,

$$\begin{aligned} p(\mathbf{v} \mid \mathbf{f}) &= \sum_{m} p(\mathbf{v}, \mathbf{I}^{(m)} \mid \mathbf{f}) \\ &= \sum_{m} p(\mathbf{v} \mid \mathbf{I}^{(m)}, \mathbf{f}) P(\mathbf{I}^{(m)}) \end{aligned} \tag{11-5-6}$$

where $P(\mathbf{I}^{(m)})$ is the probability of the sequence $\mathbf{I} = \mathbf{I}^{(m)}$, for $m = 1, 2, \ldots, M^N$ and M is the size of the signal constellation.

Channel Estimation Based on Average over Data Sequences As indicated in the above discussion, when both $\mathbf{I}$ and $\mathbf{f}$ are unknown, one approach is to estimate the impulse response $\mathbf{f}$ after averaging the probability density $p(\mathbf{v}, \mathbf{I} \mid \mathbf{f})$ over all possible data sequences. Thus, we have

$$\begin{aligned} p(\mathbf{v} \mid \mathbf{f}) &= \sum_m p(\mathbf{v} \mid \mathbf{I}^{(m)}, \mathbf{f}) P(\mathbf{I}^{(m)}) \\ &= \sum_m \left[\frac{1}{(2\pi\sigma^2)^N} \exp\left(-\frac{\|\mathbf{v} - \mathbf{A}^{(m)}\mathbf{f}\|^2}{2\sigma^2} \right) \right] P(\mathbf{I}^{(m)}) \end{aligned} \tag{11-5-7}$$

Then, the estimate of $\mathbf{f}$ that maximizes $p(\mathbf{v} \mid \mathbf{f})$ is the solution of the equation

$$\begin{aligned} \frac{\partial p(\mathbf{v} \mid \mathbf{f})}{\partial \mathbf{f}} &= \sum_m P(\mathbf{I}^{(m)}) \\ (\mathbf{A}^{(m)t}\mathbf{A}^{(m)}\mathbf{f} - \mathbf{A}^{(m)t}\mathbf{v}) \exp\left(-\frac{\|\mathbf{v} - \mathbf{A}^{(m)}\mathbf{f}\|^2}{2\sigma^2} \right) &= 0 \end{aligned} \tag{11-5-8}$$

Hence, the estimate of $\mathbf{f}$ may be expressed as

$$\begin{aligned} \mathbf{f} = &\left[\sum_m P(\mathbf{I}^{(m)}) \mathbf{A}^{(m)t}\mathbf{A}^{(m)} g(\mathbf{v}, \mathbf{A}^{(m)}, \mathbf{f}) \right]^{-1} \\ &\times \sum_m P(\mathbf{I}^{(m)}) g(\mathbf{v}, \mathbf{A}^{(m)}, \mathbf{f}) \mathbf{A}^{(m)t}\mathbf{v} \end{aligned} \tag{11-5-9}$$

where the function $g(\mathbf{v}, \mathbf{A}^{(m)}, \mathbf{f})$ is defined as

$$g(\mathbf{v}, \mathbf{A}^{(m)}, \mathbf{f}) = \exp\left(-\frac{\|\mathbf{v} - \mathbf{A}^{(m)}\mathbf{f}\|^2}{2\sigma^2} \right) \tag{11-5-10}$$

The resulting solution for the optimum $\mathbf{f}$ is denoted by $\mathbf{f}_{ML}$.

Equation (11-5-9) is a nonlinear equation for the estimate of the channel impulse response, given the received signal vector $\mathbf{v}$. It is generally difficult to obtain the optimum solution by solving (11-5-9) directly. On the other hand, it is relatively simple to devise a numerical method that solves for $\mathbf{f}_{ML}$ recursively. Specifically, we may write

$$\begin{aligned} \mathbf{f}^{(k+1)} = &\left[\sum_m P(\mathbf{I}^{(m)}) \mathbf{A}^{(m)t}\mathbf{A}^{(m)} g(\mathbf{v}, \mathbf{A}^{(m)}, \mathbf{f}^{(k)}) \right]^{-1} \\ &\times \sum_m P(\mathbf{I}^{(m)}) g(\mathbf{v}, \mathbf{A}^{(m)}, \mathbf{f}^{(k)}) \mathbf{A}^{(m)t}\mathbf{v} \end{aligned} \tag{11-5-11}$$

Once $\mathbf{f}_{ML}$ is obtained from the solution of (11-5-9) or (11-5-11), we may

simply use the estimate in the minimization of the metric $DM(\mathbf{I}, \mathbf{f}_{ML})$, given by (11-5-3), over all the possible data sequences. Thus, $\mathbf{I}_{ML}$ is the sequence $\mathbf{I}$ that mimimizes $DM(\mathbf{I}, \mathbf{f}_{ML})$, i.e.,

$$\min_{\mathbf{I}} DM(\mathbf{I}, \mathbf{f}_{ML}) = \min_{\mathbf{I}} \|\mathbf{v} - \mathbf{A}\mathbf{f}_{ML}\|^2 \tag{11-5-12}$$

We know that the Viterbi algorithm is the computationally efficient algorithm for performing the minimization of $DM(\mathbf{I}, \mathbf{f}_{ML})$ over $\mathbf{I}$.

This algorithm has two major drawbacks. First, the recursion for $\mathbf{f}_{LM}$ given by (11-5-11) is computationally intensive. Second, and, perhaps, more importantly, the estimate $\mathbf{f}_{ML}$ is not as good as the maximum-likelihood estimate $\mathbf{f}_{ML}(\mathbf{I})$ that is obtained when the sequence $\mathbf{I}$ is known. Consequently, the error rate performance of the blind equalizer (the Viterbi algorithm) based on the estimate $\mathbf{f}_{ML}$ is poorer than that based on $\mathbf{f}_{ML}(\mathbf{I})$. Next, we consider joint channel and data estimation.

Joint Channel and Data Estimation Here, we consider the joint optimization of the performance index $DM(\mathbf{I}, \mathbf{f})$ given by (11-5-3). Since the elements of the impulse response vector $\mathbf{f}$ are continuous and the elements of the data vector $\mathbf{I}$ are discrete, one approach is to determine the maximum-likelihood estimate of $\mathbf{f}$ for each possible data sequence and, then, to select the data sequence that minimizes $DM(\mathbf{I}, \mathbf{f})$ for each corresponding channel estimate. Thus, the channel estimate corresponding to the mth data sequence $\mathbf{I}^{(m)}$ is

$$\mathbf{f}_{ML}(\mathbf{I}^{(m)}) = (\mathbf{A}^{(m)t}\mathbf{A}^{(m)})^{-1}\mathbf{A}^{(m)t}\mathbf{v}. \tag{11-5-13}$$

For the mth data sequence, the metric $DM(\mathbf{I}, \mathbf{f})$ becomes

$$DM(\mathbf{I}^{(m)}, \mathbf{f}_{ML}(\mathbf{I}^{(m)})) = \|\mathbf{v} - \mathbf{A}^{(m)}\mathbf{f}_{ML}(\mathbf{I}^{(m)})\|^2 \tag{11-5-14}$$

Then, from the set of M^N possible sequences, we select the data sequence that minimizes the cost function in (11-5-14), i.e., we determine

$$\min_{\mathbf{I}^{(m)}} DM(\mathbf{I}^{(m)}, \mathbf{f}_{ML}(\mathbf{I}^{(m)})) \tag{11-5-15}$$

The approach described above is an exhaustive computational search method with a computational complexity that grows exponentially with the length of the data block. We may select $N = L$, and, thus, we shall have one channel estimate for each of the M^L surviving sequences. Thereafter, we may continue to maintain a separate channel estimate for each surviving path of the Viterbi algorithm search through the trellis.

A similar approach has been proposed by Seshadri (1991). In essence, Seshadri's algorithm is a type of generalized Viterbi algorithm (GVA) that retains $K \geq 1$ best estimates of the transmitted data sequence into each state

of the trellis and the corresponding channel estimates. In Seshadri's GVA, the search is identical to the conventional VA from the beginning up to the L stage of the trellis, i.e., up to the point where the received sequence $(v_1, v_2, \ldots, v_L)$ has been processed. Hence, up to the L stage, an exhaustive search is performed. Associated with each data sequence $\mathbf{I}^{(m)}$, there is a corresponding channel estimate $\mathbf{f}_{ML}(\mathbf{I}^{(m)})$. From this stage on, the search is modified, to retain $K \geq 1$ surviving sequences and associated channel estimates per state instead of only one sequence per state. Thus, the GVA is used for processing the received signal sequence $\{v_n, n \geq L+1\}$. The channel estimate is updated recursively at each stage using the LMS algorithm to further reduce the computational complexity. Simulation results given in the paper by Seshadri (1991) indicate that this GVA blind equalization algorithm performs rather well at moderate signal-to-noise ratios with $K = 4$. Hence, there is a modest increase in the computational complexity of the GVA compared with that for the conventional VA. However, there are additional computations involved with the estimation and updating of the channel estimates $\mathbf{f}(\mathbf{I}^{(m)})$ associated with each of the surviving data estimates.

An alternative joint estimation algorithm that avoids the least-squares computation for channel estimation has been devised by Zervas *et al.* (1991). In this algorithm, the order for performing the joint minimization of the performance index $DM(\mathbf{I}, \mathbf{f})$ is reversed. That is, a channel impulse response, say $\mathbf{f} = \mathbf{f}^{(1)}$ is selected and then the conventional VA is used to find the optimum sequence for this channel impulse response. Then, we may modify $\mathbf{f}^{(1)}$ in some manner to $\mathbf{f}^{(2)} = \mathbf{f}^{(1)} + \Delta\mathbf{f}^{(1)}$ and repeat the optimization over the data sequences $\{\mathbf{I}^{(m)}\}$.

Based on this general approach, Zervas developed a new ML blind equalization algorithm, which is called a *quantized-channel algorithm*. The algorithm operates over a grid in the channel space, which becomes finer and finer by using the ML criterion to confine the estimated channel in the neighborhood of the original unknown channel. This algorithm leads to an efficient parallel implementation, and its storage requirements are only those of the VA.

11-5-2 Stochastic Gradient Algorithm

Another class of blind equalization algorithms are stochastic-gradient iterative equalization schemes that apply a memoryless nonlinearity in the output of a linear FIR equalization filter in order to generate the "desired response" in each iteration.

Let us begin with an initial guess of the coefficients of the optimum equalizer, which we denote by $\{c_n\}$. Then, the convolution of the channel response with the equalizer response may be expressed as

$$\{c_n\} \bigstar \{f_n\} = \{\delta_n\} + \{e_n\} \tag{11-5-16}$$

where $\{\delta_n\}$ is the unit sample sequence and $\{e_n\}$ denotes the error sequence

that results from our initial guess of the equalizer coefficients. If we convolve the equalizer impulse response with the received sequence $\{v_n\}$, we obtain

$$\begin{aligned}\{\hat{I}_n\} &= \{v_n\} \star \{c_n\} \\ &= \{I_n\} \star \{f_n\} \star \{c_n\} + \{\eta_n\} \star \{c_n\} \\ &= \{I_n\} \star (\{\delta_n\} + \{e_n\}) + \{\eta_n\} \star \{c_n\} \\ &= \{I_n\} + \{I_n\} \star \{e_n\} + \{\eta_n\} \star \{c_n\}\end{aligned} \tag{11-5-17}$$

The term $\{I_n\}$ in (11-5-17) represents the desired data sequence, the term $\{I_n\} \star \{e_n\}$ represents the residual ISI, and the term $\{\eta_n\} \star \{c_n\}$ represents the additive noise. Our problem is to utilize the deconvolved sequence $\{\hat{I}_n\}$ to find the "best" estimate of a desired response, denoted in general by $\{d_n\}$. In the case of adaptive equalization using a training sequence, $\{d_n\} = \{I_n\}$. In a blind equalization mode, we shall generate a desired response from $\{\hat{I}_n\}$.

The mean square error (MSE) criterion may be employed to determine the "best" estimate of $\{I_n\}$ from the observed equalizer output $\{\hat{I}_n\}$. Since the transmitted sequence $\{I_n\}$ has a nongaussian pdf, the MSE estimate is a nonlinear transformation of $\{\hat{I}_n\}$. In general, the "best" estimate $\{d_n\}$ is given by

$$\begin{aligned} d_n &= g(\hat{I}_n) && \text{(memoryless)} \\ d_n &= g(\hat{I}_n, \hat{I}_{n-1}, \ldots, \hat{I}_{n-m}) && (m\text{th-order memory}) \end{aligned} \tag{11-5-18}$$

where $g(\ )$ is a nonlinear function. The sequence $\{d_n\}$ is then used to generate an error signal, which is fed back into the adaptive equalization filter, as shown in Fig. 11-5-1.

A well-known classical estimation problem is the following. If the equalizer output $\hat{I}_n$ is expressed as

$$\hat{I}_n = I_n + \tilde{\eta}_n \tag{11-5-19}$$

where $\tilde{\eta}_n$ is assumed to be zero-mean gaussian (the central limit theorem may

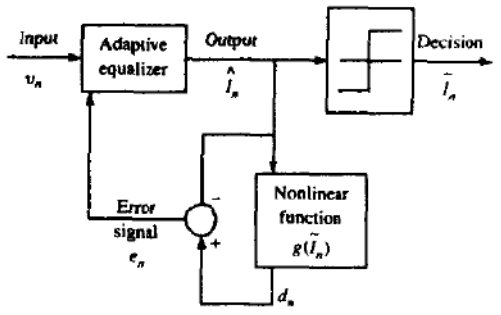

FIGURE 11-5-1 Adaptive blind equalization with stochastic gradient algorithms.

TABLE 11-5-1 STOCHASTIC GRADIENT ALGORITHMS FOR BLIND EQUALIZATION

Equalizer tap coefficients	$\{c_n, 0 \le n \le N-1\}$
Received signal sequence	$\{v_n\}$
Equalizer output sequence	$\{\hat{I}_n\} = \{v_n\} \star \{c_n\}$
Equalizer error sequence	$\{e_n\} = g(\hat{I}_n) - \hat{I}_n$
Tap coefficient update equation	$\mathbf{c}_{n+1} = \mathbf{c}_n + \Delta \mathbf{v}_n^* e_n$

Algorithm	Nonlinearity: $g(\hat{I}_n)$
Godard	$\frac{\hat{I}_n}{\lvert\hat{I}_n\rvert}(\lvert\hat{I}_n\rvert + R_2\lvert\hat{I}_n\rvert - \lvert\hat{I}_n\rvert^3),\ R_2 = \frac{E\{\lvert I_n\rvert^4\}}{E\{\lvert I_n\rvert^2\}}$
Sato	$\zeta\ \text{csgn}(\hat{I}_n),\ \zeta = \frac{E\{[\text{Re}(I_n)]^2\}}{E\{\lvert\text{Re}(I_n)\rvert\}}$
Benveniste–Goursat	$\hat{I}_n + k_1(\hat{I}_n - I_n) + k_2\lvert\hat{I}_n - \bar{I}_n\rvert[\zeta\ \text{csgn}(\hat{I}_n) - \bar{I}_n]$, k_1 and k_2 are positive constants
Stop-and-Go	$\hat{I}_n + \frac{1}{2}A(\hat{I}_n - \bar{I}_n) + \frac{1}{2}B(\hat{I}_n - \bar{I}_n)^*$ $(A, B) = (2, 0), (1, 1), (1, -1)$, or $(0, 0)$, depending on the signs of decision-directed error $\hat{I}_n - \bar{I}_n$ and the error $\zeta\ \text{csgn}(\hat{I}_n) - \bar{I}_n$

be invoked here for the residual ISI and the additive noise), $\{I_n\}$ and $\{\tilde{\eta}_n\}$ are statistically independent, and $\{I_n\}$ are statistically independent and identically distributed random variables, then the MSE estimate of $\{I_n\}$ is

$$d_n = E(I_n \mid \bar{I}_n) \tag{11-5-20}$$

which is a nonlinear function of the equalizer output when $\{I_n\}$ is nongaussian.

Table 11-5-1 illustrates the general form of existing blind equalization algorithms that are based on LMS adaptation. We observe that the basic difference among these algorithms lies in the choice of the memoryless nonlinearity. The most widely used algorithm in practice is the *Godard algorithm*, sometimes also called the *constant-modulus algorithm* (CMA).

It is apparent from Table 11-5-1 that the output sequence $\{d_n\}$ obtained by taking a nonlinear function of the equalizer output plays the role of the desired response or a training sequence. It is also apparent that these algorithms are simple to implement, since they are basically LMS-type algorithms. As such, we expect that the convergence characteristics of these algorithms will depend on the autocorrelation matrix of the received data $\{v_n\}$.

With regard to convergence, the adaptive LMS-type algorithms converge in the mean when

$$E[v_n g^*(\hat{I}_n)] = E[v_n \hat{I}_n^*] \tag{11-5-21}$$

and, in the mean square sense, when (superscript H denotes the conjugate transpose)

$$\begin{aligned} E[\mathbf{c}_n^H v_n g^*(\hat{I}_n)] &= E[\mathbf{c}_n^H v_n \hat{I}_n^*] \\ E[\hat{I}_n g^*(\hat{I}_n)] &= E[\lvert\hat{I}_n\rvert^2] \end{aligned} \tag{11-5-22}$$

Therefore, it is required that the equalizer output $\{\hat{I}_n\}$ satisfy (11-5-22). Note that (11-5-22) states that the autocorrelation of $\{\hat{I}_n\}$ (the right-hand side) equals the cross-correlation between $\hat{I}_n$ and a nonlinear transformation of $\hat{I}_n$ (left-hand side). Processes that satisfy this property are called *Bussgang* (1952), as named by Bellini (1986). In summary, the algorithms given in Table 11-5-1 converge when the equalizer output sequence $\hat{I}_n$ satisfies the Bussgang property.

The basic limitation of stochastic gradient algorithms is their relatively slow convergence. Some improvement in the convergence rate can be achieved by modifying the adaptive algorithms from LMS-type to recursive-least-square (RLS) type.

Godard Algorithm As indicated above, the Godard blind equalization algorithm is a steepest-descent algorithm that is widely used in practice when a training sequence is not available. Let us describe this algorithm in more detail.

Godard considered the problem of combined equalization and carrier phase recovery and tracking. The carrier phase tracking is performed at baseband, following the equalizer as shown in Fig. 11-5-2. Based on this structure, we may express the equalizer output as

$$\hat{I}_k = \sum_{n=-K}^{K} c_n v_{k-n} \tag{11-5-23}$$

and the input to the decision device as $\hat{I}_k \exp(-j\hat{\phi}_k)$, where $\hat{\phi}_k$ is the carrier phase estimate in the kth symbol interval.

If the desired symbol were known, we could form the error signal

$$\varepsilon_k = I_k - \hat{I}_k e^{-j\hat{\phi}_k} \tag{11-5-24}$$

and minimize the MSE with respect to $\hat{\phi}_k$ and $\{c_n\}$, i.e.,

$$\min_{\hat{\phi}_k, \mathbf{C}} E(|I_k - \hat{I}_k e^{-j\hat{\phi}_k}|^2) \tag{11-5-25}$$

FIGURE 11-5-2 Godard scheme for combined adaptive (blind) equalization and carrier phase tracking.

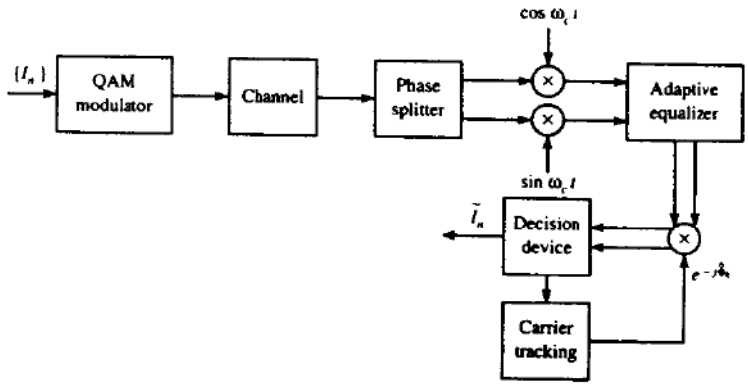

This criterion leads us to use the LMS algorithm for recursively estimating $\mathbf{C}$ and ϕ_k. The LMS algorithm based on knowledge of the transmitted sequence is

$$\hat{\mathbf{C}}_{k+1} = \hat{\mathbf{C}}_k + \Delta_c(I_k - \hat{I}_k e^{-j\hat{\phi}_k})\mathbf{V}_k^* e^{j\hat{\phi}_k} \tag{11-5-26}$$

$$\hat{\phi}_{k+1} = \hat{\phi}_k + \Delta_\phi \operatorname{Im}(I_k \hat{I}_k^* e^{j\hat{\phi}_k}) \tag{11-5-27}$$

where Δ_c and Δ_ϕ are the step-size parameters for the two recursive equations. Note that these recursive equations are coupled together. Unfortunately, these equations will not converge, in general, when the desired symbol sequence $\{I_k\}$ is unknown.

The approach proposed by Godard is to use a criterion that depends on the amount of intersymbol interference at the output of the equalizer but one that is independent of the QAM signal constellation and the carrier phase. For example, a cost function that is independent of carrier phase and has the property that its minimum leads to a small MSE is

$$G^{(p)} = E(|\hat{I}_k|^p - |I_k|^p)^2 \tag{11-5-28}$$

where p is a positive and real integer. Minimization of $G^{(p)}$ with respect to the equalizer coefficients results in the equalization of the signal amplitude only. Based on this observation, Godard selected a more general cost function, called the *dispersion of order p*, defined as

$$D^{(p)} = E(|\hat{I}_k|^p - R_p)^2 \tag{11-5-29}$$

where R_p is a positive real constant. As in the case of $G^{(p)}$, we observe that $D^{(p)}$ is independent of the carrier phase.

Minimization of $D^{(p)}$ with respect to the equalizer coefficients can be performed recursively according to the steepest-descent algorithm

$$\mathbf{C}_{k+1} = \mathbf{C}_k - \Delta_p \frac{dD^{(p)}}{d\mathbf{C}_k} \tag{11-5-30}$$

where Δ_p is the step-size parameter. By differentiating $D^{(p)}$ and dropping the expectation operation, we obtain the following LMS-type algorithm for adjusting the equalizer coefficients:

$$\hat{\mathbf{C}}_{k+1} = \hat{\mathbf{C}}_k + \Delta_p \mathbf{V}_k^* \hat{I}_k |\hat{I}_k|^{p-2}(R_p - |\hat{I}_k|^p) \tag{11-5-31}$$

where Δ_p is the step-size parameter and the optimum choice of R_p is

$$R_p = \frac{E(|I_k|^{2p})}{E(|I_k|^p)} \tag{11-5-32}$$

As expected, the recursion in (11-5-31) for $\hat{\mathbf{C}}_k$ does not require knowledge of the carrier phase. Carrier phase tracking may be carried out in a decision-directed mode according to (11-5-27).

Of particular importance is the case $p = 2$, which leads to the relatively simple algorithm

$$\begin{aligned}\hat{\mathbf{C}}_{k+1} &= \hat{\mathbf{C}}_k + \Delta_p \mathbf{V}_k^* \hat{I}_k (R_2 - |\hat{I}_k|^2) \\ \hat{\phi}_{k+1} &= \hat{\phi}_k + \Delta_\phi \operatorname{Im}(\tilde{I}_k \hat{I}_k^* e^{j\hat{\phi}_k})\end{aligned} \tag{11-5-33}$$

where $\tilde{I}_k$ is the output decision based on $\hat{I}_k$, and

$$R_2 = \frac{E(|I_k|^4)}{E(|I_k|^2)} \tag{11-5-34}$$

Convergence of the algorithm given in (11-5-33) was demonstrated in the paper by Godard (1980). Initially, the equalizer coefficients were set to zero except for the center (reference) tap, which was set according to the condition

$$|c_0|^2 > \frac{E\,|I_k|^4}{2\,|x_0|^2\,[E(|I_k|^2)]^2} \tag{11-5-35}$$

which is sufficient, but not necessary, for convergence of the algorithm. Simulation results performed by Godard on simulated telephone channels with typical frequency response characteristics and transmission rates of 7200–12 000 bits/s indicate that the algorithm in (11-5-31) performs well and leads to convergence in 5000–20 000 iterations, depending on the signal constellation. Initially, the eye pattern was closed prior to equalization. The number of iterations required for convergence is about an order of magnitude greater than the number required to equalize the channels with a known training sequence. No apparent difficulties were encountered in using the decision-directed phase estimation algorithm in (11-5-33) from the beginning of the equalizer adjustment process.

11-5-3 Blind Equalization Algorithms Based on Second- and Higher-Order Signal Statistics

It is well known that second-order statistics (autocorrelation) of the received signal sequence provide information on the magnitude of the channel characteristics, but not on the phase. However, this statement is not correct if the autocorrelation function of the received signal is periodic, as is the case for a digitally modulated signal. In such a case, it is possible to obtain a measurement of the amplitude and the phase of the channel from the received signal. This cyclostationarity property of the received signal forms the basis for a channel estimation algorithm devised by Tong *et al.* (1993).

It is also possible to estimate the channel response from the received signal by using higher-order statistical methods. In particular, the impulse response of a linear, discrete-time-invariant system can be obtained explicitly from cumulants of the received signal, provided that the channel input is nongaussian. We describe the following simple method for estimation of the channel

impulse response from fourth-order cumulants of the received signal sequence. The fourth-order cumulant is defined as

$$\begin{aligned} c(v_k, v_{k+m}, v_{k+n}, v_{k+l}) \equiv c_v(m, n, l) \\ &= E(v_k v_{k+m} v_{k+n} v_{k+l}) \\ &\quad - E(v_k v_{k+m})E(v_{k+n} v_{k+l}) \\ &\quad - E(v_k v_{k+n})E(v_{k+m} v_{k+l}) \\ &\quad - E(v_k v_{k+l})E(v_{k+m} v_{k+n}) \end{aligned} \tag{11-5-36}$$

(The fourth-order cumulant of a gaussian signal process is zero.) Consequently, it follows that

$$c_r(m, n, l) = c(I_k, I_{k+m}, I_{k+n}, I_{k+l}) \sum_{k=0}^{\infty} f_k f_{k+m} f_{k+n} f_{k+l} \tag{11-5-37}$$

For a statistically independent and identically distributed input sequence $\{I_n\}$ to the channel, $c(I_k, I_{k+m}, I_{k+n}, I_{k+l}) = k$, a constant, called the *kurtosis*. Then, if the length of the channel response is $L + 1$, we may let $m = n = l = -L$ so that

$$c_r(-L, -L, -L) = k f_L f_0^3 \tag{11-5-38}$$

Similarly, if we let $m = 0$, $n = L$ and $l = p$, we obtain

$$c_r(0, L, p) = k f_L f_0^2 f_p \tag{11-5-39}$$

If we combine (11-5-38) and (11-5-39), we obtain the impulse response within a scale factor as

$$f_p = f_0 \frac{c_r(0, L, p)}{c_r(-L, -L, -L)}, \qquad p = 1, 2, \ldots, L \tag{11-5-40}$$

The cumulants $c_r(m, n, l)$ are estimated from sample averages of the received signal sequence $\{v_n\}$.

Another approach based on higher-order statistics is due to Hatzinakos and Nikias (1991). They have introduced the first polyspectra-based adaptive blind equalization method named the *tricepstrum equalization algorithm* (TEA). This method estimates the channel response characteristics by using the complex cepstrum of the fourth-order cumulants (tricepstrum) of the received signal sequence $\{v_n\}$. TEA depends only on fourth-order cumulants of $\{v_n\}$ and is capable of separately reconstructing the minimum-phase and maximum-phase characteristics of the channel. The channel equalizer coefficients are then computed from the measured channel characteristics. The basic approach used in TEA is to compute the tricepstrum of the received sequence $\{v_n\}$, which is the inverse (three-dimensional) Fourier transform of the logarithm of the trispectrum of $\{v_n\}$. (The *trispectrum* is the three-dimensional discrete Fourier transform of the fourth-order cumulant sequence $c_r(m, n, l)$). The equalizer coefficients are then computed from the cepstral coefficients.

By separating the channel estimation from the channel equalization, it is possible to use any type of equalizer for the ISI, i.e., either linear, or decision-feedback, or maximum-likelihood sequence detection. The major disadvantage with this class of algorithms is the large amount of data and the inherent computational complexity involved in the estimation of the higher-order moments (cumulants) of the received signal.

In conclusion, we have provided an overview of three classes of blind equalization algorithms that find applications in digital communications. Of the three families of algorithms described, those based on the maximum-likelihood criterion for jointly estimating the channel impulse response and the data sequence are optimal and require relatively few received signal samples for performing channel estimation. However, the computational complexity of the algorithms is large when the ISI spans many symbols. On some channels, such as the mobile radio channel, where the span of the ISI is relatively short, these algorithms are simple to implement. However, on telephone channels, where the ISI spans many symbols but is usually not too severe, the LMS-type (stochastic gradient) algorithms are generally employed.

11-6 BIBLIOGRAPHICAL NOTES AND REFERENCES

Adaptive equalization for digital communications was developed by Lucky (1965, 1966). His algorithm was based on the peak distortion criterion and led to the zero-forcing algorithm. Lucky's work was a major breakthrough, which led to the rapid development of high-speed modems within five years of publication of his work. Concurrently, the LMS algorithm was devised by Widrow (1966), and its use for adaptive equalization for complex-valued (in-phase and quadrature components) signals was described and analyzed in a tutorial paper by Proakis and Miller (1969).

A tutorial treatment of adaptive equalization algorithms that were developed during the period 1965–1975 is given by Proakis (1975). A more recent tutorial treatment of adaptive equalization is given in the paper by Qureshi (1985). The major breakthrough in adaptive equalization techniques, beginning with the work of Lucky in 1965 coupled with the development of trellis-coded modulation, which was proposed by Ungerboeck and Csajka (1976), has led to the development of commercially available high speed modems with a capability of speeds of 9600–28 800 bits/s on telephone channels.

The use of a more rapidly converging algorithm for adaptive equalization was proposed by Godard (1974). Our derivation of the RLS (Kalman) algorithm, described in Section 11-4-1, follows the approach outlined by Picinbono (1978). RLS lattice algorithms for general signal estimation applications were developed by Morf *et al.* (1977, 1979). The applications of these algorithms have been investigated by several researchers, including Makhoul (1978), Satorius and Pack (1981), Satorius and Alexander (1979), and Ling and Proakis (1982, 1984a–c, 1985). The fast RLS Kalman algorithm for adaptive equalization was first described by Falconer and Liung (1978). The above

references are just a few of the important papers that have been published on RLS algorithms for adaptive equalization and other applications.

Sato's (1975) original work on blind equalization was focused on PAM (one-dimensinal) signal constellations. Subsequently it was generalized to two-dimensional and multidimensional signal constellations in the algorithms devised by Godard (1980), Benveniste and Goursat (1984), Sato (1986), Foschini (1985), Picchi and Prati (1987), and Shalvi and Weinstein (1990). Blind equalization methods based on the use of second- and higher-order moments of the received signal were proposed by Hatzinakos and Nikias (1991) and Tong *et al.* (1994). The use of the maximum-likelihood criterion for joint channel estimation and data detection has been investigated and treated in papers by Seshadri (1991), Ghosh and Weber (1991), Zervas *et al.* (1991) and Raheli *et al.* (1995). Finally, the convergence characteristics of stochastic gradient blind equalization algorithms have been investigated by Ding (1990), Ding *et al.* (1989), and Johnson (1991).

PROBLEMS

11-1 An equivalent discrete-time channel with white gaussian noise is shown in Fig. P11-1.

a Suppose we use a linear equalizer to equalize the channel. Determine the tap coefficients c_{-1}, c_0, c_1 of a three-tap equalizer. To simplify the computation, let the AWGN be zero.

b The tap coefficients of the linear equalizer in (a) are determined recursively via the algorithm

$$\mathbf{C}_{k+1} = \mathbf{C}_k - \Delta \mathbf{g}_k, \qquad \mathbf{C}_k = [c_{-1k} \quad c_{0k} \quad c_{1k}]'$$

where $\mathbf{g}_k = \Gamma \mathbf{C}_k - \mathbf{b}$ is the gradient vector and Δ is the step size. Determine the range of values of Δ to ensure convergence of the recursive algorithm. To simplify the computation, let the AWGN be zero.

c Determine the tap weights of a DFE with two feedforward taps and one feedback gap. To simplify the computation, let the AWGN be zero.

11-2 Refer to Problem 10-18 and answer the following questions.

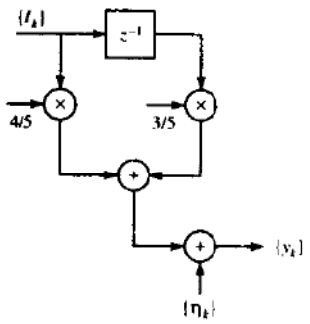

FIGURE P11-1

a Determine the maximum value of Δ that can be used to ensure that the equalizer coefficients converge during operation in the adaptive mode.

b What is the variance of the self-noise generated by the three-tap equalizer when operating in an adaptive mode, as a function of Δ? Suppose it is desired to limit the variance of the self-noise to 10% of the minimum MSE for the three-tap equalizer when $N_0 = 0.1$. What value of Δ would you select?

c If the optimum coefficients of the equalizer are computed recursively by the method of steepest descent, the recursive equation can be expressed in the form

$$\mathbf{C}_{(n+1)} = (1 - \Delta\Gamma)\mathbf{C}_{(n)} + \Delta\xi$$

where $\mathbf{I}$ is the identity matrix. The above represents a set of three coupled first-order difference equations. They can be decoupled by a linear transformation that diagonalizes the matrix Γ. That is, $\Gamma = \mathbf{U}\Lambda\mathbf{U}'$ where Λ is the diagonal matrix having the eigenvalues of Γ as its diagonal elements and $\mathbf{U}$ is the (normalized) modal matrix that can be obtained from your answer to 10-18(b). Let $\mathbf{C}' = \mathbf{U}'\mathbf{C}$ and determine the steady-state solution for $\mathbf{C}'$. From this, evaluate $\mathbf{C} = (U')^{-1}\mathbf{C}' = \mathbf{U}\mathbf{C}'$ and, thus, show that your answer agrees with the result obtained in 10-18(a).

11-3 When a periodic pseudo-random sequence of length N is used to adjust the coefficients of an N-tap linear equalizer, the computations can be performed efficiently in the frequency domain by use of the discrete Fourier transform (DFT). Suppose that $\{y_n\}$ is a sequence of N received samples (taken at the symbol rate) at the equalizer input. Then the computation of the equalizer coefficients is performed as follows.

a Compute the DFT of one period of the equalizer input sequence $\{y_n\}$, i.e.,

$$Y_k = \sum_{n=0}^{N-1} y_n e^{-j2\pi nk/N}$$

b Compute the desired equalizer spectrum

$$C_k = \frac{X_k Y_k^*}{|Y_k|^2}, \quad k = 0, 1, \ldots, N-1$$

where $\{X_i\}$ is the precomputed DFT of the training sequence.

c Compute the inverse DFT of $\{C_k\}$ to obtain the equalizer coefficients $\{c_n\}$. Show that this procedure in the absence of noise yields an equalizer whose frequency response is equal to the frequency response of the inverse folded channel spectrum at the N uniformly spaced frequencies $f_k = k/NT$, $k = 0, 1, \ldots, N-1$.

11-4 Show that the gradient vector in the minimization of the MSE may be expressed as

$$\mathbf{G}_k = -E(\varepsilon_k \mathbf{V}_k^*)$$

where the error $\varepsilon_k = I_k - \hat{I}_k$, and the estimate of $\mathbf{G}_k$, i.e.,

$$\hat{\mathbf{G}}_k = -\varepsilon_k \mathbf{V}_k^*$$

satisfies the condition that $E(\hat{\mathbf{G}}_k) = \mathbf{G}_k$.

11-5 The *tap-leakage LMS algorithm* proposed in the paper by Gitlin *et al.* (1982) may be expressed as

$$\mathbf{C}_N(n+1) = w\mathbf{C}_N(n) + \Delta\varepsilon(n)\mathbf{V}_N^*(n)$$

where $0 < w < 1$, Δ is the step size, and $\mathbf{V}_N(n)$ is the data vector at time n. Determine the condition for the convergence of the mean value of $\mathbf{C}_N(n)$.

11-6 Consider the random process

$$x(n) = gv(n) + w(n), \quad n = 0, 1, \ldots, M-1$$

where $v(n)$ is a known sequence, g is a random variable with $E(g) = 0$, and $E(g^2) = G$. The process $w(n)$ is a white noise sequence with

$$\gamma_{ww}(m) = \sigma_w^2 \delta_m$$

Determine the coefficients of the linear estimator for g, that is,

$$\hat{g} = \sum_{n=0}^{M-1} h(n)x(n)$$

that minimize the mean square error

11-7 A digital transversal filter can be realized in the frequency-sampling form with system function (see Problem 10-25)

$$H(z) = \frac{1 - z^{-M}}{M} \sum_{k=0}^{M-1} \frac{H_k}{1 - e^{j2\pi k/M} z^{-1}}$$
$$= H_1(z)H_2(z)$$

where $H_1(z)$ is the comb filter, $H_2(z)$ is the parallel bank of resonators, and $\{H_k\}$ are the values of the discrete Fourier transform (DFT).

a Suppose that this structure is implemented as an adaptive filter using the LMS algorithm to adjust the filter (DFT) parameters $\{H_k\}$. Give the time-update equation for these parameters. Sketch the adaptive filter structure.

b Suppose that this structure is used as an adaptive channel equalizer in which the desired signal is

$$d(n) = \sum_{k=0}^{M-1} A_k \cos \omega_k n, \quad \omega_k = \frac{2\pi k}{M}$$

With this form for the desired signal, what advantages are there in the LMS adaptive algorithm for the DFT coefficients $\{H_k\}$ over the direct-form structure with coefficients $\{h(n)\}$? (see Proakis, 1970).

11-8 Consider the performance index

$$J = h^2 + 40h + 28$$

Suppose that we search for the minimum of J by using the steepest-descent algorithm

$$h(n+1) = h(n) - \tfrac{1}{2}\Delta g(n)$$

where $g(n)$ is the gradient.

a Determine the range of values of Δ that provides an overdamped system for the adjustment process.

b Plot the expression for J as a function of n for a value of Δ in this range.

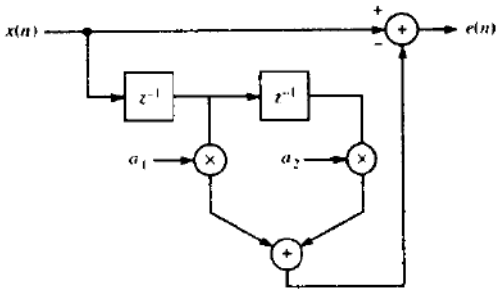

FIGURE P11-9

11-9 Determine the coefficients a_1 and a_2 for the linear predictor shown in Fig. P11-9, given that the autocorrelation $\gamma_{xx}(m)$ of the input signal is

$$\gamma_{xx}(m) = b^{|m|}, \quad 0 < b < 1$$

11-10 Determine the lattice filter and its optimum reflection coefficients corresponding to the linear predictor in Problem 11-9.

11-11 Consider the adaptive FIR filter shown in Fig. P11-11. The system $C(z)$ is characterized by the system function

$$C(z) = \frac{1}{1 - 0.9z^{-1}}$$

Determine the optimum coefficients of the adaptive transversal (FIR) filter $B(z) = b_0 + b_1 z^{-1}$ that minimize the mean square error. The additive noise is white with variance $\sigma_w^2 = 0.1$.

11-12 An $N \times N$ correlation matrix $\mathbf{\Gamma}$ has eigenvalues $\lambda_1 > \lambda_2 > \ldots > \lambda_N > 0$ and associated eigenvectors $\mathbf{v}_1, \mathbf{v}_2, \ldots, \mathbf{v}_N$. Such a matrix can be represented as

$$\mathbf{\Gamma} = \sum_{i=1}^{N} \lambda_i \mathbf{v}_i \mathbf{v}_i^{*t}$$

a If $\mathbf{\Gamma} = \mathbf{\Gamma}^{1/2}\mathbf{\Gamma}^{1/2}$, where $\mathbf{\Gamma}^{1/2}$ is the square root of $\mathbf{\Gamma}$, show that $\mathbf{\Gamma}^{1/2}$ can be represented as

$$\mathbf{\Gamma}^{1/2} = \sum_{i=1}^{N} \lambda_i^{1/2} \mathbf{v}_i \mathbf{v}_i^{*t}$$

b Using this representation, determine a procedure for computing $\mathbf{\Gamma}^{1/2}$.

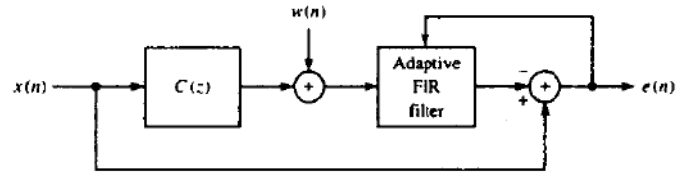

FIGURE P11-11

12

MULTICHANNEL AND MULTICARRIER SYSTEMS

In some applications, it is desirable to transmit the same information-bearing signal over several channels. This mode of transmission is used primarily in situations where there is a high probability that one or more of the channels will be unreliable from time to time. For example, radio channels such as ionospheric scatter and tropospheric scatter suffer from signal fading due to multipath, which renders the channels unreliable for short periods of time. As another example, multichannel signaling is sometimes employed in military communication systems as a means of overcoming the effects of jamming of the transmitted signal. By transmitting the same information over multiple channels, we are providing signal diversity, which the receiver can exploit to recover the information.

Another form of multichannel communications is multiple carrier transmission, where the frequency band of the channel is subdivided into a number of subchannels and information is transmitted on each of the subchannels. A rationale for subdividing the frequency band of a channel into a number of narrowband channels is given below.

In this chapter, we consider both multichannel signal transmission and multicarrier transmission. We begin with a treatment of multichannel transmission.

12-1 MULTICHANNEL DIGITAL COMMUNICATION IN AWGN CHANNELS

In this section, we confine our attention to multichannel signaling over fixed channels that differ only in attenuation and phase shift. The specific model for

the multichannel digital signaling system may be described as follows. The signal waveforms, in general are expressed as

$$s_m^{(n)}(t) = \text{Re}\{s_{lm}^{(n)}(t)e^{j2\pi f_n t}\}, \quad 0 \le t \le T$$
$$n = 1, 2, \ldots, L, \quad m = 1, 2, \ldots, M \quad (12\text{-}1\text{-}1)$$

where L is the number of channels and M is the number of waveforms. The waveforms are assumed to have equal energy and to be equally probable a priori. The waveforms $\{s_m^{(n)}(t)\}$ transmitted over the L channels are scaled by the factors $\{\alpha_n\}$, phase-shifted by $\{\phi_n\}$, and corrupted by additive noise. The equivalent lowpass signals received from the L channels may be expressed as

$$r_l^{(n)}(t) = \alpha_n e^{-j\phi_n} s_{lm}^{(n)}(t) + z_n(t), \quad 0 \le t \le T$$
$$n = 1, 2, \ldots, L, \quad m = 1, 2, \ldots, M \quad (12\text{-}1\text{-}2)$$

where $\{s_{lm}^{(n)}(t)\}$ are the equivalent lowpass transmitted waveforms and $\{z_n(t)\}$ represent the additive noise processes on the L channels. We assume that $\{z_n(t)\}$ are mutually statistically independent and identically distributed gaussian noise random processes.

We consider two types of processing at the receiver, namely, coherent detection and noncoherent detection. The receiver for coherent detection estimates the channel parameters $\{\alpha_n\}$ and $\{\phi_n\}$ and uses the estimates in computing the decision variables. Suppose we define $g_n = \alpha_n e^{-j\phi_n}$ and let $\hat{g}_n$ be the estimate of g_n. The multichannel receiver correlates each of the L received signals with a replica of the corresponding transmitted signals, multiplies each of the correlator outputs by the corresponding estimates $\{\hat{g}_n^*\}$, and sums the resulting signals. Thus, the decision variables for coherent detection are the correlation metrics

$$CM_m = \sum_{n=1}^{L} \text{Re}\left[\hat{g}_n^* \int_0^T r_l^{(n)}(t) s_{lm}^{(n)*}(t)\, dt\right], \quad m = 1, 2, \ldots, M \quad (12\text{-}1\text{-}3)$$

In noncoherent detection, no attempt is made to estimate the channel parameters. The demodulator may base its decision either on the sum of the envelopes (envelope detection) or the sum of the squared envelopes (square-law detection) of the matched filter outputs. In general, the performance obtained with envelope detection differs little from the performance obtained with square-law detection in AWGN. However, square-law detection of multichannel signaling in AWGN channels is considerably easier to analyze than envelope detection. Therefore, we confine our attention to square-law detection of the received signals of the L channels, which produces the decision variables

$$CM_m = \sum_{n=1}^{L} \left| \int_0^T r_l^{(n)}(t) s_{lm}^{(n)*}(t)\, dt \right|^2, \quad m = 1, 2, \ldots, M \quad (12\text{-}1\text{-}4)$$

Let us consider binary signaling first, and assume that $s_{l1}^{(n)}$, $n = 1, 2, \ldots, L$

are the L transmitted waveforms. Then an error is committed if $CM_2 > CM_1$, or, equivalently, if the difference $D = CM_1 - CM_2 < 0$. For noncoherent detection, this difference may be expressed as

$$D = \sum_{n=1}^{L} (|X_n|^2 - |Y_n|^2) \tag{12-1-5}$$

where the variables $\{X_n\}$ and $\{Y_n\}$ are defined as

$$\begin{aligned} X_n &= \int_0^T r_l^{(n)}(t) s_{l1}^{(n)*}(t)\, dt, \qquad n = 1, 2, \ldots, L \\ Y_n &= \int_0^T r_l^{(n)}(t) s_{l2}^{(n)*}(t)\, dt, \qquad n = 1, 2, \ldots, L \end{aligned} \tag{12-1-6}$$

The $\{X_n\}$ are mutually independent and identically distributed gaussian random variables. The same statement applies to the variables $\{Y_n\}$. However, for any n, X_n and Y_n may be correlated. For coherent detection, the difference $D = CM_1 - CM_2$ may be expressed as

$$D = \tfrac{1}{2} \sum_{n=1}^{L} (X_n Y_n^* + X_n^* Y_n) \tag{12-1-7}$$

where, by definition,

$$\begin{aligned} Y_n &= \hat{g}_n, \qquad n = 1, 2, \ldots, L \\ X_n &= \int_0^T r_l^{(n)}(t)[s_{l1}^{(n)*}(t) - s_{l2}^{(n)*}(t)]\, dt \end{aligned} \tag{12-1-8}$$

If the estimates $\{\hat{g}_n\}$ are obtained from observation of the received signal over one or more signaling intervals, as described in Appendix C, their statistical characteristics are described by the gaussian distribution. Then the $\{Y_n\}$ are characterized as mutually independent and identically distributed gaussian random variables. The same statement applies to the variables $\{X_n\}$. As in noncoherent detection, we allow for correlation between X_n and Y_n, but not between X_m and Y_n for $m \neq n$.

12-1-1 Binary Signals

In Appendix B, we derive the probability that the general quadratic form

$$D = \sum_{n=1}^{L} (A\,|X_n|^2 + B\,|Y_n|^2 + CX_n Y_n^* + C^* X_n^* Y_n) \tag{12-1-9}$$

in complex-valued gaussian random variables is less than zero. This probability, which is given in (B-21) of Appendix B, is the probability of error for

binary multichannel signaling in AWGN. A number of special cases are of particular importance.

If the binary signals are antipodal and the estimates of $\{g_n\}$ are perfect, as in coherent PSK, the probability of error takes the simple form

$$P_b = Q(\sqrt{2\gamma_b}) \tag{12-1-10}$$

where

$$\begin{aligned}\gamma_b &= \frac{\mathscr{E}}{N_0}\sum_{n=1}^{L}|g_n|^2 \\ &= \frac{\mathscr{E}}{N_0}\sum_{n=1}^{L}\alpha_n^2\end{aligned} \tag{12-1-11}$$

is the SNR per bit. If the channels are all identical, $\alpha_n = \alpha$ for all n and, hence,

$$\gamma_b = \frac{L\mathscr{E}}{N_0}\alpha^2 \tag{12-1-12}$$

We observe that $L\mathscr{E}$ is the total transmitted signal energy for the L signals. The interpretation of this result is that the receiver combines the energy from the L channels in an optimum manner. That is, there is no loss in performance in dividing the total transmitted signal energy among the L channels. The same performance is obtained as in the case in which a single waveform having energy $L\mathscr{E}$ is transmitted on one channel. This behavior holds true only if the estimates $\hat{g}_n = g_n$, for all n. If the estimates are not perfect, a loss in performance occurs, the amount of which depends on the quality of the estimates, as described in Appendix C.

Perfect estimates for $\{g_n\}$ constitute an extreme case. At the other extreme, we have binary DPSK signaling. In DPSK, the estimates $\{\hat{g}_n\}$ are simply the (normalized) signal-plus-noise samples at the outputs of the matched filters in the previous signaling interval. This is the poorest estimate that one might consider using in estimating $\{g_n\}$. For binary DPSK, the probability of error obtained from (B-21) is

$$P_b = \frac{1}{2^{2L-1}}e^{-\gamma_b}\sum_{n=1}^{L-1}c_n\gamma_b^n \tag{12-1-13}$$

where, by definition,

$$c_n = \frac{1}{n!}\sum_{k=0}^{L-1-n}\binom{2L-1}{k} \tag{12-1-14}$$

and γ_b is the SNR per bit defined in (12-1-11) and, for identical channels in (12-1-12). This result can be compared with the single-channel ($L = 1$) error probability. To simplify the comparison, we assume that the L channels have identical attenuation factors. Thus, for the same value of γ_b, the performance of the multichannel system is poorer than that of the single-channel system. That is, splitting the total transmitted energy among L channels results in a loss in performance, the amount of which depends on L.

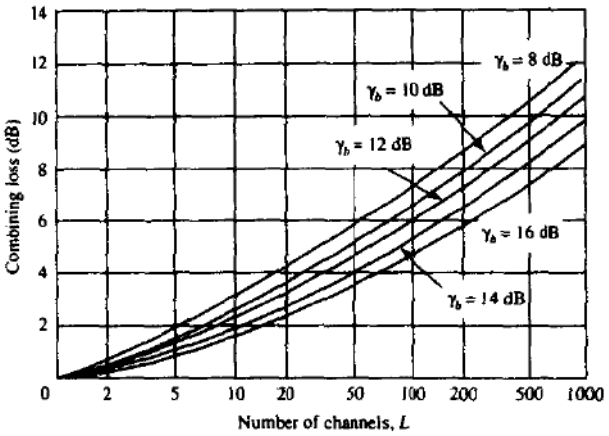

FIGURE 12-1-1 Combining loss in noncoherent detection and combination of binary multichannel signals.

A loss in performance also occurs in square-law detection of orthogonal signals transmitted over L channels. For binary orthogonal signaling, the expression for the probability of error is identical in form to that for binary DPSK given in (12-1-13), except that γ_b is replaced by $\frac{1}{2}\gamma_b$. That is, binary orthogonal signaling with noncoherent detection is 3 dB poorer than binary DPSK. However, the loss in performance due to noncoherent combination of the signals received on the L channels is identical to that for binary DPSK.

Figure 12-1-1 illustrates the loss resulting from noncoherent (square-law) combining of the L signals as a function of L. The probability of error is not shown, but it can be easily obtained from the curve of the expression

$$P_b = \tfrac{1}{2}e^{-\gamma_b} \tag{12-1-15}$$

which is the error probability of binary DPSK shown in Fig. 5-2-12 and then degrading the required SNR per bit, γ_b, by the noncoherent combining loss corresponding to the value of L.

12-1-2 M-ary Orthogonal Signals

Now let us consider M-ary orthogonal signaling with square-law detection and combination of the signals on the L channels. The decision variables are given by (12-1-4). Suppose that the signals $s_1^{(n)}(t)$, $n = 1, 2, \ldots, L$, are transmitted over the L AWGN channels. Then, the decision variables are expressed as

$$\begin{aligned} U_1 &= \sum_{n=1}^{L} |2\mathcal{E}\alpha_n + N_{n1}|^2 \\ U_m &= \sum_{n=1}^{L} |N_{nm}|^2, \qquad m = 2, 3, \ldots, M \end{aligned} \tag{12-1-16}$$

where the $\{N_{mn}\}$ are complex-valued zero-mean gaussian random variables with variance $\sigma^2 = \frac{1}{2}E(|N_{mn}|^2) = 2\mathscr{E}N_0$. Hence U_1 is described statistically as a noncentral chi-square random variable with $2L$ degrees of freedom and noncentrality parameter

$$s^2 = \sum_{n=1}^{L} (2\mathscr{E}\alpha_n)^2 = 4\mathscr{E}^2 \sum_{n=1}^{L} \alpha_n^2 \tag{12-1-17}$$

Using (2-1-118), we obtain the pdf of U_1 as

$$p(u_1) = \frac{1}{4\mathscr{E}N_0}\left(\frac{u_1}{s^2}\right)^{(L-1)/2} \exp\left(-\frac{s^2+u_1}{4\mathscr{E}N_0}\right) I_{L-1}\left(\frac{s\sqrt{u_1}}{2\mathscr{E}N_0}\right), \qquad u_1 \geq 0 \tag{12-1-18}$$

On the other hand, the $\{U_m\}$, $m = 2, 3, \ldots, M$, are statistically independent and identically chi-square-distributed random variables, each having $2L$ degrees of freedom. Using (2-1-110), we obtain the pdf for U_m as

$$p(u_m) = \frac{1}{(4\mathscr{E}N_0)^L (L-1)!} u_m^{L-1} e^{-u_m/4\mathscr{E}N_0}, \qquad u_m \geq 0$$

$$m = 2, 3, \ldots, M \tag{12-1-19}$$

The probability of a symbol error is

$$\begin{aligned} P_M &= 1 - P_c \\ &= 1 - P(U_2 < U_1, U_3 < U_1, \ldots, U_M < U_1) \\ &= 1 - \int_0^\infty [P(U_2 < u_1 \mid U_1 = u_1)]^{M-1} p(u_1)\, du_1 \end{aligned} \tag{12-1-20}$$

But

$$P(U_2 < u_1 \mid U_1 = u_1) = 1 - \exp\left(-\frac{u_1}{4\mathscr{E}N_0}\right) \sum_{k=0}^{L-1} \frac{1}{k!}\left(\frac{u_1}{4\mathscr{E}N_0}\right)^k \tag{12-1-21}$$

Hence,

$$\begin{aligned} P_M &= 1 - \int_0^\infty \left[1 - e^{-u_1/4\mathscr{E}N_0} \sum_{k=0}^{L-1} \frac{1}{k!}\left(\frac{u_1}{4\mathscr{E}N_0}\right)^k\right]^{M-1} p(u_1)\, du_1 \\ &= 1 - \int_0^\infty \left(1 - e^{-v} \sum_{k=0}^{L-1} \frac{v^k}{k!}\right)^{M-1} \left(\frac{v}{\gamma}\right)^{(L-1)/2} e^{-(\gamma+v)} I_{L-1}(2\sqrt{\gamma v})\, dv \end{aligned} \tag{12-1-22}$$

where

$$\gamma = \mathscr{E} \sum_{n=1}^{L} \alpha_n^2 / N_0$$

The integral in (12-1-22) can be evaluated numerically. It is also possible to expand the term $(1-x)^{M-1}$ in (12-1-22) and carry out the integration term by term. This approach yields an expression for P_M in terms of finite sums.

An alternative approach is to use the union bound

$$P_M < (M-1)P_2(L) \tag{12-1-23}$$

where $P_2(L)$ is the probability of error in choosing between U_1 and any one of the $M-1$ decision variables $\{U_m\}$, $m = 2, 3, \ldots, M$. From our previous discussion on the performance of binary orthogonal signaling, we have

$$P_2(L) = \frac{1}{2^{2L-1}} e^{-k\gamma_b/2} \sum_{n=0}^{L-1} c_n (\tfrac{1}{2}k\gamma_b)^n \tag{12-1-24}$$

where c_n is given by (12-1-14). For relatively small values of M, the union bound in (12-1-23) is sufficiently tight for most practical applications.

12-2 MULTICARRIER COMMUNICATIONS

From our treatment of nonideal linear filter channels in Chapters 10 and 11, we have observed that such channels introduce ISI, which degrades performance compared with the ideal channel. The degree of performance degradation depends on the frequency response characteristics. Furthermore, the complexity of the receiver increases as the span of the ISI increases.

Given a particular channel characteristic, the communication system designer must decide how to efficiently utilize the available channel bandwidth in order to transmit the information reliably within the transmitter power constraint and receiver complexity constraints. For a nonideal linear filter channel, one option is to employ a single carrier system in which the information sequence is transmitted serially at some specified rate R symbols/s. In such a channel, the time dispersion is generally much greater than the symbol rate and, hence, ISI results from the nonideal frequency response characteristics of the channel. As we have observed, an equalizer is necessary to compensate for the channel distortion.

An alternative approach to the design of a bandwidth-efficient communication system in the presence of channel distortion is to subdivide the available channel bandwidth into a number of subchannels, such that each subchannel is nearly ideal. To elaborate, suppose that $C(f)$ is the frequency response of a nonideal, band-limited channel with a bandwidth W, and that the power spectral density of the additive gaussian noise is $\Phi_{nn}(f)$. Then, we divide the bandwidth W into $N = W/\Delta f$ subbands of width Δf, where Δf is chosen sufficiently small that $|C(f)|^2/\Phi_{nn}(f)$ is approximately a constant within each subband. Furthermore, we shall select the transmitted signal power to be distributed in frequency as $P(f)$, subject to the constraint that

$$\int_W P(f)\, df \leq P_{\text{av}} \tag{12-2-1}$$

where, P_{av} is the available average power of the transmitter. Let us evaluate the capacity of the nonideal additive gaussian noise channel.

12-2-1 Capacity of a Nonideal Linear Filter Channel

Recall that the capacity of an ideal, band-limited, AWGN channel is

$$C = W \log_2\left(1 + \frac{P_{av}}{WN_0}\right) \tag{12-2-2}$$

where C is the capacity in bits/s, W is the channel bandwidth, and P_{av} is the average transmitted power. In a multicarrier system, with Δf sufficiently small, the subchannel has capacity

$$C_i = \Delta f \log_2\left[1 + \frac{\Delta f P(f_i)\,|C(f)|^2}{\Delta f \Phi_{nn}(f_i)}\right] \tag{12-2-3}$$

Hence, the total capacity of the channel is

$$C = \sum_{i=1}^{N} C_i = \Delta f \sum_{i=1}^{N} \log_2\left[1 + \frac{P(f_i)\,|C(f_i)|^2}{\Phi_{nn}(f_i)}\right] \tag{12-2-4}$$

In the limit as $\Delta f \to 0$, we obtain the capacity of the overall channel in bits/s as

$$C = \int_W \log_2\left[1 + \frac{P(f)\,|C(f)|^2}{\Phi_{nn}(f)}\right] df \tag{12-2-5}$$

Under the constraint on $P(f)$ given by (12-2-1), the choice of $P(f)$ that maximizes C may be determined by maximizing the integral

$$\int_W \left\{\log_2\left[1 + \frac{P(f)\,|C(f)|^2}{\Phi_{nn}(f)}\right] + \lambda P(f)\right\} df \tag{12-2-6}$$

where λ is a Lagrange multiplier, which is chosen to satisfy the constraint. By using the calculus of variations to perform the maximization, we find that the optimum distribution of transmitted signal power is the solution to the equation

$$\frac{1}{|C(f)|^2 P(f) + \Phi_{nn}(f)} + \lambda = 0 \tag{12-2-7}$$

Therefore, $P(f) + \Phi_{nn}(f)/|C(f)|^2$ must be a constant, whose value is adjusted to satisfy the average power constraint in (12-2-1). That is,

$$P(f) = \begin{cases} K - \Phi_{nn}(f)/|C(f)|^2 & (f \in W) \\ 0 & (f \notin W) \end{cases} \tag{12-2-8}$$

This expression for the channel capacity of a nonideal linear filter channel with additive gaussian noise is due to Shannon (1949). The basic interpretation of this result is that the signal power should be high when the channel SNR $|C(f)|^2/\Phi_{nn}(f)$ is high, and low when the channel SNR is low. This result on

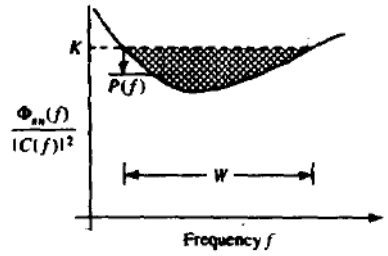

FIGURE 12-2-1 The optimum water-pouring spectrum.

the transmitted power distribution is illustrated in Fig. 12-2-1. Observe that if $\Phi_{nn}(f)/|C(f)|^2$ is interpreted as the bottom of a bowl of unit depth, and we pour an amount of water equal to P_{av} into the bowl, the water will distribute itself in the bowl so as to achieve capacity. This is called the *water-filling interpretation* of the optimum power distribution as a function of frequency.

It is interesting to note that the channel capacity is the smallest when the channel SNR $|C(f)|^2/\Phi_{nn}(f)$ is a constant for all $f \in W$. In this case, $P(f)$ is a constant for all $f \in W$. Equivalently, if the channel frequency response is ideal, i.e., $C(f) = 1$ for $f \in W$, then the worst gaussian noise power distribution, from the viewpoint of maximizing capacity, is white gaussian noise.

The above development suggests that multicarrier modulation that divides the available channel bandwidth into subbands of relatively narrow width $\Delta f = W/N$ provides a solution that could yield transmission rates close to capacity. The signal in each subband may be independently coded and modulated at a synchronous symbol rate of $1/\Delta f$, with the optimum power allocation $P(f)$. If Δf is small enough then $C(f)$ is essentially constant across each subband, so that no equalization is necessary because the ISI is negligible.

Multicarrier modulation has been used in modems for both radio and telephone channels. Multicarrier modulation has also been proposed for future digital audio broadcast applications.

A particularly suitable application of multicarrier modulation is in digital transmission over copper wire subscriber loops. The typical channel attenuation characteristics for such subscriber lines are illustrated in Fig. 12-2-2. We

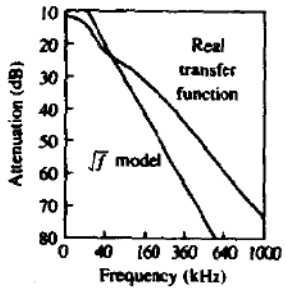

FIGURE 12-2-2 Attenuation characteristic of a 24 gauge 12 kft PIC loop. [*From Werner (1991) © IEEE.*]

observe that the attenuation increases rapidly as a function of frequency. This characteristic makes it extremely difficult to achieve a high transmission rate with a single modulated carrier and an equalizer at the receiver. The ISI penalty in performance is very large. On the other hand, multicarrier modulation with optimum power distribution provides the potential for a higher transmission rate.

The dominant noise in transmission over subscriber lines is crosstalk interference from signals carried on other telephone lines located in the same cable. The power distribution of this type of noise is also frequency-dependent, which can be taken into consideration in the allocation of the available transmitted power.

A design procedure for a multicarrier QAM system for a nonideal linear filter channel has been given by Kalet (1989). In this procedure, the overall bit rate is maximized, through the design of an optimal power division among the subcarriers and an optimum selection of the number of bits per symbol (sizes of the QAM signal constellations) for each subcarrier, under an average power constraint and under the constraint that the symbol error probabilities for all subcarriers are equal.

Below, we present an implementation of a multicarrier QAM modulator and demodulator that is based on the discrete Fourier transform (DFT) for the generation of the multiple carriers.

12-2-2 An FFT-Based Multicarrier System

In this section, we describe a multicarrier communication system that employs the fast Fourier transform (FFT) algorithm to synthesize the signal at the transmitter and to demodulate the received signal at the receiver. The FFT is simply the efficient computational tool for implementing the discrete fourier transform (DFT).

Figure 12-2-3 illustrates a block diagram of a multicarrier communication

FIGURE 12-2-3 Multicarrier communication system.

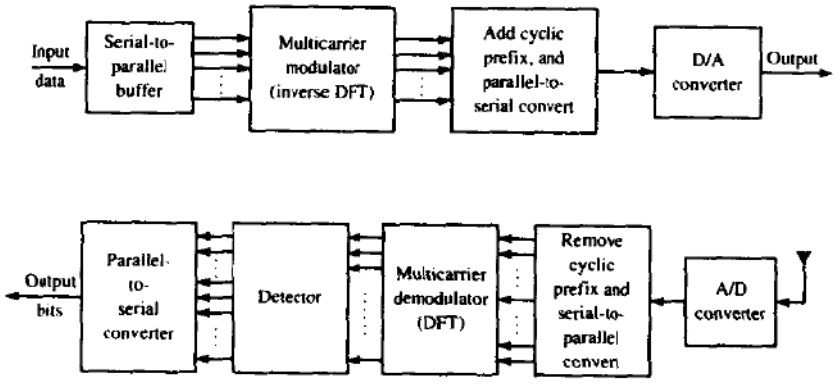

system. A serial-to-parallel buffer segments the information sequence into frames of N_f bits. The N_f bits in each frame are parsed into $\tilde{N}$ groups, where the ith group is assigned $\tilde{n}_i$ bits, and

$$\sum_{i=1}^{\tilde{N}} \tilde{n}_i = N_f \tag{12-2-9}$$

Each group may be encoded separately, so that the number of output bits from the encoder for the ith group is $n_i \geq \tilde{n}_i$.

It is convenient to view the multicarrier modulation as consisting of $\tilde{N}$ independent QAM channels, each operating at the same symbol rate $1/T$, but each channel having a distinct QAM constellation, i.e., the ith channel will employ $M_i = 2^{\tilde{n}_i}$ signal points. We denote the complex-valued signal points corresponding to the information symbols on the subchannels by X_k, $k = 0, 1, \ldots, \tilde{N} - 1$. In order to modulate the $\tilde{N}$ subcarriers by the information symbols $\{X_k\}$, we employ the inverse DFT (IDFT).

However, if we compute the $\tilde{N}$-point IDFT of $\{X_k\}$, we shall obtain a complex-valued time series, which is not equivalent to $\tilde{N}$ QAM-modulated subcarriers. Instead, we create $N = 2\tilde{N}$ information symbols by defining

$$X_{N-k} = X_k^*, \quad k = 1, \ldots, \tilde{N} - 1 \tag{12-2-10}$$

and $X_0' = \text{Re}\,(X_0)$, $X_{\tilde{N}} = \text{Im}\,(X_0)$. Thus, the symbol X_0 is split into two parts, both real. Then, the N-point IDFT yields the real-valued sequence

$$x_n = \frac{1}{\sqrt{N}} \sum_{k=0}^{N-1} X_k e^{j2\pi nk/N}, \quad n = 0, 1, \ldots, N - 1 \tag{12-2-11}$$

where $1/\sqrt{N}$ is simply a scale factor.

The sequence $\{x_n, 0 \leq n \leq N - 1\}$ corresponds to the samples of the sum $x(t)$ of $\tilde{N}$ subcarrier signals, which is expressed as

$$x(t) = \frac{1}{\sqrt{N}} \sum_{k=0}^{N-1} X_k e^{j2\pi kt/T}, \quad 0 \leq t \leq T \tag{12-2-12}$$

where T is the symbol duration. We observe that the subcarrier frequencies are $f_k = k/T$, $k = 0, 1, \ldots, \tilde{N}$. Furthermore, the discrete-time sequence $\{x_n\}$ in (12-2-10) represents the samples of $x(t)$ taken at times $t = nT/N$ where $n = 0, 1, \ldots, N - 1$.

The computation of the IDFT of the data $\{X_k\}$ as given in (12-2-10) may be viewed as multiplication of each data point X_k by a corresponding vector

$$\mathbf{v}_k = [v_{k0} \quad v_{k1} \quad \cdots \quad v_{k(N-1)}] \tag{12-2-13}$$

where

$$v_{kn} = \frac{1}{\sqrt{N}} e^{j(2\pi/N)kn} \tag{12-2-14}$$

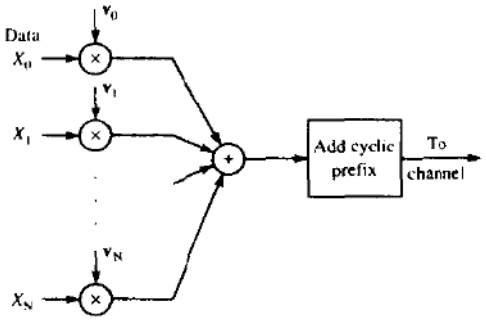

FIGURE 12-2-4 Signal synthesis for multicarrier modulation based on inverse DFT.

as illustrated in Fig. 12-2-4. In any case, the computation of the DFT is performed efficiently by the use of the FFT algorithm.

In practice, the signal samples $\{x_n\}$ are passed through a D/A converter whose output, ideally, would be the signal waveform $x(t)$. The output of the channel is the waveform

$$r(t) = x(t) \bigstar h(t) + n(t) \tag{12-2-15}$$

where $h(t)$ is the impulse response of the channel and $\bigstar$ denotes convolution. By selecting the bandwidth Δf of each subchannel to be very small, the symbol duration $T = 1/\Delta f$ is large compared with the channel time dispersion. To be specific, let us assume that the channel dispersion spans $\nu + 1$ signal samples where $\nu \ll N$. One way to avoid the effect of ISI is to insert a time guard band of duration $\nu T/N$ between transmissions of successive blocks.

An alternative method that avoids ISI is to append a cyclic prefix to each block of N signal samples $\{x_0, x_1, \ldots, x_{N-1}\}$. The cyclic prefix for this block of samples consists of the samples $x_{N-\nu}, x_{N-\nu+1}, \ldots, x_{N-1}$. These new samples are appended to the beginning of each block. Note that the addition of the cyclic prefix to the block of data increases the length of the block to $N + \nu$ samples, which may be indexed from $n = -\nu, \ldots, N-1$, where the first ν samples constitute the prefix. Then, if $\{h_n, 0 \leq n \leq \nu\}$ denotes the sampled channel impulse response, its convolution with $\{x_n, -\nu \leq n \leq N-1\}$ produces $\{r_n\}$, the received sequence. We are interested in the samples of $\{r_n\}$ for $0 \leq n \leq N-1$, from which we recover the transmitted sequence by using the N-point DFT for demodulation. Thus, the first ν samples of $\{r_n\}$ are discarded.

From a frequency-domain viewpoint, when the channel impulse response is $\{h_n, 0 \leq n \leq \nu\}$, its frequency response at the subcarrier frequencies $f_k = k/N$ is

$$H_k \equiv H\left(\frac{2\pi k}{N}\right) = \sum_{n=0}^{\nu} h_n e^{-j2\pi nk/N} \tag{12-2-16}$$

Due to the cyclic prefix, successive blocks (frames) of the transmitted

information sequence do not interfere and, hence, the demodulated sequence may be expressed as

$$\hat{X}_k = H_k X_k + \eta_k, \quad k = 0, 1, \ldots, N-1 \tag{12-2-17}$$

where $\{\hat{X}_k\}$ is the output of the N-point DFT demodulator, and η_k is the additive noise corrupting the signal. We note that by selecting $N \gg \nu$, the rate loss due to the cyclic prefix can be rendered negligible.

As shown in Fig. 12-2-3, the information is demodulated by computing the DFT of the received signal after it has been passed through an A/D converter. The DFT computation may be viewed as a multiplication of the received signal samples $\{r_n\}$ from the A/D converter by $\mathbf{v}_n^*$, where $\mathbf{v}_n$ is defined in (12-2-12). As in the case of the modulator, the DFT computation at the demodulator is performed efficiently by use of the FFT algorithm.

It is a simple matter to estimate and compensate for the channel factors $\{H_k\}$ prior to passing the data to the detector and decoder. A training signal consisting of either a known modulated sequence on each of the subcarriers or unmodulated subcarriers may be used to measure the $\{H_k\}$ at the receiver. If the channel parameters vary slowly with time, it is also possible to track the time variations by using the decisions at the output of the detector or the decoder, in a decision-directed fashion. Thus, the multicarrier system can be rendered adaptive.

Multicarrier QAM modulation of the type described above has been implemented for a variety of applications, including high-speed transmission over telephone lines, such as digital subscriber lines.

Other types of implementation besides the DFT are possible. For example, a digital filter bank that basically performs the DFT may be substituted for the FFT-based implementation when the number of subcarriers is small, e.g., $N \leq 32$. For a large number of subcarriers, e.g., $N > 32$, the FFT-based systems are computatively more efficient.

One limitation of the DFT-type modulators and demodulators arises from the relatively large sidelobes in frequency that are inherent in DFT-type filter banks. The first sidelobe is only 13 dB down from the peak at the desired subcarrier. Consequently, the DFT-based implementations are vulnerable to interchannel interference (ICI) unless a full cyclic prefix is used. If ICI is a problem, due to channel anomalies, one may resort to other types of digital filter banks that have much lower sidelobes. In particular, the class of multirate digital filter banks that have the perfect reconstruction property associated with wavelet-based filters appear to be an attractive alternative (see Tzannes *et al.*, 1994; Rizos *et al.*, 1994).

12-3 BIBLIOGRAPHICAL NOTES AND REFERENCES

Multichannel signal transmission is commonly used on time-varying channels to overcome the effects of signal fading. This topic is treated in some detail in Chapter 14, where we provide a number of references to published work. Of

particular relevance to the treatment of multichannel digital communications given in this chapter are the two publications by Price (1962a,b).

There is a large amount of literature on multicarrier digital communication systems. Such systems have been implemented and used for over 30 years. One of the earliest systems, described by Doeltz *et al.* (1957) and called Kineplex, was used for digital transmission in the HF band. Other early work on multicarrier system design has been reported in the papers by Chang (1966) and Saltzburg (1967). The use of the DFT for modulation and demodulation of multicarrier systems was proposed by Weinstein and Ebert (1971).

Of particular interest in recent years is the use of multicarrier digital transmission for data, facsimile, and video on a variety of channels, including the narrowband (4 kHz) switched telephone network, the 48 kHz group telephone band, digital subscriber lines, cellular radio, and audio broadcast. The interested reader may refer to the many papers in the literature. We cite as examples the papers by Hirosaki *et al.* (1981, 1986), Chow *et al.* (1991), and the survey paper by Bingham (1990). The paper by Kalet (1989) gives a design procedure for optimizing the rate in a multicarrier QAM system given constraints on transmitter power and channel characteristics. Finally, we cite the book by Vaidyanathan (1993) and the papers by Tzannes *et al.* (1994) and Rizos *et al.* (1994) for a treatment of multirate digital filter banks.

PROBLEMS

12-1 $X_1, X_2, \ldots, X_N$ are a set of N statistically independent and identically distributed real gaussian random variables with moments $E(X_i) = m$ and var $(X_i) = \sigma^2$.

a Define

$$U = \sum_{n=1}^{N} X_n$$

Evaluate the SNR of U, which is defined as

$$(\text{SNR})_U = \frac{[E(U)]^2}{2\sigma_U^2}$$

where σ_U^2 is the variance of U.

b Define

$$V = \sum_{n=1}^{N} X_n^2$$

Evaluate the SNR of V, which is defined as

$$(\text{SNR})_V = \frac{[E(V)]^2}{2\sigma_V^2}$$

where σ_V^2 is the variance of V.

c Plot $(\text{SNR})_U$ and $(\text{SNR})_V$ versus m^2/σ^2 on the same graph and, thus, compare the SNRs graphically.

d What does the result in (c) imply regarding coherent detection and combining versus square-law detection and combining of multichannel signals?

12-2 A binary communication system transmits the same information on two diversity channels. The two received signals are

$$r_1 = \pm\sqrt{\mathscr{E}_b} + n_1$$
$$r_2 = \pm\sqrt{\mathscr{E}_b} + n_2$$

where $E(n_1) = E(n_2) = 0$, $E(n_1^2) = \sigma_1^2$ and $E(n_2^2) = \sigma_2^2$, and n_1 and n_2 are uncorrelated gaussian variables. The detector bases its decision on the linear combination of r_1 and r_2, i.e.,

$$r = r_1 + kr_2$$

a Determine the value of k that minimizes the probability of error.

b Plot the probability of error for $\sigma_1^2 = 1$, $\sigma_2^2 = 3$, and either $k = 1$ or k is the optimum value found in (a). Compare the results.

12-3 Assess the cost of the cyclic prefix (used in multitone modulation to avoid ISI) in terms of

a extra channel bandwidth;

b extra signal energy.

12-4 Let $x(n)$ be a finite-duration signal with length N and let $X(k)$ be its N-point DFT. Suppose we pad $x(n)$ with L zeros and compute the $(N + L)$-point DFT, $X'(k)$. What is the relationship between $X(0)$ and $X'(0)$? If we plot $|X(k)|$ and $|X'(k)|$ on the same graph, explain the relationships between the two graphs.

12-5 Show that the sequence $\{x_n\}$ given by (12-2-11) corresponds to the samples of the signal $x(t)$ given by (12-2-12).

12-6 Show that the IDFT of a sequence $\{X_k, 0 \leq k \leq N-1\}$ can be computed by passing the sequence $\{X_k\}$ through a bank of N linear discrete-time filters with system functions

$$H_n(z) = \frac{1}{1 - e^{j2\pi n/N} z^{-1}}$$

12-7 Plot $P_2(L)$ for $L = 1$ and $L = 2$ as a function of $10 \log \gamma_b$ and determine the loss in SNR due to the combining loss for $\gamma_b = 10$.

13

SPREAD SPECTRUM SIGNALS FOR DIGITAL COMMUNICATIONS

Spread spectrum signals used for the transmission of digital information are distinguished by the characteristic that their bandwidth W is much greater than the information rate R in bits/s. That is, the bandwidth expansion factor $B_e = W/R$ for a spread spectrum signal is much greater than unity. The large redundancy inherent in spread spectrum signals is required to overcome the severe levels of interference that are encountered in the transmission of digital information over some radio and satellite channels. Since coded waveforms are also characterized by a bandwidth expansion factor greater than unity and since coding is an efficient method for introducing redundancy, it follows that coding is an important element in the design of spread spectrum signals.

A second important element employed in the design of spread spectrum signals is pseudo-randomness, which makes the signals appear similar to random noise and difficult to demodulate by receivers other than the intended ones. This element is intimately related with the application or purpose of such signals.

To be specific, spread spectrum signals are used for

- combatting or suppressing the detrimental effects of interference due to jamming, interference arising from other users of the channel, and self-interference due to multipath propagation;
- hiding a signal by transmitting it at low power and, thus, making it difficult for an unintended listener to detect in the presence of background noise;
- achieving message privacy in the presence of other listeners.

In applications other than communications, spread spectrum signals are used

to obtain accurate range (time delay) and range rate (velocity) measurements in radar and navigation. For the sake of brevity, we shall limit our discussion to digital communications applications.

In combatting intentional interference (jamming), it is important to the communicators that the jammer who is trying to disrupt the communication does not have prior knowledge of the signal characteristics except for the overall channel bandwidth and the type of modulation, (PSK, FSK, etc.) being used. If the digital information is just encoded as described in Chapter 8, a sophisticated jammer can easily mimic the signal emitted by the transmitter and, thus, confuse the receiver. To circumvent this possibility, the transmitter introduces an element of unpredictability or randomness (pseudo-randomness) in each of the transmitted coded signal waveforms that is known to the intended receiver but not to the jammer. As a consequence, the jammer must synthesize and transmit an interfering signal without knowledge of the pseudo-random pattern.

Interference from the other users arises in multiple-access communication systems in which a number of users share a common channel bandwidth. At any given time, a subset of these users may transmit information simultaneously over the common channel to corresponding receivers. Assuming that all the users employ the same code for the encoding and decoding of their respective information sequences, the transmitted signals in this common spectrum may be distinguished from one another by superimposing a different pseudo-random pattern, also called a *code*, in each transmitted signal. Thus, a particular receiver can recover the transmitted information intended for it by knowing the pseudo-random pattern, i.e., the key, used by the corresponding transmitter. This type of communication technique, which allows multiple users to simultaneously use a common channel for transmission of information, is called *code division multiple access* (CDMA). CDMA will be considered in Sections 13-2 and 13-3.

Resolvable multipath components resulting from time-dispersive propagation through a channel may be viewed as a form of self-interference. This type of interference may also be suppressed by the introduction of a pseudo-random pattern in the transmitted signal, as will be described below.

A message may be hidden in the background noise by spreading its bandwidth with coding and transmitting the resultant signal at a low average power. Because of its low power level, the transmitted signal is said to be "covert." It has a low probability of being intercepted (detected) by a casual listener and, hence, is also called a *low-probability-of-intercept* (LPI) signal.

Finally, message privacy may be obtained by superimposing a pseudo-random pattern on a transmitted message. The message can be demodulated by the intended receivers, who know the pseudo-random pattern or key used at the transmitter, but not by any other receivers who do not have knowledge of the key.

In the following sections, we shall describe a number of different types of spread spectrum signals, their characteristics, and their application. The

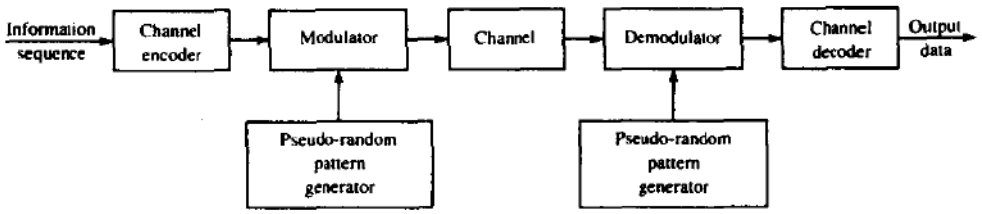

FIGURE 13-1-1 Model of spread spectrum digital communication system.

emphasis will be on the use of spread spectrum signals for combatting, jamming (antijam or AJ signals), for CDMA, and for LPI. Before discussing the signal design problem, however, we shall briefly describe the types of channel characteristics assumed for the applications cited above.

13-1 MODEL OF SPREAD SPECTRUM DIGITAL COMMUNICATION SYSTEM

The block diagram shown in Fig. 13-1-1 illustrates the basic elements of a spread spectrum digital communication system with a binary information sequence at its input at the transmitting end and at its output at the receiving end. The channel encoder and decoder and the modulator and demodulator are basic elements of the system, which were treated in Chapters 5, 7 and 8. In addition to these elements, we have two identical pseudo-random pattern generators, one that interfaces with the modulator at the transmitting end and a second that interfaces with the demodulator at the receiving end. The generators generate a pseudo-random or pseudo-noise (PN) binary-valued sequence, which is impressed on the transmitted signal at the modulator and removed from the received signal at the demodulator.

Synchronization of the PN sequence generated at the receiver with the PN sequence contained in the incoming received signal is required in order to demodulate the received signal. Initially, prior to the transmission of information, synchronization may be achieved by transmitting a fixed pseudo-random bit pattern that the receiver will recognize in the presence of interference with a high probability. After time synchronization of the generators is established, the transmission of information may commence.

Interference is introduced in the transmission of the information-bearing signal through the channel. The characteristics of the interference depend to a large extent on its origin. It may be categorized as being either broadband or narrowband relative to the bandwidth of the information-bearing signal, and either continuous or pulsed (discontinuous) in time. For example, a jamming signal may consist of one or more sinusoids in the bandwidth used to transmit the information. The frequencies of the sinusoids may remain fixed or they may change with time according to some rule. As a second example, the interference generated in CDMA by other users of the channel may be either

broadband or narrowband, depending on the type of spread spectrum signal that is employed to achieve multiple access. If it is broadband, it may be characterized as an equivalent additive white gaussian noise. We shall consider these types of interference and some others in the following sections.

Our treatment of spread spectrum signals will focus on the performance of the digital communication system in the presence of narrowband and broadband interference. Two types of modulation are considered: PSK and FSK. PSK is appropriate in applications where phase coherence between the transmitted signal and the received signal can be maintained over a time interval that is relatively long compared to the reciprocal of the transmitted signal bandwidth. On the other hand, FSK modulation is appropriate in applications where such phase coherence cannot be maintained due to time-variant effects on the communications link. This may be the case in a communications link between two high-speed aircraft or between a high-speed aircraft and a ground terminal.

The PN sequence generated at the modulator is used in conjunction with the PSK modulation to shift the phase of the PSK signal pseudo-randomly as described in Section 13-2. The resulting modulated signal is called a *direct sequence* (DS) or a *pseudo-noise* (PN) spread spectrum signal. When used in conjunction with binary or M-ary ($M > 2$) FSK, the pseudo-random sequence selects the frequency of the transmitted signal pseudo-randomly. The resulting signal is called a *frequency-hopped* (FH) spread spectrum signal. Although a number of other types of spread spectrum signals will be briefly described, the emphasis of our treatment will be on PN and FH spread spectrum signals.

13-2 DIRECT SEQUENCE SPREAD SPECTRUM SIGNALS

In the model shown in Fig. 13-1-1, we assume that the information rate at the input to the encoder is R bits/s and the available channel bandwidth is W Hz. The modulation is assumed to be binary PSK. In order to utilize the entire available channel bandwidth, the phase of the carrier is shifted pseudo-randomly according to the pattern from the PN generator at a rate W times/s. The reciprocal of W, denoted by T_c, defines the duration of a rectangular pulse, which is called a *chip* while T_c is called the *chip interval*. The pulse is the basic element in a DS spread spectrum signal.

If we define $T_b = 1/R$ to be the duration of a rectangular pulse corresponding to the transmission time of an information bit, the bandwidth expansion factor W/R may be expressed as

$$B_e = \frac{W}{R} = \frac{T_b}{T_c} \tag{13-2-1}$$

In practical systems, the ratio T_b/T_c is an integer,

$$L_c = \frac{T_b}{T_c} \tag{13-2-2}$$

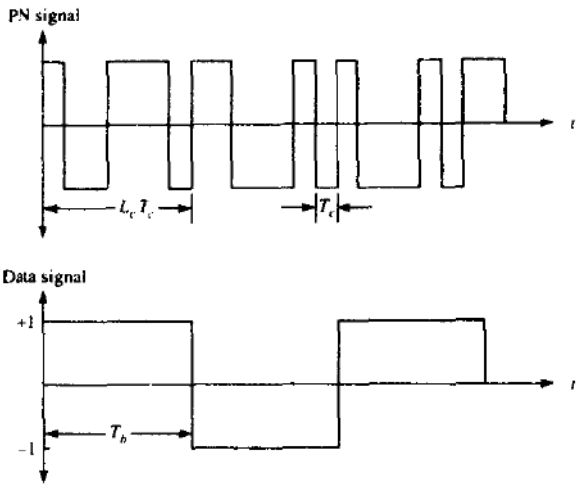

(a) PN and data signals

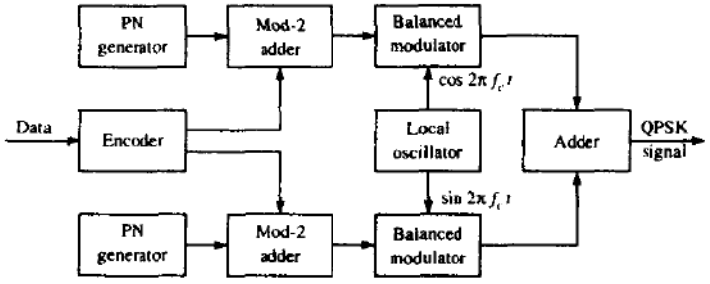

(b) DS-QPSK modulator

FIGURE 13-2-1 The PN and data signals (*a*) and the QPSK modulator (*b*) for a DS spread spectrum system.

which is the number of chips per information bit. That is, L_c is the number of phase shifts that occur in the transmitted signal during the bit duration $T_b = 1/R$. Figure 13-2-1(*a*) illustrates the relationships between the PN signal and the data signal.

Suppose that the encoder takes k information bits at a time and generates a binary linear (n, k) block code. The time duration available for transmitting the n code elements is kT_b s. The number of chips that occur in this time interval is kL_c. Hence, we may select the block length of the code as $n = kL_c$. If the encoder generates a binary convolutional code of rate k/n, the number of chips in the time interval kT_b is also $n = kL_c$. Therefore, the following discussion applies to both block codes and convolutional codes.

One method for impressing the PN sequence on the transmitted signal is to

alter directly the coded bits by modulo-2 addition with the PN sequence.† Thus, each coded bit is altered by its addition with a bit from the PN sequence. If b_i represents the ith bit of the PN sequence and c_i is the corresponding bit from the encoder, the modulo-2 sum is

$$a_i = b_i \oplus c_i \tag{13-2-3}$$

Hence, $a_i = 1$ if either $b_i = 1$ and $c_i = 0$ or $b_i = 0$ and $c_i = 1$; also, $a_i = 0$ if either $b_i = 1$ and $c_i = 1$ or $b_i = 0$ and $c_i = 0$. We may say that $a_i = 0$ when $b_i = c_i$ and $a_i = 1$ when $b_i \neq c_i$. The sequence $\{a_i\}$ is mapped into a binary PSK signal of the form $s(t) = \pm \text{Re}\,[g(t)e^{j2\pi f_c t}]$ according to the convention

$$g_i(t) = \begin{cases} g(t - iT_c) & (a_i = 0) \\ -g(t - iT_c) & (a_i = 1) \end{cases} \tag{13-2-4}$$

where $g(t)$ represents a pulse of duration T_c s and arbitrary shape.

The modulo-2 addition of the coded sequence $\{c_i\}$ and the sequence $\{b_i\}$ from the PN generator may also be represented as a multiplication of two waveforms. To demonstrate this point, suppose that the elements of the coded sequence are mapped into a binary PSK signal according to the relation

$$c_i(t) = (2c_i - 1)g(t - iT_c) \tag{13-2-5}$$

Similarly, we define a waveform $p_i(t)$ as

$$p_i(t) = (2b_i - 1)p(t - iT_c) \tag{13-2-6}$$

where $p(t)$ is a rectangular pulse of duration T_c. Then the equivalent lowpass transmitted signal corresponding to the ith coded bit is

$$\begin{aligned} g_i(t) &= p_i(t)c_i(t) \\ &= (2b_i - 1)(2c_i - 1)g(t - iT_c) \end{aligned} \tag{13-2-7}$$

This signal is identical to the one given by (13-2-4), which is obtained from the sequence $\{a_i\}$. Consequently, modulo-2 addition of the coded bits with the PN sequence followed by a mapping that yields a binary PSK signal is equivalent to multiplying a binary PSK signal generated from the coded bits with a sequence of unit amplitude rectangular pulses, each of duration T_c, and with a polarity which is determined from the PN sequence according to (13-2-6). Although it is easier to implement modulo-2 addition followed by PSK modulation instead of waveform multiplication, it is convenient, for purposes of demodulation, to consider the transmitted signal in the multiplicative form

† When four-phase PSK is desired, one PN sequence is added to the information sequence carried on the in-phase signal component and a second PN sequence is added to the information sequence carried on the quadrature component. In many PN-spread spectrum systems, the same binary information sequence is added to the two PN sequences to form the two quadrature components. Thus, a four-phase PSK signal is generated with a binary information stream.

given by (13-2-7). A functional block diagram of a four-phase PSK DS spread spectrum modulator is shown in Fig. 13-2-1(*b*).

The received equivalent lowpass signal for the ith code element is†

$$\begin{aligned} r_i(t) &= p_i(t)c_i(t) + z(t), \qquad iT_c \leq t \leq (i+1)T_c \\ &= (2b_i - 1)(2c_i - 1)g(t - iT_c) + z(t) \end{aligned} \tag{13-2-8}$$

where $z(t)$ represents the interference or jamming signal corrupting the information-bearing signal. The interference is assumed to be a stationary random process with zero mean.

If $z(t)$ is a sample function from a complex-valued gaussian process, the optimum demodulator may be implemented either as a filter matched to the waveform $g(t)$ or as a correlator, as illustrated by the block diagrams in Fig. 13-2-2. In the matched filter realization, the sampled output from the matched filter is multiplied by $2b_i - 1$, which is obtained from the PN generator at the

FIGURE 13-2-2 Possible demodulator structures for PN spread spectrum signals.

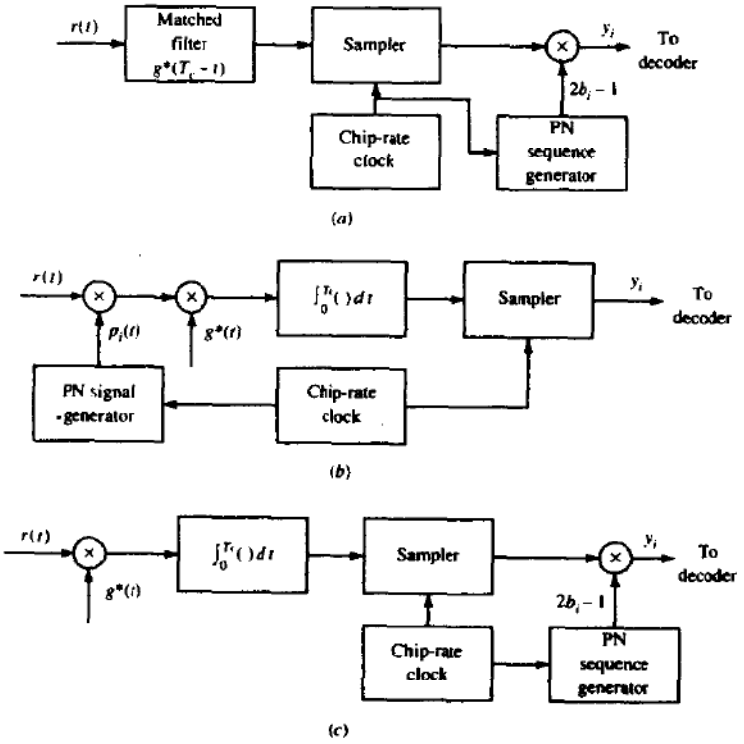

† *For simplicity, we assume that the channel attenuation* $\alpha = 1$ *and the phase shift of the channel is zero. Since coherent PSK detection is assumed, any arbitrary channel phase shift is compensated for in the demodulation.*

demodulator when the PN generator is properly synchronized. Since $(2b_i - 1)^2 = 1$ when $b_i = 0$ and $b_i = 1$, the effect of the PN sequence on the received coded bits is thus removed.

In Fig. 13-2-2, we also observe that the cross-correlation can be accomplished in either one of two ways. The first, illustrated in Fig. 13-2-2(*b*), involves premultiplying $r_i(t)$ with the waveform $p_i(t)$ generated from the output of the PN generator and then cross-correlating with $g^*(t)$ and sampling the output in each chip interval. The second method, illustrated in Fig. 13-2-2(*c*), involves cross-correlation with $g^*(t)$ first, sampling the output of the correlator and, then, multiplying this output with $2b_i - 1$, which is obtained from the PN generator.

If $z(t)$ is not a gaussian random process, the demodulation methods illustrated in Fig. 13-2-2 are no longer optimum. Nevertheless, we may still use any of these three demodulator structures to demodulate the received signal. When the statistical characteristics of the interference $z(t)$ are unknown a priori, this is certainly one possible approach. An alternative method, which is described later, utilizes an adaptive filter prior to the matched filter or correlator to suppress narrowband interference. The rationale for this second method is also described later.

In Section 13-2-1, we derive the error rate performance of the DS spread spectrum system in the presence of wideband and narrowband interference. The derivations are based on the assumption that the demodulator is any of the three equivalent structures shown in Fig. 13-2-2.

13-2-1 Error Rate Performance of the Decoder

Let the unquantized output of the demodulator be denoted by y_j, $1 \leq j \leq n$. First we consider a linear binary (n, k) block code and, without loss of generality, we assume that the all-zero code word is transmitted.

A decoder that employs soft-decision decoding computes the correlation metrics

$$CM_i = \sum_{j=1}^{n} (2c_{ij} - 1)y_j, \qquad i = 1, 2, \ldots, 2^k \tag{13-2-9}$$

where c_{ij} denotes the jth bit in the ith code word. The correlation metric corresponding to the all-zero code word is

$$\begin{aligned} CM_1 &= 2n\mathscr{E}_c + \sum_{j=1}^{n} (2c_{1j} - 1)(2b_j - 1)v_j \\ &= 2n\mathscr{E}_c - \sum_{j=1}^{n} (2b_j - 1)v_j \end{aligned} \tag{13-2-10}$$

where v_j, $1 \leq j \leq n$, is the additive noise term corrupting the jth coded bit and $\mathscr{E}_c$ is the chip energy. It is defined as

$$v_j = \text{Re}\left\{\int_0^{T_c} g^*(t)z[t + (j-1)T_c]\,dt\right\}, \qquad j = 1, 2, \ldots, n \tag{13-2-11}$$

Similarly, the correlation metric corresponding to code word $\mathbf{C}_m$ having weight w_m is

$$CM_m = 2\mathscr{E}_c n\left(1 - \frac{2w_m}{n}\right) + \sum_{j=1}^{n} (2c_{mj} - 1)(2b_j - 1)v_j \qquad (13\text{-}2\text{-}12)$$

Following the procedure used in Section 8-1-4, we shall determine the probability that $CM_m > CM_1$. The difference between CM_1 and CM_m is

$$\begin{aligned} D &= CM_1 - CM_m \\ &= 4\mathscr{E}_c w_m - 2\sum_{j=1}^{n} c_{mj}(2b_j - 1)v_j \end{aligned} \qquad (13\text{-}2\text{-}13)$$

Since the code word $\mathbf{C}_m$ has weight w_m, there are w_m nonzero components in the summation of noise terms contained in (13-2-13). We shall assume that the minimum distance of the code is sufficiently large that we can invoke the central limit theorem for the summation of noise components. This assumption is valid for PN spread spectrum signals that have a bandwidth expansion of 20 or more.† Thus, the summation of noise components is modeled as a gaussian random variable. Since $E(2b_j - 1) = 0$ and $E(v_j) = 0$, the mean of the second term in (13-2-13) is also zero.

The variance is

$$\sigma_m^2 = 4\sum_{j=1}^{n}\sum_{i=1}^{n} c_{mi}c_{mj}E[(2b_j - 1)(2b_i - 1)]E(v_i v_j) \qquad (13\text{-}2\text{-}14)$$

The sequence of binary digits from the PN generator are assumed to be uncorrelated. Hence,

$$E[(2b_j - 1)(2b_i - 1)] = \delta_{ij} \qquad (13\text{-}2\text{-}15)$$

and

$$\sigma_m^2 = 4w_m E(v^2) \qquad (13\text{-}2\text{-}16)$$

where $E(v^2)$ is the second moment of any one element from the set $\{v_j\}$. This moment is easily evaluated to yield

$$\begin{aligned} E(v^2) &= \int_0^{T_c}\int_0^{T_c} g^*(t)g(\tau)\phi_{zz}(t - \tau)\,dt\,d\tau \\ &= \int_{-\infty}^{\infty} |G(f)|^2\,\Phi_{zz}(f)\,df \end{aligned} \qquad (13\text{-}2\text{-}17)$$

† Typically, the bandwidth expansion factor in a spread spectrum signal is of the order of 100 and higher.

where $\phi_{zz}(\tau) = \frac{1}{2}E[z^*(t)z(t+\tau)]$ is the autocorrelation function and $\Phi_{zz}(f)$ is the power spectral density of the interference $z(t)$.

We observe that when the interference is spectrally flat within the bandwidth† occupied by the transmitted signal, i.e.,

$$\Phi_{zz}(f) = J_0 \quad |f| \leq \tfrac{1}{2}W \tag{13-2-18}$$

the second moment in (13-2-17) is $E(v^2) = 2\mathscr{E}_c J_0$, and, hence, the variance of the interference term in (13-2-16) becomes

$$\sigma_m^2 = 8\mathscr{E}_c J_0 w_m \tag{13-2-19}$$

In this case, the probability that $D < 0$ is

$$P_2(m) = Q\left(\sqrt{\frac{2\mathscr{E}_c}{J_0} w_m}\right) \tag{13-2-20}$$

But the energy per coded bit $\mathscr{E}_c$ may be expressed in terms of the energy per information bit $\mathscr{E}_b$ as

$$\mathscr{E}_c = \frac{k}{n}\mathscr{E}_b = R_c \mathscr{E}_b \tag{13-2-21}$$

With this substitution, (13-2-20) becomes

$$\begin{aligned} P_2(m) &= Q\left(\sqrt{\frac{2\mathscr{E}_b}{J_0} R_c w_m}\right) \\ &= Q(\sqrt{2\gamma_b R_c w_m}) \end{aligned} \tag{13-2-22}$$

where $\gamma_b = \mathscr{E}_b/J_0$ is the SNR per information bit. Finally, the code word error probability may be upper-bounded by the union bound as

$$P_m \leq \sum_{m=2}^{M} Q(\sqrt{2\gamma_b R_c w_m}) \tag{13-2-23}$$

where $M = 2^k$. Note that this expression is identical to the probability of a code word error for soft-decision decoding of a linear binary block code in an AWGN channel.

Although we have considered a binary block code in the derivation given above, the procedure is similar for an (n, k) convolutional code. The result of such a derivation is the following upper bound on the equivalent bit error probability:

$$P_b \leq \frac{1}{k} \sum_{d=d_{\text{free}}}^{\infty} \beta_d Q(\sqrt{2\gamma_b R_c d}) \tag{13-2-24}$$

The set of coefficients $\{\beta_d\}$ is obtained from an expansion of the derivative of the transfer function $T(D, N)$, as described in Section 8-2-3.

Next, we consider a narrowband interference centered at the carrier (at d.c.

† If the bandwidth of the bandpass channel is W, that of the equivalent low-pass channel is $\frac{1}{2}W$.

for the equivalent lowpass signal). We may fix the total (average) jamming power to $J_{av} = J_0 W$, where J_0 is the value of the power spectral density of an equivalent wideband interference (jamming signal). The narrowband interference is characterized by the power spectral density

$$\Phi_{zz}(f) = \begin{cases} \dfrac{J_{av}}{W_1} = \dfrac{J_0 W}{W_1} & (|f| \leq \frac{1}{2}W_1) \\ 0 & (|f| > \frac{1}{2}W_1) \end{cases} \tag{13-2-25}$$

where $W \gg W_1$.

Substitution of (13-2-25) for $\Phi_{zz}(f)$ into (13-2-17) yields

$$E(v^2) = \frac{J_{av}}{W_1} \int_{-W_1/2}^{W_1/2} |G(f)|^2 \, df \tag{13-2-26}$$

The value of $E(v^2)$ depends on the spectral characteristics of the pulse $g(t)$. In the following example, we consider two special cases.

Example 13-2-1

Suppose that $g(t)$ is a rectangular pulse as shown in Fig. 13-2-3(a) and $|G(f)|^2$ is the corresponding energy density spectrum shown in Fig. 13-2-3(b). For the narrowband interference given by (13-2-26), the variance of the total interference is

$$\begin{aligned} \sigma_m^2 &= 4w_m E(v^2) \\ &= \frac{8\mathscr{E}_c w_m T_c J_{av}}{W_1} \int_{-W_1/2}^{W_1/2} \left(\frac{\sin \pi f T_c}{\pi f T_c} \right)^2 df \\ &= \frac{8\mathscr{E}_c w_m J_{av}}{W_1} \int_{-\beta/2}^{\beta/2} \left(\frac{\sin \pi x}{\pi x} \right)^2 dx \end{aligned} \tag{13-2-27}$$

FIGURE 13-2-3 Rectangular pulse and its energy density spectrum.

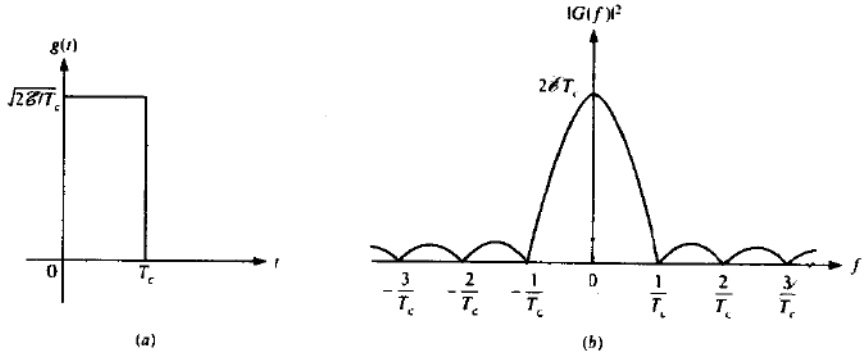

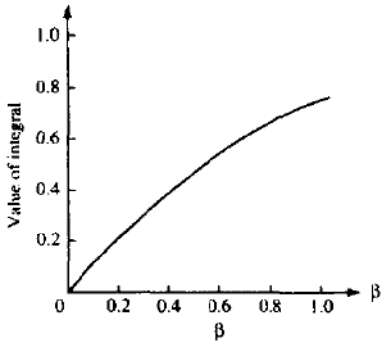

FIGURE 13-2-4 Plot of the value of the integral in (13-2-27).

where $\beta = W_1 T_c$. Figure 13-2-4 illustrates the value of this integral for $0 \leq \beta \leq 1$. We observe that the value of the integral is upper-bounded by $W_1 T_c$. Hence, $\sigma_m^2 \leq 8\mathscr{E}_c w_m T_c J_{av}$.

In the limit as W_1 becomes zero, the interference becomes an impulse at the carrier. In this case the interference is a pure frequency tone and it is usually called a *CW jamming signal.* The power spectral density is

$$\Phi_{zz}(f) = J_{av}\delta(f) \tag{13-2-28}$$

and the corresponding variance for the decision variable $D = CM_1 - CM_m$ is

$$\begin{aligned}\sigma_m^2 &= 4w_m J_{av} |G(0)|^2 \\ &= 8w_m \mathscr{E}_c T_c J_{av}\end{aligned} \tag{13-2-29}$$

The probability of a code word error for CW jamming is upper-bounded as

$$P_M \leq \sum_{m=2}^{M} Q\left(\sqrt{\frac{2\mathscr{E}_c}{J_{av} T_c} w_m}\right) \tag{13-2-30}$$

But $\mathscr{E}_c = R_c \mathscr{E}_b$. Furthermore, $T_c \approx 1/W$ and $J_{av}/W = J_0$. Therefore (13-2-30) may be expressed as

$$P_M \leq \sum_{m=2}^{M} Q\left(\sqrt{\frac{2\mathscr{E}_b}{J_0} R_c w_m}\right) \tag{13-2-31}$$

which is the result obtained previously for broadband interference. This result indicates that a CW jammer has the same effect on performance as an equivalent broadband jammer. This equivalence is discussed further below.

Example 13-2-2

Let us determine the performance of the DS spread spectrum system in the presence of a CW jammer of average power J_{av} when the transmitted signal pulse $g(t)$ is one-half cycle of a sinusoid as illustrated in Fig. 13-2-5, i.e.,

$$g(t) = \sqrt{\frac{4\mathscr{E}_c}{T_c}} \sin \frac{\pi t}{T_c}, \quad 0 \leq t \leq T_c \tag{13-2-32}$$

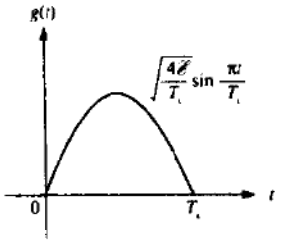

FIGURE 13-2-5 A sinusoidal signal pulse.

The variance of the interference of this pulse is

$$\sigma_m^2 = 4w_m J_{av} |G(0)|^2$$
$$= \frac{64}{\pi^2} \mathscr{E}_c T_c J_{av} w_m \tag{13-2-33}$$

Hence, the upper bound on the code word error probability is

$$P_M \leq \sum_{m=2}^{M} Q\left(\sqrt{\frac{\pi^2 \mathscr{E}_b}{4J_{av}T_c} R_c w_m}\right) \tag{13-2-34}$$

We observe that the performance obtained with this pulse is 0.9 dB better than that obtained with a rectangular pulse. Recall that this pulse shape when used in offset QPSK results in an MSK signal. MSK modulation is frequently used in DS spread spectrum systems.

The Processing Gain and the Jamming Margin An interesting interpretation of the performance characteristics for the DS spread spectrum signal is obtained by expressing the signal energy per bit $\mathscr{E}_b$ in terms of the average power. That is, $\mathscr{E}_b = P_{av}T_b$, where P_{av} is the average signal power and T_b is the bit interval. Let us consider the performance obtained in the presence of CW jamming for the rectangular pulse treated in Example 13-2-1. When we substitute for $\mathscr{E}_b$ and J_0 into (13-2-31), we obtain

$$P_M \leq \sum_{m=2}^{M} Q\left(\sqrt{\frac{2P_{av}}{J_{av}}\frac{T_b}{T_c} R_c w_m}\right) = \sum_{m=2}^{M} Q\left(\sqrt{\frac{2P_{av}}{J_{av}} L_c R_c w_m}\right) \tag{13-2-35}$$

where L_c is the number of chips per information bit and P_{av}/J_{av} is the signal-to-jamming power ratio.

An identical result is obtained with broadband jamming for which the performance is given by (13-2-23). For the signal energy per bit, we have

$$\mathscr{E}_b = P_{av}T_b = \frac{P_{av}}{R} \tag{13-2-36}$$

where R is the information rate in bits/s. The power spectral density for the jamming signal may be expressed as

$$J_0 = \frac{J_{av}}{W} \tag{13-2-37}$$

Using the relation in (13-2-36) and (13-2-37), the ratio $\mathscr{E}_b/J_0$ may be expressed as

$$\frac{\mathscr{E}_b}{J_0} = \frac{P_{av}/R}{J_{av}/W} = \frac{W/R}{J_{av}/P_{av}} \tag{13-2-38}$$

The ratio J_{av}/P_{av} is the jamming-to-signal power ratio, which is usually greater than unity. The ratio $W/R = T_b/T_c = B_c = L_c$ is just the bandwidth expansion factor, or, equivalently, the number of chips per information bit. This ratio is usually called the *processing gain* of the DS spread spectrum system. It represents the advantage gained over the jammer that is obtained by expanding the bandwidth of the transmitted signal. If we interpret $\mathscr{E}_b/J_0$ as the SNR required to achieve a specified error rate performance and W/R as the available bandwidth expansion factor, the ratio J_{av}/P_{av} is called the *jamming margin* of the DS spread spectrum system. In other words, the jamming margin is the largest value that the ratio J_{av}/P_{av} can take and still satisfy the specified error probability.

The performance of a soft-decision decoder for a linear (n, k) binary code, expressed in terms of the processing gain and the jamming margin, is

$$P_m \leq \sum_{m=2}^{M} Q\left(\sqrt{\frac{2W/R}{J_{av}/P_{av}} R_c w_m}\right) \leq (M-1)Q\left(\sqrt{\frac{2W/R}{J_{av}/P_{av}} R_c d_{min}}\right) \tag{13-2-39}$$

In addition to the processing gain W/R and J_{av}/P_{av}, we observe that the performance depends on a third factor, namely, $R_c w_m$. This factor is the *coding gain*. A lower bound on this factor is $R_c d_{min}$. Thus the jamming margin achieved by the DS spread spectrum signal depends on the processing gain and the coding gain.

Uncoded DS Spread Spectrum Signals The performance results given above for DS spread spectrum signals generated by means of an (n, k) code may be specialized to a trivial type of code, namely, a binary repetition code. For this case, $k = 1$ and the weight of the nonzero code word is $w = n$. Thus, $R_c w = 1$ and, hence, the performance of the binary signaling system reduces to

$$\begin{aligned} P_2 &= Q\left(\sqrt{\frac{2\mathscr{E}_b}{J_0}}\right) \\ &= Q\left(\sqrt{\frac{2W/R}{J_{av}/P_{av}}}\right) \end{aligned} \tag{13-2-40}$$

Note that the trivial (repetition) code gives no coding gain. It does result in a processing gain of W/R.

Example 13-2-3

Suppose that we wish to achieve an error rate performance of 10^{-6} or less with an uncoded DS spread spectrum system. The available bandwidth expansion factor is $W/R = 1000$. Let us determine the jamming margin.

The $\mathscr{E}_b/J_0$ required to achieve a bit error probability of 10^{-6} with uncoded binary PSK is 10.5 dB. The processing gain is $10 \log_{10} 1000 = 30$ dB. Hence the maximum jamming-to-signal power that can be tolerated, i.e., the jamming margin, is

$$10 \log_{10} \frac{J_{av}}{P_{av}} = 30 - 10.5 = 19.5 \text{ dB}$$

Since this is the jamming margin achieved with an uncoded DS spread spectrum system, it may be increased by coding the information sequence.

There is another way to view the modulation and demodulation processes for the uncoded (repetition code) DS spread spectrum system. At the modulator, the signal waveform generated by the repetition code with rectangular pulses, for example, is identical to a unit amplitude rectangular pulse $s(t)$ of duration T_b or its negative, depending on whether the information bit is 1 or 0, respectively. This may be seen from (13-2-7), where the coded chips $\{c_i\}$ within a single information bit are either all 1s or 0s. The PN sequence multiplies either $s(t)$ or $-s(t)$. Thus, when the information bit is a 1, the L_c PN chips generated by the PN generator are transmitted with the same polarity. On the other hand, when the information bit is a 0, the L_c PN chips when multiplied by $-s(t)$ are reversed in polarity.

The demodulator for the repetition code, implemented as a correlator, is illustrated in Fig. 13-2-6. We observe that the integration interval in the integrator is the bit interval T_b. Thus, the decoder for the repetition code is eliminated and its function is subsumed in the demodulator.

Now let us qualitatively assess the effect of this demodulation process on

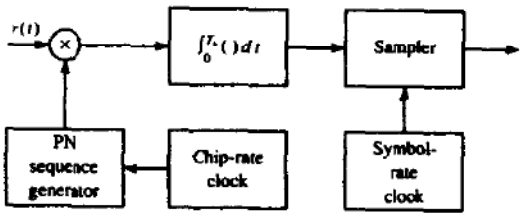

FIGURE 13-2-6 Correlation-type demodulator for a repetition code.

the interference $z(t)$. The multiplication of $z(t)$ by the output of the PN generator, which is expressed as

$$w(t) = \sum_i (2b_i - 1)p(t - iT_c)$$

yields

$$v(t) = w(t)z(t)$$

The waveforms $w(t)$ and $z(t)$ are statistically independent random processes each with zero mean and autocorrelation functions $\phi_{ww}(\tau)$ and $\phi_{zz}(\tau)$, respectively. The product $v(t)$ is also a random process having an autocorrelation function equal to the product of $\phi_{ww}(\tau)$ with $\phi_{zz}(\tau)$. Hence, the power spectral density of the process $v(t)$ is equal to the convolution of the power spectral density of $w(t)$ with the power spectral density of $z(t)$.

The effect of convolving the two spectra is to spread the power in bandwidth. Since the bandwidth of $w(t)$ occupies the available channel bandwith W, the result of convolution of the two spectra is to spread the power spectral density of $z(t)$ over the frequency band of width W. If $z(t)$ is a narrowband process, i.e., its power spectral density has a width much less than W, the power spectral density of the process $v(t)$ will occupy a bandwidth equal to at least W.

The integrator used in the cross-correlation shown in Fig. 13-2-6 has a bandwidth approximately equal to $1/T_b$. Since $1/T_b \ll W$, only a fraction of the total interference power appears at the output of the correlator. This fraction is approximately equal to the ratio of bandwidths $1/T_b$ to W. That is,

$$\frac{1/T_b}{W} = \frac{1}{WT_b} = \frac{T_c}{T_b} = \frac{1}{L_c}$$

In other words, the multiplication of the interference with the signal from the PN generator spreads the interference to the signal bandwidth W, and the narrowband integration following the multiplication sees only the fraction $1/L_c$ of the total interference. Thus, the performance of the uncoded DS spread spectrum system is enhanced by the processing gain L_c.

Linear Code Concatenated with a Binary Repetition Code As illustrated above, a binary repetition code provides a margin against an interference or jamming signal but yields no coding gain. To obtain an improvement in performance, we may use a linear (n_1, k) block or convolutional code, where $n_1 \leq n = kL_c$. One possibility is to select $n_1 < n$ and to repeat each code bit n_2 times such that $n = n_1 n_2$. Thus, we can construct a linear (n_1, k) code by concatenating the (n_1, k) code with a binary $(n_2, 1)$ repetition code. This may be viewed as a trivial form of code concatenation where the outer code is the (n_1, k) code and the inner code is the repetition code.

Since the repetition code yields no coding gain, the coding gain achieved by the combined code must reduce to that achieved by the (n_1, k) outer code. It

is demonstrated that this is indeed the case. The coding gain of the overall combined code is

$$R_c w_m = \frac{k}{n} w_m, \qquad m = 2, 3, \ldots, 2^k$$

But the weights $\{w_m\}$ for the combined code may be expressed as

$$w_m = n_2 w_m^0$$

where $\{w_m^0\}$ are the weights of the outer code. Therefore, the coding gain of the combined code is

$$R_c w_m = \frac{k}{n_1 n_2} n_2 w_m^0 = \frac{k}{n_1} w_m^0 = R_c^0 w_m^0 \tag{13-2-41}$$

which is just the coding gain obtained from the outer code.

A coding gain is also achieved if the (n_1, k) outer code is decoded using hard decisions. The probability of a bit error obtained with the $(n_2, 1)$ repetition code (based on soft-decision decoding) is

$$p = Q\left(\sqrt{\frac{2n_2 \mathscr{E}_c}{J_0}}\right) = Q\sqrt{\frac{2\mathscr{E}_b}{J_0} R_c^0}\Big)$$

$$= Q\left(\sqrt{\frac{2W/R}{J_{\text{av}}/P_{\text{av}}} R_c^0}\right) \tag{13-2-42}$$

Then the code word error probability for a linear (n_1, k) block code is upper-bounded as

$$P_M \leq \sum_{m=t+1}^{n_1} \binom{n_1}{m} p^m (1-p)^{n_1 - m} \tag{13-2-43}$$

where $t = \lfloor \frac{1}{2}(d_{\min} - 1) \rfloor$, or as

$$P_M \leq \sum_{m=2}^{M} [4p(1-p)]^{w_m^0/2} \tag{13-2-44}$$

where the latter is a Chernoff bound. For an (n_1, k) binary convolutional code, the upper bound on the bit error probability is

$$P_b \leq \sum_{d=d_{\text{free}}}^{\infty} \beta_d P_2(d) \tag{13-2-45}$$

where $P_2(d)$ is defined by (8-2-28) for odd d and by (8-2-29) for even d.

Concatenated Coding for DS Spread Spectrum Systems It is apparent from the above discussion that an improvement in performance can be obtained by replacing the repetition code by a more powerful code that will

yield a coding gain in addition to the processing gain. Basically, the objective in a DS spread spectrum system is to construct a long, low-rate code having a large minimum distance. This may be best accomplished by using code concatenation. When binary PSK is used in conjunction with DS spread spectrum, the elements of a concatenated code word must be expressed in binary form.

Best performance is obtained when soft-decision decoding is used on both the inner and outer codes. However, an alternative, which usually results in reduced complexity for the decoder, is to employ soft-decision decoding on the inner code and hard-decision decoding on the outer code. The expressions for the error rate performance of these decoding schemes depend, in part, on the type of codes (block or convolutional) selected for the inner and outer codes. For example, the concatenation of two block codes may be viewed as an overall long binary (n, k) block code having a performance given by (13-2-39). The performance of other code combinations may also be readily derived. For the sake of brevity, we shall not consider such code combinations.

13-2-2 Some Applications of DS Spread Spectrum Signals

In this subsection, we shall briefly consider the use of coded DS spread spectrum signals for three specific applications. One is concerned with providing immunity against a jamming signal. In the second, a communication signal is hidden in the background noise by transmitting the signal at a very low power level. The third application is concerned with accommodating a number of simultaneous signal transmissions on the same channel, i.e., CDMA.

Antijamming Application In Section 13-2-1, we derived the error rate performance for a DS spread spectrum signal in the presence of either a narrow band or a wideband jamming signal. As examples to illustrate the performance of a digital communications system in the presence of a jamming signal, we shall select three codes. One is the Golay (24, 12), which is characterized by the weight distribution given in Table 8-1-1 and has a minimum distance $d_{\min} = 8$. The second code is an expurgated Golay (24, 11) obtained by selecting 2048 code words of constant weight 12. Of course this expurgated code is nonlinear. These two codes will be used in conjunction with a repetition code. The third code to be considered is a maximum-length shift-register code.

The error rate performance of the Golay (24, 12) with soft-decision decoding is

$$P_M \leq \left[759Q\left(\sqrt{\frac{8W/R}{J_{av}/P_{av}}}\right) + 2576Q\left(\sqrt{\frac{12W/R}{J_{av}/P_{av}}}\right) + 759Q\left(\sqrt{\frac{16W/R}{J_{av}/P_{av}}}\right) + Q\left(\sqrt{\frac{24W/R}{J_{av}/P_{av}}}\right)\right] \tag{13-2-46}$$

where W/R is the processing gain and J_{av}/P_{av} is the jamming margin. Since $n = n_1 n_2 = 12W/R$ and $n_1 = 24$, each coded bit is, in effect, repeated $n_2 = W/2R$ times. For example, if $W/R = 100$ (a processing gain of 20 dB), the block length of the repetition code is $n_2 = 50$.

If hard-decision decoding is used, the probability of error for a coded bit is

$$p = Q\left(\sqrt{\frac{W/R}{J_{av}/P_{av}}}\right) \tag{13-2-47}$$

and the corresponding probability of a code word error is upper-bounded as

$$P_M \leq \sum_{m=4}^{24} \binom{24}{m} p^m (1-p)^{24-m} \tag{13-2-48}$$

As an alternative, we may use the Chernoff bound for hard-decision decoding, which is

$$\begin{aligned} P_M \leq\ & 759[4p(1-p)]^4 + 2576[4p(1-p)]^6 \\ & + 759[4p(1-p)]^8 + [4p(1-p)]^{12} \end{aligned} \tag{13-2-49}$$

Figure 13-2-7 illustrates the performance of the Golay (24, 12) as a function of the jamming margin J_{av}/P_{av}, with the processing gain as a parameter. The Chernoff bound was used to compute the error probability for hard-decision decoding. The error probability for soft-decision decoding is dominated by the term

$$759Q\left(\sqrt{\frac{8W/R}{J_{av}/P_{av}}}\right)$$

and that for hard-decision decoding is dominated by the term $759[4p(1-p)]^4$. Hence, the coding gain for soft-decision decoding † is at most $10 \log 4 = 6$ dB. We note that the two curves corresponding to $W/R = 1000$ (30 dB) are identical in shape to the ones for $W/R = 100$ (20 dB), except that the latter are shifted by 10 dB to the right relative to the former. This shift is simply the difference in processing gain between these two DS spread spectrum signals.

The error rate performance of the expurgated Golay (24, 11) is upper-bounded as

$$P_M \leq 2047Q\left(\sqrt{\frac{11W/R}{J_{av}/P_{av}}}\right) \tag{13-2-50}$$

for soft-decision decoding and as‡

$$P_M \leq 2047[4p(1-p)]^6 \tag{13-2-51}$$

† The coding gain is less than 6 dB due to the multiplicative factor of 759, which increases the error probability relative to the performance of the binary uncoded system.

‡ We remind the reader that the union bound is not very tight for large signal sets.

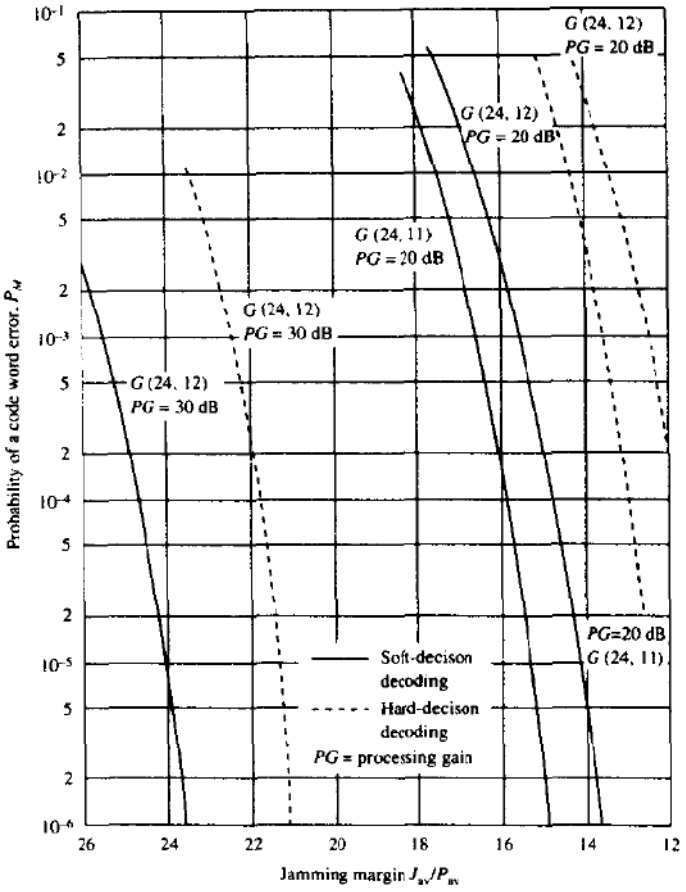

FIGURE 13-2-7 Performance of Golay codes used in DS spread spectrum signal.

for hard-decision decoding, where p is given as

$$p = Q\left(\sqrt{\frac{11W/R}{J_{av}/P_{av}}}\right) \tag{13-2-52}$$

The performance characteristics of this code are also plotted in Fig. 13-2-7 for $W/R = 100$. We observe that this expurgated Golay (24, 11) code performs about 1 dB better than the Golay (24, 12) code.

Instead of using a block code concatenated with a low-rate $(1/n_2)$ repetition code, let us consider using a single low-rate code. A particularly suitable set of low-rate codes is the set of maximum-length shift-register codes described in Section 8-1-3. We recall that for this set of codes,

$$\begin{aligned}(n, k) &= (2^m - 1, m)\\ d_{\min} &= 2^{m-1}\end{aligned} \tag{13-2-53}$$

All code words except the all-zero word have an identical weight of 2^{m-1}. Hence, the error rate for soft-decision decoding is upper-bounded as†

$$\begin{aligned} P_M &\leq (M-1)Q\left(\sqrt{\frac{2W/R}{J_{av}/P_{av}} R_c d_{min}}\right) \\ &\leq 2^m Q\left(\sqrt{\frac{2W/R}{J_{av}/P_{av}} \frac{m2^{m-1}}{2^m-1}}\right) \\ &\leq 2^m \exp\left(-\frac{W/R}{J_{av}/P_{av}} \frac{m2^{m-1}}{2^m-1}\right) \end{aligned} \tag{13-2-54}$$

For moderate values of m, $R_c d_{min} \approx \frac{1}{2}m$ and, hence, (13-2-54) may be expressed as

$$P_M \leq 2^m Q\left(\sqrt{\frac{W/R}{J_{av}/P_{av}} m}\right) \leq 2^m \exp\left(-\frac{mW/R}{2J_{av}P_{av}}\right) \tag{13-2-55}$$

Hence, the coding gain is at most $10 \log \frac{1}{2}m$.

For example, if we select $m = 10$ then $n = 2^{10} - 1 = 1023$. Since $n = kW/R = mW/R$, it follows that $W/R \approx 102$. Thus, we have a processing gain of about 20 dB and a coding gain of 7 dB. This performance is comparable to that obtained with the expurgated Golay (24, 11) code. Higher coding gains can be achieved with larger values of m.

If hard-decision decoding is used for the maximum-length shift-register codes, the error rate is upper-bounded by the Chernoff bound as

$$P_M \leq (M-1)[4p(1-p)]^{d_{min}/2} = (2^m - 1)[4p(1-p)]^{2^{m-2}} \tag{13-2-56}$$

where p is given as

$$p = Q\left(\sqrt{\frac{2W/R}{J_{av}/P_{av}} R_c}\right) = Q\left(\sqrt{\frac{2W/R}{J_{av}/P_{av}} \frac{m}{2^m-1}}\right) \tag{13-2-57}$$

For $m = 10$, the code word error rate P_M is comparable to that obtained with the expurgated Golay (24, 11) code for hard-decision decoding.

The reslts given above illustrate the performance that can be obtained with a single level of coding. Greater coding gains can be achieved with concatenated codes.

† The $M = 2^m$ waveforms generated by a maximum-length shift-register code form a simplex set (see Problem 8-13). The exact expression for the error probability, given in Section 5-2-4, may be used for large values of M, where the union bound becomes very loose.

Low-Detectability Signal Transmission In this application, the signal is purposely transmitted at a very low power level relative to the background channel noise and thermal noise that is generated in the front end of the receiver. If the DS spread spectrum signal occupies a bandwidth W and the spectral density of the additive noise is N_0 W/Hz, the average noise power in the bandwidth W is $N_{av} = WN_0$.

The average received signal power at the intended receiver is P_{av}. If we wish to hide the presence of the signal from receivers that are in the vicinity of the intended receiver, the signal is transmitted at a low power level such that $P_{av}/N_{av} \ll 1$. The intended receiver can recover the information-bearing signal with the aid of the processing gain and the coding gain. However, any other receiver that has no prior knowledge of the PN sequence is unable to take advantage of the processing gain and the coding gain. Hence, the presence of the information-bearing signal is difficult to detect. We say that the signal has a *low probability* of being *intercepted* (LPI) and it is called an *LPI signal.*

The probability of error results given in Section 13-2-1 also apply to the demodulation and decoding of LPI signals at the intended receiver.

Code Division Multiple Access The enhancement in performance obtained from a DS spread spectrum signal through the processing gain and coding gain can be used to enable many DS spread spectrum signals to occupy the same channel bandwidth provided that each signal has its own distinct PN sequence. Thus, it is possible to have several users transmit messages simultaneously over the same channel bandwidth. This type of digital communication in which each user (transmitter-receiver pair) has a distinct PN code for transmitting over a common channel bandwidth is called either *code division multiple access* (CDMA) or *spread spectrum multiple access* (SSMA).

In the demodulation of each PN signal, the signals from the other simultaneous users of the channel appear as an additive interference. The level of interference varies, depending on the number of users at any given time. A major advantage of CDMA is that a large number of users can be accommodated if each transmits messages for a short period of time. In such a multiple access system, it is relatively easy either to add new users or to decrease the number of users without disrupting the system.

Let us determine the number of simultaneous signals that can be supported in a CDMA system.† For simplicity, we assume that all signals have identical average powers. Thus, if there are N_u simultaneous users, the desired signal-to-noise interference power ratio at a given receiver is

$$\frac{P_{av}}{J_{av}} = \frac{P_{av}}{(N_u - 1)P_{av}} = \frac{1}{N_u - 1} \tag{13-2-58}$$

† In this section the interference from other users is treated as a random process. This is the case if there is no cooperation among the users. In Chapter 15 we consider CDMA transmission in which interference from other users is known and is suppressed by the receiver.

Hence, the performance for soft-decision decoding at the given receiver is upper-bounded as

$$P_M \leq \sum_{m=2}^{M} Q\left(\sqrt{\frac{2W/R}{N_u - 1} R_c w_m}\right) \leq (M-1) Q\left(\sqrt{\frac{2W/R}{N_u - 1} R_c d_{\min}}\right) \tag{13-2-59}$$

In this case, we have assumed that the interference from other users is gaussian.

As an example, suppose that the desired level of performance (error probability of 10^{-6}) is achieved when

$$\frac{W/R}{N_u - 1} R_c d_{\min} = 20$$

Then the maximum number of users that can be supported in the CDMA system is

$$N_u = \frac{W/R}{20} R_c d_{\min} + 1 \tag{13-2-60}$$

If $W/R = 100$ and $R_c d_{\min} = 4$, as obtained with the Golay (24, 12) code, the maximum number is $N_u = 21$. If $W/R = 1000$ and $R_c d_{\min} = 4$, this number becomes $N_u = 201$.

In determining the maximum number of simultaneous users of the channel, we have implicitly assumed that the PN code sequences are mutually orthogonal and the interference from other users adds on a power basis only. However, orthogonality among a number of PN code sequences is not easily achieved, especially if the number of PN code sequences required is large. In fact, the selection of a good set of PN sequences for a CDMA system is an important problem that has received considerable attention in the technical literature. We shall briefly discuss this problem in Section 13-2-3.

13-2-3 Effect of Pulsed Interference on DS Spread Spectrum Systems

Thus far, we have considered the effect of continuous interference or jamming on a DS spread spectrum signal. We have observed that the processing gain and coding gain provide a means for overcoming the detrimental effects of this type of interference. However, there is a jamming threat that has a dramatic effect on the performance of a DS spread spectrum system. That jamming signal consists of pulses of spectrally flat noise that covers the entire signal bandwidth W. This is usually called *pulsed interference* or *partial-time jamming*.

Suppose the jammer has an average power J_{av} in the signal bandwidth W. Hence $J_0 = J_{av}/W$. Instead of transmitting continuously, the jammer transmits pulses at a power J_{av}/α for α% of the time, i.e., the probability that the jammer is transmitting at a given instant is α. For simplicity, we assume that

an interference pulse spans an integral number of signaling intervals and, thus, it affects an integral number of bits. When the jammer is not transmitting, the transmitted bits are assumed to be received error-free, and when the jammer is transmitting, the probability of error for an uncoded DS spread spectrum system is $Q(\sqrt{2\alpha\mathscr{E}_b/J_0})$. Hence, the average probability of a bit error is

$$P_2(\alpha) = \alpha Q(\sqrt{2\alpha\mathscr{E}_b/J_0}) = \alpha Q\left(\sqrt{\frac{2\alpha W/R}{J_{av}/P_{av}}}\right) \tag{13-2-61}$$

The jammer selects the duty cycle α to maximize the error probability. On differentiating (13-2-61) with respect to α, we find that the worst-case pulse jamming occurs when

$$\alpha^* = \begin{cases} \dfrac{0.71}{\mathscr{E}_b/J_0} & (\mathscr{E}_b/J_0 \geq 0.71) \\ 1 & (\mathscr{E}_b/J_0 < 0.71) \end{cases} \tag{13-2-62}$$

and the corresponding error probability is

$$P_2 = \begin{cases} \dfrac{0.083}{\mathscr{E}_b/J_0} = \dfrac{0.083 J_{av}/P_{av}}{W/R} & (\mathscr{E}_b/J_0 > 0.71) \\ Q\left(\sqrt{\dfrac{2W/R}{J_{av}/P_{av}}}\right) & (\mathscr{E}_b/J_0 < 0.71) \end{cases} \tag{13-2-63}$$

The error rate performance given by (13-2-61) for $\alpha = 1.0$, 0.1, and 0.01 along with the worst-case performance based on α^* is plotted in Fig. 13-2-8.

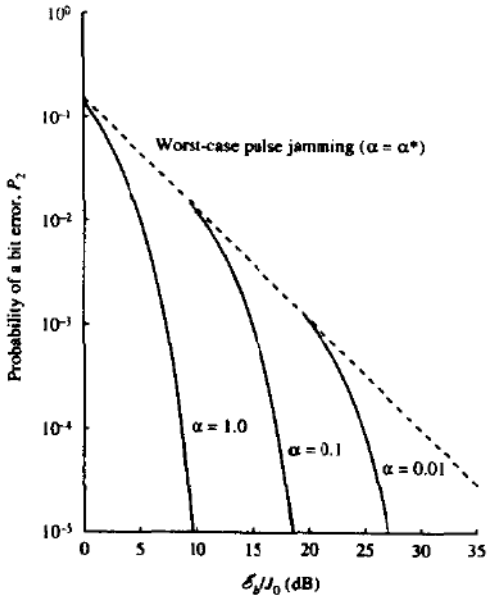

FIGURE 13-2-8 Performance of DS binary PSK with pulse jamming.

By comparing the error rate for continuous gaussian noise jamming with worst-case pulse jamming, we observe a large difference in performance, which is approximately 40 dB at an error rate of 10^{-6}.

We should point out that the above analysis applies when the jammer pulse duration is equal to or greater than the bit duration. In addition, we should indicate that practical considerations may prohibit the jammer from achieving high peak power (small values of α). Nevertheless, the error probability given by (13-2-63) serves as an upper bound on the performance of the uncoded binary PSK in worst-case pulse jamming. Clearly, the performance of the DS spread spectrum system in the presence of such jamming is extremely poor.

If we simply add coding to the DS spread spectrum system, the improvement over the uncoded system is the coding gain. Thus, $\mathscr{E}_b/J_0$ is reduced by the coding gain, which in most cases is limited to less than 10 dB. The reason for the poor performance is that the jamming signal pulse duration may be selected to affect many consecutive coded bits when the jamming signal is turned on. Consequently, the code word error probability is high due to the burst characteristics of the jammer.

In order to improve the performance, we should interleave the coded bits prior to transmission over the channel. The effect of the interleaving, as discussed in Section 8-1-9, is to make the coded bits that are hit by the jammer statistically independent.

The block diagram of the digital communication system that includes interleaving/deinterleaving is shown in Fig. 13-2-9. Also shown is the possibility that the receiver knows the jammer state, i.e., that it knows when the jammer is on or off. Knowledge of the jammer state (called *side information*) is sometimes available from channel measurements of noise power levels in adjacent frequency bands. In our treatment, we consider two

FIGURE 13-2-9 Block diagram of AJ communication system.

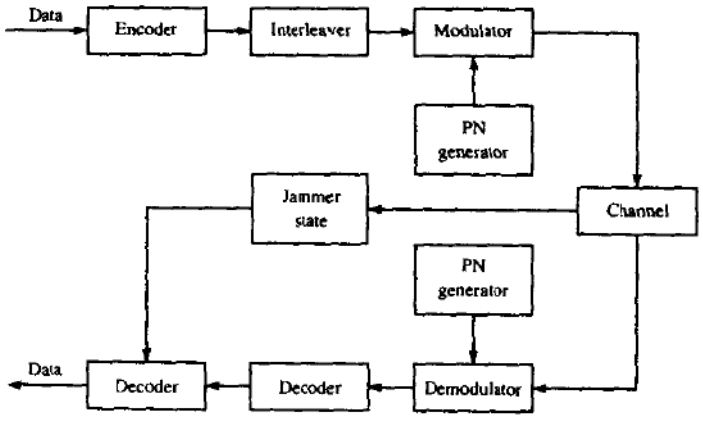

extreme cases, namely, no knowledge of the jammer state or complete knowledge of the jammer state. In any case, the random variable ζ representing the jammer state is characterized by the probabilities

$$P(\zeta = 1) = \alpha, \quad P(\zeta = 0) = 1 - \alpha$$

When the jammer is on, the channel is modeled as an AWGN with power spectral density $N_0 = J_0/\alpha = J_{av}/\alpha W$; and when the jammer is off, there is no noise in the channel. Knowledge of the jammer state implies that the decoder knows when $\zeta = 1$ and when $\zeta = 0$, and uses this information in the computation of the correlation metrics. For example, the decoder may weight the demodulator output for each coded bit by the reciprocal of the noise power level in the interval. Alternatively, the decoder may give zero weight (erasure) to a jammed bit.

First, let us consider the effect of jamming without knowledge of the jammer state. The interleaver/deinterleaver pair is assumed to result in statistically independent jammer hits of the coded bits. As an example of the performance achieved with coding, we cite the performance results from the paper of Martin and McAdam (1980). There the performance of binary convolutional codes is evaluated for worst-case pulse jamming. Both hard and soft-decision Viterbi decoding are considered. Soft decisions are obtained by quantizing the demodulator output to eight levels. For this purpose, a uniform quantizer is used for which the threshold spacing is optimized for the pulse jammer noise level. The quantizer plays the important role of limiting the size of the demodulator output when the pulse jammer is on. The limiting action ensures that any hit on a coded bit does not heavily bias the corresponding path metrics.

The optimum duty cycle for the pulse jammer in the coded system is generally inversely proportional to the SNR, but its value is different from that given by (13-2-62) for the uncoded system. Figure 13-2-10 illustrates graphically the optimal jammer duty cycle for both hard- and soft-decision decoding of the rate 1/2 convolutional codes. The corresponding error rate results for this worst-case pulse jammer are illustrated in Figs 13-2-11 and 13-2-12 for rate 1/2 codes with constraint lengths $3 \leq K \leq 9$. For example, note that at $P_2 = 10^{-6}$, the $K = 7$ convolutional code with soft-decision decoding requires $\mathscr{E}_b/J_0 = 7.6$ dB, whereas hard-decision decoding requires $\mathscr{E}_b/J_0 = 11.7$ dB. This 4.1 dB difference in SNR is relatively large. With continuous gaussian noise, the corresponding SNRs for an error rate of 10^{-6} are 5 dB for soft-decision decoding and 7 dB for hard-decision decoding. Hence, the worst-case pulse jammer has degraded the performance by 2.6 dB for soft-decision decoding and by 4.7 dB for hard-decision decoding. These levels of degradation increase as the constraint length of the convolutional code is decreased. The important point, however, is that the loss in SNR due to jamming has been reduced from 40 dB for the uncoded system to less than 5 dB for the coded system based on a $K = 7$, rate 1/2 convolutional code.

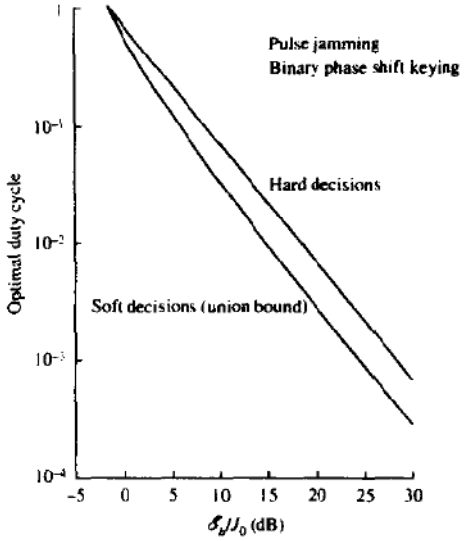

FIGURE 13-2-10 Optimal duty cycle for pulse jammer. [*From Martin and McAdam (1980). © 1980 IEEE.*]

A simpler method for evaluating the performance of a coded AJ communication system is to use the cutoff rate parameter R_0 as proposed by Omura and Levitt (1982). For example, with binary-coded modulation, the cutoff rate may be expressed as

$$R_0 = 1 - \log(1 + D_\alpha) \tag{13-2-64}$$

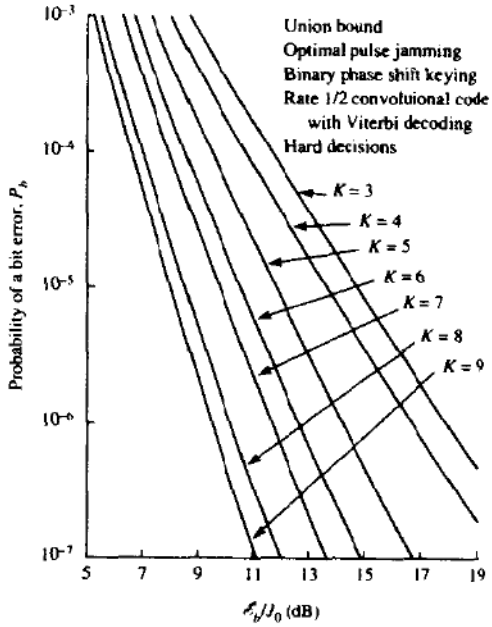

FIGURE 13-2-11 Performance of rate 1/2 convolutional codes with hard-decision Viterbi decoding binary PSK with optimal pulse jamming. [*From Martin and McAdam (1980). © 1980 IEEE.*]

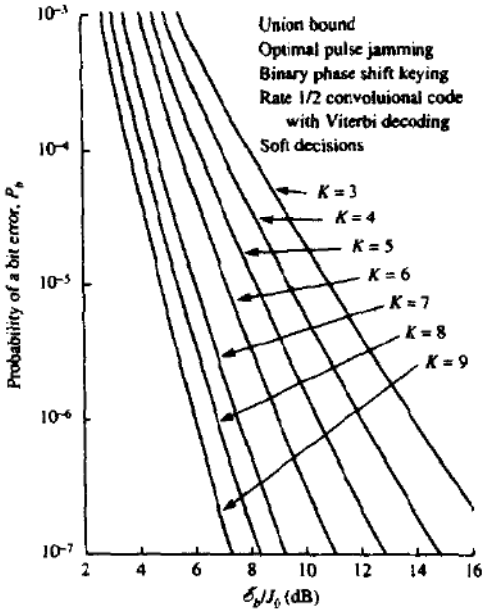

FIGURE 13-2-12 Performance of rate 1/2 convolutional codes with soft-decision Viterbi decoding binary PSK with optimal pulse jamming. [*From Martin and McAdam (1980). © 1980 IEEE.*]

where the factor D_α depends on the channel noise characteristics and the decoder processing. Recall that for binary PSK in an AWGN channel and soft-decision decoding,

$$D_\alpha = e^{-\mathscr{E}_c/N_0} \tag{13-2-65}$$

where $\mathscr{E}_c$ is the energy per coded bit; and for hard-decision decoding,

$$D_\alpha = \sqrt{4p(1-p)} \tag{13-2-66}$$

where p is the probability of a coded bit error. Here, we have $N_0 \equiv J_0$.

For a coded binary PSK, with pulse jamming, Omura and Levitt (1982) have shown that

$$D_\alpha = \alpha e^{-\alpha \mathscr{E}_c/N_0} \quad \text{for soft-decision decoding with knowledge of jammer state} \tag{13-2-67}$$

$$D_\alpha = \min_{\lambda \geq 0} \{[\alpha \exp(\lambda^2 \mathscr{E}_c N_0/\alpha) + 1 - \alpha] \exp(-2\lambda \mathscr{E}_c)\}$$

for soft-decision decoding with no knowledge of jammer state (13-2-68)

$$D_\alpha = \alpha\sqrt{4p(1-p)} \quad \text{for hard-decision decoding with knowledge of the jammer state} \tag{13-2-69}$$

$$D_\alpha = \sqrt{4\alpha p(1-\alpha p)} \quad \text{for hard-decision decoding with no knowledge of the jammer state} \tag{13-2-70}$$

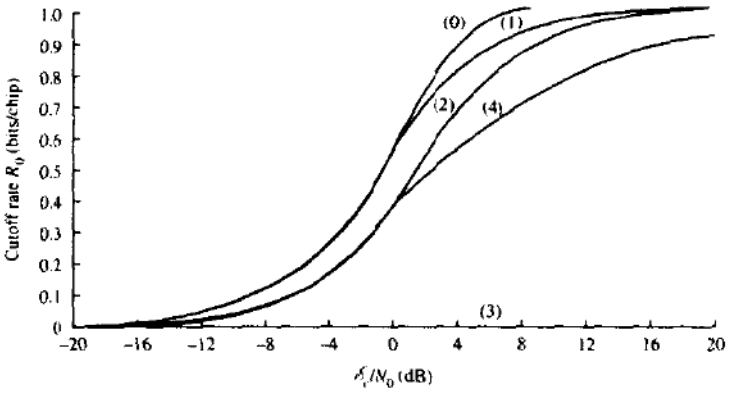

Key
(0) Soft-decision decoding in AWGN ($\alpha \neq 1$)
(1) Soft-decision with jammer state information
(2) Hard-decision with jammer state information
(3) Soft-decision with no jammer state information
(4) Hard-decision with no jammer state information

FIGURE 13-2-13 Cutoff rate for coded DS binary PSK modulation. [*From Omura and Levitt (1982).* © *1982 IEEE.*]

where the probability of error for hard-decision decoding of binary PSK is

$$p = Q\left(\sqrt{\frac{2\alpha\mathscr{E}_c}{N_0}}\right)$$

The graphs for R_0 as a function of $\mathscr{E}_c/N_0$ are illustrated in Fig. 13-2-13 for the cases given above. Note that these graphs represent the cutoff rate for the worst-case value of $\alpha = \alpha^*$ that maximizes D_α (minimizes R_0) for each value of $\mathscr{E}_c/N_0$. Furthermore, note that with soft-decision decoding and no knowledge of the jammer state, $R_0 = 0$. This situation results from the fact that the demodulator output is not quantized.

The graphs in Fig. 13-2-13 may be used to evaluate the performance of coded systems. To demonstrate the procedure, suppose that we wish to determine the SNR required to achieve an error probability of 10^{-6} with coded binary PSK in worst-case pulse jamming. To be specific, we assume that we have a rate 1/2, $K = 7$ convolutional code. We begin with the performance of the rate 1/2, $K = 7$ convolutional code with soft-decision decoding in an AWGN channel. At $P_2 = 10^{-6}$, the SNR required is found from Fig. 8-2-21 to be

$$\mathscr{E}_b/N_0 = 5 \text{ dB}$$

Since the code is rate 1/2, we have

$$\mathscr{E}_c/N_0 = 2 \text{ dB}$$

Now, we go to the graphs in Fig. 13-2-13 and find that for the AWGN channel (reference system) with $\mathscr{E}_c/N_0 = 2$ dB, the corresponding value of the cutoff rate is

$$R_0 = 0.74 \text{ bits/symbol}$$

If we have another channel with different noise characteristics (a worst-case pulse noise channel) but with the same value of the cutoff rate R_0, then the upper bound on the bit error probability is the same, i.e., 10^{-6} in this case. Consequently, we can use this rate to determine the SNR required for the worst-case pulse jammer channel. From the graphs in Fig. 13-2-13, we find that

$$\frac{\mathscr{E}_c}{J_0} = \begin{cases} 10 \text{ dB} & \text{for hard-decision decoding with no knowledge of jammer state} \\ 5 \text{ dB} & \text{for hard-decision decoding with knowledge of jammer state} \\ 3 \text{ dB} & \text{for soft-decision decoding with knowledge of jammer state} \end{cases}$$

Therefore, the corresponding values of $\mathscr{E}_b/J_0$ for the rate 1/2, $K = 7$ convolutional are 13, 8, and 6 dB, respectively.

This general approach may be used to generate error rate graphs for coded binary signals in a worst-case pulse jamming channel by using corresponding error rate graphs for the AWGN channel. The approach we describe above is easily generalized to M-ary coded signals as indicated by Omura and Levitt (1982).

By comparing the cutoff rate for coded DS binary PSK modulation shown in Fig. 13-2-13, we note that for rates below 0.7, there is no penalty in SNR with soft-decision decoding and jammer state information compared with the performance on the AWGN channel ($\alpha = 1$). On the other hand, at $R_0 = 0.7$, there is a 6 dB difference in performance between the SNR in an AWGN channel and that required for hard-decision decoding with no jammer state information. At rates below 0.4, there is no penalty in SNR with hard-decision decoding if the jammer state is unknown. However, there is the expected 2 dB loss in hard-decision decoding compared with soft-decision decoding in the AWGN channel.

13-2-4 Generation of PN Sequences

The generation of PN sequences for spread spectrum applications is a topic that has received considerable attention in the technical literature. We shall briefly discuss the construction of some PN sequences and present a number of important properties of the autocorrelation and cross-correlation functions of such sequences. For a comprehensive treatment of this subject, the interested reader may refer to the book by Golomb (1967).

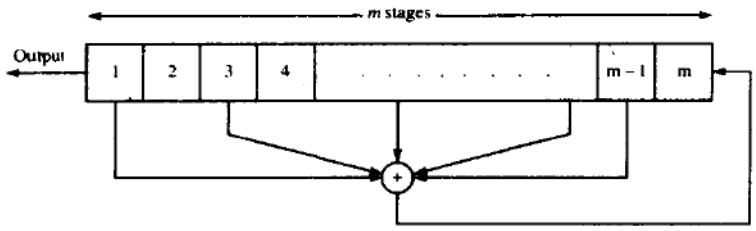

FIGURE 13-2-14 General m-stage shift register with linear feedback.

By far the most widely known binary PN sequences are the maximum-length shift-register sequences introduced in Section 8-1-3 in the context of coding and suggested again in Section 13-2-2 for use as low-rate codes. A maximum-length shift-register sequence, or m-sequence for short, has length $n = 2^m - 1$ bits and is generated by an m-stage shift register with linear feedback as illustrated in Fig. 13-2-14. The sequence is periodic with period n. Each period of the sequence contains 2^{m-1} ones and $2^{m-1} - 1$ zeros.

In DS spread spectrum applications the binary sequence with elements $\{0, 1\}$ is mapped into a corresponding sequence of positive and negative pulses according to the relation

$$p_i(t) = (2b_i - 1)p(t - iT)$$

where $p_i(t)$ is the pulse corresponding to the element b_i in the sequence with elements $\{0, 1\}$. Equivalently, we may say that the binary sequence with elements $\{0, 1\}$ is mapped into a corresponding binary sequence with elements $\{-1, 1\}$. We shall call the equivalent sequence with elements $\{-1, 1\}$ a *bipolar sequence*, since it results in pulses of positive and negative amplitudes.

An important characteristic of a periodic PN sequence is its periodic autocorrelation function, which is usually defined in terms of the bipolar sequence as

$$\phi(j) = \sum_{i=1}^{n} (2b_i - 1)(2b_{i+j} - 1), \qquad 0 \leq j \leq n - 1 \tag{13-2-71}$$

where n is the period. Clearly, $\phi(j + rn) = \phi(j)$ for any integer value r.

Ideally, a pseudo-random sequence should have an autocorrelation function with the property that $\phi(0) = n$ and $\phi(j) = 0$ for $1 \leq j \leq n - 1$. In the case of m sequences, the periodic autocorrelation function is

$$\phi(j) = \begin{cases} n & (j = 0) \\ -1 & (1 \leq j \leq n - 1) \end{cases} \tag{13-2-72}$$

For large values of n, i.e., for long m sequences, the size of the off-peak values of $\phi(j)$ relative to the peak value $\phi(j)/\phi(0) = -1/n$ is small and, from a practical viewpoint, inconsequential. Therefore, m sequences are almost ideal when viewed in terms of their autocorrelation function.

In antijamming applications of PN spread spectrum signals, the period of the sequence must be large in order to prevent the jammer from learning the feedback connections of the PN generator. However, this requirement is impractical in most cases because the jammer can determine the feedback connections by observing only $2m$ chips from the PN sequence. This vulnerability of the PN sequence is due to the linearity property of the generator. To reduce the vulnerability to a jammer, the output sequences from several stages of the shift register or the outputs from several distinct m sequences are combined in a nonlinear way to produce a nonlinear sequence that is considerably more difficult for the jammer to learn. Further reduction in vulnerability is achieved by frequently changing the feedback connections and/or the number of stages in the shift register according to some prearranged plan formulated between the transmitter and the intended receiver.

In some applications, the cross-correlation properties of PN sequences are as important as the autocorrelation properties. For example, in CDMA, each user is assigned a particular PN sequence. Ideally, the PN sequences among users should be mutually orthogonal so that the level of interference experienced by any one user from transmissions of other users adds on a power basis. However, the PN sequences used in practice exhibit some correlation.

To be specific, we consider the class of m sequences. It is known (Sarwate and Pursley, 1980) that the periodic cross-correlation function between any pair of m sequences of the same period can have relatively large peaks. Table 13-2-1 lists the peak magnitude $\phi_{\max}$ for the periodic cross-correlation between pairs of m sequences for $3 \leq m \leq 12$. The table also shows the number of m sequences of length $n = 2^m - 1$ for $3 \leq m \leq 12$. As we can see, the number of m sequences of length n increases rapidly with m. We also observe that, for most sequences, the peak magnitude $\phi_{\max}$ of the cross-correlation function is a large percentage of the peak value of the autocorrelation function.

Such high values for the cross-correlations are undesirable in CDMA.

TABLE 13-2-1 PEAK CROSS-CORRELATION OF m SEQUENCES AND GOLD SEQUENCES

m	$n = 2^m - 1$	Number of m sequences	Peak cross-correlation $\phi_{\max}$	$\phi_{\max}/\phi(0)$	$t(m)$	$t(m)/\phi(0)$
3	7	2	5	0.71	5	0.71
4	15	2	9	0.60	9	0.60
5	31	6	11	0.35	9	0.29
6	63	6	23	0.36	17	0.27
7	127	18	41	0.32	17	0.13
8	255	16	95	0.37	33	0.13
9	511	48	113	0.22	33	0.06
10	1023	60	383	0.37	65	0.06
11	2047	176	287	0.14	65	0.03
12	4095	144	1407	0.34	129	0.03

Although it is possible to select a small subset of m sequences that have relatively smaller cross-correlation peak values, the number of sequences in the set is usually too small for CDMA applications.

PN sequences with better periodic cross-correlation properties than m sequences have been given by Gold (1967, 1968) and Kasami (1966). They are derived from m sequences as described below.

Gold and Kasami proved that certain pairs of m sequences of length n exhibit a three-valued cross-correlation function with values $\{-1, -t(m), t(m)-2\}$, where

$$t(m) = \begin{cases} 2^{(m+1)/2} + 1 & (\text{odd } m) \\ 2^{(m+2)/2} + 1 & (\text{even } m) \end{cases} \tag{13-2-73}$$

For example, if $m = 10$ then $t(10) = 2^6 + 1 = 65$ and the three possible values of the periodic cross-correlation function are $\{-1, -65, 63\}$. Hence the maximum cross-correlation for the pair of m sequences is 65, while the peak for the family of 60 possible sequences generated by a 10-stage shift register with different feedback connections is $\phi_{max} = 383$—about a sixfold difference in peak values. Two m sequences of length n with a periodic cross-correlation function that takes on the possible values $\{-1, -t(m), t(m)-2\}$ are called *preferred sequences.*

From a pair of preferred sequences, say $\mathbf{a} = [a_1 a_2 \ldots a_n]$ and $\mathbf{b} = [b_1 b_2 \ldots b_n]$, we construct a set of sequences of length n by taking the modulo-2 sum of $\mathbf{a}$ with the n cyclicly shifted versions of $\mathbf{b}$ or vice versa. Thus, we obtain n new periodic sequences† with period $n = 2^m - 1$. We may also include the original sequences $\mathbf{a}$ and $\mathbf{b}$ and, thus, we have a total of $n + 2$ sequences. The $n + 2$ sequences constructed in this manner are called *Gold sequences.*

Example 13-2-4

Let us consider the generation of Gold sequences of length $n = 31 = 2^5 - 1$. As indicated above for $m = 5$, the cross-correlation peak is

$$t(5) = 2^3 + 1 = 9$$

Two preferred sequences, which may be obtained from Peterson and Weldon (1972), are described by the polynomials

$$g_1(p) = p^5 + p^2 + 1$$
$$g_2(p) = p^5 + p^4 + p^2 + p + 1$$

† An equivalent method for generating the n new sequences is to employ a shift register of length $2m$ with feedback connections specified by the polynomial $h(p) = g_1(p)g_2(p)$, where $g_1(p)$ and $g_2(p)$ are the polynomials that specify the feedback connections of the m-stage shift registers that generate the m sequences $\mathbf{a}$ and $\mathbf{b}$.

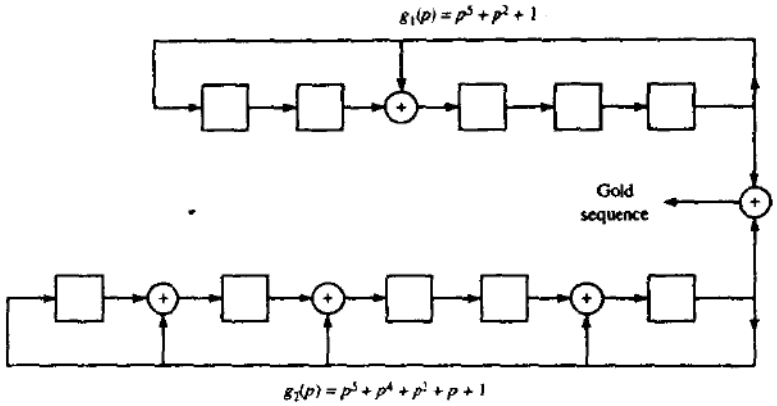

FIGURE 13-2-15 Generation of Gold sequences of length 31.

The shift registers for generating the two m sequences and the corresponding Gold sequences are shown in Fig. 13-2-15. In this case, there are 33 different sequences, corresponding to the 33 relative phases of the two m sequences. Of these, 31 sequences are non-maximal-length sequences.

With the exception of the sequences **a** and **b**, the set of Gold sequences does not comprise maximum-length shift-register sequences of length n. Hence, their autocorrelation functions are not two-valued. Gold (1968) has shown that the cross-correlation function for any pair of sequences from the set of $n + 2$ Gold sequences is three-valued with possible values $\{-1, -t(m), t(m) - 2\}$, where $t(m)$ is given by (13-2-73). Similarly, the off-peak autocorrelation function for a Gold sequence takes on values from the set $\{-1, -t(m), t(m) - 2\}$. Hence, the off-peak values of the autocorrelation function are upper-bounded by $t(m)$.

The values of the off-peak autocorrelation function and the peak cross-correlation function, i.e., $t(m)$, for Gold sequences is listed in Table 13-2-1. Also listed are the values normalized by $\phi(0)$.

It is interesting to compare the peak cross-correlation value of Gold sequences with a known lower bound on the cross-correlation between any pair of binary sequences of period n in a set of M sequences. A lower bound developed by Welch (1974) for ϕ_{max} is

$$\phi_{max} \geq n\sqrt{\frac{M-1}{Mn-1}} \tag{13-2-74}$$

which, for large values of n and M, is well approximated as $\sqrt{n}$. For Gold sequences, $n = 2^m - 1$ and, hence, the lower bound is $\phi_{max} \approx 2^{m/2}$. This bound is lower by $\sqrt{2}$ for odd m and by 2 for even m relative to $\phi_{max} = t(m)$ for Gold sequences.

A procedure similar to that used for generating Gold sequences will generate a smaller set of $M = 2^{m/2}$ binary sequences of period $n = 2^m - 1$, where m is even. In this procedure, we begin with an m sequence **a** and we form a binary sequence **b** by taking every $2^{m/2} + 1$ bit of **a**. Thus, the sequence **b** is formed by decimating **a** by $2^{m/2} + 1$. It can be verified that the resulting **b** is periodic with period $2^{m/2} - 1$. For example, if $m = 10$, the period of **a** is $n = 1023$ and the period of **b** is 31. Hence, if we observe 1023 bits of the sequence **b**, we shall see 33 repetitions of the 31-bit sequence. Now, by taking $n = 2^m - 1$ bits of the sequences **a** and **b**, we form a new set of sequences by adding, modulo-2, the bits from **a** and the bits from **b** and all $2^{m/2} - 2$ cyclic shifts of the bits from **b**. By including **a** in the set, we obtain a set of $2^{m/2}$ binary sequences of length $n = 2^m - 1$. These are called *Kasami sequences*. The autocorrelation and cross-correlation functions of these sequences take on values from the set $\{-1, -(2^{m/2} + 1), 2^{m/2} - 1\}$. Hence, the maximum cross-correlation value for any pair of sequences from the set is

$$\phi_{\max} = 2^{m/2} + 1 \tag{13-2-75}$$

This value of $\phi_{\max}$ satisfies the Welch lower bound for a set of $2^{m/2}$ sequences of length $n = 2^m - 1$. Hence, the Kasami sequences are optimal.

Besides the well-known Gold and Kasami sequences, there are other binary sequences appropriate for CDMA applications. The interested reader may refer to the work of Scholtz (1979), Olsen (1977), and Sarwate and Pursley (1980).

Finally, we wish to indicate that, although we have discussed the periodic cross-correlation function between pairs of periodic sequences, many practical CDMA systems may use information bit durations that encompass only fractions of a periodic sequence. In such cases, it is the partial-period cross-correlation between two sequences that is important. A number of papers deal with this problem, including those by Lindholm (1968), Wainberg and Wolf (1970), Fredricsson (1975), Bekir *et al.* (1978), and Pursley (1979).

13-3 FREQUENCY-HOPPED SPREAD SPECTRUM SIGNALS

In a *frequency-hopped* (FH) spread spectrum communications system the available channel bandwidth is subdivided into a large number of contiguous frequency slots. In any signaling interval, the transmitted signal occupies one or more of the available frequency slots. The selection of the frequency slot(s) in each signaling interval is made pseudo-randomly according to the output from a PN generator. Figure 13-3-1 illustrates a particular frequency-hopped pattern in the time-frequency plane.

A block diagram of the transmitter and receiver for a frequency-hopped spread spectrum system is shown in Fig. 13-3-2. The modulation is usually either binary or M-ary FSK. For example, if binary FSK is employed, the modulator selects one of two frequencies corresponding to the transmission of

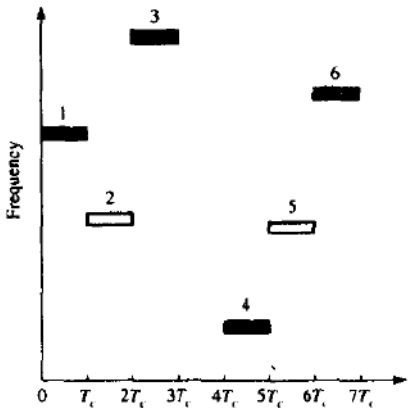

FIGURE 13-3-1 An example of a frequency-hopped (FH) pattern.

either a 1 or a 0. The resulting FSK signal is translated in frequency by an amount that is determined by the output sequence from the PN generator, which, in turn, is used to select a frequency that is synthesized by the frequency synthesizer. This frequency is mixed with the output of the modulator and the resultant frequency-translated signal is transmitted over the channel. For example, m bits from the PN generator may be used to specify $2^m - 1$ possible frequency translations.

At the receiver, we have an identical PN generator, synchronized with the received signal, which is used to control the output of the frequency synthesizer. Thus, the pseudo-random frequency translation introduced at the transmitter is removed at the receiver by mixing the synthesizer output with the received signal. The resultant signal is demodulated by means of an FSK demodulator. A signal for maintaining synchronism of the PN generator with the frequency-translated received signal is usually extracted from the received signal.

Although PSK modulation gives better performance than FSK in an

FIGURE 13-3-2 Block diagram of a FH spread spectrum system.

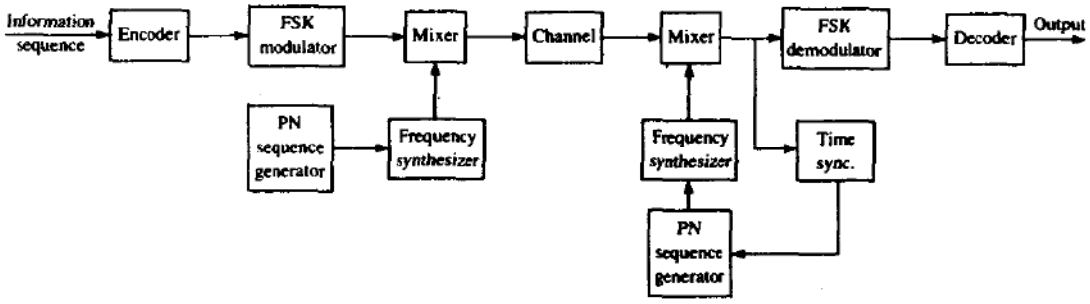

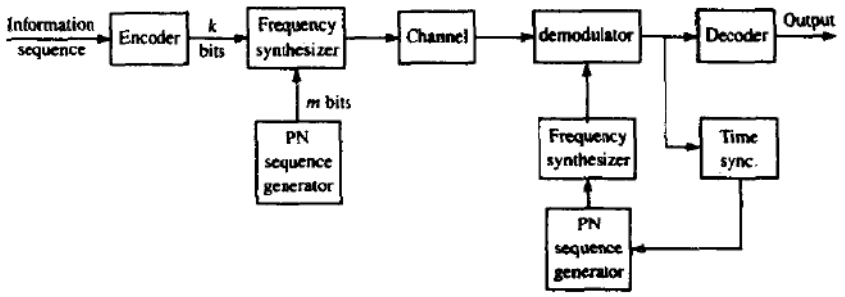

FIGURE 13-3-3 Block diagram of an independent tone FH spread spectrum system.

AWGN channel, it is difficult to maintain phase coherence in the synthesis of the frequencies used in the hopping pattern and, also, in the propagation of the signal over the channel as the signal is hopped from one frequency to another over a wide bandwidth. Consequently, FSK modulation with noncoherent detection is usually employed with FH spread spectrum signals.

In the frequency-hopping system depicted in Fig. 13-3-2, the carrier frequency is pseudo-randomly hopped in every signaling interval. The M information-bearing tones are contiguous and separated in frequency by $1/T_c$, where T_c is the signaling interval. This type of frequency hopping is called *block hopping*.

Another type of frequency hopping that is less vulnerable to some jamming strategies is independent tone hopping. In this scheme, the M possible tones from the modulator are assigned widely dispersed frequency slots. One method for accomplishing this is illustrated in Fig. 13-3-3. Here, the m bits from the PN generator and the k information bits are used to specify the frequency slots for the transmitted signal.

The frequency-hopping rate is usually selected to be either equal to the (coded or uncoded) symbol rate or faster than that rate. If there are multiple hops per symbol, we have a fast-hopped signal. On the other hand, if the hopping is performed at the symbol rate, we have a slow-hopped signal.

Fast frequency hopping is employed in AJ applications when it is necessary to prevent a type of jammer, called a *follower jammer*, from having sufficient time to intercept the frequency and retransmit it along with adjacent frequencies so as to create interfering signal components. However, there is a penalty incurred in subdividing a signal into several frequency-hopped elements because the energy from these separate elements is combined noncoherently. Consequently, the demodulator incurs a penalty in the form of a noncoherent combining loss as described in Section 12-1.

FH spread spectrum signals are used primarily in digital communications systems that require AJ projection and in CDMA, where many users share a common bandwidth. In most cases, a FH signal is preferred over a DS spread spectrum signal because of the stringent synchronization requirements

inherent in DS spread spectrum signals. Specifically, in a DS system, timing and synchronization must be established to within a fraction of the chip interval $T_c \approx 1/W$. On the other hand, in an FH system, the chip interval is the time spent in transmitting a signal in a particular frequency slot of bandwidth $B \ll W$. But this interval is approximately $1/B$, which is much larger than $1/W$. Hence the timing requirements in a FH system are not as stringent as in a PN system.

In Sections 13-3-2 and 13-3-3, we shall focus on the AJ and CDMA applications of FH spread spectrum signals. First, we shall determine the error rate performance of an uncoded and a coded FH signal in the presence of broadband AWGN interference. Then we shall consider a more serious type of interference that arises in AJ and CDMA applications, called *partial-band interference*. The benefits obtained from coding for this type of interference are determined. We conclude the discussion in Section 13-3-3 with an example of an FH CDMA system that was designed for use by mobile users with a satellite serving as the channel.

13-3-1 Performance of FH Spread Spectrum Signals in AWGN Channel

Let us consider the performance of a FH spread spectrum signal in the presence of broadband interference characterized statistically as AWGN with power spectral density J_0. For binary orthogonal FSK with noncoherent detection and slow frequency hopping (1 hop/bit), the probability of error, derived in Section 5-4-1, is

$$P_2 = \tfrac{1}{2} e^{-\gamma_b/2} \tag{13-3-1}$$

where $\gamma_b = \mathscr{E}_b/J_0$. On the other hand, if the bit interval is subdivided into L subintervals and FH binary FSK is transmitted in each subinterval, we have a fast FH signal. With square-law combining of the output signals from the corresponding matched filters for the L subintervals, the error rate performance of the FH signal, obtained from the results in Section 12-1, is

$$P_2(L) = \frac{1}{2^{2L-1}} e^{-\gamma_b/2} \sum_{i=0}^{L-1} K_i (\tfrac{1}{2}\gamma_b)^i \tag{13-3-2}$$

where the SNR per bit is $\gamma_b = \mathscr{E}_b/J_0 = L\gamma_c$, γ_c is the SNR per chip in the L-chip symbol, and

$$K_i = \frac{1}{i!} \sum_{r=0}^{L-1-i} \binom{2L-1}{r} \tag{13-3-3}$$

We recall that, for a given SNR per bit γ_b, the error rate obtained from (13-3-2) is larger than that obtained from (13-3-1). The difference in SNR for a given error rate and a given L is called the *noncoherent combining loss*, which was described and illustrated in Section 12-1.

Coding improves the performance of the FH spread spectrum system by an

amount, which we call the *coding gain*, that depends on the code parameters. Suppose we use a linear binary (n, k) block code and binary FSK modulation with one hop per coded bit for transmitting the bits. With soft-decision decoding of the square-law -demodulated FSK signal, the probability of a code word error is upper-bounded as

$$P_M \leq \sum_{m=2}^{M} P_2(m) \tag{13-3-4}$$

where $P_2(m)$ is the error probability in deciding between the mth code word and the all-zero code word when the latter has been transmitted. The expression for $P_2(m)$ was derived in Section 8-1-4 and has the same form as (13-3-2) and (13-3-3), with L being replaced by w_m and γ_b by $\gamma_b R_c w_m$, where w_m is the weight of the mth code word and R_c is the code rate. The product $R_c w_m$, which is not less than $R_c d_{\min}$, represents the coding gain. Thus, we have the performance of a block coded FH system with slow frequency hopping in broadband interference.

The probability of error for fast frequency hopping with n_2 hops per coded bit is obtained by reinterpreting the binary event probability $P_2(m)$ in (13-3-4). The n_2 hops per coded bit may be interpreted as a repetition code, which, when combined with a nontrivial (n_1, k) binary linear code having weight distribution $\{w_m\}$, yields an $(n_1 n_2, k)$ binary linear code with weight distribution $\{n_2 w_m\}$. Hence, $P_2(m)$ has the form given in (13-3-2), with L replaced by $n_2 w_m$ and γ_b by $\gamma_b R_c n_2 w_m$, where $R_c = k/n_1 n_2$. Note that $\gamma_b R_c n_2 w_m = \gamma_b w_m k/n_1$, which is just the coding gain obtained from the nontrivial (n_1, k) code. Consequently, the use of the repetition code will result in an increase in the noncoherent combining loss.

With hard-decision decoding and slow frequency hopping, the probability of a coded bit error at the output of the demodulator for noncoherent detection is

$$p = \tfrac{1}{2} e^{-\gamma_b R_c/2} \tag{13-3-5}$$

The code word error probability is easily upper-bounded, by use of the Chernoff bound, as

$$P_M \leq \sum_{m=2}^{M} [4p(1-p)]^{w_m/2} \tag{13-3-6}$$

However, if fast frequency hopping is employed with n_2 hops per coded bit, and the square-law-detected outputs from the corresponding matched filters for the n_2 hops are added as in soft-decision decoding to form the two decision variables for the coded bits, the bit error probability p is also given by (13-3-2), with L replaced by n_2 and γ_b replaced by $\gamma_b R_c n_2$, where R_c is the rate of the nontrivial (n_1, k) code. Consequently, the performance of the fast FH system in broadband interference is degraded relative to the slow FH system by an amount equal to the noncoherent combining loss of the signals received from the n_2 hops.

We have observed that for both hard-decision and soft-decision decoding, the use of the repetition code in a fast-frequency-hopping system yields no coding gain. The only coding gain obtained comes from the (n_1, k) block code. Hence, the repetition code is inefficient in a fast FH system with noncoherent combining. A more efficient coding method is one in which either a single low-rate binary code or a concatenated code is employed. Additional improvements in performance may be obtained by using nonbinary codes in conjunction with M-ary FSK. Bounds on the error probability for this case may be obtained from the results given in Section 12-1.

Although we have evaluated the performance of linear block codes only in the above discussion, it is relatively easy to derive corresponding performance results for binary convolutional codes. We leave as an exercise for the reader the derivation of the bit error probability for soft-decision Viterbi decoding and hard-decision Viterbi decoding of FH signals corrupted by broadband interference.

Finally, we observe that $\mathscr{E}_b$, the energy per bit, can be expressed as $\mathscr{E}_b = P_{av}/R$, where R is the information rate in bits per second and $J_0 = J_{av}/W$. Therefore, γ_b may be expressed as

$$\gamma_b = \frac{\mathscr{E}_b}{J_0} = \frac{W/R}{J_{av}/P_{av}} \tag{13-3-7}$$

In this expression, we recognize W/R as the processing gain and J_{av}/P_{av} as the jamming margin for the FH spread spectrum signal.

13-3-2 Performance of FH Spread Spectrum Signals in Partial-Band Interference

The partial-band interference considered in this subsection is modeled as a zero-mean gaussian random process with a flat power spectral density over a fraction α of the total bandwidth W and zero elsewhere. In the region or regions where the power spectral density is nonzero, its value is $\Phi_{zz}(f) = J_0/\alpha$, $0 < \alpha \leq 1$. This model of the interference may be applied to a jamming signal or to interference from other users in a FH CDMA system.

Suppose that the partial-band interference comes from a jammer who may select α to optimize the effect on the communications system. In an uncoded pseudo-randomly hopped (slow-hopping) FH system with binary FSK modulation and noncoherent detection, the received signal will be jammed with probability α and it will not be jammed with probability $1 - \alpha$. When it is jammed, the probability of error is $\frac{1}{2}\exp(-\mathscr{E}_b\alpha/2J_0)$, and when it is not jammed, the demodulation is error-free. Consequently, the average probability of error is

$$P_2(\alpha) = \tfrac{1}{2}\alpha \exp\left(-\frac{\alpha\mathscr{E}_b}{2J_0}\right) \tag{13-3-8}$$

where $\mathscr{E}_b/J_0$ may also be expressed as $(W/R)/(J_{av}/P_{av})$.

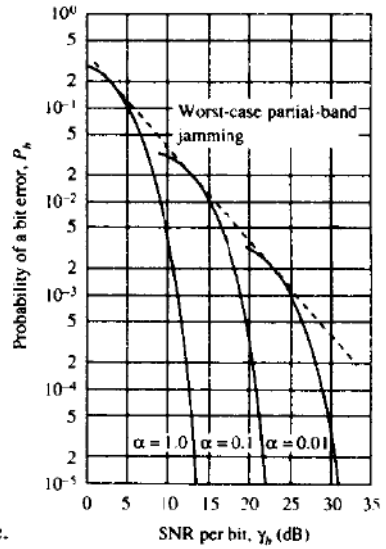

FIGURE 13-3-4 Performance of binary FSK with partial-band interference.

Figure 13-3-4 illustrates the error rate as a function of $\mathscr{E}_b/J_0$ for several values of α. The jammer's optimum strategy is to select the value of α that maximizes the error probability. By differentiating $P_2(\alpha)$ and solving for the extremum with the restriction that $0 \leq \alpha \leq 1$, we find that

$$\alpha^* = \begin{cases} \dfrac{1}{\mathscr{E}_b/2J_0} = 2\dfrac{J_{av}/P_{av}}{W/R} & (\mathscr{E}_b/J_0 \geq 2) \\ 1 & (\mathscr{E}_b/J_0 < 2) \end{cases} \tag{13-3-9}$$

The corresponding error probability for the worst-case partial-band jammer is

$$P_2 = \frac{e^{-1}}{\mathscr{E}_b/J_0} = \left[e\left(\frac{W/R}{J_{av}/P_{av}}\right)\right]^{-1} \tag{13-3-10}$$

Whereas the error probability decreases exponentially for full-band jamming, we now find that the error probability decreases only inversely with $\mathscr{E}_b/J_0$ for the worst-case partial-band jamming. This result is similar to the error rate performance of binary FSK in a Rayleigh fading channel (see Section 14-3) and to the uncoded DS spread spectrum system corrupted by worst-case pulse jamming (see Section 13-2-3).

As we shall demonstrate below, signal diversity obtained by means of coding provides a significant improvement in performance relative to uncoded signals. This same approach to signal design is also effective for signaling over a fading channel, as we shall demonstrate in Chapter 14.

To illustrate the benefits of diversity in a FH spread spectrum signal with partial-band interference, we assume that the same information symbol is

transmitted by binary FSK on L independent frequency hops. This may be accomplished by subdividing the signaling interval into L subintervals, as described previously for fast frequency hopping. After the hopping pattern is removed, the signal is demodulated by passing it through a pair of matched filters whose outputs are square-law-detected and sampled at the end of each subinterval. The square-law-detected signals corresponding to the L frequency hops are weighted and summed to form the two decision variables (metrics), which are denoted as U_1 and U_2.

When the decision variable U_1 contains the signal components, U_1 and U_2 may be expressed as

$$\begin{aligned} U_1 &= \sum_{k=1}^{L} \beta_k \, |2\mathscr{E}_c + N_{1k}|^2 \\ U_2 &= \sum_{k=1}^{L} \beta_k \, |N_{2k}|^2 \end{aligned} \tag{13-3-11}$$

where $\{\beta_k\}$ represent the weighting coefficients, $\mathscr{E}_c$ is the signal energy per chip in the L-chip symbol, and $\{N_{jk}\}$ represent the additive gaussian noise terms at the output of the matched filters.

The coefficients are optimally selected to prevent the jammer from saturating the combiner should the transmitted frequencies be successfully hit in one or more hops. Ideally, β_k is selected to be equal to the reciprocal of the variance of the corresponding noise terms $\{N_k\}$. Thus, the noise variance for each chip is normalized to unity by this weighting and the corresponding signal is also scaled accordingly. This means that when the signal frequencies on a particular hop are jammed, the corresponding weight is very small. In the absence of jamming on a given hop, the weight is relatively large. In practice, for partial-bound noise jamming, the weighting may be accomplished by use of an AGC having a gain that is set on the basis of noise power measurements obtained from frequency bands adjacent to the transmitted tones. This is equivalent to having side information (knowledge of jammer state) at the decoder.

Suppose that we have broadband gaussian noise with power spectral density N_0 and partial-band interference, over αW of the frequency band, which is also gaussian with power spectral density J_0/α. In the presence of partial-band interference, the second moments of the noise terms N_{1k} and N_{2k} are

$$\sigma_k^2 = \tfrac{1}{2}E(|N_{1k}|^2) = \tfrac{1}{2}E(|N_{2k}|^2) = 2\mathscr{E}_c\left(N_0 + \frac{J_0}{\alpha}\right) \tag{13-3-12}$$

In this case, we select $\beta_k = 1/\sigma_k^2 = [2\mathscr{E}_c(N_0 + J_0/\alpha)]^{-1}$. In the absence of partial-band interference, $\sigma_k^2 = 2\mathscr{E}_c N_0$ and, hence, $\beta_k = (2\mathscr{E}_c N_0)^{-1}$. Note that β_k is a random variable.

An error occurs in the demodulation if $U_2 > U_1$. Although it is possible to determine the exact error probability, we shall resort to the Chernoff bound,

which yields a result that is much easier to evaluate and interpret. Specifically, the Chernoff (upper) bounds in the error probability is

$$\begin{aligned} P_2 &= P(U_2 - U_1 > 0) \leq E\{\exp[\nu(U_2 - U_1)]\} \\ &= E\left\{\exp\left[-\nu \sum_{k=1}^{L} \beta_k(|2\mathscr{E}_c + N_{1k}|^2 - |N_{2k}|^2)\right]\right\} \end{aligned} \tag{13-3-13}$$

where ν is a variable that is optimized to yield the tightest possible bound.

The averaging in (13-3-13) is performed with respect to the statistics of the noise components and the statistics of the weighting coefficients $\{\beta_k\}$, which are random as a consequence of the statistical nature of the interference. Keeping the $\{\beta_k\}$ fixed and averaging over the noise statistics first, we obtain

$$\begin{aligned} P_2(\boldsymbol{\beta}) &= E\left[\exp\left(-\nu \sum_{k=1}^{L} \beta_k |2\mathscr{E}_c + N_{1k}|^2 + \nu \sum_{k=1}^{L} \beta_k |N_{2k}|^2\right)\right] \\ &= \prod_{k=1}^{L} E[\exp(-\nu\beta_k |2\mathscr{E}_c + N_{1k}|^2)]E[\exp(\nu\beta_k |N_{2k}|^2)] \\ &= \prod_{k=1}^{L} \frac{1}{1-4\nu^2} \exp\left(\frac{-4\mathscr{E}_c^2\beta_k\nu}{1+2\nu}\right) \end{aligned} \tag{13-3-14}$$

Since the FSK tones are jammed with probability α, it follows that $\beta_k = [2\mathscr{E}(N_0 + J_0/\alpha)]^{-1}$ with probability α and $(2\mathscr{E}_c N_0)^{-1}$ with probability $1-\alpha$. Hence, the Chernoff bound is

$$\begin{aligned} P_2 &\leq \prod_{k=1}^{L} \left\{\frac{\alpha}{1-4\nu^2} \exp\left[\frac{-2\mathscr{E}_c\nu}{(N_0 + J_0/\alpha)(1+2\nu)}\right] + \frac{1-\alpha}{1-4\nu^2} \exp\left[\frac{-2\mathscr{E}_c\nu}{N_0(1+2\nu)}\right]\right\} \\ &= \left\{\frac{\alpha}{1-4\nu^2} \exp\left[\frac{-2\mathscr{E}_c\nu}{(N_0 + J_0/\alpha)(1+2\nu)}\right] + \frac{1-\alpha}{1-4\nu^2} \exp\left[\frac{-2\mathscr{E}_c\nu}{N_0(1+2\nu)}\right]\right\}^L \end{aligned} \tag{13-3-15}$$

The next step is to optimize the bound in (13-3-15) with respect to the variable ν. In its present form, however, the bound is messy to manipulate. A significant simplification occurs if we assume that $J_0/\alpha \gg N_0$, which renders the second term in (13-3-15) negligible compared with the first. Alternatively, we let $N_0 = 0$, so that the bound on P_2 reduces to

$$P_2 \leq \left\{\frac{\alpha}{1-4\nu^2} \exp\left[\frac{-2\alpha\nu\mathscr{E}_c}{J_0(1+2\nu)}\right]\right\}^L \tag{13-3-16}$$

The minimum value of this bound with respect to ν and the maximum with respect to α (worst-case partial-band interference) is easily shown to occur when $\alpha = 3J_0/\mathscr{E}_c \leq 1$ and $\nu = \frac{1}{4}$. For these values of the parameters, (13-3-16) reduces to

$$P_2 \leq P_2(L) = \left(\frac{4}{e\gamma_c}\right)^L = \left(\frac{1.47}{\gamma_c}\right)^L, \qquad \gamma_c = \frac{\mathscr{E}_c}{J_0} = \frac{\mathscr{E}_b}{LJ_0} \geq 3 \tag{13-3-17}$$

where γ_c is the SNR per chip in the L-chip symbol. Equivalently,

$$P_2 \leq \left[\frac{1.47(J_{av}/P_{av})}{W/R}\right]^L, \quad \frac{W/R}{L(J_{av}/P_{av})} \geq 3 \tag{13-3-18}$$

The result in (13-3-17) was first derived by Viterbi and Jacobs (1975).

We observe that the probability of error for the worst-case partial-band interference decreases exponentially with an increase in the SNR per chip γ_c. This result is very similar to the performance characteristics of diversity techniques for Rayleigh fading channels (see Section 14-4). We may express the right-hand side of (13-3-17) in the form

$$P_2(L) = \exp[-\gamma_b h(\gamma_c)] \tag{13-3-19}$$

where the function $h(\gamma_c)$ is defined as

$$h(\gamma_c) = -\frac{1}{\gamma_c}\left[\ln\left(\frac{4}{\gamma_c}\right) - 1\right] \tag{13-3-20}$$

A plot of $h(\gamma_c)$ is given in Fig. 13-3-5. We observe that the function has a maximum value of $\frac{1}{4}$ at $\gamma_c = 4$. Consequently, there is an optimum SNR per chip of $10 \log \gamma_c = 6$ dB. At the optimum SNR, the error rate is upper-bounded as

$$P_2 \leq P_2(L_{opt}) = e^{-\gamma_b/4} \tag{13-3-21}$$

When we compare the error probability bound in (13-3-21) with the error probability for binary FSK in spectrally flat noise, which is given by (13-3-1), we see that the combined effect of worst-case partial-band interference and the noncoherent combining loss in the square-law combining of the L chips is 3 dB. We emphasize, however, that for a given $\mathscr{E}_b/J_0$, the loss is greater when the order of diversity is not optimally selected.

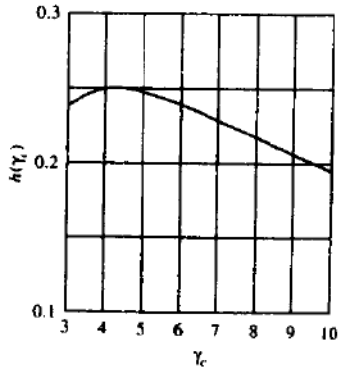

FIGURE 13-3-5 Graph of the function $h(\gamma_c)$.

Coding provides a means for improving the performance of the frequency-hopped system corrupted by partial-band interference. In particular, if a block orthogonal code is used, with $M = 2^k$ code words and Lth-order diversity per code word, the probability of a code word error is upper-bounded as

$$P_M \leq (2^k - 1)P_2(L) = (2^k - 1)\left(\frac{1.47}{\gamma_c}\right)^L = (2^k - 1)\left(\frac{1.47}{k\gamma_b/L}\right)^L \quad (13\text{-}3\text{-}22)$$

and the equivalent bit error probability is upper-bounded as

$$P_b \leq 2^{k-1}\left(\frac{1.47}{k\gamma_b/L}\right)^L \quad (13\text{-}3\text{-}23)$$

Figure 13-3-6 illustrates the probability of a bit error for $L = 1, 2, 4, 8$ and

FIGURE 13-3-6 Performance of binary and octal FSK with L-order diversity for a channel with worst-case partial-band interference.

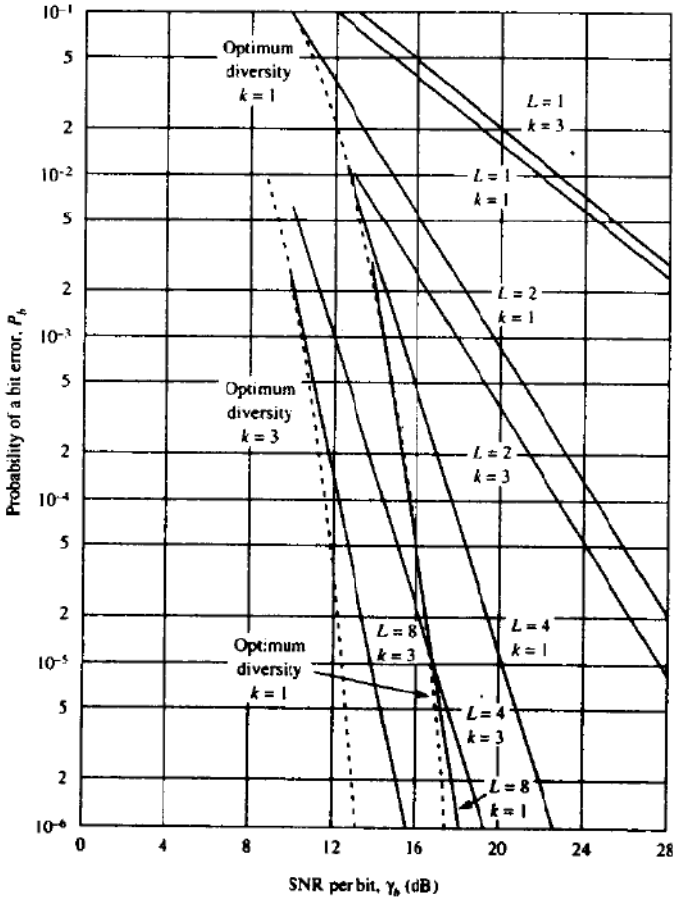

$k = 1, 3$. With an optimum choice of diversity, the upper bound can be expressed as

$$P_b \leq 2^{k-1} \exp(-\tfrac{1}{4}k\gamma_b) = \tfrac{1}{2}\exp[-k(\tfrac{1}{4}\gamma_b - \ln 2)] \qquad (13\text{-}3\text{-}24)$$

Thus, we have an improvement in performance by an amount equal to $10 \log [k(1 - 2.77/\gamma_b)]$. For example, if $\gamma_b = 10$ and $k = 3$ (octal modulation) then the gain is 3.4 dB, while if $k = 5$ then the gain is 5.6 dB.

Additional gains can be achieved by employing concatenated codes in conjunction with soft-decision decoding. In the example below, we employ a dual-k convolutional code as the outer code and a Hadamard code as the inner code on the channel with partial-band interference.

Example 13-3-1

Suppose we use a Hadamard $H(n, k)$ constant weight code with on-off keying (OOK) modulation for each code bit. The minimum distance of the code is $d_{\min} = \frac{1}{2}n$, and, hence, the effective order of diversity obtained with OOK modulation is $\frac{1}{2}d_{min} = \frac{1}{4}n$. There are $\frac{1}{2}n$ frequency-hopped tones transmitted per code word. Hence,

$$\gamma_c = \frac{k}{\frac{1}{2}n}\gamma_b = 2R_c\gamma_b \qquad (13\text{-}3\text{-}25)$$

when this code is used alone. The bit error rate performance for soft-decision decoding of these codes for the partial-band interference channel is upper-bounded as

$$P_b \leq 2^{k-1}P_2(\tfrac{1}{2}d_{\min}) = 2^{k-1}\left(\frac{1.47}{2R_c\gamma_b}\right)^{n/4} \qquad (13\text{-}3\text{-}26)$$

Now, if a Hadamard (n, k) code is used as the inner code and a rate 1/2 dual-k convolutional code (see Section 8-2-6) is the outer code, the bit error performance in the presence of worst-case partial-band interference is (see (8-2-40))

$$P_b \leq \frac{2^{k-1}}{2^k - 1}\sum_{m=4}^{\infty}\beta_m P_2(\tfrac{1}{2}md_{\min}) = \frac{2^{k-1}}{2^k - 1}\sum_{m=4}^{\infty}\beta_m P_2(\tfrac{1}{4}mn) \qquad (13\text{-}3\text{-}27)$$

where $P_2(L)$ is given by (13-3-17) with

$$\gamma_c = \frac{k}{n}\gamma_b = R_c\gamma_b \qquad (13\text{-}3\text{-}28)$$

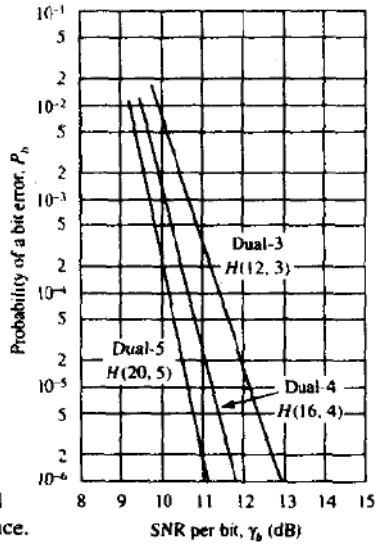

FIGURE 13-3-7 Performance of dual-k codes concatenated with Hadamard codes for a channel with worst-case partial-band interference.

Figure 13-3-7 illustrates the performance of the dual-k codes for $k = 5$, 4, and 3 concatenated with the Hadamard $H(20, 5)$, $H(16, 4)$, and $H(12, 3)$ codes, respectively.

In the above discussion, we have focused on soft-decision decoding. On the other hand, the performance achieved with hard-decision decoding is significantly (several decibels) poorer than that obtained with soft-decision decoding. In a concatenated coding scheme, however, a mixture involving soft-decision decoding of the inner code and hard-decision decoding of the outer code represents a reasonable compromise between decoding complexity and performance.

Finally, we wish to indicate that another serious threat in a FH spread spectrum system is partial-band multitone jamming. This type of interference is similar in effect to partial-band spectrally flat noise jamming. Diversity obtained through coding is an effective means for improving the performance of the FH system. An additional improvement is achieved by properly weighting the demodulator outputs so as to suppress the effects of the jammer.

13-3-3 A CDMA System Based on FH Spread Spectrum Signals

In Section 13-2-2, we considered a CDMA system based on use of DS spread spectrum signals. As previously indicated, it is also possible to have a CDMA system based on FH spread spectrum signals. Each transmitter–receiver pair in such a system is assigned its own pseudo-random frequency-hopping pattern.

Aside from this distinguishing feature, the transmitters and receivers of all the users may be identical in that they may have identical encoders, decoders, modulators, and demodulators.

CDMA systems based on FH spread spectrum signals are particularly attractive for mobile (land, air, sea) users because timing requirements are not as stringent as in a PN spread spectrum signal. In addition, frequency synthesis techniques and associated hardware have been developed that make it possible to frequency-hop over bandwidths that are significantly larger than those currently possible with DS spread spectrum systems. Consequently, larger processing gains are possible with FH. The capacity of CDMA with FH is also relatively high. Viterbi (1978) has shown that with dual-k codes and M-ary FSK modulation, it is possible to accomodate up to $\frac{3}{8}W/R$ simultaneous users who transmit at an information rate R bits/s over a channel with bandwidth W.

One of the earliest CDMA systems based on FH coded spread spectrum signals was built to provide multiple-access tactical satellite communications for small mobile (land, sea, air) terminals each of which transmitted relatively short messages over the channel intermittently. The system was called the *Tactical Transmission System* (TATS) and it is described in a paper by Drouilhet and Bernstein (1969).

An octal Reed–Solomon (7, 2) code is used in the TATS system. Thus, two 3 bit information symbols from the input to the encoder are used to generate a seven-symbol code word. Each 3 bit coded symbol is transmitted by means of octal FSK modulation. The eight possible frequencies are spaced $1/T_c$ Hz apart, where T_c is the time (chip) duration of a single frequency transmission. In addition to the seven symbols in a code word, an eighth symbol is included. That symbol and its corresponding frequency are fixed and transmitted at the beginning of each code word for the purpose of providing timing and frequency synchronization† at the receiver. Consequently, each code word is transmitted in $8T_c$ s.

TATS was designed to transmit at information rates of 75 and 2400 bits/s. Hence, $T_c = 10$ ms and 312.5 μs, respectively. Each frequency tone corresponding to a code symbol is frequency-hopped. Hence, the hopping rate is 100 hops/s at the 75 bits/s rate and 3200 hops/s at the 2400 bits/s rate.

There are $M = 2^6 = 64$ code words in the Reed–Solomon (7, 2) code and the minimum distance of the code is $d_{\min} = 6$. This means that the code provides an effective order of diversity equal to 6.

At the receiver, the received signal is first dehopped and then demodulated by passing it through a parallel bank of eight matched filters, where each filter is tuned to one of the eight possible frquencies. Each filter output is envelope-detected, quantized to 4 bits (one of 16 levels), and fed to the decoder. The decoder takes the 56 filter outputs corresponding to the

† Since mobile users are involved, there is a Doppler frequency offset associated with transmission. This frequency offset must be tracked and compensated for in the demodulation of the signal. The sync symbol is used for this purpose.

reception of each seven-symbol code word and forms 64 decision variables corresponding to the 64 possible code words in the (7, 2) code by linearly combining the appropriate envelope detected outputs. A decision is made in favor of the code word having the largest decision variable.

By limiting the matched filter outputs to 16 levels, interference (crosstalk) from other users of the channel causes a relatively small loss in performance (0.75 dB with strong interference on one chip and 1.5 dB with strong interference on two chips out of the seven). The AGC used in TATS has a time constant greater than the chip interval T_c, so that no attempt is made to perform optimum weighting of the demodulator outputs as described in Section 13-3-2.

The derivation of the error probability for the TATS signal in AWGN and worst-case partial-band interference is left as an exercise for the reader (Problems 13-23 and 13-24).

13-4 OTHER TYPES OF SPREAD SPECTRUM SIGNALS

DS and FH are the most common forms of spread spectrum signals used in practice. However, other methods may be used to introduce pseudo-randomness in a spread spectrum signal. One method, which is analogous to FH, is *time* hopping (TH). In TH, a time interval, which is selected to be much larger than the reciprocal of the information rate, is subdivided into a large number of time slots. The coded information symbols are transmitted in a pseudo-randomly selected time slot as a block of one or more code words. PSK modulation may be used to transmit the coded bits.

For example, suppose that a time interval T is subdivided into 1000 time slots of width $T/1000$ each. With an information bit rate of R bits/s, the number of bits to be transmitted in T s is RT. Coding increases this number to RT/R_c bits, where R_c is the coding rate. Consequently, in a time interval of $T/1000$ s, we must transmit RT/R_c bits. If binary PSK is used as the modulation method, the bit rate is $1000R/R_c$ and the bandwidth required is approximately $W = 1000R/R_c$.

A block diagram of a transmitter and a receiver for a TH spread spectrum system is shown in Fig. 13-4-1. Due to the burst characteristics of the transmitted signal, buffer storage must be provided at the transmitter in a TH system, as shown in Fig. 13-4-1. A buffer may also be used at the receiver to provide a uniform data stream to the user.

Just as partial-band interference degrades an uncoded FH spread spectrum system, partial-time (pulsed) interference has a similar effect on a TH spread spectrum system. Coding and interleaving are effective means for combatting this type of interference, as we have already demonstrated for FH and DS systems. Perhaps the major disadvantage of a TH system is the stringent timing requirements compared not only with FH but, also, with DS.

Other types of spread spectrum signals can be obtained by combining DS,

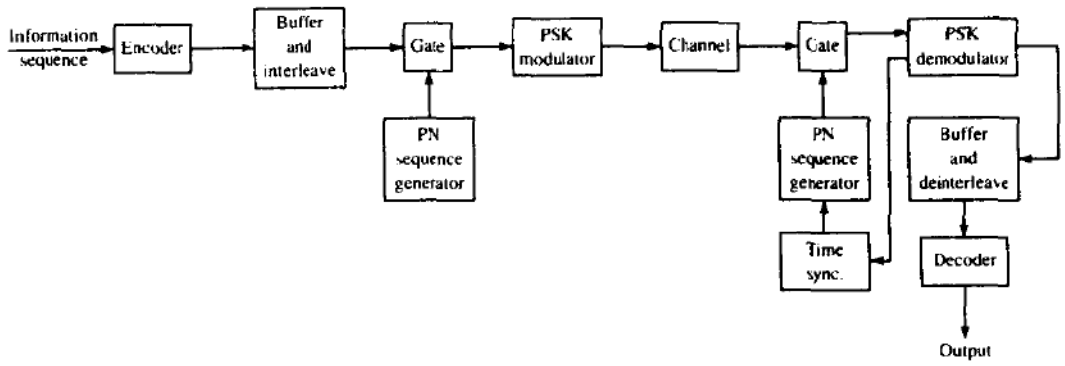

FIGURE 13-4-1 Block diagram of time-hopping (TH) spread spectrum system.

FH, and TH. For example, we may have a hybrid DS/FH, which means that a PN sequence is used in combination with frequency hopping. The signal transmitted on a single hop consists of a DS spread spectrum signal which is demodulated coherently. However, the received signals from different hops are combined noncoherently (envelope or square-law combining). Since coherent detection is performed within a hop, there is an advantage obtained relative to a pure FH system. However, the price paid for the gain in performance is an increase in complexity, greater cost, and more stringent timing requirements.

Another possible hybrid spread spectrum signal is DS/TH. This does not seem to be as practical as DS/FH, primarily because of an increase in system complexity and more stringent timing requirements.

13-5 SYNCHRONIZATION OF SPREAD SPECTRUM SYSTEMS

Time synchronization of the receiver to the received spread spectrum signal may be separated into two phases. There is an initial acquisition phase and a tracking phase after the signal has been initially acquired.

Acquisition In a direct sequence spread spectrum system, the PN code must be time-synchronized to within a small fraction of the chip interval $T_c \approx 1/W$. The problem of initial synchronization may be viewed as one in which we attempt to synchronize in time the receiver clock to the transmitter clock. Usually, extremely accurate and stable time clocks are used in spread spectrum systems. Consequently, accurate time clocks result in a reduction of the time uncertainty between the receiver and the transmitter. However, there is always an initial timing uncertainty due to range uncertainty between the transmitter and the receiver. This is especially a problem when communication is taking place between two mobile users. In any case, the usual procedure for establishing initial synchronization is for the transmitter to send a known

pseudo-random data sequence to the receiver. The receiver is continuously in a search mode looking for this sequence in order to establish initial synchronization.

Let us suppose that the initial timing uncertainty is T_u and the chip duration is T_c. If initial synchronization is to take place in the presence of additive noise and other interference, it is necessary to dwell for $T_d = NT_c$ in order to test synchronism at each time instant. If we search over the time uncertainty interval in (coarse) time steps of $\frac{1}{2}T_c$ then the time required to establish initial synchronization is

$$T_{\text{init sync}} = \frac{T_u}{\frac{1}{2}T_c} NT_c = 2NT_u \tag{13-5-1}$$

Clearly, the synchronization sequence transmitted to the receiver must be at least as long as $2NT_c$ in order for the receiver to have sufficient time to perform the necessary search in a serial fashion.

In principle, matched filtering or cross-correlation are optimum methods for establishing initial synchronization. A filter matched to the known data waveform generated from the known pseudo-random sequence continuously looks for exceedence of a predetermined threshold. When this occurs, initial synchronization is established and the demodulator enters the "data receive" mode.

Alternatively, we may use a *sliding correlator* as shown in Fig. 13-5-1. The correlator cycles through the time uncertainty, usually in discrete time intervals of $\frac{1}{2}T_c$, and correlates the received signal with the known synchronization sequence. The cross-correlation is performed over the time interval NT_c (N chips) and the correlator output is compared with a threshold to determine if the known signal sequence is present. If the threshold is not exceeded, the known reference sequence is advanced in time by $\frac{1}{2}T_c$ s and the correlation process is repeated. These operations are performed until a signal is detected or until the search has been performed over the time uncertainty interval T_u. In the latter case, the search process is then repeated.

A similar process may also be used for FH signals. In this case, the problem is to synchronize the PN code that controls the hopped frequency pattern. To accomplish this initial synchronization, a known frequency hopped signal is

FIGURE 13-5-1 A sliding correlator for DS signal acquisition.

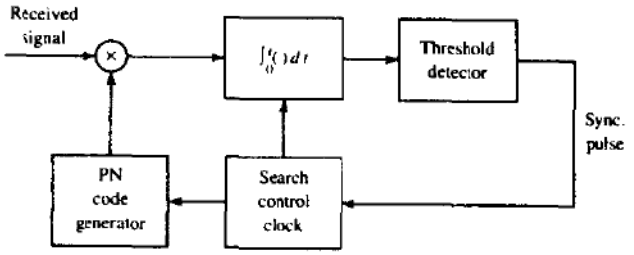

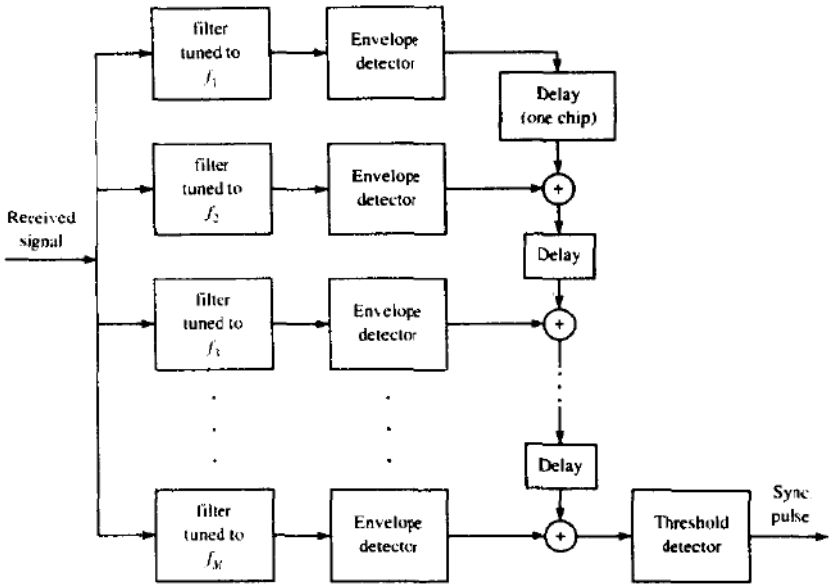

FIGURE 13-5-2 System for acquisition of a FH signal.

transmitted to the receiver. The initial acquisition system at the receiver looks for this known FH signal pattern. For example, a bank of matched filters tuned to the transmitted frequencies in the known pattern may be employed. Their outputs must be properly delayed, envelope- or square-law-detected, weighted, if necessary, and added (noncoherent integration) to produce the signal output which is compared with a threshold. A signal present is declared when the threshold is exceeded. The search process is usually performed continuously in time until a threshold is exceeded. A block diagram illustrating this signal acquisition scheme is given in Fig. 13-5-2. As an alternative, a single matched-filter–envelope detector pair may be used, preceded by a frequency-hopping pattern generator and followed by a post-detection integrator and a threshold detector. This configuration, shown in Fig. 13-5-3, is based on a serial search and is akin to the sliding correlator for DS spread spectrum signals.

The sliding correlator for the DS signals or its counterpart shown in Fig. 13-5-3 for FH signals basically perform a serial search that is generally time-consuming. As an alternative, one may introduce some degree of parallelism by having two or more such correlators operating in parallel and searching over nonoverlapping time slots. In such a case, the search time is reduced at the expense of a more complex and costly implementation. Figure 13-5-2 represents such a parallel realization for the FH signals.

During the search mode, there may be false alarms that occur at the designed false alarm rate of the system. To handle the occasional false alarms, it is necessary to have an additional method or circuit that checks to confirm

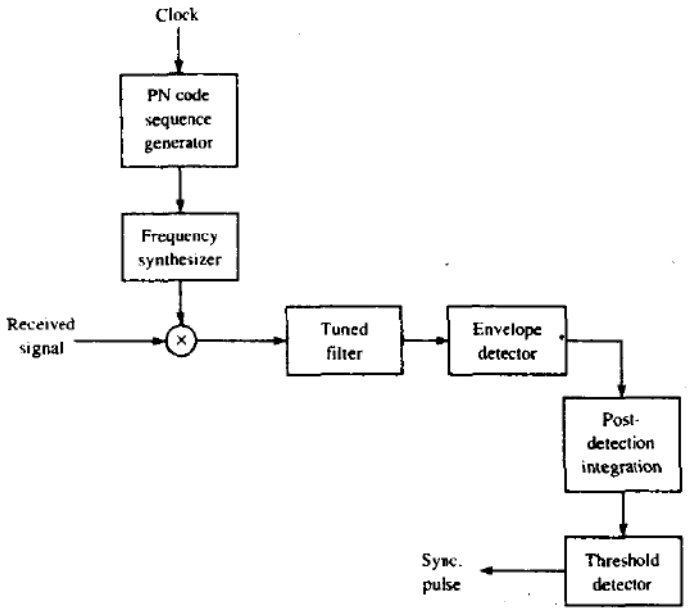

FIGURE 13-5-3 Alternative system for acquisition of a FH signal.

that the received signal at the output of the correlator remains above the threshold. With such a detection strategy, a large noise pulse that causes a false alarm will cause only a temporary exceedence of the threshold. On the other hand, when a signal is present, the correlator or matched filter output will stay above the threshold for the duration of the transmitted signal. Thus, if confirmation fails, the search is resumed.

Another initial search strategy, called a *sequential search*, has been investigated by Ward (1965, 1977). In this method, the dwell time at each delay in the search process is made variable by employing a correlator with a variable integration period whose (biased) output is compared with two thresholds. Thus, there are three possible decisions:

1 if the upper threshold is exceed by the correlator output, initial synchronization is declared established;

2 if the correlator output falls below the lower threshold, the signal is declared absent at that delay and the search process resumes at a different delay;

3 if the correlator output falls between the two thresholds, the integration time is increased by one chip and the resulting output is compared with the two thresholds again.

Hence, steps 1, 2, and 3 are repeated for each chip interval until the correlator output either exceeds the upper threshold or falls below the lower threshold.

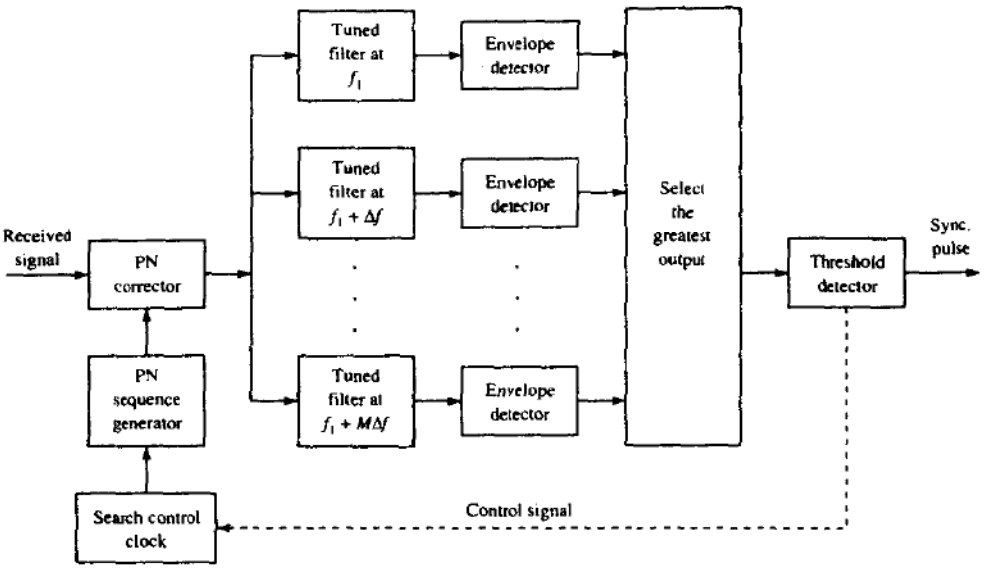

FIGURE 13-5-4 Initial search for Doppler frequency offset in a DS system.

The sequential search method falls in the class of sequential estimation methods proposed by Wald (1947), which are known to result in a more efficient search in the sense that the average search time is minimized. Hence, the search time for a sequential search is less than that for the fixed dwell time integrator.

In the above discussion, we have considered only time uncertainty in establishing initial synchronization. However, another aspect of initial synchronization is frequency uncertainty. If the transmitter and/or the receiver are mobile, the relative velocity between them results in a Doppler frequency shift in the received signal relative to the transmitted signal. Since the receiver does not usually know the relative velocity, a priori, the Doppler frequency shift is unknown and must be determined by means of a frequency search method. Such a search is usually accomplished in parallel over a suitably quantized frequency uncertainty interval and serially over the time uncertainty interval. A block diagram of this scheme is shown in Fig. 13-5-4. Appropriate Doppler frequency search methods can also be devised for FH signals.

Tracking Once the signal is acquired, the initial search process is stopped and fine synchronization and tracking begins. The tracking maintains the PN code generator at the receiver in synchronism with the incoming signal. Tracking includes both fine chip synchronization and, for coherent demodulation, carrier phase tracking.

The commonly used tracking loop for a DS spread spectrum signal is the

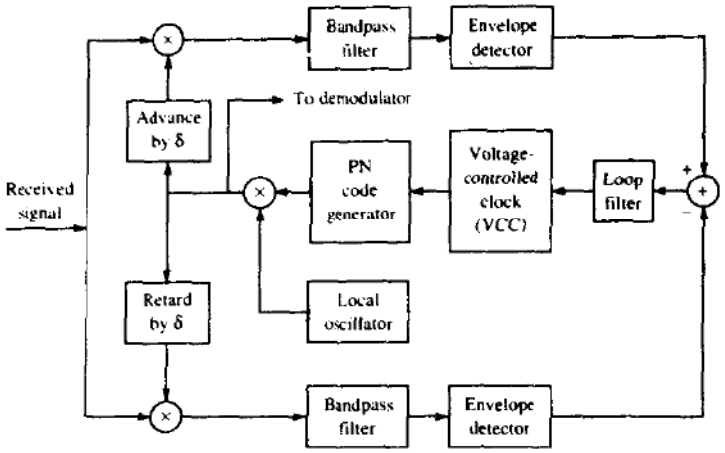

FIGURE 13-5-5 Delay-locked loop (DLL) for PN code tracking.

delay-locked loop (DLL), which is shown in Fig. 13-5-5. In this tracking loop, the received signal is applied to two multipliers, where it is multiplied by two outputs from the local PN code generator, which are delayed relative to each other by an amount $2\delta \leq T_c$. Thus, the product signals are the cross-correlations between the received signal and the PN sequence at the two values of delay. These products are bandpass-filtered and envelope- (or square-law-) detected and then subtracted. This difference signal is applied to the loop filter that drives the voltage controlled clock (VCC). The VCC serves as the clock for the PN code signal generator.

If the synchronism is not exact, the filtered output from one correlator will exceed the other and the VCC will be appropriately advanced or delayed. At the equilibrium point, the two filtered correlator outputs will be equally displaced from the peak value, and the PN code generator output will be exactly synchronized to the received signal that is fed to the demodulator. We observe that this implementation of the DLL for tracking a DS signal is equivalent to the early–late gate bit tracking synchronizer previously discussed in Section 6-3-2 and shown in Fig. 6-3-5.

An alternative method for time tracking a DS signal is to use a *tau-dither loop* (TDL), illustrated by the block diagram in Fig. 13-5-6. The TDL employs a single "arm" instead of the two "arms" shown in Fig. 13-5-5. By providing a suitable gating waveform, it is possible to make this "single-arm" implementation appear to be equivalent to the "two-arm" realization. In this case, the cross-correlation is regularly sampled at two values of delay, by stepping the code clock forward or backward in time by an amount δ. The envelope of the cross-correlation that is sampled at $\pm\delta$ has an amplitude modulation whose phase relative to the tau-dither modulator determines the sign of the tracking error.

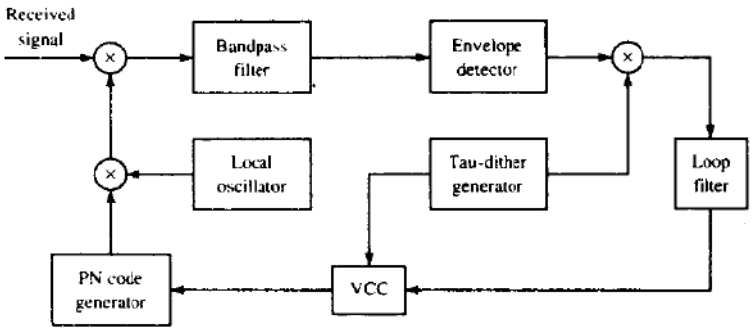

FIGURE 13-5-6 Tau-dither loop (TDL).

A major advantage of the TDL is the less costly implementation resulting from elimination of one of the two arms that are employed in the conventional DLL. A second and less apparent advantage is that the TDL does not suffer from performance degradation that is inherent in the DLL when the amplitude gain in the two arms is not properly balanced.

The DLL (and its equivalent, the TDL) generate an error signal by sampling the signal correlation function at $\pm\delta$ off the peak as shown in Fig. 13-5-7(a). This generates an error signal as shown in Fig. 13-5-7(b). The analysis of the performance of the DLL is similar to that for the phase-locked loop (PLL) carried out in Section 6-3. If it were not for the envelope detectors in the two arms of the DLL, the loop would resemble a Costas loop. In general, the variance of the time estimation error in the DLL is inversely proportional to the loop SNR, which depends on the input SNR to the loop and the loop bandwidth. Its performance is somewhat degraded as in the squaring PLL by the nonlinearities inherent in the envelope detectors, but this degradation is relatively small.

FIGURE 13-5-7 Autocorrelation function and tracking error signal for DLL.

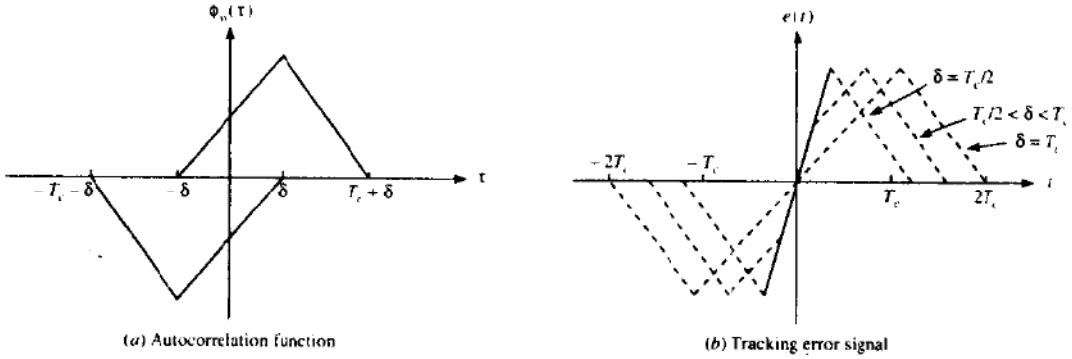

(a) Autocorrelation function

(b) Tracking error signal

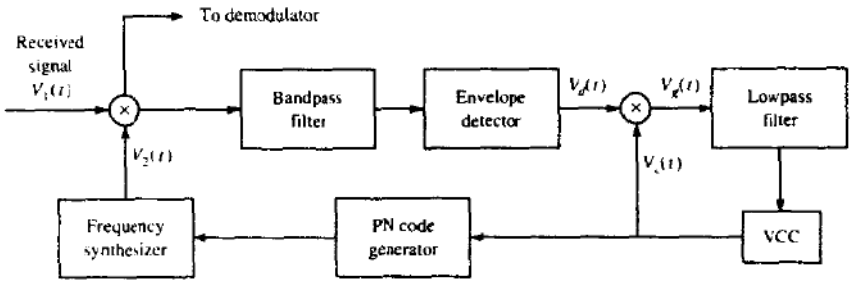

(*a*) Tracking loop for FH signals

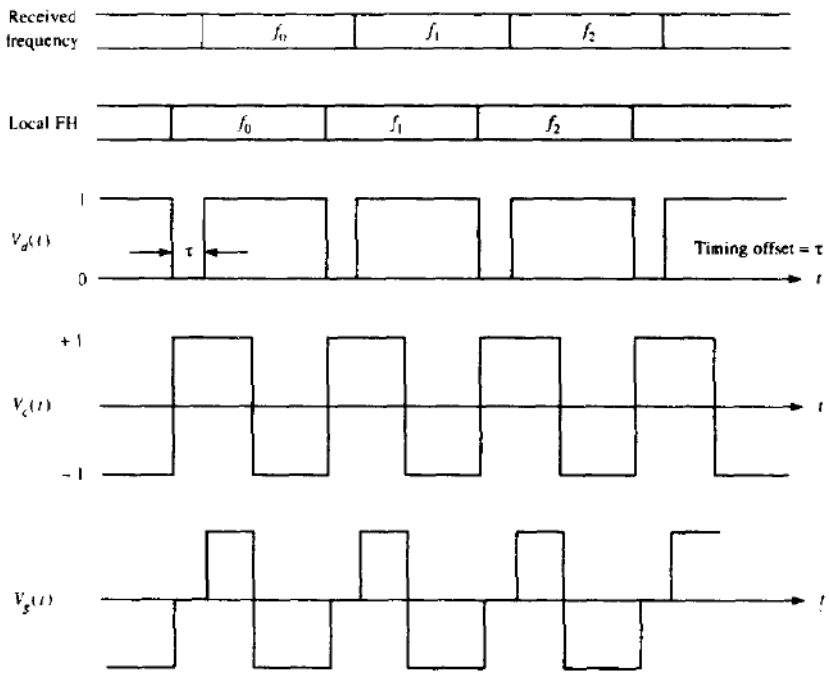

(*b*) Wavefront for tracking an FH signal

FIGURE 13-5-8 Trracking method for FH signals. [*From Pickholtz* et al. *(1982).* © *1982 IEEE.*]

A typical tracking technique for FH spread spectrum signals is illustrated in Fig. 13-5-8(*a*). This method is also based on the premise that, although initial acquisition has been achieved, there is a small timing error between the received signal and the receiver clock. The bandpass filter is tuned to a single intermediate frequency and its bandwidth is of the order of $1/T_c$, where T_c is the chip interval. Its output is envelope-detected and then multiplied by the clock signal to produce a three-level signal, as shown in Fig. 13-5-8(*b*), which

drives the loop filter. Note that when the chip transitions from the locally generated sinusoidal waveform do not occur at the same time as the transitions in the incoming signal, the output of the loop filter will be either negative or positive, depending on whether the VCC is lagging or advanced relative to the timing of the input signal. This error signal from the loop filter will provide the control signal for adjusting the VCC timing signal so as to drive the frequency synthesized pulsed sinusoid to proper synchronism with the received signal.

13-6 BIBLIOGRAPHICAL NOTES AND REFERENCES

The introductory treatment of spread spectrum signals and their performance that we have given in this chapter is necessarily brief. Detailed and more specialized treatments of signal acquisition techniques, code tracking methods, and hybrid spread spectrum systems, as well as other general topics on spread spectrum signals and systems, can be found in the vast body of technical literature that now exists on the subject.

Historically, the primary application of spread spectrum communications has been in the development of secure (AJ) digital communication systems for military use. In fact, prior to 1970, most of the work on the design and development of spread spectrum communications was classified. Since then, this trend has been reversed. The open literature now contains numerous publications on all aspects of spread spectrum signal analysis and design. Moreover, we have recently seen publications dealing with the application of spread spectrum signaling techniques to commercial communications such as interoffice radio communications (see Pahlavan, 1985) and mobile-user radio communications (see Yue, 1983).

A historical perspective on the development of spread spectrum communication systems covering the period 1920–1960 is given in a paper by Scholtz (1982). Tutorial treatments focusing on the basic concepts are found in the papers by Scholtz (1977) and Pickholtz *et al.* (1982). These papers also contain a large number of references to previous work. In addition, there are two papers by Viterbi (1979, 1985) that provide a basic review of the performance characteristics of DS and FH signaling techniques.

Comprehensive treatments of various aspects of analysis and design of spread spectrum signals and systems, including synchronization techniques are now available in the texts by Simon *et al.* (1985), Ziemer and Peterson (1985), and Holmes (1982). In addition to these texts, there are several special issues of the *IEEE Transactions on Communications* devoted to spread spectrum communications (August 1977 and May 1982) and the *IEEE Transactions on Selected Areas in Communication* (September 1985, May 1989, May 1990, and June 1993). These issues contain a collection of papers devoted to a variety of topics, including multiple access techniques, synchronization techniques, and performance analyses with various types of interference. A number of important papers that have been published in IEEE journals have also been reprinted in book form by the IEEE Press (Dixon, 1976; Cook *et al.* 1983).

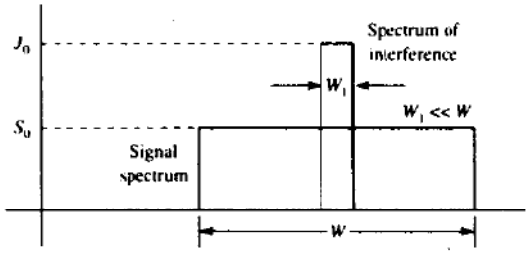

FIGURE P13-2

Finally, we recommend the book by Golomb (1967) as a basic reference on shift register sequences for the reader who wishes to delve deeper into this topic.

PROBLEMS

13-1 Following the procedure outlined in Example 13-2-2, determine the error rate performance of a DS spread spectrum system in the presence of CW jamming when the signal pulse is

$$g(t) = \sqrt{\frac{16\mathcal{E}_c}{3T_c}} \cos^2\left[\frac{\pi}{T_c}(t - \tfrac{1}{2}T_c)\right], \quad 0 \le t \le T_c$$

13-2 The sketch in Fig. P13-2 illustrates the power spectral densities of a PN spread spectrum signal and narrowband interference in an uncoded (trivial repetition code) digital communication system. Referring to Fig. 13-2-6, which shows the demodulator for this signal, sketch the (approximate) spectral characteristics of the signal and the interference after the multiplication of $r(t)$ with the output of the PN generator. Determine the fraction of the total interference that appears at the output of the correlator when the number of PN chips per bit is L_c.

13-3 Consider the concatenation of a Reed–Solomon $(31, 3)$ ($q = 32$-ary alphabet) as the outer code with a Hadamard $(16, 5)$ binary code as the inner code in a DS spread spectrum system. Assume that soft-decision decoding is performed on both codes. Determine an upper (union) bound on the probability of a bit error based on the minimum distance of the concatenated code.

13-4 The Hadamard $(n, k) = (2^m, m + 1)$ codes are low-rate codes with $d_{\min} = 2^{m-1}$. Determine the performance of this class of codes for DS spread spectrum signals with binary PSK modulation and either soft-decision or hard-decision decoding.

13-5 A rate 1/2 convolutional code with $d_{\text{free}} = 10$ is used to encode a data sequence occurring at a rate of 1000 bits/s. The modulation is binary PSK. The DS spread-spectrum sequence has a chip rate of 10 MHz.

a Determine the coding gain.

b Determine the processing gain.

c Determine the jamming margin assuming an $\mathcal{E}_b/J_0 = 10$.

13-6 A total of 30 equal-power users are to share a common communication channel by CDMA. Each user transmits information at a rate of 10 kbits/s via DS spread-spectrum and binary PSK. Determine the minimum chip rate to obtain a bit error

probability of 10^{-5}. Additive noise at the receiver may be ignored in this computation.

13-7 A CDMA system is designed based on DS spread spectrum with a processing gain of 1000 and binary PSK modulation. Determine the number of users if each user has equal power and the desired level of performance is an error probability of 10^{-6}. Repeat the computation if the processing gain is changed to 500.

13-8 A DS spread-spectrum system transmits at a rate of 1000 bits/s in the presence of a tone jammer. The jammer power is 20 dB greater than the desired signal and the required $\mathscr{E}_b/J_0$ to achieve satisfactory performance is 10 dB.

a Determine the spreading bandwidth required to meet the specifications.

b If the jammer is a pulse jammer, determine the pulse duty cycle that results in worst-case jamming and the corresponding probability of error.

13-9 A CDMA system consists of 15 equal-power users that transmit information at a rate of 10 000 bits/s, each using a DS spread spectrum signal operating at a chip rate of 1 MHz. The modulation is binary PSK.

a Determine the $\mathscr{E}_b/J_0$, where J_0 is the spectral density of the combined interference.

b What is the processing gain?

c How much should the processing gain be increased to allow for doubling the number of users without affecting the output SNR?

13-10 A DS binary PSK spread spectrum signal has a processing gain of 500. What is the jamming margin against a continuous-tone jammer if the desired error probability is 10^{-5}?

13-11 Repeat Problem 13-10 if the jammer is a pulsed-noise jammer with a duty cycle of 1%.

13-12 Consider the DS spread spectrum signal

$$c(t) = \sum_{n=-\infty}^{\infty} c_n p(t - nT_c)$$

where c_n is a periodic m sequence with a period $N = 127$ and $p(t)$ is a rectangular pulse of duration $T_c = 1\ \mu$s. Determine the power spectral density of the signal $c(t)$.

13-13 Suppose that $\{c_{1i}\}$ and $\{c_{2i}\}$ are two binary (0, 1) periodic sequences with periods N_1 and N_2, respectively. Determine the period of the sequence obtained by forming the modulo-2 sum of $\{c_{1i}\}$ and $\{c_{2i}\}$.

13-14 An $m = 10$ ML shift register is used to generate the pseudorandom sequence in a DS spread spectrum system. The chip duration is $T_c = 1\ \mu$s, and the bit duration is $T_b = NT_c$, where N is the length (period) of the m sequence.

a Determine the processing gain of the system in dB.

b Determine the jamming margin if the required $\mathscr{E}_b/J_0 = 10$ and the jammer is a tone jammer with an average power J_{av}.

13-15 A FH binary orthogonal FSK system employs an $m = 15$ stage linear feedback shift register that generates an ML sequence. Each state of the shift register selects one of L nonoverlapping frequency bands in the hopping pattern. The bit rate is 100 bits/s and the hop rate is once per bit. The demodulator employs noncoherent detection.

a Determine the hopping bandwidth for this channel.

b What is the processing gain?

c What is the probability of error in the presence of AWGN?

13-16 Consider the FH binary orthogonal FSK system described in Problem 13-15. Suppose that the hop rate is increased to 2 hops/bit. The receiver uses square-law combining to combine the signal over the two hops.
- **a** Determine the hopping bandwidth for the channel.
- **b** What is the processing gain?
- **c** What is the error probability in the presence of AWGN?

13-17 In a fast FH spread-spectrum system, the information is transmitted via FSK, with noncoherent detection. Suppose there are $N = 3$ hops/bit, with hard-decision decoding of the signal in each hop.
- **a** Determine the probability of error for this system in an AWGN channel with power spectral density $\frac{1}{2}N_0$ and an SNR = 13 dB (total SNR over the three hops).
- **b** Compare the result in (a) with the error probability of a FH spread-spectrum system that hops once per bit.

13-18 A slow FH binary FSK system with noncoherent detection operates at $\mathscr{E}_b/J_0 = 10$, with a hopping bandwidth of 2 GHz, and a bit rate of 10 kbits/s.
- **a** What is the processing gain for the system?
- **b** If the jammer operates as a partial-band jammer, what is the bandwidth occupancy for worst-case jamming?
- **c** What is the probability of error for the worst-case partial-band jammer?

13-19 Determine the error probability for a FH spread spectrum signal in which a binary convolutional code is used in combination with binary FSK. The interference on the channel is AWGN. The FSK demodulator outputs are square-law detected and passed to the decoder, which performs optimum soft-decision Viterbi decoding as described in Section 8-2. Assume that the hopping rate is 1 hop per coded bit.

13-20 Repeat Problem 13-19 for hard-decision Viterbi decoding.

13-21 Repeat Problem 13-19 when fast frequency hopping is performed at a hopping rate of L hops per coded bit.

13-22 Repeat Problem 13-19 when fast frequency hopping is performed with L hops per coded bit and the decoder is a hard-decision Viterbi decoder. The L chips per coded bit are square-law-detected and combined prior to the hard decision.

13-23 The TATS signal described in Section 13-3-3 is demodulated by a parallel bank of eight matched filters (octal FSK), and each filter output is square-law-detected. The eight outputs obtained in each of seven signal intervals (56 total outputs) are used to form the 64 possible decision variables corresponding to the Reed-Solomon (7, 2) code. Determine an upper (union) bound of the code word error probability for AWGN and soft-decision decoding.

13-24 Repeat Problem 13-23 for the worst-case partial-band interference channel.

13-25 Derive the results in (13-2-62) and (13-2-63) from (13-2-61).

13-26 Show that (13-3-14) follows from (13-3-13).

13-27 Derive (13-3-17) from (13-3-16).

13-28 The generator polynomials for constructing Gold code sequences of length $n = 7$ are

$$g_1(p) = p^3 + p + 1$$
$$g_2(p) = p^3 + p^2 + 1$$

Generate all the Gold codes of length 7 and determine the cross-correlations of one sequence with each of the others.

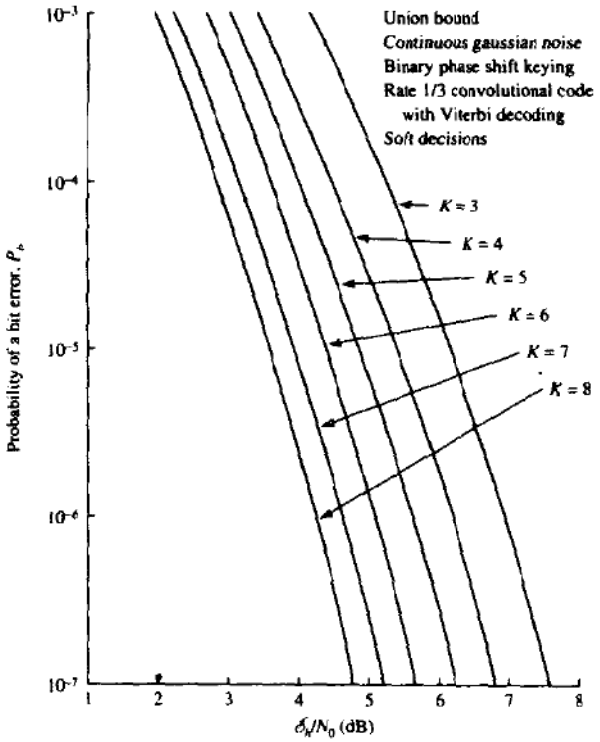

FIGURE P13-29

13-29 In Section 13-2-3, we demonstrated techniques for evaluating the error probability of a coded system with interleaving in pulse interference by using the cutoff rate parameter R_0. Use the error probability curves given in Fig. P13-29 for rate 1/2 and 1/3 convolutional codes with soft-decision Viterbi decoding to determine the corresponding error rates for a coded system in pulse interference. Perform this computation for $K = 3$, 5, and 7.

13-30 In coded and interleaved DS binary PSK modulation with pulse jamming and soft-decision decoding, the cutoff rate is

$$R_0 = 1 - \log_2 (1 + \alpha e^{-\alpha \mathscr{E}_c/N_0})$$

where α is the fraction of the time the system is being jammed, $\mathscr{E}_c = \mathscr{E}_b R$, R is the bit rate, and $N_0 \equiv J_0$.

a Show that the SNR per bit, $\mathscr{E}_b/N_0$, can be expressed as

$$\frac{\mathscr{E}_b}{N_0} = \frac{1}{\alpha R} \ln \frac{\alpha}{2^{1-R_0} - 1}$$

b Determine the value of α that maximizes the required $\mathscr{E}_b/N_0$ (worst-case pulse jamming) and the resulting maximum value of $\mathscr{E}_b/N_0$.

b Plot the graph of $10 \log (\mathscr{E}_b/rN_0)$ versus R_0, where $r = R_0/R$, for worst-case pulse jamming and for AWGN ($\alpha = 1$). What conclusions do you reach regarding the effect of worst-case pulse jamming?

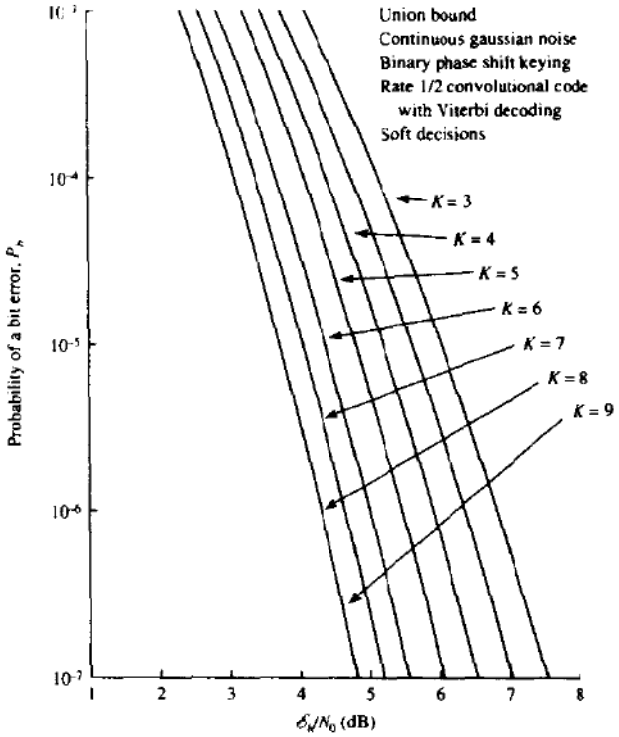

FIGURE P13-29 (*Continued*).

13-31 In a coded and interleaved frequency-hopped q-ary FSK modulation with partial band jamming and coherent demodulation with soft-decision decoding, the cutoff rate is

$$R_0 = \log_2 \left[\frac{q}{1 + (q-1)\alpha e^{-\alpha \mathscr{E}_c/2N_0}} \right]$$

where α is the fraction of the band being jammed, $\mathscr{E}_c$ is the chip (or tone) energy, and $N_0 = J_0$.

a Show that the SNR per bit can be expressed as

$$\frac{\mathscr{E}_b}{N_0} = \frac{2}{\alpha R} \ln \frac{(q-1)\alpha}{q2^{-R_0} - 1}$$

b Determine the value of α that maximizes the required $\mathscr{E}_b/N_0$ (worst-case partial band jamming) and the resulting maximum value of $\mathscr{E}_b/N_0$.

c Define $r = R_0/R$ in the result for $\mathscr{E}_b/N_0$ from (b), and plot $10 \log (\mathscr{E}_b/rN_0)$ versus the normalized cutoff rate $R_0/\log_2 q$ for $q = 2, 4, 8, 16, 32$. Compare these graphs with the results of Problem 13-30(c). What conclusions do you reach regarding the effect of worst-case partial band jamming? What is the effect of increasing the alphabet size q? What is the penalty in SNR between the results in Problem 13-30(c) and q-ary FSK as $q \to \infty$?

14

DIGITAL COMMUNICATION THROUGH FADING MULTIPATH CHANNELS

The previous chapters have described the design and performance of digital communications systems for transmission on either the classical AWGN channel or a linear filter channel with AWGN. We observed that the distortion inherent in linear filter channels requires special signal design techniques and rather sophisticated adaptive equalization algorithms in order to achieve good performance.

In this chapter, we consider the signal design, receiver structure, and receiver performance for more complex channels, namely, channels having randomly time-variant impulse responses. This characterization serves as a model for signal transmission over many radio channels such as shortwave ionospheric radio communication in the 3–30 MHz frequency band (HF), tropospheric scatter (beyond-the-horizon) radio communications in the 300–3000 MHz frequency band (UHF) and 3000–30 000 MHz frequency band (SHF), and ionospheric forward scatter in the 30–300 MHz frequency band (VHF). The time-variant impulse responses of these channels are a consequence of the constantly changing physical characteristics of the media. For example, the ions in the ionospheric layers that reflect the signals transmitted in the HF frequency band are always in motion. To the user of the channel, the motion of the ions appears to be random. Consequently, if the same signal is transmitted at HF in two widely separated time intervals, the two received signals will be different. The time-varying responses that occur are treated in statistical terms.

We shall begin our treatment of digital signalling over fading multipath channels by first developing a statistical characterization of the channel. Then we shall evaluate the performance of several basic digital signaling techniques for communication over such channels. The performance results will demons-

trate the severe penalty in SNR that must be paid as a consequence of the fading characteristics of the received signal. We shall then show that the penalty in SNR can be dramatically reduced by means of efficient modulation/coding and demodulation/decoding techniques.

14-1 CHARACTERIZATION OF FADING MULTIPATH CHANNELS

If we transmit an extremely short pulse, ideally an impulse, over a time-varying multipath channel, the received signal might appear as a train of pulses, as shown in Fig. 14-1-1. Hence, one characteristic of a multipath medium is the time spread introduced in the signal that is transmitted through the channel.

A second characteristic is due to the time variations in the structure of the medium. As a result of such time variations, the nature of the multipath varies with time. That is, if we repeat the pulse-sounding experiment over and over, we shall observe changes in the received pulse train, which will include changes in the sizes of the individual pulses, changes in the relative delays among the pulses, and, quite often, changes in the number of pulses observed in the received pulse train as shown in Fig. 14-1-1. Moreover, the time variations appear to be unpredictable to the user of the channel. Therefore, it is reasonable to characterize the time-variant multipath channel statistically.

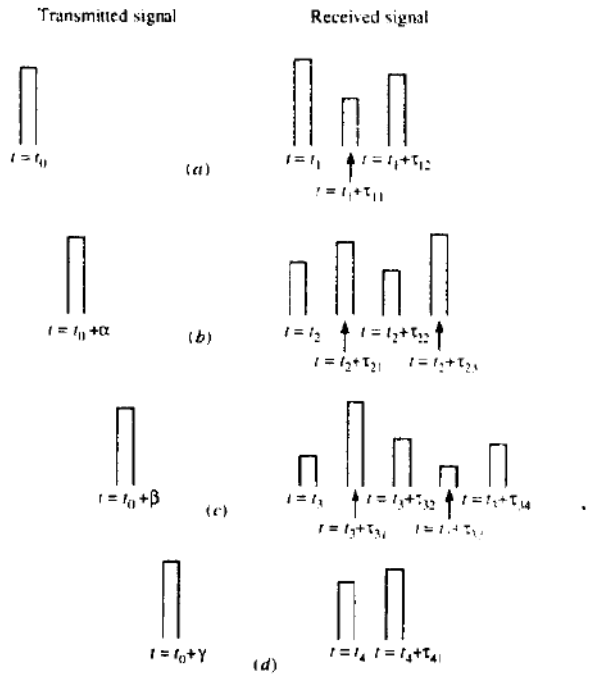

FIGURE 14-1-1 Example of the response of a time-variant multipath channel to a very narrow pulse.

Toward this end, let us examine the effects of the channel on a transmitted signal that is represented in general as

$$s(t) = \text{Re}\left[s_l(t)e^{j2\pi f_c t}\right] \tag{14-1-1}$$

We assume that there are multiple propagation paths. Associated with each path is a propagation delay and an attenuation factor. Both the propagation delays and the attenuation factors are time-variant as a result of changes in the structure of the medium. Thus, the received bandpass signal may be expressed in the form

$$x(t) = \sum_n \alpha_n(t)s(t - \tau_n(t)) \tag{14-1-2}$$

where $\alpha_n(t)$ is the attenuation factor for the signal received on the nth path and $\tau_n(t)$ is the propagation delay for the nth path. Substitution for $s(t)$ from (14-1-1) into (14-1-2) yields the result

$$x(t) = \text{Re}\left\{\left[\sum_n \alpha_n(t)e^{-j2\pi f_c \tau_n(t)}s_l(t - \tau_n(t))\right]e^{j2\pi f_c t}\right\} \tag{14-1-3}$$

It is apparent from (14-1-3) that the equivalent lowpass received signal is

$$r_l(t) = \sum_n \alpha_n(t)e^{-j2\pi f_c \tau_n(t)}s_l(t - \tau_n(t)) \tag{14-1-4}$$

Since $r_l(t)$ is the response of an equivalent lowpass channel to the equivalent lowpass signal $s_l(t)$, it follows that the equivalent lowpass channel is described by the time-variant impulse response

$$c(\tau; t) = \sum_n \alpha_n(t)e^{-j2\pi f_c \tau_n(t)}\delta(\tau - \tau_n(t)) \tag{14-1-5}$$

For some channels, such as the tropospheric scatter channel, it is more appropriate to view the received signal as consisting of a continuum of multipath components. In such a case, the received signal $x(t)$ is expressed in the integral form

$$x(t) = \int_{-\infty}^{\infty} \alpha(\tau; t)s(t - \tau)\,d\tau \tag{14-1-6}$$

where $\alpha(\tau; t)$ denotes the attenuation of the signal components at delay τ and at time instant t. Now substitution for $s(t)$ from (14-1-1) into (14-1-6) yields

$$x(t) = \text{Re}\left\{\left[\int_{-\infty}^{\infty} \alpha(\tau; t)e^{-j2\pi f_c \tau}s_l(t - \tau)\,d\tau\right]e^{j2\pi f_c t}\right\} \tag{14-1-7}$$

Since the integral in (14-1-7) represents the convolution of $s_l(t)$ with an equivalent lowpass time-variant impulse response $c(\tau; t)$, it follows that

$$c(\tau; t) = \alpha(\tau; t)e^{-j2\pi f_c \tau} \tag{14-1-8}$$

where $c(\tau; t)$ represents the response of the channel at time t due to an impulse applied at time $t - \tau$. Thus (14-1-8) is the appropriate definition of the equivalent lowpass impulse response when the channel results in continuous multipath and (14-1-5) is appropriate for a channel that contains discrete multipath components.

Now let us consider the transmission of an unmodulated carrier at frequency f_c. Then $s_l(t) = 1$ for all t, and, hence, the received signal for the case of discrete multipath, given by (14-1-4), reduces to

$$r_l(t) = \sum_n \alpha_n(t) e^{-j2\pi f_c \tau_n(t)}$$

$$= \sum_n \alpha_n(t) e^{-j\theta_n(t)} \qquad (14\text{-}1\text{-}9)$$

where $\theta_n(t) = 2\pi f_c \tau_n(t)$. Thus, the received signal consists of the sum of a number of time-variant vectors (phasors) having amplitudes $\alpha_n(t)$ and phases $\theta_n(t)$. Note that large dynamic changes in the medium are required for $\alpha_n(t)$ to change sufficiently to cause a significant change in the received signal. On the other hand, $\theta_n(t)$ will change by 2π rad whenever τ_n changes by $1/f_c$. But $1/f_c$ is a small number and, hence, θ_n can change by 2π rad with relatively small motions of the medium. We also expect the delays $\tau_n(t)$ associated with the different signal paths to change at different rates and in an unpredictable (random) manner. This implies that the received signal $r_l(t)$ in (14-1-9) can be modeled as a random process. When there are a large number of paths, the central limit theorem can be applied. That is, $r_l(t)$ may be modeled as a complex-valued gaussian random process. This means that the time-variant impulse response $c(\tau; t)$ is a complex-valued gaussian random process in the t variable.

The multipath propagation model for the channel embodied in the received signal $r_l(t)$, given in (14-1-9), results in signal fading. The fading phenomenon is primarily a result of the time variations in the phases $\{\theta_n(t)\}$. That is, the randomly time-variant phases $\{\theta_n(t)\}$ associated with the vectors $\{\alpha_n e^{-j\theta_n}\}$ at times result in the vectors adding destructively. When that occurs, the resultant received signal $r_l(t)$ is very small or practically zero. At other times, the vectors $\{\alpha_n e^{-j\theta_n}\}$ add constructively, so that the received signal is large. Thus, the amplitude variations in the received signal, termed *signal fading*, are due to the time-variant multipath characteristics of the channel.

When the impulse response $c(\tau; t)$ is modeled as a zero-mean complex-valued gaussian process, the envelope $|c(\tau; t)|$ at any instant t is Rayleigh-distributed. In this case the channel is said to be a *Rayleigh fading channel.* In the event that there are fixed scatterers or signal reflectors in the medium, in addition to randomly moving scatterers, $c(\tau; t)$ can no longer be modeled as having zero mean. In this case, the envelope $|c(\tau; t)|$ has a Rice distribution and the channel is said to be a *Ricean fading channel.* Another probability distribution function that has been used to model the envelope of fading

signals is the Nakagami-m distribution. These fading channel models are considered in Section 14-1-2.

14-1-1 Channel Correlation Functions and Power Spectra

We shall now develop a number of useful correlation functions and power spectral density functions that define the characteristics of a fading multipath channel. Our starting point is the equivalent lowpass impulse response $c(\tau; t)$, which is characterized as a complex-valued random process in the t variable. We assume that $c(\tau; t)$ is wide-sense-stationary. Then we define the autocorrelation function of $c(\tau; t)$ as

$$\phi_c(\tau_1, \tau_2; \Delta t) = \tfrac{1}{2}E[c^*(\tau_1; t)c(\tau_2; t + \Delta t)] \tag{14-1-10}$$

In most radio transmission media, the attenuation and phase shift of the channel associated with path delay τ_1 is uncorrelated with the attenuation and phase shift associated with path delay τ_2. This is usually called *uncorrelated scattering*. We make the assumption that the scattering at two different delays is uncorrelated and incorporate it into (14-1-10) to obtain

$$\tfrac{1}{2}E[c^*(\tau_1; t)c(\tau_2; t + \Delta t)] = \phi_c(\tau_1; \Delta t)\delta(\tau_1 - \tau_2) \tag{14-1-11}$$

If we let $\Delta t = 0$, the resulting autocorrelation function $\phi_c(\tau; 0) \equiv \phi_c(\tau)$ is simply the average power output of the channel as a function of the time delay τ. For this reason, $\phi_c(\tau)$ is called the *multipath intensity profile* or *the delay power spectrum* of the channel. In general, $\phi_c(\tau; \Delta t)$ gives the average power output as a function of the time delay τ and the difference Δt in observation time.

In practice, the function $\phi_c(\tau; \Delta t)$ is measured by transmitting very narrow pulses or, equivalently, a wideband signal and cross-correlating the received signal with a delayed version of itself. Typically, the measured function $\phi_c(\tau)$ may appear as shown in Fig. 14-1-2. The range of values of τ over which $\phi_c(\tau)$

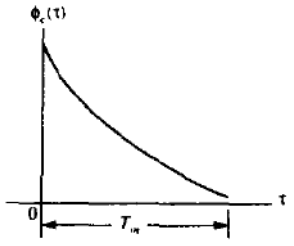

FIGURE 14-1-2 Multipath intensity profile.

is essentially nonzero is called the *multipath spread of the channel* and is denoted by T_m.

A completely analogous characterization of the time-variant multipath channel begins in the frequency domain. By taking the Fourier transform of $c(\tau; t)$ we obtain the time-variant transfer function $C(f; t)$, where f is the frequency variable. Thus,

$$C(f; t) = \int_{-\infty}^{\infty} c(\tau; t) e^{-j2\pi f\tau}\, d\tau \tag{14-1-12}$$

If $c(\tau; t)$ is modeled as a complex-valued zero-mean gaussian random process in the t variable, it follows that $C(f; t)$ also has the same statistics. Under the assumption that the channel is wide-sense-stationary, we define the autocorrelation function

$$\phi_C(f_1, f_2; \Delta t) = \tfrac{1}{2} E[C^*(f_1; t) C(f_2; t + \Delta t)] \tag{14-1-13}$$

Since $C(f; t)$ is the Fourier transform of $c(\tau; t)$, it is not surprising to find that $\phi_C(f_1, f_2; \Delta t)$ is related to $\phi_C(\tau; \Delta t)$ by the Fourier transform. The relationship is easily established by substituting (14-1-12) into (14-1-13). Thus,

$$\begin{aligned}
\phi_C(f_1, f_2; \Delta t) &= \tfrac{1}{2} \int_{-\infty}^{\infty} \int_{-\infty}^{\infty} E[c^*(\tau_1; t) c(\tau_2; t + \Delta t)] e^{j2\pi(f_1\tau_1 - f_2\tau_2)}\, d\tau_1\, d\tau_2 \\
&= \int_{-\infty}^{\infty} \int_{-\infty}^{\infty} \phi_c(\tau_1; \Delta t) \delta(\tau_1 - \tau_2) e^{j2\pi(f_1\tau_1 - f_2\tau_2)}\, d\tau_1\, d\tau_2 \\
&= \int_{-\infty}^{\infty} \phi_c(\tau_1; \Delta t) e^{j2\pi(f_1 - f_2)\tau_1}\, d\tau_1 \\
&= \int_{-\infty}^{\infty} \phi_c(\tau_1; \Delta t) e^{-j2\pi \Delta f \tau_1}\, d\tau_1 \equiv \phi_C(\Delta f; \Delta t)
\end{aligned} \tag{14-1-14}$$

where $\Delta f = f_2 - f_1$. From (14-1-14), we observe that $\phi_C(\Delta f; \Delta t)$ is the Fourier transform of the multipath intensity profile. Furthermore, the assumption of uncorrelated scattering implies that the autocorrelation function of $C(f; t)$ in frequency is a function of only the frequency difference $\Delta f = f_2 - f_1$. Therefore, it is appropriate to call $\phi_C(\Delta f; \Delta t)$ the *spaced-frequency, spaced-time correlation function of the channel.* It can be measured in practice by transmitting a pair of sinusoids separated by Δf and cross-correlating the two separately received signals with a relative delay Δt.

Suppose we set $\Delta t = 0$ in (14-1-14). Then, with $\phi_C(\Delta f; 0) \equiv \phi_C(\Delta f)$ and $\phi_c(\tau; 0) \equiv \phi_c(\tau)$, the transform relationship is simply

$$\phi_C(\Delta f) = \int_{-\infty}^{\infty} \phi_c(\tau) e^{-j2\pi \Delta f \tau}\, d\tau \tag{14-1-15}$$

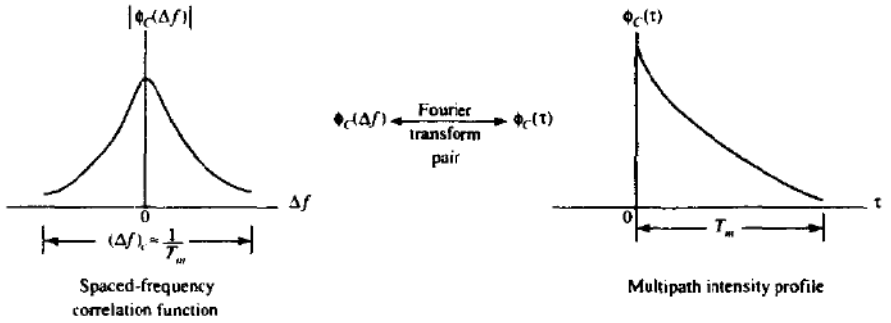

FIGURE 14-1-3 Relationship between $\phi_C(\Delta f)$ and $\phi_c(\tau)$.

The relationship is depicted graphically in Fig. 14-1-3. Since $\phi_C(\Delta f)$ is an autocorrelation function in the frequency variable, it provides us with a measure of the frequency coherence of the channel. As a result of the Fourier transform relationship between $\phi_C(\Delta f)$ and $\phi_c(\tau)$, the reciprocal of the multipath spread is a measure of the *coherence bandwidth of the channel.* That is,

$$(\Delta f)_c \approx \frac{1}{T_m} \tag{14-1-16}$$

where $(\Delta f)_c$ denotes the coherence bandwidth. Thus, two sinusoids with frequency separation greater than $(\Delta f)_c$ are affected differently by the channel. When an information-bearing signal is transmitted through the channel, if $(\Delta f)_c$ is small in comparison to the bandwidth of the transmitted signal, the channel is said to be *frequency-selective.* In this case, the signal is severely distorted by the channel. On the other hand, if $(\Delta f)_c$ is large in comparison with the bandwidth of the transmitted signal, the channel is said to be *frequency-nonselective.*

We now focus our attention on the time variations of the channel as measured by the parameter Δt in $\phi_C(\Delta f; \Delta t)$. The time variations in the channel are evidenced as a Doppler broadening and, perhaps, in addition as a Doppler shift of a spectral line. In order to relate the Doppler effects to the time variations of the channel, we define the Fourier transform of $\phi_C(\Delta f; \Delta t)$ with respect to the variable Δt to be the function $S_C(\Delta f; \lambda)$. That is,

$$S_C(\Delta f; \lambda) = \int_{-\infty}^{\infty} \phi_C(\Delta f; \Delta t) e^{-j2\pi\lambda\,\Delta t}\, d\Delta t \tag{14-1-17}$$

With Δf set to zero and $S_C(0; \lambda) \equiv S_C(\lambda)$, the relation in (14-1-17) becomes

$$S_C(\lambda) = \int_{-\infty}^{\infty} \phi_C(\Delta t) e^{-j2\pi\lambda\,\Delta t}\, d\Delta t \tag{14-1-18}$$

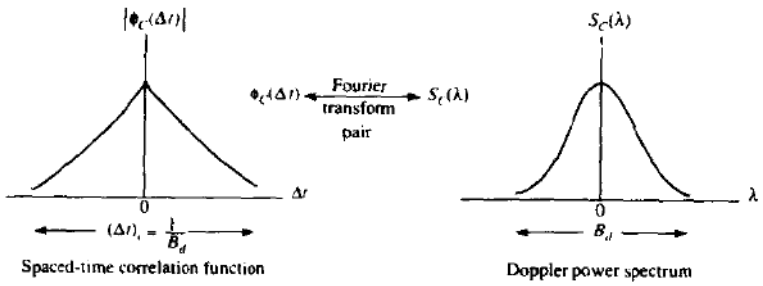

FIGURE 14-1-4 Relationship between $\phi_C(\Delta t)$ and $S_C(\lambda)$.

The function $S_C(\lambda)$ is a power spectrum that gives the signal intensity as a function of the Doppler frequency λ. Hence, we call $S_C(\lambda)$ the *Doppler power spectrum of the channel.*

From (14-1-18), we observe that if the channel is time-invariant, $\phi_C(\Delta t) = 1$ and $S_C(\lambda)$ becomes equal to the delta function $\delta(\lambda)$. Therefore, when there are no time variations in the channel, there is no spectral broadening observed in the transmission of a pure frequency tone.

The range of values of λ over which $S_C(\lambda)$ is essentially nonzero is called the *Doppler spread B_d of the channel.* Since $S_C(\lambda)$ is related to $\phi_C(\Delta t)$ by the Fourier transform, the reciprocal of B_d is a measure of the coherence time of the channel. That is,

$$(\Delta t)_c \approx \frac{1}{B_d} \tag{14-1-19}$$

where $(\Delta t)_c$ denotes the *coherence time.* Clearly, a slowly changing channel has a large coherence time or, equivalently, a small Doppler spread. Figure 14-1-4 illustrates the relationship between $\phi_C(\Delta t)$ and $S_C(\lambda)$.

We have now established a Fourier transform relationship between $\phi_C(\Delta f; \Delta t)$ and $\phi_c(\tau; \Delta t)$ involving the variables $(\tau, \Delta f)$, and a Fourier transform relationship between $\phi_C(\Delta f; \Delta t)$ and $S_C(\Delta f; \lambda)$ involving the variables $(\Delta t, \lambda)$. There are two additional Fourier transform relationships that we can define, which serve to relate $\phi_c(\tau; \Delta t)$ to $S_C(\Delta f; \lambda)$ and, thus, close the loop. The desired relationship is obtained by defining a new function, denoted by $S(\tau; \lambda)$, to be the Fourier transform of $\phi_c(\tau; \Delta t)$ in the Δt variable. That is,

$$S(\tau; \lambda) = \int_{-\infty}^{\infty} \phi_c(\tau; \Delta t) e^{-j2\pi\lambda\,\Delta t}\, d\Delta t \tag{14-1-20}$$

It follows that $S(\tau; \lambda)$ and $S_C(\Delta f; \lambda)$ are a Fourier transform pair. That is,

$$S(\tau; \lambda) = \int_{-\infty}^{\infty} S_C(\Delta f; \lambda) e^{j2\pi\tau\,\Delta f}\, d\Delta f \tag{14-1-21}$$

Furthermore, $S(\tau; \lambda)$ and $\phi_C(\Delta f; \Delta t)$ are related by the double Fourier transform

$$S(\tau; \lambda) = \int_{-\infty}^{\infty} \int_{-\infty}^{\infty} \phi_C(\Delta f; \Delta t) e^{-j2\pi\lambda \Delta t} e^{j2\pi\tau \Delta f} d\Delta t \, d\Delta f \qquad (14\text{-}1\text{-}22)$$

This new function $S(\tau; \lambda)$ is called the *scattering function of the channel.* It provides us with a measure of the average power output of the channel as a function of the time delay τ and the Doppler frequency λ.

The relationships among the four functions $\phi_C(\Delta f; \Delta t)$, $\phi_c(\tau; \Delta t)$, $\phi_C(\Delta f; \lambda)$, and $S(\tau; \lambda)$ are summarized in Fig. 14-1-5.

FIGURE 14-1-5 Relationships among the channel correlation functions and power spectra. [*From Green (1962), with permission.*]

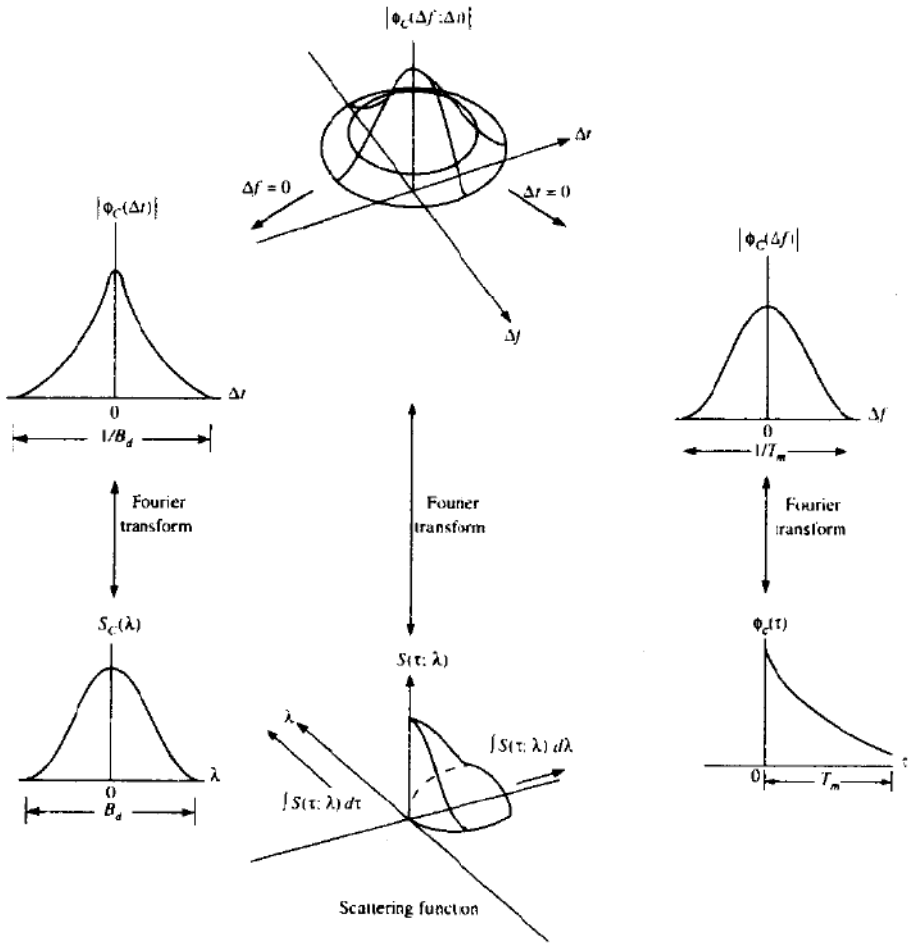

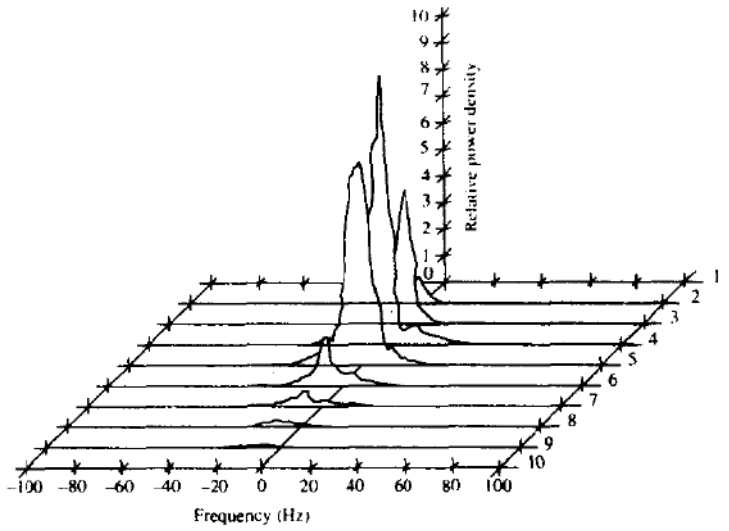

FIGURE 14-1-6 Scattering function of a medium-range tropospheric scatter channel. The taps delay increment is 0.1 μs.

The scattering function $S(\tau; \lambda)$ measured on a 150 mi tropospheric scatter link is shown in Fig. 14-1-6. The signal used to probe the channel had a time resolution of 0.1 μs. Hence, the time-delay axis is quantized in increments of 0.1 μs. From the graph, we observe that the multipath spread $T_m = 0.7$ μs. On the other hand, the Doppler spread, which may be defined as the 3 dB bandwidth of the power spectrum for each signal path, appears to vary with each signal path. For example, in one path it is less than 1 Hz, while in some other paths it is several hertz. For our purposes, we shall take the largest of these 3 dB bandwidths of the various paths and call that the *Doppler spread.*

14-1-2 Statistical Models for Fading Channels

There are several probability distributions that can be considered in attempting to model the statistical characteristics of the fading channel. When there are a large number of scatterers in the channel that contribute to the signal at the receiver, as is the case in ionospheric or tropospheric signal propagation, application of the central limit theorem leads to a gaussian process model for the channel impulse response. If the process is zero-mean, then the envelope of the channel response at any time instant has a Rayleigh probability distribution and the phase is uniformly distributed in the interval $(0, 2\pi)$. That is,

$$p_R(r) = \frac{2r}{\Omega} e^{-r^2/\Omega}, \quad r \geq 0 \tag{14-1-23}$$

where

$$\Omega = E(R^2) \tag{14-1-24}$$

We observe that the Rayleigh distribution is characterized by the single parameter $E(R^2)$.

An alternative statistical model for the envelope of the channel response is the Nakagami-m distribution given by the pdf in (2-1-147). In constrast to the Rayleigh distribution, which has a single parameter that can be used to match the fading channel statistics, the Nakagami-m is a two-parameter distribution, namely, involving the parameter m and the second moment $\Omega = E(R^2)$. As a consequence, this distribution provides more flexibility and accuracy in matching the observed signal statistics. The Nakagami-m distribution can be used to model fading channel conditions that are either more or less severe than the Rayleigh distribution, and it includes the Rayleigh distribution as a special case ($m = 1$). For example, Turin (1972) and Suzuki (1977) have shown that the Nakagami-m distribution is the best fit for data signals received in urban radio multipath channels.

The Rice distribution is also a two-parameter distribution. It may be expressed by the pdf given in (2-1-141), where the parameters are s and σ^2. Recall that s^2 is called the *noncentrality parameter* in the equivalent chi-square distribution. It represents the power in the nonfading signal components, sometimes called *specular components*, of the received signal.

There are many radio channels in which fading is encountered that are basically line-of-sight (LOS) communication links with multipath components arising from secondary reflections, or signal paths, from surrounding terrain. In such channels, the number of multipath components is small, and, hence, the channel may be modeled in a somewhat simpler form. We cite two channel models as examples.

As the first example, let us consider an airplane to ground communication link in which there is the direct path and a single multipath component at a delay t_0 relative to the direct path. The impulse response of such a channel may be modeled as

$$c(\tau; t) = \alpha\delta(\tau) + \beta(t)\delta(\tau - \tau_0(t)) \tag{14-1-25}$$

where α is the attenuation factor of the direct path and $\beta(t)$ represents the time-variant multipath signal component resulting from terrain reflections. Often, $\beta(t)$ can be characterized as a zero-mean gaussian random process. The transfer function for this channel model may be expressed as

$$C(f; t) = \alpha + \beta(t)e^{-j2\pi f\tau_0(t)} \tag{14-1-26}$$

This channel fits the Ricean fading model defined previously. The direct path with attenuation α represents the specular component and $\beta(t)$ represents the Rayleigh fading component.

A similar model has been found to hold for microwave LOS radio channels

used for long-distance voice and video transmission by telephone companies throughout the world. For such channels, Rummler (1979) has developed a three-path model based on channel measurements performed on typical LOS links in the 6 GHz frequency band. The differential delay on the two multipath components is relatively small, and, hence, the model developed by Rummler is one that has a channel transfer function

$$C(f) = a[1 - \beta e^{-j2\pi(f - f_0)\tau_0}] \tag{14-1-27}$$

where a is the overall attenuation parameter, β is called a shape parameter which is due to the multipath components, f_0 is the frequency of the fade minimum, and τ_0 is the relative time delay between the direct and the multipath components. This simplified model was used to fit data derived from channel measurements.

Rummler found that the parameters a and β may be characterized as random variables that, for practical purposes, are nearly statistically independent. From the channel measurements, he found that the distribution of β has the form $(1 - \beta)^{2.3}$. The distribution of a is well modeled by the lognormal distribution, i.e., $-\log a$ is gaussian. For $\beta > 0.5$, the mean of $-20 \log a$ was found to be 25 dB and the standard deviation was 5 dB. For smaller values of β, the mean decreases to 15 dB. The delay parameter determined from the measurements was $\tau_0 = 6.3$ ns. The magnitude-square response of $C(f)$ is

$$|C(f)|^2 = a^2[1 + \beta^2 - 2\beta \cos 2\pi(f - f_0)\tau_0] \tag{14-1-28}$$

$|C(f)|$ is plotted in Fig. 14-1-7 as a function of the frequency $f - f_0$ for $\tau_0 = 6.3$ ns. Note that the effect of the multipath component is to create a deep attenuation at $f = f_0$ and at multiples of $1/\tau_0 \approx 159$ MHz. By comparison, the typical channel bandwidth is 30 MHz. This model was used by Lundgren and Rummler (1979) to determine the error rate performance of digital radio systems.

FIGURE 14-1-7 Magnitude frequency response of LOS channel model

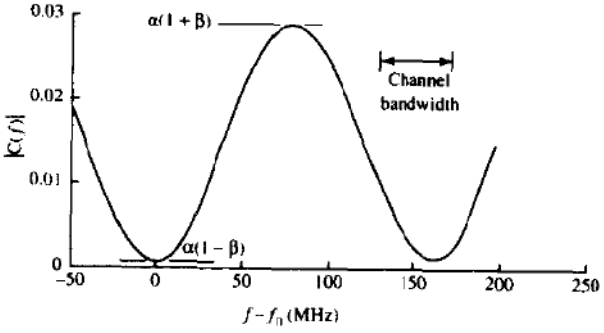

14-2 THE EFFECT OF SIGNAL CHARACTERISTICS ON THE CHOICE OF A CHANNEL MODEL

Having discussed the statistical characterization of time-variant multipath channels generally in terms of the correlation functions described in Section 14-1, we now consider the effect of signal characteristics on the selection of a channel model that is appropriate for the specified signal. Thus, let $s_l(t)$ be the equivalent lowpass signal transmitted over the channel and let $S_l(f)$ denote its frequency content. Then the equivalent lowpass received signal, exclusive of additive noise, may be expressed either in terms of the time domain variables $c(\tau; t)$ and $s_l(t)$ as

$$r_l(t) = \int_{-\infty}^{\infty} c(\tau; t) s_l(t - \tau)\, d\tau \tag{14-2-1}$$

or in terms of the frequency functions $C(f; t)$ and $S_l(f)$ as

$$r_l(t) = \int_{-\infty}^{\infty} C(f; t) S_l(f) e^{j2\pi ft}\, df \tag{14-2-2}$$

Suppose we are transmitting digital information over the channel by modulating (either in amplitude, or in phase, or both) the basic pulse $s_l(t)$ at a rate $1/T$, where T is the signaling interval. It is apparent from (14-2-2) that the time-variant channel characterized by the transfer function $C(f; t)$ distorts the signal $S_l(f)$. If $S_l(f)$ has a bandwidth W greater than the coherence bandwidth $(\Delta f)_c$ of the channel, $S_l(f)$ is subjected to different gains and phase shifts across the band. In such a case, the channel is said to be *frequency-selective*. Additional distortion is caused by the time variations in $C(f; t)$. This type of distortion is evidenced as a variation in the received signal strength, and has been termed *fading*. It should be emphasized that the frequency selectivity and fading are viewed as two different types of distortion. The former depends on the multipath spread or, equivalently, on the coherence bandwidth of the channel relative to the transmitted signal bandwidth W. The latter depends on the time variations of the channel, which are grossly characterized by the coherence time $(\Delta t)_c$ or, equivalently, by the Doppler spread B_d.

The effect of the channel on the transmitted signal $s_l(t)$ is a function of our choice of signal bandwidth and signal duration. For example, if we select the signaling interval T to satisfy the condition $T \gg T_m$, the channel introduces a negligible amount of intersymbol interference. If the bandwidth of the signal pulse $s_l(t)$ is $W \approx 1/T$, the condition $T \gg T_m$ implies that

$$W \ll \frac{1}{T_m} \approx (\Delta f)_c \tag{14-2-3}$$

That is, the signal bandwidth W is much smaller than the coherence bandwidth of the channel. Hence, the channel is frequency-nonselective. In other words,

all of the frequency components in $S_l(f)$ undergo the same attenuation and phase shift in transmission through the channel. But this implies that, within the bandwidth occupied by $S_l(f)$, the time-variant transfer function $C(f; t)$ of the channel is a complex-valued constant in the frequency variable. Since $S_l(f)$ has its frequency content concentrated in the vicinity of $f = 0$, $C(f; t) = C(0; t)$. Consequently, (14-2-2) reduces to

$$r_l(t) = C(0; t)\int_{-\infty}^{\infty} S_l(f)e^{j2\pi ft}\,df$$

$$= C(0; t)s_l(t) \tag{14-2-4}$$

Thus, when the signal bandwidth W is much smaller than the coherence bandwidth $(\Delta f)_c$ of the channel, the received signal is simply the transmitted signal multiplied by a complex-valued random process $C(0; t)$, which represents the time-variant characteristics of the channel. In this case, we say that the multipath components in the received are not resolvable because $W \ll (\Delta f)_c$.

The transfer function $C(0; t)$ for a frequency-nonselective channel may be expressed in the form

$$C(0; t) = \alpha(t)e^{-j\phi(t)} \tag{14-2-5}$$

where $\alpha(t)$ represents the envelope and $\phi(t)$ represents the phase of the equivalent lowpass channel. When $C(0; t)$ is modeled as a zero-mean complex-valued gaussian random process, the envelope $\alpha(t)$ is Rayleigh-distributed for any fixed value of t and $\phi(t)$ is uniformly distributed over the interval $(-\pi, \pi)$. The rapidity of the fading on the frequency-nonselective channel is determined either from the correlation function $\phi_C(\Delta t)$ or from the Doppler power spectrum $S_C(\lambda)$. Alternatively, either of the channel parameters $(\Delta t)_c$ or B_d can be used to characterize the rapidity of the fading.

For example, suppose it is possible to select the signal bandwidth W to satisfy the condition $W \ll (\Delta f)_c$ and the signaling interval T to satisfy the condition $T \ll (\Delta t)_c$. Since T is smaller than the coherence time of the channel, the channel attenuation and phase shift are essentially fixed for the duration of at least one signaling interval. When this condition holds, we call the channel a *slowly fading channel.* Furthermore, when $W \approx 1/T$, the conditions that the channel be frequency-nonselective and slowly fading imply that the product of T_m and B_d must satisfy the condition $T_m B_d < 1$.

The product $T_m B_d$ is called the *spread factor* of the channel. If $T_m B_d < 1$, the channel is said to be *underspread*; otherwise, it is *overspread.* The multipath spread, the Doppler spread, and the spread factor are listed in Table 14-2-1 for several channels. We observe from this table that several radio channels, including the moon when used as a passive reflector, are underspread. Consequently, it is possible to select the signal $s_l(t)$ such that these channels are frequency-nonselective and slowly fading. The slow-fading condition

TABLE 14-2-1 MULTIPATH SPREAD, DOPPLER SPREAD, AND SPREAD FACTOR FOR SEVERAL TIME-VARIANT MULTIPATH CHANNELS

Type of channel	Multipath duration	Doppler spread	Spread factor
Shortwave ionospheric propagation (HF)	10^{-3}–10^{-2}	10^{-1}–1	10^{-4}–10^{-2}
Ionospheric propagation under disturbed auroral conditions (HF)	10^{-3}–10^{-2}	10–100	10^{-2}–1
Ionospheric forward scatter (VHF)	10^{-4}	10	10^{-3}
Tropospheric scatter (SHF)	10^{-6}	10	10^{-5}
Orbital scatter (X band)	10^{-4}	10^{3}	10^{-1}
Moon at max. libration (f_0 = 0.4 kmc)	10^{-2}	10	10^{-1}

implies that the channel characteristics vary sufficiently slowly that they can be measured.

In Section 14-3, we shall determine the error rate performance for binary signaling over a frequency-nonselective slowly fading channel. This channel model is, by far, the simplest to analyze. More importantly, it yields insight into the performance characteristics for digital signaling on a fading channel and serves to suggest the type of signal waveforms that are effective in overcoming the fading caused by the channel.

Since the multipath components in the received signal are not resolvable when the signal bandwidth W is less than the coherence bandwidth $(\Delta f)_c$ of the channel, the received signal appears to arrive at the receiver via a single fading path. On the other hand, we may choose $W \gg (\Delta f)_c$, so that the channel becomes frequency-selective. We shall show later that, under this condition, the multipath components in the received signal are resolvable with a resolution in time delay of $1/W$. Thus, we shall illustrate that the frequency-selective channel can be modeled as a tapped delay line (transversal) filter with time-variant tap coefficients. We shall then derive the performance of binary signaling over such a frequency-selective channel model.

14-3 FREQUENCY-NONSELECTIVE, SLOWLY FADING CHANNEL

In this section, we derive the error rate performance of binary PSK and binary FSK when these signals are transmitted over a frequency-nonselective, slowly fading channel. As described in Section 14-2, the frequency-nonselective channel results in multiplicative distortion of the transmitted signal $s_l(t)$. Furthermore, the condition that the channel fades slowly implies that the multiplicative process may be regarded as a constant during at least one

signaling interval. Consequently, if the transmitted signal is $s_l(t)$, the received equivalent lowpass signal in one signaling interval is

$$r_l(t) = \alpha e^{-j\phi} s_l(t) + z(t), \quad 0 \le t \le T \tag{14-3-1}$$

where $z(t)$ represents the complex-valued white gaussian noise process corrupting the signal.

Let us assume that the channel fading is sufficiently slow that the phase shift ϕ can be estimated from the received signal without error. In that case, we can achieve ideal coherent detection of the received signal. Thus, the received signal can be processed by passing it through a matched filter in the case of binary PSK or through a pair of matched filters in the case of binary FSK. One method that we can use to determine the performance of the binary communications systems is to evaluate the decision variables and from these determine the probability of error. However, we have already done this for a fixed (time-invariant) channel. That is, for a fixed attenuation α, we have previously derived the probability of error for binary PSK and binary FSK. From (5-2-5), the expression for the error rate of binary PSK as a function of the received SNR γ_b is

$$P_2(\gamma_b) = Q(\sqrt{2\gamma_b}) \tag{14-3-2}$$

where $\gamma_b = \alpha^2 \mathscr{E}_b / N_0$. The expression for the error rate of binary FSK, detected coherently, is given by (5-2-10) as

$$P_2(\gamma_b) = Q(\sqrt{\gamma_b}) \tag{14-3-3}$$

We view (14-3-2) and (14-3-3) as conditional error probabilities, where the condition is that α is fixed. To obtain the error probabilities when α is random, we must average $P_2(\gamma_b)$, given in (14-3-2) and (14-3-3), over the probability density function of γ_b. That is, we must evaluate the integral

$$P_2 = \int_0^\infty P_2(\gamma_b) p(\gamma_b)\, d\gamma_b \tag{14-3-4}$$

where $p(\gamma_b)$ is the probability density function of γ_b when α is random.

Rayleigh Fading Since α is Rayleigh-distributed, α^2 has a chi-square probability distribution with two degrees of freedom. Consequently, γ_b also is chi-square-distributed. It is easily shown that

$$p(\gamma_b) = \frac{1}{\bar{\gamma}_b} e^{-\gamma_b/\bar{\gamma}_b}, \quad \gamma_b \ge 0 \tag{14-3-5}$$

where $\bar{\gamma}_b$ is the average signal-to-noise ratio, defined as

$$\bar{\gamma}_b = \frac{\mathscr{E}_b}{N_0} E(\alpha^2) \tag{14-3-6}$$

The term $E(\alpha^2)$ is simply the average value of α^2.

Now we can substitute (14-3-5) into (14-3-4) and carry out the integration for $P_2(\gamma_b)$ as given by (14-3-2) and (14-3-3). The result of this integration for binary PSK is

$$P_2 = \frac{1}{2}\left(1 - \sqrt{\frac{\bar{\gamma}_b}{1 + \bar{\gamma}_b}}\right) \tag{14-3-7}$$

If we repeat the integration with $P_2(\gamma_b)$ given by (14-3-3), we obtain the probability of error for binary FSK, detected coherently, in the form

$$P_2 = \frac{1}{2}\left(1 - \sqrt{\frac{\bar{\gamma}_b}{2 + \bar{\gamma}_b}}\right) \tag{14-3-8}$$

In arriving at the error rate results in (14-3-7) and (14-3-8), we have assumed that the estimate of the channel phase shift, obtained in the presence of slow fading, is noiseless. Such an ideal condition may not hold in practice. In such a case, the expressions in (14-3-7) and (14-3-8) should be viewed as representing the best achievable performance in the presence of Rayleigh fading. In Appendix C we consider the problem of estimating the phase in the presence of noise and we evaluate the error rate performance of binary and multiphase PSK.

On channels for which the fading is sufficiently rapid to preclude the estimation of a stable phase reference by averaging the received signal phase over many signaling intervals, DPSK, is an alternative signaling method. Since DPSK requires phase stability over only two consecutive signaling intervals, this modulation technique is quite robust in the presence of signal fading. In deriving the performance of binary DPSK for a fading channel, we begin again with the error probability for a nonfading channel, which is

$$P_2(\gamma_b) = \tfrac{1}{2}e^{-\gamma_b} \tag{14-3-9}$$

This expression is substituted into the integral in (14-3-4) along with $p(\gamma_b)$ obtained from (14-3-5). Evaluation of the resulting integral yields the probability of error for binary DPSK, in the form

$$P_2 = \frac{1}{2(1 + \bar{\gamma}_b)} \tag{14-3-10}$$

If we choose not to estimate the channel phase shift at all, but instead employ a noncoherent (envelope or square-law) detector with binary, orthogonal FSK signals, the error probability for a nonfading channel is

$$P_2(\gamma_b) = \tfrac{1}{2}e^{-\gamma_b/2} \tag{14-3-11}$$

When we average $P_2(\gamma_b)$ over the Rayleigh fading channel attenuation, the resulting error probability is

$$P_2 = \frac{1}{2 + \bar{\gamma}_b} \tag{14-3-12}$$

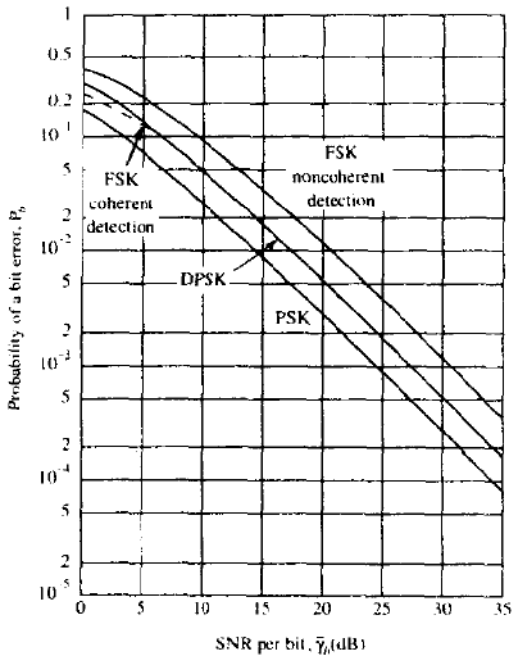

FIGURE 14-3-1 Performance of binary signaling on a Rayleigh fading channel.

The error probabilities in (14-3-7), (14-3-8), (14-3-10), and (14-3-12) are illustrated in Fig. 14-3-1. In comparing the performance of the four binary signaling systems, we focus our attention on the probabilities of error for large SNR, i.e., $\bar{\gamma}_b \gg 1$. Under this condition, the error rates in (14-3-7), (14-3-8), (14-3-10), and (14-3-12) simplify to

$$P_2 \approx \begin{cases} 1/4\bar{\gamma}_b & \text{for coherent PSK} \\ 1/2\bar{\gamma}_b & \text{for coherent, orthogonal FSK} \\ 1/2\bar{\gamma}_b & \text{for DPSK} \\ 1/\bar{\gamma}_b & \text{for noncoherent, orthogonal FSK} \end{cases} \tag{14-3-13}$$

From (14-3-13), we observe that coherent PSK is 3 dB better than DPSK and 6 dB better than noncoherent FSK. More striking, however, is the observation that the error rates decrease only inversely with SNR. In contrast, the decrease in error rate on a nonfading channel is exponential with SNR. This means that, on a fading channel, the transmitter must transmit a large amount of power in order to obtain a low probability of error. In many cases, a large amount of power is not possible, technically and/or economically. An alternative solution to the problem of obtaining acceptable performance on a fading channel is the use of redundancy, which can be obtained by means of diversity techniques, as discussed in Section 14-4.

Nakagami Fading If α is characterized statistically by the Nakagami-m distribution, the random variable $\gamma = \alpha^2 \mathcal{E}_b/N_0$ has the pdf (see Problem 14-15)

$$p(\gamma) = \frac{m^m}{\Gamma(m)\bar{\gamma}^m} \gamma^{m-1} e^{-m\gamma/\bar{\gamma}} \tag{14-3-14}$$

where $\bar{\gamma} = E(\alpha^2)\mathcal{E}/N_0$.

The average probability of error for any of the modulation methods is simply obtained by averaging the appropriate error probability for a nonfading channel over the fading signal statistics.

As an example of the performance obtained with Nakagami-m fading statistics, Fig. 14-3-2 illustrates the probability of error of binary PSK with m as a parameter. We recall that $m = 1$ corresponds to Rayleigh fading. We observe that the performance improves as m is increased above $m = 1$, which is indicative of the fact that the fading is less severe. On the other hand, when $m < 1$, the performance is worse than Rayleigh fading.

Other Fading Signal Statistics Following the procedure described above, one can determine the performance of the various modulation methods for other types of fading signal statistics, such as the Rice distribution.

Error probability results for Rice-distributed fading statistics can be found in the paper by Lindsey (1964), while for Nakagami-m fading statistics, the

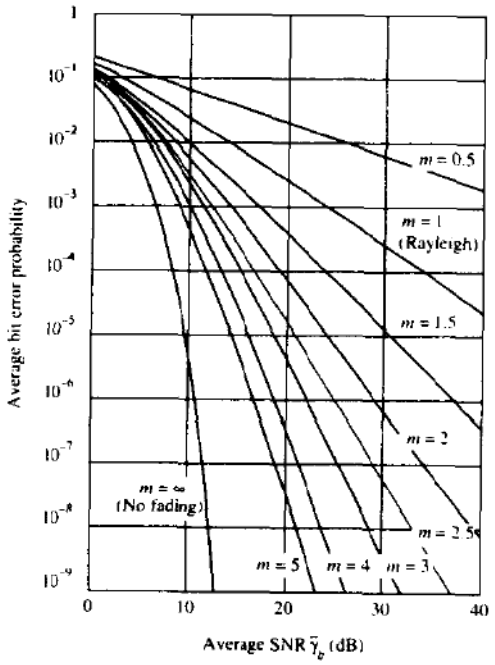

FIGURE 14-3-2 Average error probability for two-phase PSK symbol in nondiversity reception.

reader may refer to the papers by Espósito (1967), Miyagaki *et al.* (1978), Charash (1979), Al-Hussaini *et al.* (1985), and Beaulieu *et al.* (1991).

14-4 DIVERSITY TECHNIQUES FOR FADING MULTIPATH CHANNELS

Diversity techniques are based on the notion that errors occur in reception when the channel attenuation is large, i.e., when the channel is in a deep fade. If we can supply to the receiver several replicas of the same information signal transmitted over independently fading channels, the probability that all the signal components will fade simultaneously is reduced considerably. That is, if p is the probability that any one signal will fade below some critical value then p^L is the probability that all L independently fading replicas of the same signal will fade below the critical value. There are several ways in which we can provide the receiver with L independently fading replicas of the same information-bearing signal.

One method is to employ *frequency diversity*. That is, the same information-bearing signal is transmitted on L carriers, where the separation between successive carriers equals or exceeds the coherence bandwidth $(\Delta f)_c$ of the channel.

A second method for achieving L independently fading versions of the same information-bearing signal is to transmit the signal in L different time slots, where the separation between successive time slots equals or exceeds the coherence time $(\Delta t)_c$ of the channel. This method is called *time diversity*.

Note that the fading channel fits the model of a bursty error channel. Furthermore, we may view the transmission of the same information either at different frequencies or in difference time slots (or both) as a simple form of repetition coding. The separation of the diversity transmissions in time by $(\Delta t)_c$ or in frequency by $(\Delta f)_c$ is basically a form of block-interleaving the bits in the repetition code in an attempt to break up the error bursts and, thus, to obtain independent errors. Later in the chapter, we shall demonstrate that, in general, repetition coding is wasteful of bandwidth when compared with nontrivial coding.

Another commonly used method for achieving diversity employs multiple antennas. For example, we may employ a single transmitting antenna and multiple receiving antennas. The latter must be spaced sufficiently far apart that the multipath components in the signal have significantly different propagation delays at the antennas. Usually a separation of at least 10 wavelengths is required between two antennas in order to obtain signals that fade independently.

A more sophisticated method for obtaining diversity is based on the use of a signal having a bandwidth much greater than the coherence bandwidth $(\Delta f)_c$ of the channel. Such a signal with bandwidth W will resolve the multipath components and, thus, provide the receiver with several independently fading signal paths. The time resolution is $1/W$. Consequently, with a multipath

spread of T_m s, there are $T_m W$ resolvable signal components. Since $T_m \approx 1/(\Delta f)_c$, the number of resolvable signal components may also be expressed as $W/(\Delta f)_c$. Thus, the use of a wideband signal may be viewed as just another method for obtaining frequency diversity of order $L \approx W/(\Delta f)_c$. The optimum receiver for processing the wideband signal will be derived in Section 14-5. It is called a *RAKE correlator* or a *RAKE matched filter* and was invented by Price and Green (1958).

There are other diversity techniques that have received some consideration in practice, such as angle-of-arrival diversity and polarization diversity. However, these have not been as widely used as those described above.

14-4-1 Binary Signals

We shall now determine the error rate performance for a binary digital communications system with diversity. We begin by describing the mathematical model for the communications system with diversity. First of all, we assume that there are L diversity channels, carrying the same information-bearing signal. Each channel is assumed to be frequency-nonselective and slowly fading with Rayleigh-distributed envelope statistics. The fading processes among the L diversity channels are assumed to be mutually statistically independent. The signal in each channel is corrupted by an additive zero-mean white gaussian noise process. The noise processes in the L channels are assumed to be mutually statistically independent, with identical autocorrelation functions. Thus, the equivalent low-pass received signals for the L channels can be expressed in the form

$$r_{lk}(t) = \alpha_k e^{-j\phi_k} s_{km}(t) + z_k(t), \qquad k = 1, 2, \ldots, L, \quad m = 1, 2 \tag{14-4-1}$$

where $\{\alpha_k e^{-j\phi_k}\}$ represent the attenuation factors and phase shifts for the L channels, $s_{km}(t)$ denotes the mth signal transmitted on the kth channel, and $z_k(t)$ denotes the additive white gaussian noise on the kth channel. All signals in the set $\{s_{km}(t)\}$ have the same energy.

The optimum demodulator for the signal received from the kth channel consists of two matched filters, one having the impulse response

$$b_{k1}(t) = s_{k1}^*(T - t) \tag{14-4-2}$$

and the other having the impulse response

$$b_{k2}(t) = s_{k2}^*(T - t) \tag{14-4-3}$$

Of course, if binary PSK is the modulation method used to transmit the information, then $s_{k1}(t) = -s_{k2}(t)$. Consequently, only a single matched filter is required for binary PSK. Following the matched filters is a combiner that forms the two decision variables. The combiner that achieves the best performance is one in which each matched filter output is multiplied by the corresponding complex-valued (conjugate) channel gain $\alpha_k e^{j\phi_k}$. The effect of this multiplication is to compensate for the phase shift in the channel and to

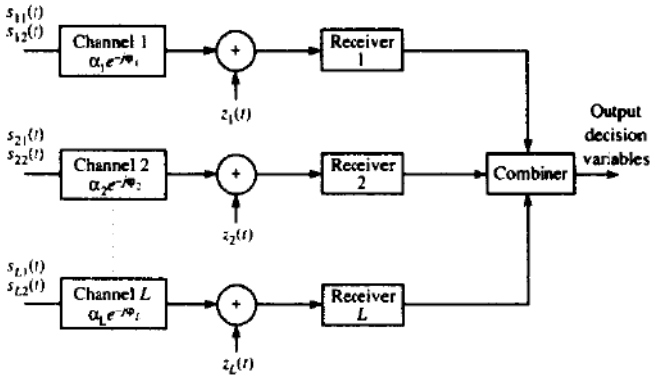

FIGURE 14-4-1 Model of binary digital communications system with diversity.

weight the signal by a factor that is proportional to the signal strength. Thus, a strong signal carries a larger weight than a weak signal. After the complex-valued weighting operation is performed, two sums are formed. One consists of the real parts of the weighted outputs from the matched filters corresponding to a transmitted 0. The second consists of the real part of the outputs from the matched filters corresponding to a transmitted 1. This optimum combiner is called a *maximal ratio combiner* by Brennan (1959). Of course, the realization of this optimum combiner is based on the assumption that the channel attenuations $\{\alpha_k\}$ and the phase shifts $\{\phi_k\}$ are known perfectly. That is, the estimates of the parameters $\{\alpha_k\}$ and $\{\phi_k\}$ contain no noise. (The effect of noisy estimates on the error rate performance of multiphase PSK is considered in Appendix C.

A block diagram illustrating the model for the binary digital communications system described above is shown in Fig. 14-4-1.

Let us first consider the performance of binary PSK with Lth-order diversity. The output of the maximal ratio combiner can be expressed as a single decision variable in the form

$$U = \text{Re}\left(2\mathscr{E}\sum_{k=1}^{L}\alpha_k^2 + \sum_{k=1}^{L}\alpha_k N_k\right)$$
$$= 2\mathscr{E}\sum_{k=1}^{L}\alpha_k^2 + \sum_{k=1}^{L}\alpha_k N_{kr} \tag{14-4-4}$$

where N_{kr} denotes the real part of the complex-valued gaussian noise variable

$$N_k = e^{j\phi_k}\int_0^T z_k(t)s_k^*(t)\,dt \tag{14-4-5}$$

We follow the approach used in Section 14-3 in deriving the probability of error. That is, the probability of error conditioned on a fixed set of attenuation

factors $\{\alpha_k\}$ is obtained first. Then the conditional probability of error is averaged over the probability density function of the $\{\alpha_k\}$.

Rayleigh Fading For a fixed set of $\{\alpha_k\}$ the decision variable U is gaussian with mean

$$E(U) = 2\mathscr{E}\sum_{k=1}^{L}\alpha_k^2 \tag{14-4-6}$$

and variance

$$\sigma_U^2 = 2\mathscr{E}N_0\sum_{k=1}^{L}\alpha_k^2 \tag{14-4-7}$$

For these values of the mean and variance, the probability that U is less than zero is simply

$$P_2(\gamma_b) = Q(\sqrt{2\gamma_b}) \tag{14-4-8}$$

where the SNR per bit, γ_b, is given as

$$\begin{aligned}\gamma_b &= \frac{\mathscr{E}}{N_0}\sum_{k=1}^{L}\alpha_k^2 \\ &= \sum_{k=1}^{L}\gamma_k\end{aligned} \tag{14-4-9}$$

where $\gamma_k = \mathscr{E}\alpha_k^2/N_0$ is the instantaneous SNR on the kth channel. Now we must determine the probability density function $p(\gamma_b)$. This function is most easily determined via the characteristic function of γ_b. First of all, we note that for $L = 1$, $\gamma_b \equiv \gamma_1$ has a chi-square probability density function given in (14-3-5). The characteristic function of γ_1 is easily shown to be

$$\begin{aligned}\psi_{\gamma_1}(jv) &= E(e^{jv\gamma_1}) \\ &= \frac{1}{1 - jv\bar{\gamma}_c}\end{aligned} \tag{14-4-10}$$

where $\bar{\gamma}_c$ is the average SNR per channel, which is assumed to be identical for all channels. That is,

$$\bar{\gamma}_c = \frac{\mathscr{E}}{N_0}E(\alpha_k^2) \tag{14-4-11}$$

independent of k. This assumption applies for the results throughout this section. Since the fading on the L channels is mutually statistically independent, the $\{\gamma_k\}$ are statistically independent, and, hence, the characteristic function for the sum γ_b is simply the result in (14-4-10) raised to the Lth power, i.e.,

$$\psi_{\gamma_b}(jv) = \frac{1}{(1 - jv\bar{\gamma}_c)^L} \tag{14-4-12}$$

But this is the characteristic function of a chi-square-distributed random variable with $2L$ degrees of freedom. It follows from (2-1-107) that the probability density function $p(\gamma_b)$ is

$$p(\gamma_b) = \frac{1}{(L-1)!\bar{\gamma}_c^L}\gamma_b^{L-1}e^{-\gamma_b/\bar{\gamma}_c} \tag{14-4-13}$$

The final step in this derivation is to average the conditional error probability given in (14-4-8) over the fading channel statistics. Thus, we evaluate the integral

$$P_2 = \int_0^\infty P_2(\gamma_b)p(\gamma_b)\,d\gamma_b \tag{14-4-14}$$

There is a closed-form solution for (14-4-14), which can be expressed as

$$P_2 = [\tfrac{1}{2}(1-\mu)]^L \sum_{k=0}^{L-1}\binom{L-1+k}{k}[\tfrac{1}{2}(1+\mu)]^k \tag{14-4-15}$$

where, by definition,

$$\mu = \sqrt{\frac{\bar{\gamma}_c}{1+\bar{\gamma}_c}} \tag{14-4-16}$$

When the average SNR per channel, $\bar{\gamma}_c$, satisfies the condition $\bar{\gamma}_c \gg 1$, the term $\frac{1}{2}(1+\mu) \approx 1$ and the term $\frac{1}{2}(1-\mu) \approx 1/4\bar{\gamma}_c$. Furthermore,

$$\sum_{k=0}^{L-1}\binom{L-1+k}{k} = \binom{2L-1}{L} \tag{14-4-17}$$

Therefore, when $\bar{\gamma}_c$ is sufficiently large (greater than 10 dB), the probability of error in (14-4-15) can be approximated as

$$P_2 \approx \left(\frac{1}{4\bar{\gamma}_c}\right)^L\binom{2L-1}{L} \tag{14-4-18}$$

We observe from (14-4-18) that the probability of error varies as $1/\bar{\gamma}_c$ raised to the Lth power. Thus, with diversity, the error rate decreases inversely with the Lth power of the SNR.

Having obtained the performance of binary PSK with diversity, we now turn our attention to binary, orthogonal FSK that is detected coherently. In this case, the two decision variables at the output of the maximal ratio combiner may be expressed as

$$\begin{aligned} U_1 &= \mathrm{Re}\left(2\mathscr{E}\sum_{k=1}^{L}\alpha_k^2 + \sum_{k=1}^{L}\alpha_k N_{k1}\right) \\ U_2 &= \mathrm{Re}\left(\sum_{k=1}^{L}\alpha_k N_{k2}\right) \end{aligned} \tag{14-4-19}$$

where we have assumed that signal $s_{k1}(t)$ was transmitted and where $\{N_{k1}\}$ and $\{N_{k2}\}$ are the two sets of noise component at the output of the matched filters.

The probability of error is simply the probability that $U_2 > U_1$. This computation is similar to the one performed for PSK, except that we now have twice the noise power. Consequently, when the $\{\alpha_k\}$ are fixed, the conditional probability of error is

$$P_2(\gamma_b) = Q(\sqrt{\gamma_b}) \tag{14-4-20}$$

We use (14-4-13) to average $P_2(\gamma_b)$ over the fading. It is not surprising to find that the result given in (14-4-15) still applies, with $\bar{\gamma}_c$ replaced by $\frac{1}{2}\bar{\gamma}_c$. That is, (14-4-15) is the probability of error for binary, orthogonal FSK with coherent detection, where the parameter μ is defined as

$$\mu = \sqrt{\frac{\bar{\gamma}_c}{2 + \bar{\gamma}_c}} \tag{14-4-21}$$

Furthermore, for large values of $\bar{\gamma}_c$, the performance P_2 can be approximated as

$$P_2 \approx \left(\frac{1}{2\bar{\gamma}_c}\right)^L \binom{2L-1}{L} \tag{14-4-22}$$

In comparing (14-4-22) with (14-4-18), we observe that the 3 dB difference in performance between PSK and orthogonal FSK with coherent detection, which exists in a nonfading, nondispersive channel, is the same also in a fading channel.

In the above discussion of binary PSK and FSK, detected coherently, we assumed that noiseless estimates of the complex-valued channel parameters $\{\alpha_k e^{-j\phi_k}\}$ were used at the receiver. Since the channel is time-variant, the parameters $\{\alpha_k e^{-j\phi_k}\}$ cannot be estimated perfectly. In fact, on some channels, the time variations may be sufficiently fast to preclude the implementation of coherent detection. In such a case, we should consider using either DPSK or FSK with noncoherent detection.

Let us consider DPSK first. In order for DPSK to be a viable digital signaling method, the channel variations must be sufficiently slow so that the channel phase shifts $\{\phi_k\}$ do not change appreciably over two consecutive signaling intervals. In our analysis, we assume that the channel parameters $\{\alpha_k e^{-j\phi_k}\}$ remain constant over two successive signaling intervals. Thus the combiner for binary DPSK will yield as an output the decision variable

$$U = \mathrm{Re}\left[\sum_{k=1}^{L} (2\mathscr{E}\alpha_k e^{-j\phi_k} + N_{k2})(2\mathscr{E}\alpha_k e^{j\phi_k} + N_{k1}^*)\right] \tag{14-4-23}$$

where $\{N_{k1}\}$ and $\{N_{k2}\}$ denote the received noise components at the output of the matched filters in the two consecutive signaling intervals. The probability of error is simply the probability that $U < 0$. Since U is a special case of the general quadratic form in complex-valued gaussian random variables treated in Appendix B, the probability of error can be obtained directly from the results given in that appendix. Alternatively, we may use the error probability given in (12-1-3), which applies to binary DPSK transmitted over L time-invariant

channels, and average it over the Rayleigh fading channel statistics. Thus, we have the conditional error probability

$$P_2(\gamma_b) = (\tfrac{1}{2})^{2L-1} e^{-\gamma_b} \sum_{k=0}^{L-1} b_k \gamma_b^2 \tag{14-4-24}$$

where γ_b is given by (14-4-9) and

$$b_k = \frac{1}{k!} \sum_{n=0}^{L-1-k} \binom{2L-1}{n} \tag{14-4-25}$$

The average of $P_2(\gamma_b)$ over the fading channel statistics given by $p(\gamma_b)$ in (14-4-13) is easily shown to be

$$P_2 = \frac{1}{2^{2L-1}(L-1)!(1+\bar{\gamma}_c)^L} \sum_{k=0}^{L-1} b_k (L-1+k)! \left(\frac{\bar{\gamma}_c}{1+\bar{\gamma}_c}\right)^k \tag{14-4-26}$$

We indicate that the result in (14-4-26) can be manipulated into the form given in (14-4-15), which applies also to coherent PSK and FSK. For binary DPSK, the parameter μ in (14-4-15) is defined as (see Appendix C)

$$\mu = \frac{\bar{\gamma}_c}{1+\bar{\gamma}_c} \tag{14-4-27}$$

For $\bar{\gamma}_c \gg 1$, the error probability in (14-4-26) can be approximated by the expression

$$P_2 \approx \left(\frac{1}{2\bar{\gamma}_c}\right)^L \binom{2L-1}{L} \tag{14-4-28}$$

Orthogonal FSK with noncoherent detection is the final signaling technique that we consider in this section. It is appropriate for both slow and fast fading. However, the analysis of the performance presented below is based on the assumption that the fading is sufficiently slow so that the channel parameters $\{\alpha_k e^{-j\phi_k}\}$ remain constant for the duration of the signaling interval. The combiner for the multichannel signals is a square-law combiner. Its output consists of the two decision variables

$$\begin{aligned} U_1 &= \sum_{k=1}^{L} |2\mathscr{E}\alpha_k e^{-j\phi_k} + N_{k1}|^2 \\ U_2 &= \sum_{k=1}^{L} |N_{k2}|^2 \end{aligned} \tag{14-4-29}$$

where U_1 is assumed to contain the signal. Consequently the probability of error is the probability that $U_2 > U_1$.

As in DPSK, we have a choice of two approaches in deriving the performance of FSK with square-law combining. In Section 12-1, we indicated that the expression for the error probability for square-law combined FSK is the same as that for DPSK with γ_b replaced by $\frac{1}{2}\gamma_b$. That is, the FSK system requires 3 dB of additional SNR to achieve the same performance on a time-invariant channel. Consequently, the conditional error probability for DPSK given in (14-4-24) applies to square-law-combined FSK when γ_b is replaced by $\frac{1}{2}\gamma_b$. Furthermore, the result obtained by averaging (14-4-24) over the fading, which is given by (14-4-26), must also apply to FSK with $\bar{\gamma}_c$ replaced by $\frac{1}{2}\bar{\gamma}_c$. But we also stated previously that (14-4-26) and (14-4-15) are equivalent. Therefore, the error probability given in (14-4-15) also applies to square-law-combined FSK with the parameter μ defined as

$$\mu = \frac{\bar{\gamma}_c}{2 + \bar{\gamma}_c} \tag{14-4-30}$$

An alternative derivation used by Pierce (1958) to obtain the probability that the decision variable $U_2 > U_1$ is just as easy as the method described above. It begins with the probability density functions $p(U_1)$ and $p(U_2)$. Since the complex-valued random variables $\{\alpha_k e^{-j\phi_k}\}$, $\{N_{k1}\}$, and $\{N_{k2}\}$ are zero-mean gaussian-distributed, the decision variables U_1 and U_2 are distributed according to a chi-square probability distribution with $2L$ degrees of freedom. That is,

$$p(U_1) = \frac{1}{(2\sigma_1^2)^L (L-1)!} U_1^{L-1} \exp\left(-\frac{U_1}{2\sigma_1^2}\right) \tag{14-4-31}$$

where

$$\begin{aligned}\sigma_1^2 &= \tfrac{1}{2}E(|2\mathscr{E}\alpha_k e^{-j\phi_k} + N_{k1}|^2) \\ &= 2\mathscr{E}N_0(1 + \bar{\gamma}_c)\end{aligned}$$

Similarly,

$$p(U_2) = \frac{2}{(2\sigma_2^2)^L (L-1)!} U_2^{L-1} \exp\left(-\frac{U_2}{2\sigma_2^2}\right) \tag{14-4-32}$$

where

$$\sigma_2^2 = 2\mathscr{E}N_0$$

The probability of error is just the probability that $U_2 > U_1$. It is left as an exercise for the reader to show that this probability is given by (14-4-15), where μ is defined by (14-4-30).

When $\bar{\gamma}_c \gg 1$, the performance of square-law-detected FSK can be simplified as we have done for the other binary multichannel systems. In this case, the error rate is well approximated by the expression

$$P_2 \approx \left(\frac{1}{\bar{\gamma}_c}\right)^L \binom{2L-1}{L} \tag{14-4-33}$$

The error rate performance of PSK, DPSK, and square-law-detected

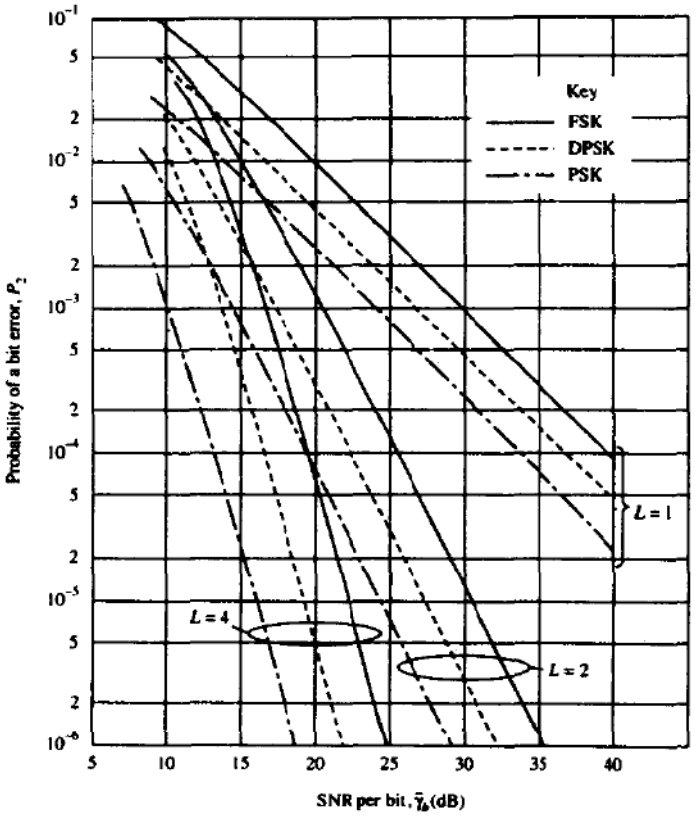

FIGURE 14-4-2 Performance of binary signals with diversity.

orthogonal FSK is illustrated in Fig. 14-4-2 for $L = 1$, 2, and 4. The performance is plotted as a function of the average SNR per bit, $\bar{\gamma}_b$, which is related to the average SNR per channel, $\bar{\gamma}_c$, by the formula

$$\bar{\gamma}_b = L\bar{\gamma}_c \tag{14-4-34}$$

The results in Fig. 14-4-2 clearly illustrate the advantage of diversity as a means for overcoming the severe penalty in SNR caused by fading.

14-4-2 Multiphase Signals

Multiphase signaling over a Rayleigh fading channel is the topic presented in some detail in Appendix C. Our main purpose in this section is to cite the general result for the probability of a symbol error in M-ary PSK and DPSK systems and the probability of a bit error in four-phase PSK and DPSK.

The general result for the probability of a symbol error in M-ary PSK and DPSK is

$$P_M = \frac{(-1)^{L-1}(1-\mu^2)^L}{\pi(L-1)!}\left(\frac{\partial^{L-1}}{\partial b^{L-1}}\left\{\frac{1}{b-\mu^2}\left[\frac{\pi}{M}(M-1)\right.\right.\right.$$
$$\left.\left.\left. - \frac{\mu \sin(\pi/M)}{\sqrt{b-\mu^2\cos^2(\pi/M)}}\cot^{-1}\frac{-\mu\cos(\pi/M)}{\sqrt{b-\mu^2\cos^2(\pi/M)}}\right]\right\}\right)_{b=1} \quad (14\text{-}4\text{-}35)$$

where

$$\mu = \sqrt{\frac{\bar{\gamma}_c}{1+\bar{\gamma}_c}} \quad (14\text{-}4\text{-}36)$$

for coherent PSK and

$$\mu = \frac{\bar{\gamma}_c}{1+\bar{\gamma}_c} \quad (14\text{-}4\text{-}37)$$

for DPSK. Again, $\bar{\gamma}_c$ is the average received SNR per channel. The SNR per bit is $\bar{\gamma}_b = L\bar{\gamma}_c/k$, where $k = \log_2 M$.

The bit error rate for four-phase PSK and DPSK is derived on the basis that the pair of information bits is mapped into the four phases according to a Gray code. The expression for the bit error rate derived in Appendix C is

$$P_b = \frac{1}{2}\left[1 - \frac{\mu}{\sqrt{2-\mu^2}}\sum_{k=0}^{L-1}\binom{2k}{k}\left(\frac{1-\mu^2}{4-2\mu^2}\right)^k\right] \quad (14\text{-}4\text{-}38)$$

where μ is again given by (14-4-36) and (14-4-37) for PSK and DPSK, respectively.

Figure 14-4-3 illustrates the probability of a symbol error of DPSK and coherent PSK for $M = 2$, 4, and 8 with $L = 1$. Note that the difference in performance between DPSK and coherent PSK is approximately 3 dB for all three values of M. In fact, when $\bar{\gamma}_b \gg 1$ and $L = 1$, (14-4-35) is well approximated as

$$P_M \approx \frac{M-1}{(M\log_2 M)[\sin^2(\pi/M)]\bar{\gamma}_b} \quad (14\text{-}4\text{-}39)$$

for DPSK and as

$$P_M \approx \frac{M-1}{(M\log_2 M)[\sin^2(\pi/M)]2\bar{\gamma}_b} \quad (14\text{-}4\text{-}40)$$

for PSK. Hence, at high SNR, coherent PSK is 3 dB better than DPSK on a Rayleigh fading channel. This difference also holds as L is increased.

Bit error probabilities are depicted in Fig. 14-4-4 for two-phase, four-phase, and eight-phase DPSK signaling with $L = 1$, 2, and 4. The expression for the bit error probability of eight-phase DPSK with Gray encoding is not given here, but it is available in the paper by Proakis (1968). In this case, we observe

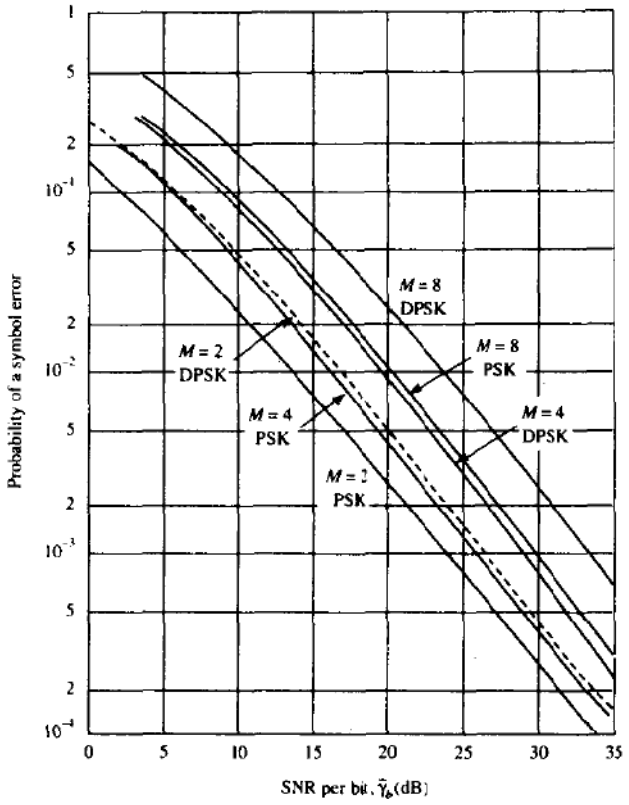

FIGURE 14-4-3 Probability of symbol error for PSK and DPSK for Rayleigh fading.

that the performances for two- and four-phase DPSK are (approximately) the same, while that for eight-phase DPSK is about 3 dB poorer. Although we have not shown the bit error probability for coherent PSK, it can be demonstrated that two- and four-phase coherent PSK also yield approximately the same performance.

14-4-3 *M*-ary Orthogonal Signals

In this sub-section, we determine the performance of M-ary orthogonal signals transmitted over a Rayleigh fading channel and we assess the advantages of higher-order signal alphabets relative to a binary alphabet. The orthogonal signals may be viewed as M-ary FSK with a minimum frequency separation of an integer multiple of $1/T$, where T is the signaling interval. The same information-bearing signal is transmitted on L diversity channels. Each diversity channel is assumed to be frequency-nonselective and slowly fading, and the fading processes on the L channels are assumed to be mutually

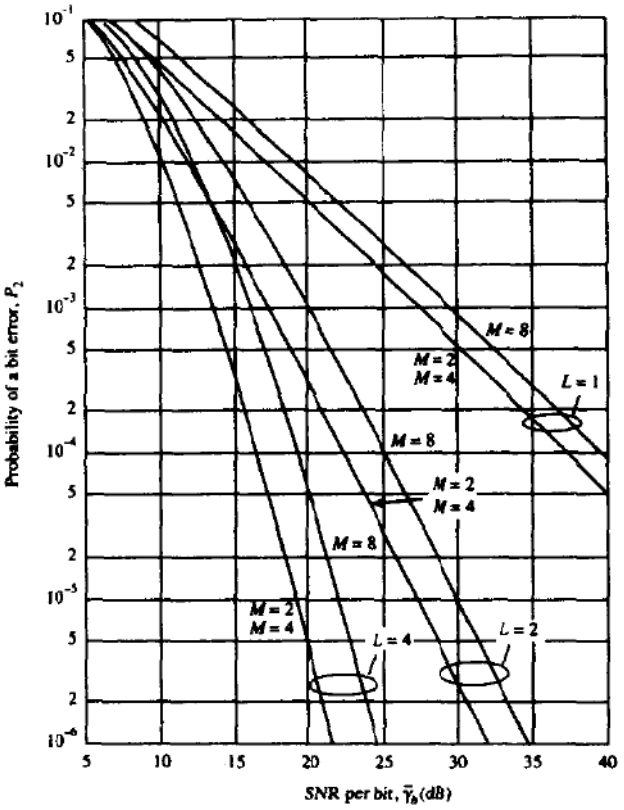

FIGURE 14-4-4 Probability of a bit error for DPSK with diversity for Rayleigh fading.

statistically independent. An additive white gaussian noise process corrupts the signal on each diversity channel. We assume that the additive noise processes are mutually statistically independent.

Although it is relatively easy to formulate the structure and analyze the performance of a maximal ratio combiner for the diversity channels in the M-ary communication system, it is more likely that a practical system would employ noncoherent detection. Consequently, we confine our attention to square-law combining of the diversity signals. The output of the combiner containing the signal is

$$U_1 = \sum_{k=1}^{L} |2\mathcal{E}\alpha_k e^{-j\phi_k} + N_{k1}|^2 \tag{14-4-41}$$

while the outputs of the remaining $M - 1$ combiners are

$$U_m = \sum_{k=1}^{L} |N_{km}|^2, \quad m = 2, 3, 4, \ldots, M \tag{14-4-42}$$

The probability of error is simply 1 minus the probability that $U_1 > U_m$ for $m = 2, 3, \ldots, M$. Since the signals are orthogonal and the additive noise processes are mutually statistically independent, the random variables $U_1, U_2, \ldots, U_M$ are also mutually statistically independent. The probability density function of U_1 was given in (14-4-31). On the other hand, $U_2, \ldots, U_M$ are identically distributed and described by the marginal probability density function in (14-4-32). With U_1 fixed, the joint probability $P(U_2 < U_1, U_3 < U_1, \ldots, U_m < U_1)$ is equal to $P(U_2 < U_1)$ raised to the $M-1$ power. Now,

$$\begin{aligned} P(U_2 < U_1) &= \int_0^{U_1} p(U_2)\, dU_2 \\ &= 1 - \exp\left(-\frac{U_1}{2\sigma_2^2}\right) \sum_{k=0}^{L-1} \frac{1}{k!} \left(\frac{U_1}{2\sigma_2^2}\right)^k \end{aligned} \tag{14-4-43}$$

where $\sigma_2^2 = 2\mathscr{E}N_0$. The $M-1$ power of this probability is then averaged over the probability density function of U_1 to yield the probability of a correct decision. If we subtract this result from unity, we obtain the probability of error in the form given by Hahn (1962)

$$\begin{aligned} P_M &= 1 - \int_0^\infty \frac{1}{(2\sigma_1^2)^L (L-1)!} U_1^{L-1} \exp\left(-\frac{U_1}{2\sigma_2^2}\right) \\ &\quad \times \left[1 - \exp\left(-\frac{U_1}{2\sigma_2^2}\right) \sum_{k=0}^{L-1} \frac{1}{k!} \left(\frac{U_1}{2\sigma_2^2}\right)^k\right]^{M-1} dU_1 \\ &= 1 - \int_0^\infty \frac{1}{(1+\bar{\gamma}_c)^L (L-1)!} U_1^{L-1} \exp\left(-\frac{U_1}{1+\bar{\gamma}_c}\right) \\ &\quad \times \left(1 - e^{-U_1} \sum_{k=0}^{L-1} \frac{U_1^k}{k!}\right)^{M-1} dU_1 \end{aligned} \tag{14-4-44}$$

where $\bar{\gamma}_c$ is the average SNR per diversity channel. The average SNR per bit is $\bar{\gamma}_b = L\bar{\gamma}_c / \log_2 M = L\bar{\gamma}_c / k$.

The integral in (14-4-44) can be expressed in closed form as a double summation. This can be seen if we write

$$\left(\sum_{k=0}^{L-1} \frac{U_1^k}{k!}\right)^m = \sum_{k=0}^{m(L-1)} \beta_{km} U_1^k \tag{14-4-45}$$

where β_{km} is the set of coefficients in the above expansion. Then it follows that (14-4-44) reduces to

$$\begin{aligned} P_M &= \frac{1}{(L-1)!} \sum_{m=1}^{M-1} \frac{(-1)^{m+1} \binom{M-1}{m}}{(1+m+m\bar{\gamma}_c)^L} \\ &\quad \times \sum_{k=0}^{m(L-1)} \beta_{km} (L-1+k)! \left(\frac{1+\bar{\gamma}_c}{1+m+m\bar{\gamma}_c}\right)^k \end{aligned} \tag{14-4-46}$$

When there is no diversity ($L = 1$), the error probability in (14-4-46) reduces to the simple form

$$P_M = \sum_{m=1}^{M-1} \frac{(-1)^{m+1}\binom{M-1}{m}}{1 + m + m\bar{\gamma}_c} \tag{14-4-47}$$

The symbol error rate P_M may be converted to an equivalent bit error rate by multiplying P_M with $2^{k-1}/(2^k - 1)$.

Although the expression for P_M given in (14-4-46) is in closed form, it is computationally cumbersome to evaluate for large values of M and L. An alternative is to evaluate P_M by numerical integration using the expression in (14-4-44). The results illustrated in the following graphs were generated from (14-4-44).

First of all, let us observe the error rate performance of M-ary orthogonal signaling with square-law combining as a function of the order of diversity. Figures 14-4-5 and 14-4-6 illustrate the characteristics of P_M for $M = 2$ and 4 as

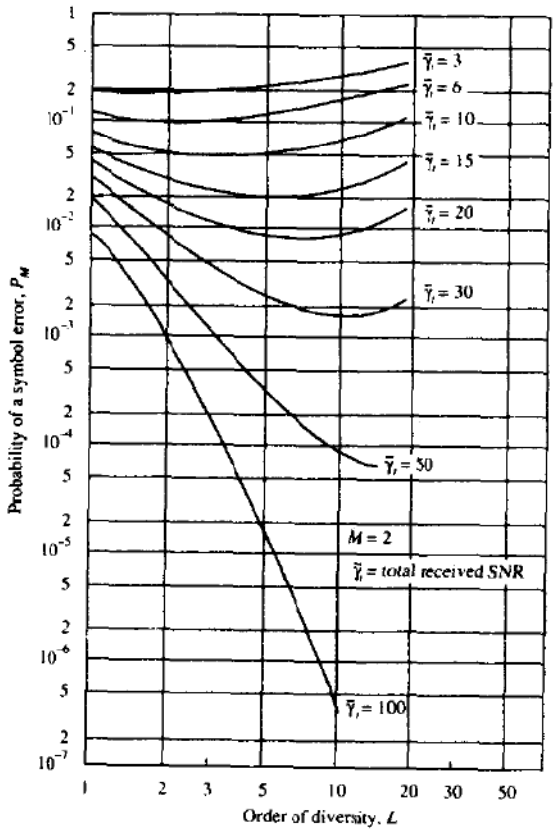

FIGURE 14-4-5 Performance of square-law-detected binary orthogonal signals as a function of diversity.

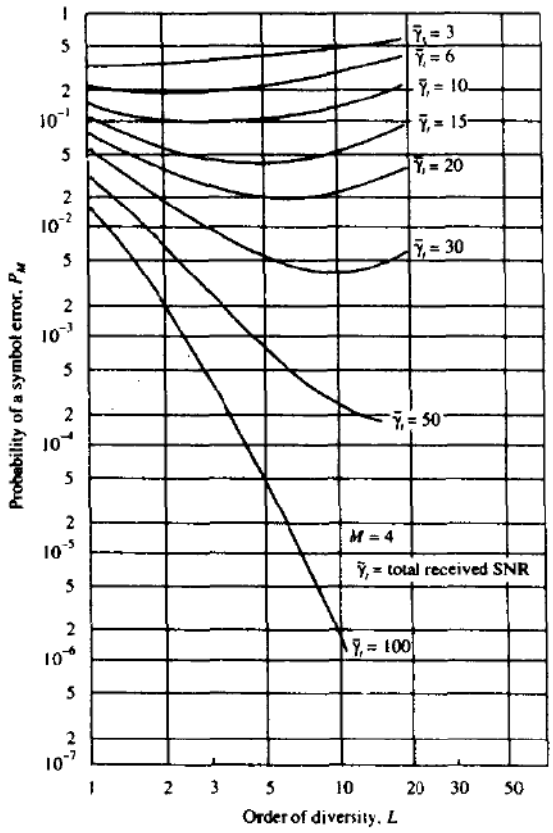

FIGURE 14-4-6 Performance of square-law-detected $M = 4$ orthogonal signals as a function of diversity.

a function of L when the total SNR, defined as $\bar{\gamma}_t = L\bar{\gamma}_c$, remains fixed. These results indicate that there is an optimum order of diversity for each $\bar{\gamma}_t$. That is, for any $\bar{\gamma}_t$, there is a value of L for which P_M is a minimum. A careful observation of these graphs reveals that the minimum in P_M is obtained when $\bar{\gamma}_c = \bar{\gamma}_t/L \approx 3$. This result appears to be independent of the alphabet size M.

Second, let us observe the error rate P_M as a function of the average SNR per bit, defined as $\bar{\gamma}_b = L\bar{\gamma}_c/k$. (If we interpret M-ary orthogonal FSK as a form of coding† and the order of diversity as the number of times a symbol is repeated in a repetition code then $\bar{\gamma}_b = \bar{\gamma}_c/R_c$, where $R_c = k/L$ is the code rate.) The graphs of P_M versus $\bar{\gamma}_b$ for $M = 2, 4, 8, 16, 32$ and $L = 1, 2, 4$ are shown in Fig. 14-4-7. These results illustrate the gain in performance as M increases and L increases. First, we note that a significant gain in performance is obtained by increasing L. Second, we note that the gain in performance obtained with an increase in M is relatively small when L is small. However,

† In Section 14-6, we show that M-ary orthogonal FSK with diversity may be viewed as a block orthogonal code.

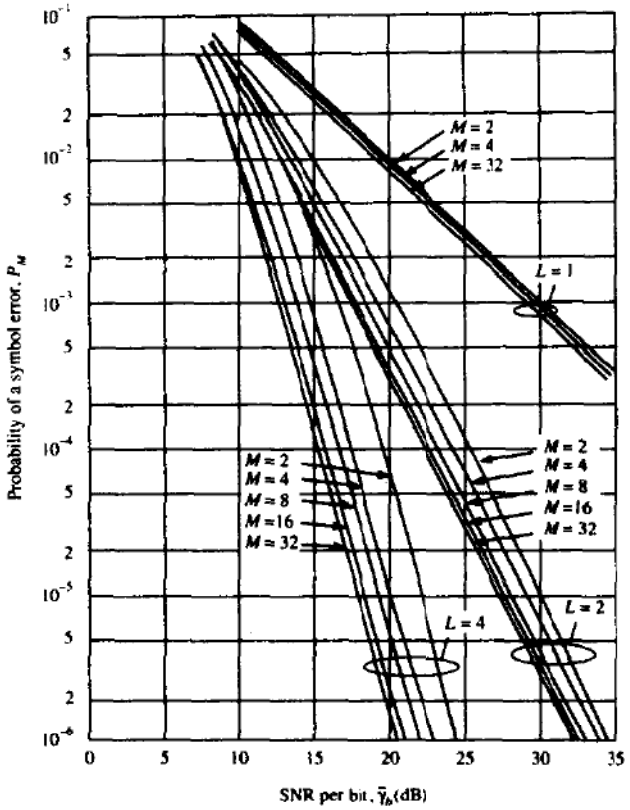

FIGURE 14-4-7 Performance of orthogonal signaling with M and L as parameters.

as L increases, the gain achieved by increasing M also increases. Since an increase in either parameter results in an expansion of bandwidth, i.e.,

$$B_e = \frac{LM}{\log_2 M}$$

the results illustrated in Fig. 14-4-7 indicate that an increase in L is more efficient than a corresponding increase in M. As we shall see in Section 14-6, coding is a bandwidth-effective means for obtaining diversity in the signal transmitted over the fading channel.

Chernoff Bound Before concluding this section, we develop a Chernoff upper bound on the error probability of binary orthogonal signaling with Lth-order diversity, which will be useful in our discussion of coding for fading channels, the topic of Section 14-6. Our starting point is the expression for the two decision variables U_1 and U_2 given by (14-4-29), where U_1 consists of the

square-law-combined signal-plus-noise terms and U_2 consists of square-law-combined noise terms. The binary probability of error, denoted here by $P_2(L)$, as

$$\begin{aligned} P_2(L) &= P(U_2 - U_1 > 0) \\ &= P(X > 0) = \int_0^\infty p(x)\,dx \end{aligned} \tag{14-4-48}$$

where the random variable X is defined as

$$X = U_2 - U_1 = \sum_{k=1}^{L} (|N_{k2}|^2 - |2\mathcal{E}\alpha_k + N_{k1}|^2) \tag{14-4-49}$$

The phase terms $\{\phi_k\}$ in U_1 have been dropped since they do not affect the performance of the square-law detector.

Let $S(X)$ denote the unit step function. Then the error probability in (14-4-48) can be expressed in the form

$$P_2(L) = E[S(X)] \tag{14-4-50}$$

Following the development in Section 2-1-5, the Chernoff bound is obtained by overbounding the unit step function by an exponential function. That is,

$$S(X) \leq e^{\zeta X}, \quad \zeta \geq 0 \tag{14-4-51}$$

where the parameter ζ is optimized to yield a tight bound. Thus, we have

$$P_2(L) = E[S(X)] \leq E(e^{\zeta X}) \tag{14-4-52}$$

Upon substituting for the random variable X from (14-4-49) and noting that the random variables in the summation are mutually statistically independent, we obtain the result

$$P_2(L) \leq \prod_{k=1}^{L} E(e^{\zeta|N_{k2}|^2}) E(e^{-\zeta|2\mathcal{E}\alpha_k + N_{k1}|^2}) \tag{14-4-53}$$

But

$$E(e^{\zeta|N_{k2}|^2}) = \frac{1}{1 - 2\zeta\sigma_2^2}, \quad \zeta < \frac{1}{2\sigma_2^2} \tag{14-4-54}$$

and

$$E(e^{-\zeta|2\mathcal{E}\alpha_k + N_{k1}|^2}) = \frac{1}{1 + 2\zeta\sigma_1^2}, \quad \zeta > \frac{-1}{2\sigma_1^2} \tag{14-4-55}$$

where $\sigma_2^2 = 2\mathcal{E}N_0$, $\sigma_1^2 = 2\mathcal{E}N_0(1 + \bar{\gamma}_c)$, and $\bar{\gamma}_c$ is the average SNR per diversity channel. Note that σ_1^2 and σ_2^2 are independent of k, i.e., the additive noise terms on the L diversity channels as well as the fading statistics are identically distributed. Consequently, (14-4-53) reduces to

$$P_2(L) \leq \left[\frac{1}{(1 - 2\zeta\sigma_2^2)(1 + 2\zeta\sigma_1^2)}\right]^L, \quad 0 \leq \zeta \leq \frac{1}{2\sigma_2^2} \tag{14-4-56}$$

By differentiating the right-hand side of (14-4-56) with respect to ζ, we find that the upper bound is minimized when

$$\zeta = \frac{\sigma_1^2 - \sigma_2^2}{4\sigma_1^2\sigma_2^2} \tag{14-4-57}$$

Substitution of (14-4-57) for ζ into (14-4-56) yields the Chernoff upper bound in the form

$$P_2(L) \leq \left[\frac{4(1+\bar{\gamma}_c)}{(2+\bar{\gamma}_c)^2}\right]^L \tag{14-4-58}$$

It is interesting to note that (14-4-58) may also be expressed as

$$P_2(L) \leq [4p(1-p)]^L \tag{14-4-59}$$

where $p = 1/(2+\bar{\gamma}_c)$ is the probability of error for binary orthogonal signaling on a fading channel without diversity.

A comparison of the Chernoff bound in (14-4-58) with the exact error probability for binary orthogonal signaling and square-law combining of the L diversity signals, which is given by the expression

$$\begin{aligned} P_2(L) &= \left(\frac{1}{1+\bar{\gamma}_c}\right)^L \sum_{k=0}^{L-1} \binom{L-1+k}{k} \left(\frac{1+\bar{\gamma}_c}{2+\bar{\gamma}_c}\right)^k \\ &= p^L \sum_{k=0}^{L-1} \binom{L-1+k}{k} (1-p)^k \end{aligned} \tag{14-4-60}$$

reveals the tightness of the bound. Figure (14-4-8) illustrates this comparison.

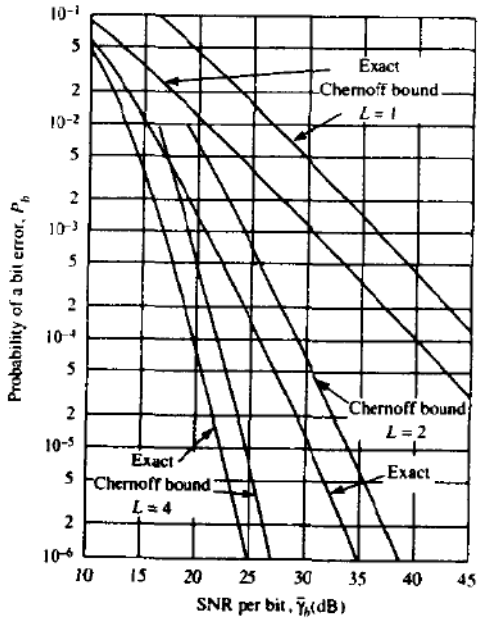

FIGURE 14-4-8 *Comparison of Chernoff bound with exact error probability.*

We observe that the Chernoff upper bound is approximately 6 dB from the exact error probability for $L = 1$, but, as L increases, it becomes tighter. For example, the difference between the bound and the exact error probability is about 2.5 dB when $L = 4$.

Finally we mention that the error probability for M-ary orthogonal signaling with diversity can be upper-bounded by means of the union bound

$$P_M \leq (M-1)P_2(L) \tag{14-4-61}$$

where we may use either the exact expression given in (14-4-60) or the Chernoff bound in (14-4-58) for $P_2(L)$.

14-5 DIGITAL SIGNALING OVER A FREQUENCY-SELECTIVE, SLOWLY FADING CHANNEL

When the spread factor of the channel satisfies the condition $T_m B_d \ll 1$, it is possible to select signals having a bandwidth $W \ll (\Delta f)_c$ and a signal duration $T \ll (\Delta t)_c$. Thus, the channel is frequency-nonselective and slowly fading. In such a channel, diversity techniques can be employed to overcome the severe consequences of fading.

When a bandwidth $W \gg (\Delta f)_c$ is available to the user, the channel can be subdivided into a number of frequency-division multiplexed (FDM) subchannels having a mutual separation in center frequencies of at least $(\Delta f)_c$. Then the same signal can be transmitted on the FDM subchannels, and, thus, frequency diversity is obtained. In this section, we describe an alternative method.

14-5-1 A Tapped-Delay-Line Channel Model

As we shall now demonstrate, a more direct method for achieving basically the same result is to employ a wideband signal covering the bandwidth W. The channel is still assumed to be slowly fading by virtue of the assumption that $T \ll (\Delta t)_c$. Now suppose that W is the bandwidth occupied by the real bandpass signal. Then the band occupancy of the equivalent lowpass signal $s_l(t)$ is $|f| \leq \frac{1}{2}W$. Since $s_l(t)$ is band-limited to $|f| \leq \frac{1}{2}W$, application of the sampling theorem results in the signal representation

$$s_l(t) = \sum_{n=-\infty}^{\infty} s_l\left(\frac{n}{W}\right) \frac{\sin[\pi W(t - n/W)]}{\pi W(t - n/W)} \tag{14-5-1}$$

The Fourier transform of $s_l(t)$ is

$$S_l(f) = \begin{cases} \dfrac{1}{W} \displaystyle\sum_{n=-\infty}^{\infty} s_l(n/W) e^{-j2\pi fn/W} & (|f| \leq \tfrac{1}{2}W) \\ 0 & (|f| > \tfrac{1}{2}W) \end{cases} \tag{14-5-2}$$

The noiseless received signal from a frequency-selective channel was previously expressed in the form

$$r_l(t) = \int_{-\infty}^{\infty} C(f;t)S_l(f)e^{j2\pi ft}\,df \tag{14-5-3}$$

where $C(f;t)$ is the time-variant transfer function. Substitution for $S_l(f)$ from (14-5-2) into (14-5-3) yields

$$\begin{aligned} r_l(t) &= \frac{1}{W}\sum_{n=-\infty}^{\infty} s_l(n/W)\int_{-\infty}^{\infty} C(f;t)e^{j2\pi f(t-n/W)}\,df \\ &= \frac{1}{W}\sum_{n=-\infty}^{\infty} s_l(n/W)c(t-n/W;t) \end{aligned} \tag{14-5-4}$$

where $c(\tau;t)$ is the time-variant impulse response. We observe that (14-5-4) has the form of a convolution sum. Hence, it can also be expressed in the alternative form

$$r(t) = \frac{1}{W}\sum_{n=-\infty}^{\infty} s_l(t-n/W)c(n/W;t) \tag{14-5-5}$$

It is convenient to define a set of time-variable channel coefficients as

$$c_n(t) = \frac{1}{W}c\left(\frac{n}{W};t\right) \tag{14-5-6}$$

Then (14-5-5) expressed in terms of these channel coefficients becomes

$$r(t) = \sum_{n=-\infty}^{\infty} c_n(t)s_l(t-n/W) \tag{14-5-7}$$

The form for the received signal in (14-5-7) implies that the time-variant frequency-selective channel can be modeled or represented as a tapped delay line with tap spacing $1/W$ and tap weight coefficients $\{c_n(t)\}$. In fact, we deduce from (14-5-7) that the lowpass impulse response for the channel is

$$c(\tau;t) = \sum_{n=-\infty}^{\infty} c_n(t)\delta(\tau-n/W) \tag{14-5-8}$$

and the corresponding time-variant transfer function is

$$C(f;t) = \sum_{n=-\infty}^{\infty} c_n(t)e^{-j2\pi fn/W} \tag{14-5-9}$$

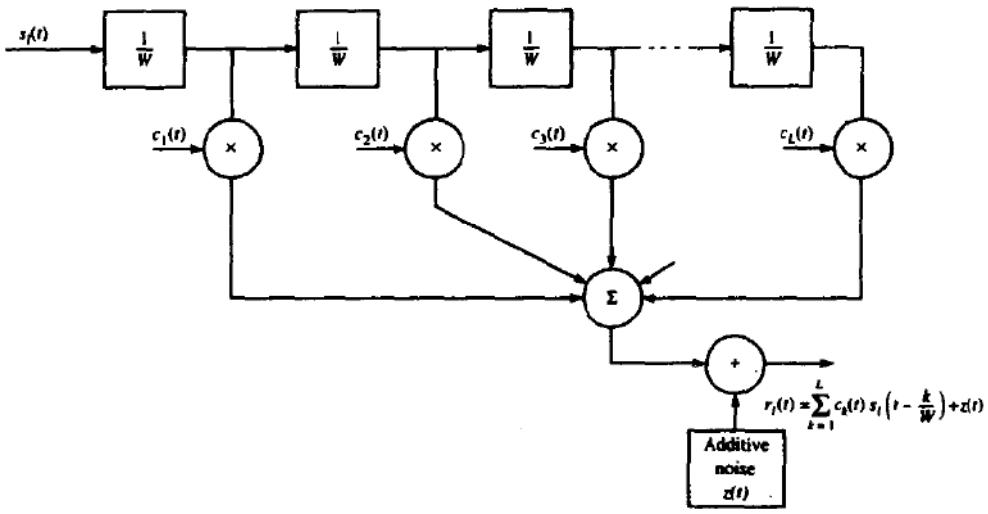

FIGURE 14-5-1 Trapped delay line model of frequency-selective channel.

Thus, with an equivalent lowpass signal having a bandwidth $\frac{1}{2}W$, where $W \gg (\Delta f)_c$, we achieve a resolution of $1/W$ in the multipath delay profile. Since the total multipath spread is T_m, for all practical purposes the tapped delay line model for the channel can be truncated at $L = [T_m W] + 1$ taps. Then the noiseless received signal can be expressed in the form

$$r_l(t) = \sum_{n=1}^{L} c_n(t) s_l\left(t - \frac{n}{W}\right) \tag{14-5-10}$$

The truncated tapped delay line model is shown in Fig. 14-5-1. In accordance with the statistical characterization of the channel presented in Section 14-1, the time-variant tap weights $\{c_n(t)\}$ are complex-valued stationary random processes. In the special case of Rayleigh fading, the magnitudes $|c_n(t)| = \alpha_n(t)$ are Rayleigh-distributed and the phases $\phi_n(t)$ are uniformly distributed. Since the $\{c_n(t)\}$ represent the tap weights corresponding to the L different delays $\tau = n/W$, $n = 1, 2, \ldots, L$, the uncorrelated scattering assumption made in Section 7-1 implies that the $\{c_n(t)\}$ are mutually uncorrelated. When the $\{c_n(t)\}$ are gaussian random processes, they are statistically independent.

14-5-2 The RAKE Demodulator

We now consider the problem of digital signaling over a frequency-selective channel that is modeled by a tapped delay line with statistically independent time-variant tap weights $\{c_n(t)\}$. It is apparent at the outset, however, that the tapped delay line model with statistically independent tap weights provides us

with L replicas of the same transmitted signal at the receiver. Hence, a receiver that processes the received signal in an optimum manner will achieve the performance of an equivalent Lth-order diversity communications system.

Let us consider binary signaling over the channel. We have two equal-energy signals $s_{l1}(t)$ and $s_{l2}(t)$, which are either antipodal or orthogonal. Their time duration T is selected to satisfy the condition $T \gg T_m$. Thus, we may neglect any intersymbol interference due to multipath. Since the bandwidth of the signal exceeds the coherent bandwidth of the channel, the received signal is expressed as

$$\begin{aligned} r_l(t) &= \sum_{k=1}^{L} c_k(t) s_{li}(t - k/W) + z(t) \\ &= v_i(t) + z(t), \quad 0 \leq t \leq T, \quad i = 1, 2 \end{aligned} \tag{14-5-11}$$

where $z(t)$ is a complex-valued zero-mean white gaussian noise process. Assume for the moment that the channel tap weights are known. Then the optimum receiver consists of two filters matched to $v_1(t)$ and $v_2(t)$, followed by samplers and a decision circuit that selects the signal corresponding to the largest output. An equivalent optimum receiver employs cross correlation instead of matched filtering. In either case, the decision variables for coherent detection of the binary signals can be expressed as

$$\begin{aligned} U_m &= \text{Re}\left[\int_0^T r_l(t) v_m^*(t)\, dt\right] \\ &= \text{Re}\left[\sum_{k=1}^{L} \int_0^T r_l(t) c_k^*(t) s_{lm}^*(t - k/W)\, dt\right], \quad m = 1, 2 \end{aligned} \tag{14-5-12}$$

Figure 14-5-2 illustrates the operations involved in the computation of the decision variables. In this realization of the optimum receiver, the two reference signals are delayed and correlated with the received signal $r_l(t)$.

An alternative realization of the optimum receiver employs a single delay line through which is passed the received signal $r_l(t)$. The signal at each tap is correlated with $c_k(t)s_{lm}^*(t)$, where $k = 1, 2, \ldots, L$ and $m = 1, 2$. This receiver structure is shown in Fig. 14-5-3. In effect, the tapped delay line receiver attempts to collect the signal energy from all the received signal paths that fall within the span of the delay line and carry the same information. Its action is somewhat analogous to an ordinary garden rake and, consequently, the name "RAKE receiver" has been coined for this receiver structure by Price and Green (1958).

14-5-3 Performance of RAKE Receiver

We shall now evaluate the performance of the RAKE receiver under the condition that the fading is sufficiently slow to allow us to estimate $c_k(t)$ perfectly (without noise). Furthermore, within any one signaling interval, $c_k(t)$

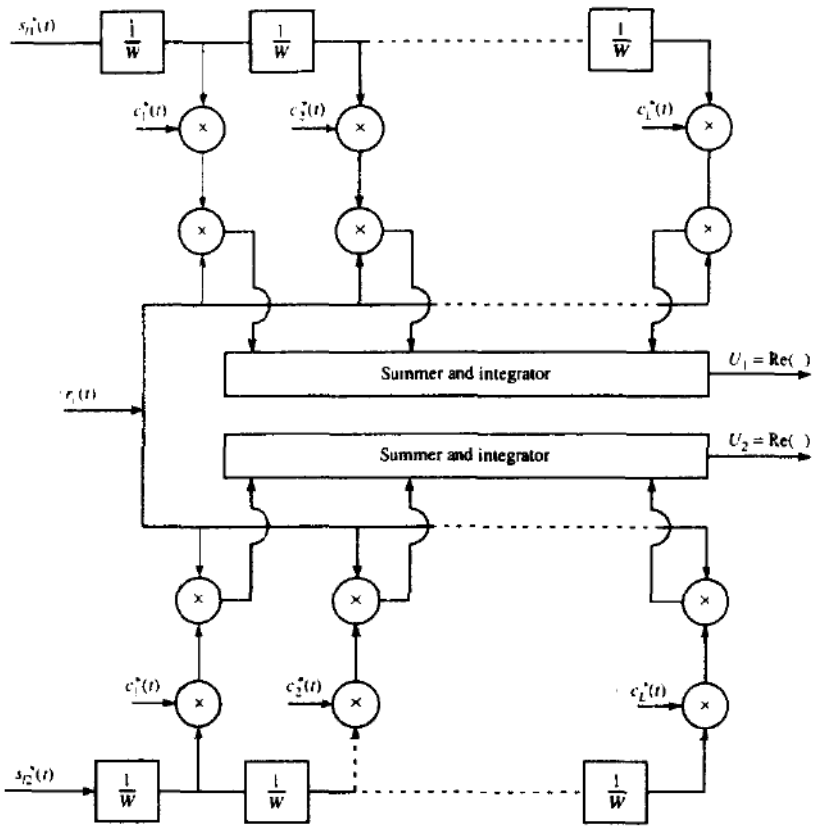

FIGURE 14-5-2 Optimum demodulator for wideband binary signals (delayed reference configuration).

is treated as a constant and denoted as c_k. Thus the decision variables in (14-5-12) may be expressed in the form

$$U_m = \text{Re}\left[\sum_{k=1}^{L} c_k^* \int_0^T r(t) s_{lm}^*(t - k/W)\, dt\right], \quad m = 1, 2 \qquad (14\text{-}5\text{-}13)$$

Suppose the transmitted signal is $s_{l1}(t)$; then the received signal is

$$r_l(t) = \sum_{n=1}^{L} c_n s_{l1}(t - n/W) + z(t), \quad 0 \leq t \leq T \qquad (14\text{-}5\text{-}14)$$

Substitution of (14-5-14) into (14-5-13) yields

$$U_m = \text{Re}\left[\sum_{k=1}^{L} c_k^* \sum_{n=1}^{L} c_n \int_0^T s_{l1}(t - n/W) s_{lm}^*(t - k/W)\, dt\right] + \text{Re}\left[\sum_{k=1}^{L} c_k^* \int_0^T z(t) s_{lm}^*(t - k/W)\, dt\right], \quad m = 1, 2 \qquad (14\text{-}5\text{-}15)$$

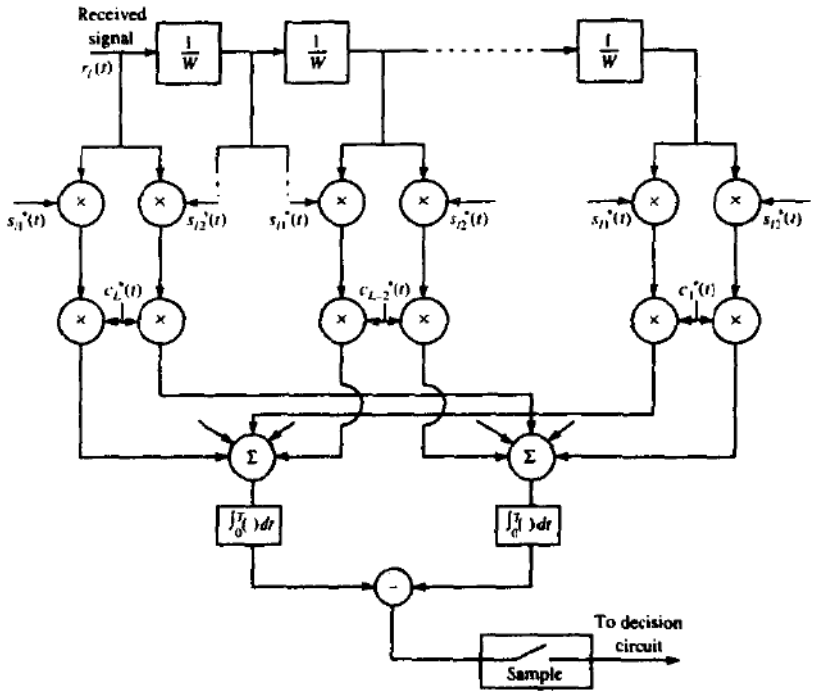

FIGURE 14-5-3 Optimum demodulator for wideband binary signals (delayed received signal configuration).

Usually the wideband signals $s_{l1}(t)$ and $s_{l2}(t)$ are generated from pseudo-random sequences, which result in signals that have the property

$$\int_0^T s_{li}(t - n/W)s_{li}^*(t - k/W)\,dt \approx 0, \quad k \neq n, \quad i = 1, 2 \qquad (14\text{-}5\text{-}16)$$

If we assume that our binary signals are designed to satisfy this property then (14-5-15) simplifies to†

$$U_m = \text{Re}\left[\sum_{k=1}^{L} |c_k|^2 \int_0^T s_{l1}(t - k/W)s_{lm}^*(t - k/W)\,dt\right] + \text{Re}\left[\sum_{k=1}^{L} c_k^* \int_0^T z(t)s_{lm}^*(t - k/W)\,dt\right], \quad m = 1, 2 \qquad (14\text{-}5\text{-}17)$$

† Although the orthogonality property specified by (14-5-16) can be satisfied by proper selection of the pseudo-random sequences, the cross-correlation of $s_{l1}(t - n/W)$ with $s_{li}^*(t - k/W)$ gives rise to a signal-dependent self-noise, which ultimately limits the performance. For simplicity, we do not consider the self-noise term in the following calculations. Consequently, the performance results presented below should be considered as lower bounds (ideal RAKE). An approximation to the performance of the RAKE can be obtained by treating the self-noise as an additional gaussian noise component with noise power equal to its variance.

When the binary signals are antipodal, a single decision variable suffices. In this case, (14-5-17) reduces to

$$U_1 = \text{Re}\left(2\mathscr{E}\sum_{k=1}^{L}\alpha_k^2 + \sum_{k=1}^{L}\alpha_k N_k\right) \tag{14-5-18}$$

where $\alpha_k = |c_k|$ and

$$N_k = e^{j\phi_k}\int_0^T z(t)s_1^*(t - k/W)\,dt \tag{14-5-19}$$

But (14-5-18) is identical to the decision variable given in (14-4-4), which corresponds to the output of a maximal ratio combiner in a system with Lth-order diversity. Consequently, the RAKE receiver with perfect (noiseless) estimates of the channel tap weights is equivalent to a maximal ratio combiner in a system with Lth-order diversity. Thus, when all the tap weights have the same mean-square value, i.e., $E(\alpha_k^2)$ is the same for all k, the error rate performance of the RAKE receiver is given by (14-4-15) and (14-4-16). On the other hand, when the mean square values $E(\alpha_k^2)$ are not identical for all k, the derivation of the error rate performance must be repeated since (14-4-15) no longer applies.

We shall derive the probability of error for binary antipodal and orthogonal signals under the condition that the mean-square values of $\{\alpha_k\}$ are distinct. We begin with the conditional error probability

$$P_2(\gamma_b) = Q(\sqrt{\gamma_b(1 - \rho_r)}) \tag{14-5-20}$$

where $\rho_r = -1$ for antipodal signals, $\rho_r = 0$ for orthogonal signals, and

$$\begin{aligned}\gamma_b &= \frac{\mathscr{E}}{N_0}\sum_{k=1}^{L}\alpha_k^2 \\ &= \sum_{k=1}^{L}\gamma_k\end{aligned} \tag{14-5-21}$$

Each of the $\{\gamma_k\}$ is distributed according to a chi-squared distribution with two degrees of freedom. That is,

$$p(\gamma_k) = \frac{1}{\bar{\gamma}_k}e^{-\gamma_k/\bar{\gamma}_k} \tag{14-5-22}$$

where $\bar{\gamma}_k$ is the average SNR for the kth path, defined as

$$\bar{\gamma}_k = \frac{\mathscr{E}}{N_0}E(\alpha_k^2) \tag{14-5-23}$$

Furthermore, from (14-4-10) we know that the characteristic function of γ_k is

$$\psi_{\gamma_k}(jv) = \frac{1}{1 - jv\bar{\gamma}_k} \tag{14-5-24}$$

Since γ_b is the sum of L statistically independent components $\{\gamma_k\}$, the characteristic function of γ_b is

$$\psi_{\gamma_b}(jv) = \prod_{k=1}^{L} \frac{1}{1 - jv\bar{\gamma}_k} \tag{14-5-25}$$

The inverse Fourier transform of the characteristic function in (14-5-25) yields the probability density function of γ_b in the form

$$p(\gamma_b) = \sum_{k=1}^{L} \frac{\pi_k}{\bar{\gamma}_k} e^{-\gamma_b/\bar{\gamma}_k}, \qquad \gamma_b \geq 0 \tag{14-5-26}$$

where π_k is defined as

$$\pi_k = \prod_{\substack{i=1 \\ i \neq k}}^{L} \frac{\bar{\gamma}_k}{\bar{\gamma}_k - \bar{\gamma}_i} \tag{14-5-27}$$

When the conditional error probability in (14-5-20) is averaged over the probability density function given in (14-5-26), the result is

$$P_2 = \tfrac{1}{2} \sum_{k=1}^{L} \pi_k \left[1 - \sqrt{\frac{\bar{\gamma}_k(1 - \rho_r)}{2 + \bar{\gamma}_k(1 - \rho_r)}} \right] \tag{14-5-28}$$

This error probability can be approximated as ($\bar{\gamma}_k \gg 1$)

$$P_2 \approx \binom{2L-1}{L} \prod_{k=1}^{L} \frac{1}{2\bar{\gamma}_k(1 - \rho_r)} \tag{14-5-29}$$

By comparing (14-5-29) for $\rho_r = -1$ with (14-4-18), we observe that the same type of asymptotic behavior is obtained for the case of unequal SNR per path and the case of equal SNR per path.

In the derivation of the error rate performance of the RAKE receiver, we assumed that the estimates of the channel tap weights are perfect. In practice, relatively good estimates can be obtained if the channel fading is sufficiently slow, e.g., $(\Delta t)_c/T \geq 100$, where T is the signaling interval. Figure 14-5-4 illustrates a method for estimating the tap weights when the binary signaling waveforms are orthogonal. The estimate is the output of the lowpass filter at each tap. At any one instant in time, the incoming signal is either $s_{l1}(t)$ or $s_{l2}(t)$. Hence, the input to the lowpass filter used to estimate $c_k(t)$ contains signal plus noise from one of the correlators and noise only from the other correlator. This method for channel estimation is not appropriate for antipodal signals, because the addition of the two correlator outputs results in signal cancellation. Instead, a single correlator can be employed for antipodal signals. Its output is fed to the input of the lowpass filter after the information-bearing signal is removed. To accomplish this, we must introduce a delay of one signaling interval into the channel estimation procedure, as illustrated in Fig. 14-5-5.

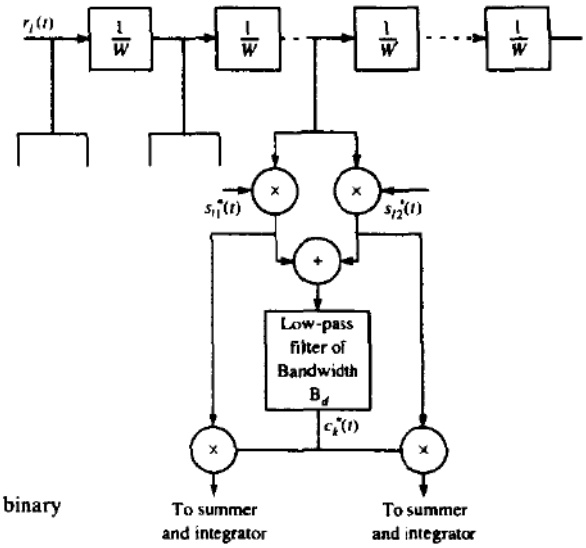

FIGURE 14-5-4 Channel tap weight estimation with binary orthogonal signals.

FIGURE 14-5-5 Channel tap weight estimation with binary antipodal signals.

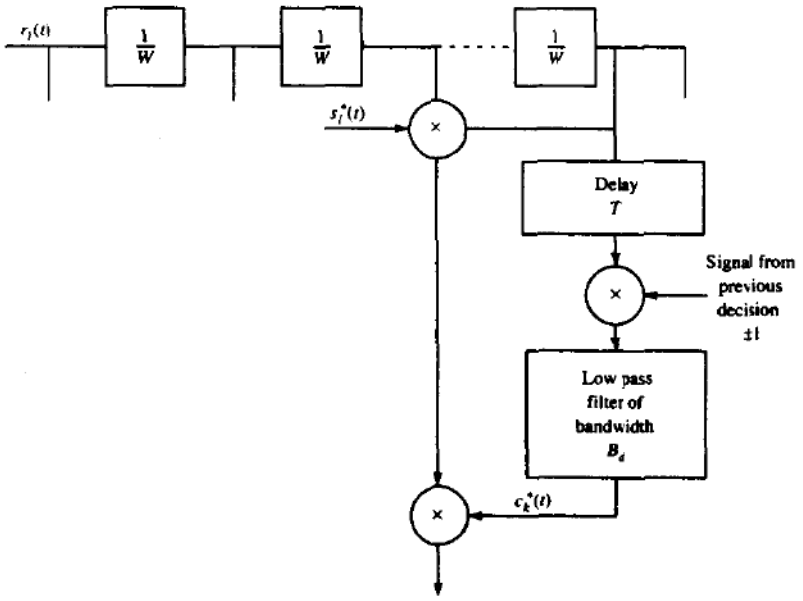

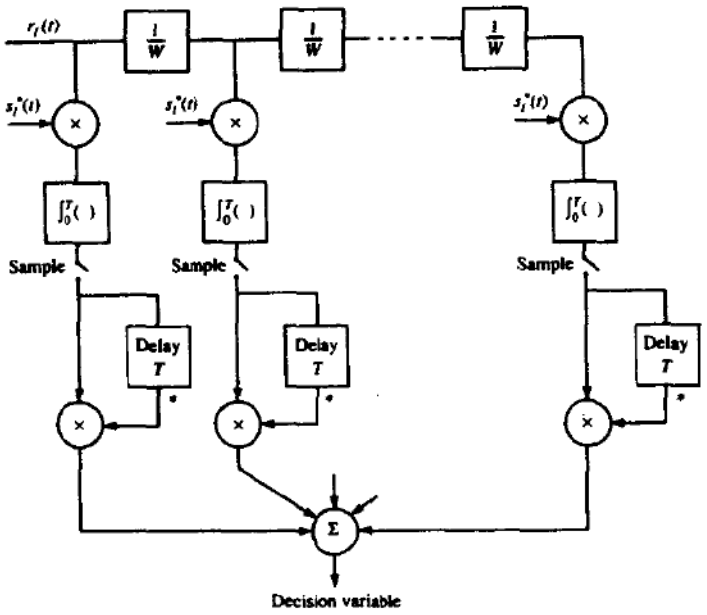

FIGURE 14-5-6 RAKE demodulator for DPSK signals.

That is, first the receiver must decide whether the information in the received signal is +1 or −1 and, then, it uses the decision to remove the information from the correlator output prior to feeding it to the lowpass fiter.

If we choose not to estimate the tap weights of the frequency-selective channel, we may use either DPSK signaling or noncoherently detected orthogonal signaling. The RAKE receiver structure for DPSK is illustrated in Fig 14-5-6. It is apparent that when the transmitted signal waveform $s_l(t)$ satisfies the orthogonality property given in (14-5-16), the decision variable is identical that given in (14-4-23) for an Lth-order diversity system. Consequently, the error rate performance of the RAKE receiver for a binary DPSK is identical to that given in (14-4-15) with $\mu = \bar{\gamma}_c/(1 + \bar{\gamma}_c)$, when all the signal paths have the same SNR $\bar{\gamma}_c$. On the other hand, when the SNRs $\{\bar{\gamma}_k\}$ are distinct, the error probability can be obtained by averaging (14-4-24), which is the probability of error conditioned on a time-invariant channel, over the probability density function of γ_b given by (14-5-26). The result of this integration is

$$P_2 = (\tfrac{1}{2})^{2L-1} \sum_{m=0}^{L-1} m! b_m \sum_{k=1}^{L} \frac{\pi_k}{\bar{\gamma}_k} \left(\frac{\bar{\gamma}_k}{1 + \bar{\gamma}_k} \right)^{m+1} \tag{14-5-30}$$

where π_k is defined in (14-5-27) and b_m in (14-4-25).

Finally, we consider binary orthogonal signaling over the frequency-selective channel with square-law detection at the receiver. This type of signal

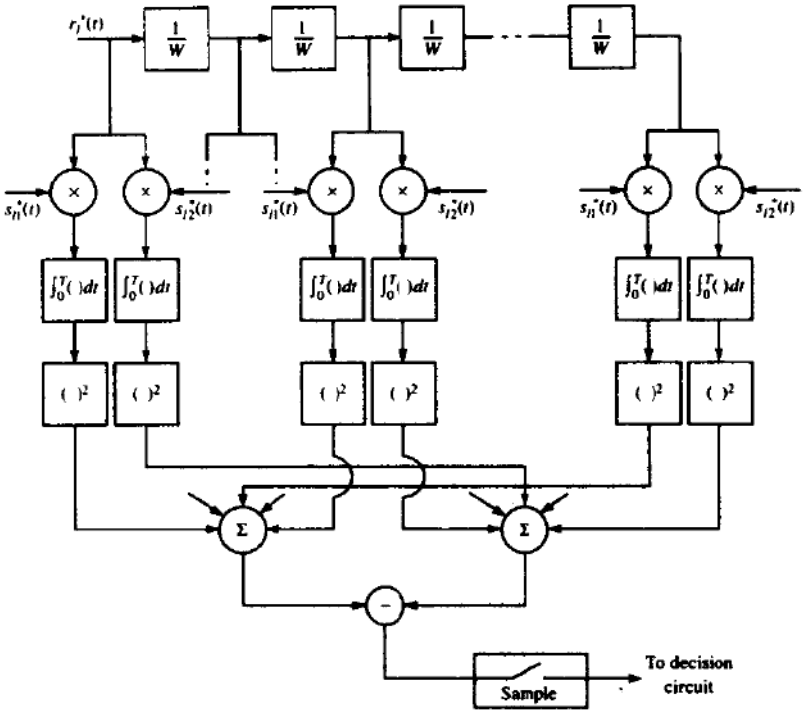

FIGURE 14-5-7 RAKE demodulator for square-law combination of orthogonal signals.

is appropriate when either the fading is rapid enough to preclude a good estimate of the channel tap weights or the cost of implementing the channel estimators is high. The RAKE receiver with square-law combining of the signal from each tap is illustrated in Fig. 14-5-7. In computing its performance, we again assume that the orthogonality property given in (14-5-16) holds. Then the decision variables at the output of the RAKE are

$$U_1 = \sum_{k=1}^{L} |2\mathscr{E}c_k + N_{k1}|^2$$
$$U_2 = \sum_{k=1}^{L} |N_{k2}|^2 \tag{14-5-31}$$

where we have assumed that $s_{l1}(t)$ was the transmitted signal. Again we observe that the decision variables are identical to the ones given in (14-4-29), which apply to orthogonal signals with Lth-order diversity. Therefore, the performance of the RAKE receiver for square-law-detected orthogonal signals is given by (14-4-15) with $\mu = \bar{\gamma}_c/(2 + \bar{\gamma}_c)$ when all the signal paths have the same SNR. If the SNRs are distinct, we can average the conditional error probability given by (14-4-24), with γ_b replaced by $\frac{1}{2}\gamma_b$, over the probability

density function $p(\gamma_b)$ given in (14-5-26). The result of this averaging is given by (14-5-30), with $\bar{\gamma}_k$ replaced by $\frac{1}{2}\bar{\gamma}_k$.

In the above analysis, the RAKE demodulator shown in Fig. 14-5-7 for square-law combination of orthogonal signals is assumed to contain a signal component at each delay. If that is not the case, its performance will be degraded, since some of the tap correlators will contribute only noise. Under such conditions, the low-level, noise-only contributions from the tap correlators should be excluded from the combiner, as shown by Chyi *et al.* (1988).

This concludes our discussion of signaling over a frequency-selective channel. The configurations of the RAKE receiver presented in this section can be easily generalized to multilevel signaling. In fact, if M-ary PSK or DPSK is chosen, the RAKE structures presented in this section remain unchanged. Only the PSK and DPSK detectors that follow the RAKE correlator are different.

14-6 CODED WAVEFORMS FOR FADING CHANNELS

Up to this point, we have demonstrated that diversity techniques are very effective in overcoming the detrimental effects of fading caused by the time-variant dispersive characteristics of the channel. Time- and/or frequency-diversity techniques may be viewed as a form of repetition (block) coding of the information sequence. From this point of view, the combining techniques described previously represent soft-decision decoding of the repetition code. Since a repetition code is a trivial form of coding, we shall now consider the additional benefits derived from more efficient types of codes. In particular, we demonstrate that coding provides an efficient means for obtaining diversity on a fading channel. The amount of diversity provided by a code is directly related to its minimum distance.

As explained in Section 14-4, time diversity is obtained by transmitting the signal components carrying the same information in multiple time intervals mutually separated by an amount equal to or exceeding the coherence time $(\Delta t)_c$ of the channel. Similarly, frequency diversity is obtained by transmitting the signal components carrying the same information in multiple frequency slots mutually separated by an amount of at least equal to the coherence bandwidth $(\Delta f)_c$ of the channel. Thus, the signal components carrying the same information undergo statistically independent fading.

To extend these notions to a coded information sequence, we simply require that the signal waveform corresponding to a particular code or code symbol fade independently of the signal waveform corresponding to any other code bit or code symbol. This requirement may result in inefficient utilization of the available time-frequency space, with the existence of large unused portions in this two-dimensional signaling space. To reduce the inefficiency, a number of code words may be interleaved in time or in frequency or both, in such a manner that the waveform corresponding to the bits or symbols of a given code word fade independently. Thus, we assume that the time-frequency signaling

space is partitioned into nonoverlapping time-frequency cells. A signal waveform corresponding to a code bit or code symbol is transmitted within such a cell.

In addition to the assumption of statistically independent fading of the signal components of a given code word, we also assume that the additive noise components corrupting the received signals are white gaussian processes that are statistically independent and identically distributed among the cells in the time-frequency space. Also, we assume that there is sufficient separation between adjacent cells so that intercell interference is negligible.

An important issue is the modulation technique that is used to transmit the coded information sequence. If the channel fades slowly enough to allow the establishment of a phase reference then PSK or DPSK may be employed. If this is not possible then FSK modulation with noncoherent detection at the receiver is appropriate. In our treatment, we assume that it is not possible to establish a phase reference or phase references for the signals in the different cells occupied by the transmitted signal. Consequently, we choose FSK modulation with noncoherent detection.

A model of the digital communications system for which the error rate performance will be evaluated is shown in Fig. 14-6-1. The encoder may be binary, nonbinary, or a concatenation of a nonbinary encoder with a binary encoder. Furthermore, the code generated by the encoder may be a block code, a convolutional code, or, in the case of concatenation, a mixture of a block code and a convolutional code.

In order to explain the modulation, demodulation, and decoding for FSK-type (orthogonal) signals, consider a linear binary block code in which k information bits are encoded into a block of n bits. For simplicity and without loss of generality, let us assume that all n bits of a code word are transmitted simultaneously over the channel on multiple frequency cells. A code word $\mathbf{C}_i$ having bits $\{c_{ij}\}$ is mapped into FSK signal waveforms in the following way. If $c_{ij} = 0$, the tone f_{0j} is transmitted, and if $c_{ij} = 1$, the tone f_{1j} is transmitted. This means that $2n$ tones or cells are available to transmit the n bits of the code word, but only n tones are transmitted in any signaling interval. Since each code word conveys k bits of information, the bandwidth expansion factor for FSK is $B_e = 2n/k$.

The demodulator for the received signal separates the signal into $2n$

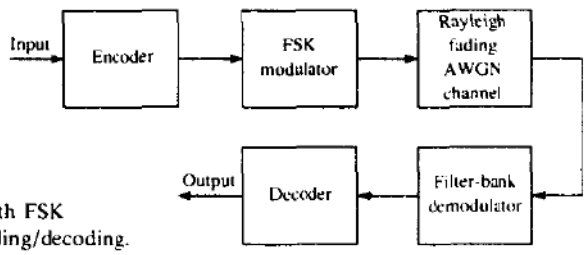

FIGURE 14-6-1 Model of communications system with FSK modulation/demodulation and encoding/decoding.

spectral components corresponding to the available tone frequencies at the transmitter. Thus, the demodulator can be realized as a bank of $2n$ filters, where each filter is matched to one of the possible transmitted tones. The outputs of the $2n$ filters are detected noncoherently. Since the Rayleigh fading and the additive white gaussian noises in the $2n$ frequency cells are mutually statistically independent and identically distributed random processes, the optimum maximum-likelihood soft-decision decoding criterion requires that these filter responses be square-law-detected and appropriately combined for each code word to form the $M = 2^k$ decision variables. The code word corresponding to the maximum of the decision variables is selected. If hard-decision decoding is employed, the optimum maximum-likelihood decoder selects the code word having the smallest Hamming distance relative to the received code word.

Although the discussion above assumed the use of a block code, a convolutional encoder can be easily accommodated in the block diagram shown in Fig. 14-6-1. For example, if a binary convolutional code is employed, each bit in the output sequence may be transmitted by binary FSK. The maximum-likelihood soft-decision decoding criterion for the convolutional code can be efficiently implemented by means of the Viterbi algorithm, in which the metrics for the surviving sequences at any point in the trellis consist of the square-law-combined outputs for the corresponding paths through the trellis. On the other hand, if hard-decision decoding is employed, the Viterbi algorithm is implemented with Hamming distance as the metric.

14-6-1 Probability of Error for Soft-Decision Decoding of Linear Binary Block Codes

Consider the decoding of a linear binary (n, k) code transmitted over a Rayleigh fading channel, as described above. The optimum soft-decision decoder, based on the maximum-likelihood criterion, forms the $M = 2^k$ decision variables

$$U_i = \sum_{j=1}^{n} [(1 - c_{ij})\,|y_{0j}|^2 + c_{ij}\,|y_{1j}|^2]$$

$$= \sum_{j=1}^{n} [|y_{0j}|^2 + c_{ij}(|y_{1j}|^2 - |y_{0j}|^2)], \qquad i = 1, 2, \ldots, 2^k \tag{14-6-1}$$

where $|y_{rj}|^2$, $j = 1, 2, \ldots, n$, and $r = 0, 1$ represent the squared envelopes at the outputs of the $2n$ filters that are tuned to the $2n$ possible transmitted tones. A decision is made in favor of the code word corresponding to the largest decision variable of the set $\{U_i\}$.

Our objective in this section is the determination of the error rate performance of the soft-decision decoder. Toward this end, let us assume that the all-zero code word $\mathbf{C}_1$ is transmitted. The average received signal-to-noise

ratio per tone (cell) is denoted by $\bar{\gamma}_c$. The total received SNR for the n tones in $n\bar{\gamma}_c$ and, hence, the average SNR per bit is

$$\begin{aligned}\bar{\gamma}_b &= \frac{n}{k}\bar{\gamma}_c \\ &= \frac{\bar{\gamma}_c}{R_c}\end{aligned} \tag{14-6-2}$$

where R_c is the code rate.

The decision variable U_1 corresponding to the code word $\mathbf{C}_1$ is given by (14-6-1) with $c_{ij} = 0$ for all j. The probability that a decision is made in favor of the mth code word is just

$$\begin{aligned}P_2(m) &= P(U_m > U_1) = P(U_1 - U_m < 0) \\ &= P\left[\sum_{j=1}^{n}(c_{1j} - c_{mj})(|y_{1j}|^2 - |y_{0j}|^2) < 0\right] \\ &= P\left[\sum_{j=1}^{w_m}(|y_{0j}|^2 - |y_{1j}|^2) < 0\right]\end{aligned} \tag{14-6-3}$$

where w_m is the weight of the mth code word. But the probability in (14-6-3) is just the probability of error for square-law combining of binary orthogonal FSK with w_mth-order diversity. That is,

$$P_2(m) = p^{w_m}\sum_{k=0}^{w_m-1}\binom{w_m - 1 + k}{k}(1-p)^k \tag{14-6-4}$$

$$\leq p^{w_m}\sum_{k=0}^{w_m-1}\binom{w_m - 1 + k}{k} = \binom{2w_m - 1}{w_m}p^{w_m} \tag{14-6-5}$$

where

$$p = \frac{1}{2 + \bar{\gamma}_c} = \frac{1}{2 + R_c\bar{\gamma}_b} \tag{14-6-6}$$

As an alternative, we may use the Chernoff upper bound derived in Section 14-4, which in the present notation is

$$P_2(m) \leq [4p(1-p)]^{w_m} \tag{14-6-7}$$

The sum of the binary error events over the $M-1$ nonzero-weight code words gives an upper bound on the probability of error. Thus,

$$P_M \leq \sum_{m=2}^{M} P_2(m) \tag{14-6-8}$$

Since the minimum distance of the linear code is equal to the minimum weight, it follows that

$$(1 + R_c\bar{\gamma}_b)^{-w_m} \leq (2 + R_c\bar{\gamma}_b)^{-d_{\min}}$$

The use of this relation in conjunction with (14-6-5) and (14-6-8) yields a simple, albeit looser, upper bound that may be expressed in the form

$$P_M < \frac{\sum_{m=2}^{M} \binom{2w_m - 1}{w_m}}{(2 + R_c \bar{\gamma}_b)^{d_{\min}}} \tag{14-6-9}$$

This simple bound indicates that the code provides an effective order of diversity equal to $d_{\min}$. An even simpler bound is the union bound

$$P_M < (M-1)[4p(1-p)]^{d_{\min}} \tag{14-6-10}$$

which is obtained from the Chernoff bound given in (14-6-7).

As an example serving to illustrate the benefits of coding for a Rayleigh fading channel, we have plotted in Fig. 14-6-2 the performance obtained with the extended Golay (24, 12) code and the performance of binary FSK and quarternay FSK each with dual diversity. Since the extended Golay code requires a total of 48 cells and $k = 12$, the bandwidth expansion factor $B_e = 4$. This is also the bandwidth expansion factor for binary and quaternary FSK with $L = 2$. Thus, the three types of waveforms are compared on the basis of the same bandwidth expansion factor. Note that at $P_b = 10^{-4}$, the Golay code outperforms quaternary FSK by more than 6 dB, and at $P_b = 10^{-5}$, the difference is approximately 10 dB.

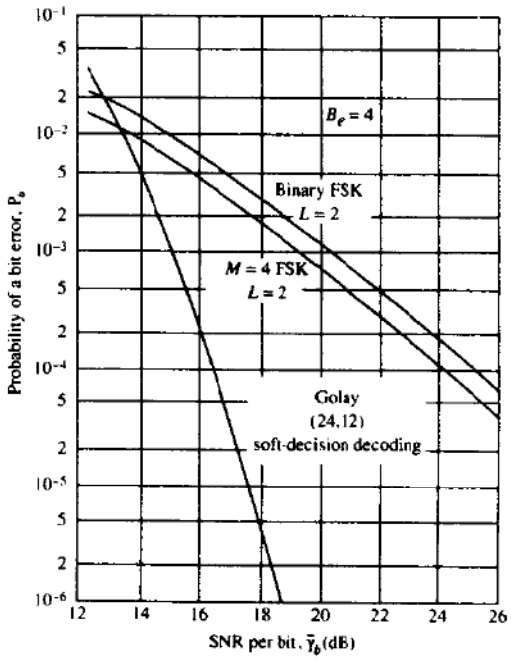

FIGURE 14-6-2 Example of performance obtained with conventional diversity versus coding for $B_e = 4$.

The reason for the superior performance of the Golay code is its large minimum distance ($d_{\min} = 8$), which translates into an equivalent eighth-order ($L = 8$) diversity. In contrast, the binary and quaternary FSK signals have only second-order diversity. Hence, the code makes more efficient use of the available channel bandwidth. The price that we must pay for the superior performance of the code is the increase in decoding complexity.

14-6-2 Probability of Error for Hard-Decision Decoding of Linear Binary Block Codes

Bounds on the performance obtained with hard-decision decoding of a linear binary (n, k) code have already been given in Section 8-1-5. These bounds are applicable to a general binary-input binary-output memoryless (binary symmetric) channel and, hence, they apply without modification to a Rayleigh fading AWGN channel with statistically independent fading of the symbols in the code word. The probability of a bit error needed to evaluate these bounds when binary FSK with noncoherent detection is used as the modulation and demodulation technique is given by (14-6-6).

A particularly interesting result is obtained when we use the Chernoff upper bound on the error probability for hard-decision decoding given by (8-1-89). That is,

$$P_2(m) \leq [4p(1-p)]^{m/2} \tag{14-6-11}$$

and P_M is upper-bounded by (14-6-8). In comparison, the Chernoff upper bound for $P_2(m)$ when soft-decision decoding is employed is given by (14-6-7). We observe that the effect of hard-decision decoding is a reduction in the distance between any two code words by a factor of 2. When the minimum distance of a code is relatively small, the reduction of the distances by a factor of 2 is much more noticeable in a fading channel than in a nonfading channel.

For illustrative pruposes we have plotted in Fig. 14-6-3 the performance of the Golay (23, 12) code when hard-decision and soft-decision decoding are used. The difference in performance at $P_b = 10^{-5}$ is approximately 6 dB. This is a significant difference in performance compared with the 2 dB difference between soft- and hard-decision decoding in a nonfading AWGN channel. We also note that the difference in performance increases as P_b decreases. In short, these results indicate the benefits of a soft-decision decoding over hard-decision decoding on a Rayleigh fading channel.

14-6-3 Upper Bounds on the Performance of Convolutional Codes for a Rayleigh Fading Channel

In this subsection, we derive the performance of binary convolutional codes when used on a Rayleigh fading AWGN channel. The encoder accepts k binary digits at a time and puts out n binary digits at a time. Thus, the code rate is $R_c = k/n$. The binary digits at the output of the encoder are transmitted

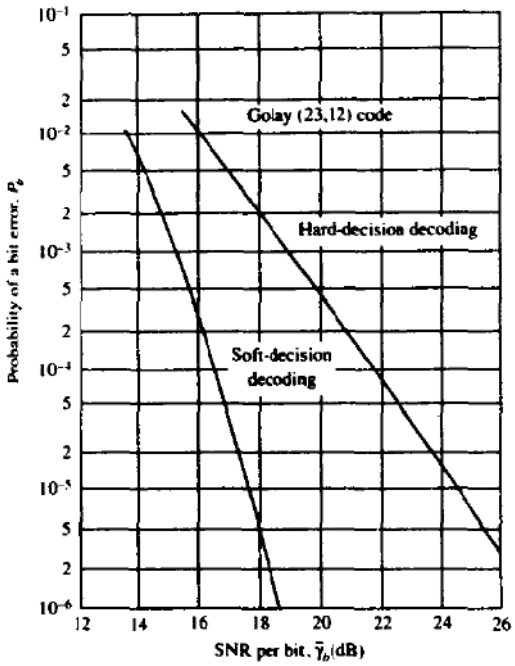

FIGURE 14-6-3 Comparison of performance between hard- and soft-decision decoding.

over the Rayleigh fading channel by means of binary FSK, which is square-law-detected at the receiver. The decoder for either soft- or hard-decision decoding performs maximum-likelihood sequence estimation, which is efficiently implemented by means of the Viterbi algorithm.

First, we consider soft-decision decoding. In this case, the metrics computed in the Viterbi algorithm are simply sums of square-law-detected outputs from the demodulator. Suppose the all-zero sequence is transmitted. Following the procedure outlined in Section 8-2-3, it is easily shown that the probability of error in a pairwise comparison of the metric corresponding to the all-zero sequence with the metric corresponding to another sequence that merges for the first time at the all-zero state is

$$P_2(d) = p^d \sum_{k=0}^{d-1} \binom{d-1+k}{k} (1-p)^k \tag{14-6-12}$$

where d is the number of bit positions in which the two sequences differ and p is given by (14-6-6). That is, $P_2(d)$ is just the probability of error for binary FSK with square-law detection and dth-order diversity. Alternatively, we may use the Chernoff bound in (14-6-7) for $P_2(d)$. In any case, the bit error probability is upperbounded, as shown in Section 8-2-3 by the expression

$$P_b < \frac{1}{k} \sum_{d=d_{\text{free}}}^{\infty} \beta_d P_2(d) \tag{14-6-13}$$

where the weighting coefficients $\{\beta_d\}$ in the summation are obtained from the expansion of the first derivative of the transfer function $T(D, N)$, given by (8-2-25).

When hard-decision decoding is performed at the receiver, the bounds on the error rate performance for binary convolutional codes derived in Section 8-2-4 apply. That is, P_b is again upper-bounded by the expression in (14-6-13), where $P_2(d)$ is defined by (8-2-28) for odd d and by (8-2-29) for even d, or upper-bounded (Chernoff bound) by (8-2-31), and p is defined by (14-6-6).

As in the case of block coding, when the respective Chernoff bounds are used for $P_2(d)$ with hard-decision and soft-decision decoding, it is interesting to note that the effect of hard-decision decoding is to reduce the distances (diversity) by a factor of 2 relative to soft-decision decoding.

The following numerical results illustrate the error rate performance of binary, rate $1/n$, maximal free distance convolutional codes for $n = 2$, 3, and 4 with soft-decision Viterbi decoding. First of all, Fig. 14-6-4 shows the performance of the rate 1/2 convolutional codes for constraint lengths 3, 4, and 5. The bandwidth expansion factor for binary FSK modulation is $B_e = 2n$. Since an increase in the constraint length results in an increase in the complexity of the decoder to go along with the corresponding increase in the minimum free distance, the system designer can weigh these two factors in the selection of the code.

Another way to increase the distance without increasing the constraint

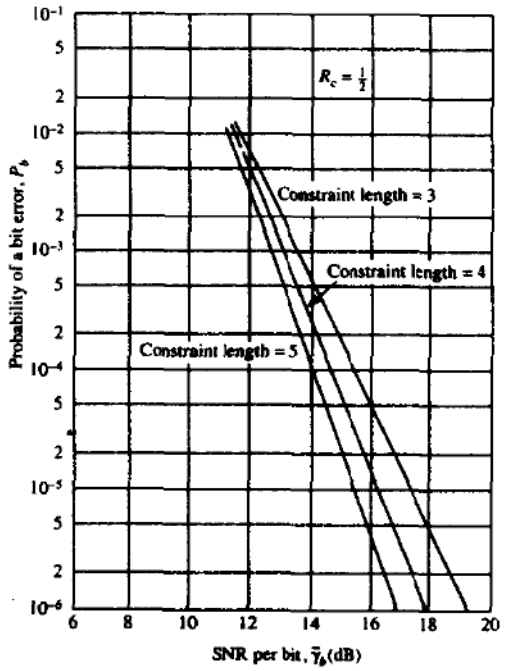

FIGURE 14-6-4 Performance of rate 1/2 binary convolutional codes with soft decision decoding.

length of the code is to repeat each output bit m times. This is equivalent to reducing the code rate by a factor of m or expanding the bandwidth by the same factor. The result is a convolutional code that has a minimum free distance of md_{free}, where d_{free} is the minimum free distance of the original code without repetitions. Such a code is almost as good, from the viewpoint of minimum distance, as a maximum free distance, rate $1/mn$ code. The error rate performance with repetitions is upper-bounded by

$$P_b < \frac{1}{k} \sum_{d_{free}}^{\infty} \beta_d P_2(md) \qquad (14\text{-}6\text{-}14)$$

where $P_2(md)$ is given by (14-6-12). Figure (14-6-5) illustrates the performance of the rate 1/2 codes with repetitions ($m = 1, 2, 3, 4$) for constraint length 5.

14-6-4 Use of Constant-Weight Codes and Concatenated Codes for a Fading Channel

Our treatment of coding for a Rayleigh fading channel to this point was based on the use of binary FSK as the modulation technique for transmitting each of the binary digits in a code word. For this modulation technique, all the 2^k code

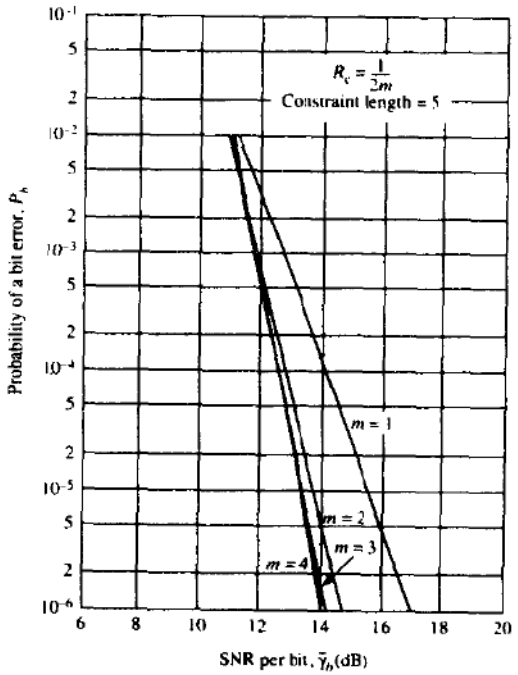

FIGURE 14-6-5 Performance of rate $1/2m$, constraint length 5, binary convolutional codes with soft-decision decoding.

words in the (n, k) code have identical transmitted energy. Furthermore, under the condition that the fading on the n transmitted tones is mutually statistically independent and identically distributed, the average received signal energy for the $M = 2^k$ possible code words is also identical. Consequently, in a soft-decision decoder, the decision is made in favor of the code word having the largest decision variable.

The condition that the received code words have identical average SNR has an important ramification in the implementation of the receiver. If the received code words do not have identical average SNR, the receiver must provide bias compensation for each received code word so as to render it equal energy. In general, the determination of the appropriate bias terms is difficult to implement because it requires the estimation of the average received signal power; hence, the equal-energy condition on the received code words considerably simplifies the receiver processing.

There is an alternative modulation method for generating equal-energy waveforms from code words when the code is constant-weight, i.e., when every code word has the same number of 1s. Note that such a code is nonlinear. Nevertheless, suppose we assign a single tone or cell to each bit position of the 2^k code words. Thus, an (n, k) binary block code has n tones assigned. Waveforms are constructed by transmitting the tone corresponding to a particular bit in a code word if that bit is a 1; otherwise, that tone is not transmitted for the duration of the interval. This modulation technique for transmitting the coded bits is called *on–off keying* (OOK). Since the code is constant-weight, say w, every coded waveform consists of w transmitted tones that depend on the positions of the 1s in each of the code words.

As in FSK, all tones in the OOK signal that are transmitted over the channel are assumed to fade independently across the frequency band and in time from one code word to another. The received signal envelope for each tone is described statistically by the Rayleigh distribution. Statistically independent additive white gaussian noise is assumed to be present in each frequency cell.

The receiver employs maximum-likelihood (soft-decision) decoding to map the received waveform into one of the M possible transmitted code words. For this purpose, n matched filters are employed, each matched to one of the n frequency tones. For the assumed statistical independence of the signal fading for the n frequency cells and additive white gaussian noise, the envelopes of the matched filter outputs are squared and combined to form the M decision variables

$$U_i = \sum_{j=1}^{n} c_{ij} |y_j|^2, \quad i = 1, 2, \ldots, 2^k \tag{14-6-15}$$

where $|y_j|^2$ corresponds to the squared envelope of the filter corresponding to the jth frequency, where $j = 1, 2, \ldots, n$.

It may appear that the constant-weight condition severely restricts our choice of codes. This is not the case, however. To illustrate this point, we

briefly describe some methods for constructing constant-weight codes. This discussion is by no means exhaustive.

Method 1: Nonlinear Transformation of a Linear Code In general, if in each word of an arbitrary binary code we substitute one binary sequence for every occurrence of a 0 and another sequence for each 1, a constant-weight binary block code will be obtained if the two substitution sequences are of equal weights and lengths. If the length of the sequence is v and the original code is an (n, k) code then the resulting constant-weight code will be an (vn, k) code. The weight will be n times the weight of the substitution sequence, and the minimum distance will be the minimum distances of the original code times the distances between the two substitution sequences. Thus, the use of complementary sequences when v is even results in a code with minimum distance $vd_{\min}$ and weight $\frac{1}{2}vn$.

The simplest form of this method is the case $v = 2$, in which every 0 is replaced by the pair 01 and every 1 is replaced by the complementary sequence 10 (or vice versa). As an example, we take as the initial code the (24, 12) extended Golay code. The parameters of the original and the resultant constant-weight code are given in Table 14-6-1.

Note that this substitution process can be viewed as a separate encoding. This secondary encoding clearly does not alter the information content of a code word—it merely changes the form in which it is transmitted. Since the new code word is composed of pairs of bits—one "on" and one "off"—the use of OOK transmission of this code word produces a waveform that is identical to that obtained by binary FSK modulation for the underlying linear code.

Method 2: Expurgation In this method, we start with an arbitrary binary block code and select from it a subset consisting of all words of a certain weight. Several different constant-weight codes can be obtained from one initial code by varying the choice of the weight w. Since the code words of the resulting expurgated code can be viewed as a subset of all possible permutations of any one code word in the set, the term *binary expurgated permutation modulation* (BEXPERM) has been used by Gaarder (1971) to describe such a code. In fact, the constant-weight binary block codes constructed by the other

TABLE 14-6-1 EXAMPLE OF CONSTANT-WEIGHT CODE FORMED BY METHOD 1

Code parameters	Original Golay	Constant-weight
n	24	48
k	12	12
M	4096	4096
$d_{\min}$	8	16
w	variable	24

TABLE 14-6-2 EXAMPLES OF CONSTANT-WEIGHT CODES FORMED BY EXPURGATION

Parameters	Original	Constant weight No. 1	Constant weight No. 2
n	24	24	24
k	12	9	11
M	4096	759	2576
$d_{\min}$	8	≥ 8	≥ 8
w	variable	8	12

methods may also be viewed as BEXPERM codes. This method of generating constant-weight codes is in a sense opposite to the first method in that the word length n is held constant and the code size M is changed. The minimum distance for the constant-weight subset will clearly be no less than that of the original code. As an example, we consider the Golay (24, 12) code and form the two different constant-weight codes shown in Table 14-6-2.

Method 3: Hadamard Matrices This method might appear to form a constant-weight binary block code directly, but it actually is a special case of the method of expurgation. In this method, a Hadamard matrix is formed as described in Section 8-1-2, and a constant-weight code is created by selection of rows (code words) from this matrix. Recall that a Hadamard matrix is an $n \times n$ matrix (n even integer) of 1s and 0s with the property that any row differs from any other row in exactly $\frac{1}{2}n$ positions. One row of the matrix is normally chosen as being all 0s.

In each of the other rows, half of the elements are 0s and the other half 1s. A Hadamard code of size $2(n-1)$ code words is obtained by selecting these $n-1$ rows and their complements. By selecting $M = 2^k \leq 2(n-1)$ of these code words, we obtain a Hadamard code, which we denote by $H(n, k)$, where each code word conveys k information bits. The resulting code has constant weight $\frac{1}{2}n$ and minimum distance $d_{\min} = \frac{1}{2}n$.

Since n frequency cells are used to transmit k information bits, the bandwidth expansion factor for the Hadamard $H(n, k)$ code is defined as

$$B_e = \frac{n}{k} \text{ cells per information bit}$$

which is simply the reciprocal of the code rate. Also, the average signal-to-noise ratio (SNR) per bit, denoted by $\bar{\gamma}_b$, is related to the average SNR per cell, $\bar{\gamma}_c$, by the expression

$$\begin{aligned} \bar{\gamma}_c &= \frac{k}{\frac{1}{2}n}\bar{\gamma}_b \\ &= 2\frac{k}{n}\bar{\gamma}_b = 2R_c\bar{\gamma}_b = \frac{2\bar{\gamma}_b}{B_e} \end{aligned} \tag{14-6-16}$$

Let us compare the performance of the constant-weight Hadamard codes under a fixed bandwidth constraint with a conventional M-ary orthogonal set of waveforms where each waveform has diversity L. The M orthogonal waveforms with diversity are equivalent to a block orthogonal code having a block length $n = LM$ and $k = \log_2 M$. For example, if $M = 4$ and $L = 2$, the code words of the block orthogonal code are

$$\mathbf{C}_1 = [1 \quad 1 \quad 0 \quad 0 \quad 0 \quad 0 \quad 0 \quad 0]$$

$$\mathbf{C}_2 = [0 \quad 0 \quad 1 \quad 1 \quad 0 \quad 0 \quad 0 \quad 0]$$

$$\mathbf{C}_3 = [0 \quad 0 \quad 0 \quad 0 \quad 1 \quad 1 \quad 0 \quad 0]$$

$$\mathbf{C}_4 = [0 \quad 0 \quad 0 \quad 0 \quad 0 \quad 0 \quad 1 \quad 1]$$

To transmit these code words using OOK modulation requires $n = 8$ cells, and since each code word conveys $k = 2$ bits of information, the bandwidth expansion factor $B_e = 4$. In general, we denote the block orthogonal code as $O(n, k)$. The bandwidth expansion factor is

$$B_e = \frac{n}{k} = \frac{LM}{k} \tag{14-6-17}$$

Also, the SNR per bit is related to the SNR per cell by the expression

$$\begin{aligned} \bar{\gamma}_c &= \frac{k}{L}\bar{\gamma}_b \\ &= M\left(\frac{k}{n}\right)\bar{\gamma}_b = M\frac{\bar{\gamma}_b}{B_e} \end{aligned} \tag{14-6-18}$$

Now we turn our attention to the performance characteristics of these codes. First, the exact probability of a code word (symbol) error for M-ary orthogonal signaling over a Rayleigh fading channel with diversity was given in closed form in Section 14-4. As previously indicated, this expression is rather cumbersome to evaluate, especially if either L or M or both are large. Instead, we shall use a union bound that is very convenient. That is, for a set of M orthogonal waveforms, the probability of a symbol error can be upper-bounded as

$$\begin{aligned} P_M &\leq (M-1)P_2(L) \\ &= (2^k - 1)P_2(L) < 2^k P_2(L) \end{aligned} \tag{14-6-19}$$

where $P_2(L)$, the probability of error for two orthogonal waveforms, each with diversity L, is given by (14-6-12) with $p = 1/(2 + \bar{\gamma}_c)$. The probability of bit error is obtained by multiplying P_M by $2^{k-1}/(2^k - 1)$, as explained previously.

A simple upper (union) bound on the probability of a code word error for the Hadamard $H(n, k)$ code is obtained by noting the probability of error in deciding between the transmitted code word and any other code word is bounded from above by $P_2(\frac{1}{2}d_{\min})$, where $d_{\min}$ is the minimum distance of the code. Therefore, an upper bound on P_M is

$$P_M \leq (M-1)P_2(\tfrac{1}{2}d_{\min}) < 2^k P_2(\tfrac{1}{2}d_{\min}) \tag{14-6-20}$$

Thus the "effective order of diversity" of the code for OOK modulation is $\frac{1}{2}d_{\min}$. The bit error probability may be approximated as $\frac{1}{2}P_M$, or slightly overbounded by multiplying P_M by the factor $2^{k-1}/(2^k-1)$, which is the factor used above for orthogonal codes. The latter was selected for the error probability computations given below.

Figures 14-6-6 and 14-6-7 illustrate the error rate performance of a selected number of Hadamard codes and block orthogonal codes, respectively, for several bandwidth expansion factors. The advantage resulting from an increase in the size M of the alphabet (or k, since $k = \log_2 M$) and an increase in the bandwidth expansion factor is apparent from observation of these curves. Note, for example, that the $H(20, 5)$ code when repeated twice results in a code that is denoted by ${}_2H(20, 5)$ and has a bandwidth expansion factor $B_e = 8$. Figure 14-6-8 shows the performance of the two types of codes compared on the basis of equal bandwidth expansion factors. It is observed that the error rate curves for the Hadamard codes are steeper than the corresponding curves

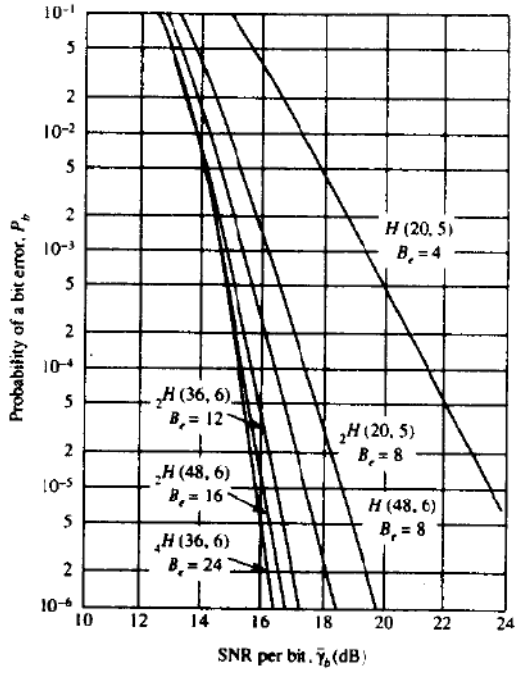

FIGURE 14-6-6 Performance of Hadamard codes.

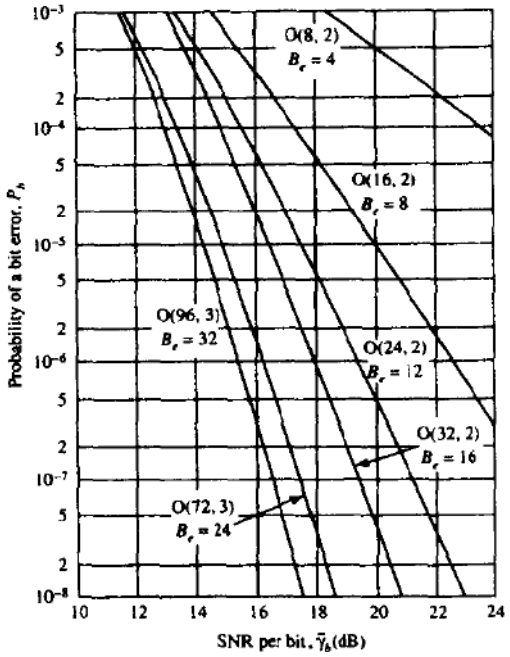

FIGURE 14-6-7 Performance of block orthogonal codes.

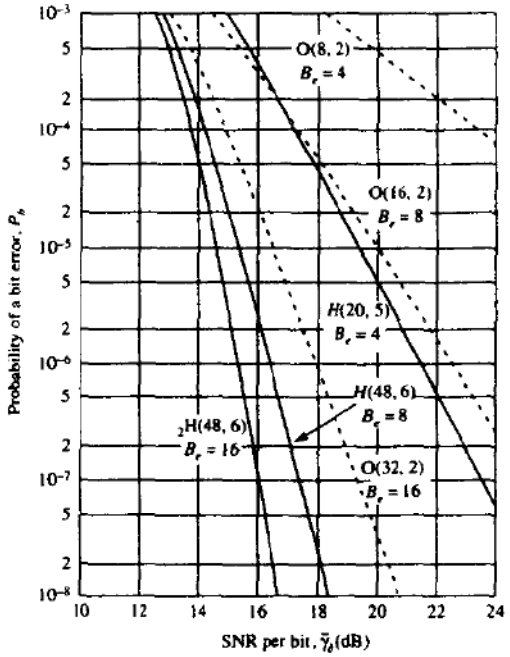

FIGURE 14-6-8 Comparison of performance between Hadamard codes and block orthogonal codes.

for the block orthogonal codes. This characteristic behavior is due simply to the fact that, for the same bandwidth expansion factor, the Hadamard codes provide more diversity than block orthogonal codes. Alternatively, one may say that Hadamard codes provide better bandwidth efficiency than block orthogonal codes. It should be mentioned, however, that at low SNR, a lower-diversity code outperforms a higher-diversity code as a consequence of the fact that, on a Rayleigh fading channel, there is an optimum distribution of the total received SNR among the diversity signals. Therefore, the curves for the block orthogonal codes will cross over the curves for the Hadamard codes at the low-SNR (high-error-rate) region.

Method 4: Concatenation In this method, we begin with two codes: one binary and the other nonbinary. The binary code is the inner code and is an (n, k) constant-weight (nonlinear) block code. The nonbinary code, which may be linear, is the outer code. To distinguish it from the inner code, we use uppercase letters, e.g., an (N, K) code, where N and K are measured in terms of symbols from a q-ary alphabet. The size q of the alphabet over which the outer code is defined cannot be greater than the number of words in the inner code. The outer code, when defined in terms of the binary inner code words rather than q-ary symbols, is the new code.

An important special case is obtained when $q = 2^k$ and the inner code size is chosen to be 2^k. Then the number of words is $M = 2^{kK}$ and the concatenated structure is an (nN, kK) code. The bandwidth expansion factor of this concatenated code is the product of the bandwidth expansions for the inner and outer codes.

Now we shall demonstrate the performance advantages obtained on a Rayleigh fading channel by means of code concatenation. Specifically, we construct a concatenated code in which the outer code is a dual-k (nonbinary) convolutional code and the inner code is either a Hadamard code or a block orthogonal code. That is, we view the dual-k code with M-ary ($M = 2^k$) orthogonal signals for modulation as a concatenated code. In all cases to be considered, soft-decision demodulation and Viterbi decoding are assumed.

The error rate performance of the dual-k convolutional codes is obtained from the derivation of the transfer function given by (8-2-39). For a rate-1/2, dual-k code with no repetitions, the bit error probability, appropriate for the case in which each k-bit output symbol from the dual-k encoder is mapped into one of $M = 2^k$ orthogonal code words, is upper-bounded as

$$P_b < \frac{2^{k-1}}{2^k - 1} \sum_{m=4}^{\infty} \beta_m P_2(m) \tag{14-6-21}$$

where $P_2(m)$ is given by (14-6-12).

For example, a rate-1/2, dual-2 code may employ a 4-ary orthogonal code $O(4, 2)$ as the inner code. The bandwidth expansion factor of the resulting concatenated code is, of course, the product of the bandwidth expansion

factors of the inner and outer codes. Thus, in this example, the rate of the outer code is 1/2 and the inner code is 1/2. Hence, $B_c = (4/2)(2) = 4$.

Note that if every symbol of the dual-k is repeated r times, this is equivalent to using an orthogonal code with diversity $L = r$. If we select $r = 2$ in the example given above, the resulting orthogonal code is denoted as O(8, 2) and the bandwidth expansion factor for the rate-1/2, dual-2 code becomes $B_c = 8$. Consequently, the term $P_2(m)$ in (14-6-21) must be replaced by $P_2(mL)$ when the orthogonal code has diversity L. Since a Hadamard code has an "effective diversity" $\frac{1}{2}d_{\min}$, it follows that when a Hadamard code is used as the inner code with a dual-k outer code, the upper bound on the bit error probability of the resulting concatenated code given by (14-6-21) still applies if $P_2(m)$ is replaced by $P_2(\frac{1}{2}md_{\min})$. With these modifications, the upper bound on the bit error probability given by (14-6-21) has been evaluated for rate-1/2, dual-k convolutional codes with either Hadamard codes or block orthogonal codes as inner codes. Thus the resulting concatenated code has a bandwidth expansion factor equal to twice the bandwidth expansion factor of the inner code.

First, we consider the performance gains due to code concatenation. Figure 14-6-9 illustrates the performance of dual-k codes with block orthogonal inner codes compared with the performance of block orthogonal codes for bandwidth expansion factors $B_c = 4$, 8, 16, and 32. The performance gains due to concatenation are very impressive. For example, at an error rate of 10^{-6} and $B_c = 8$, the dual-k code outperforms the orthogonal block code by 7.5 dB. In

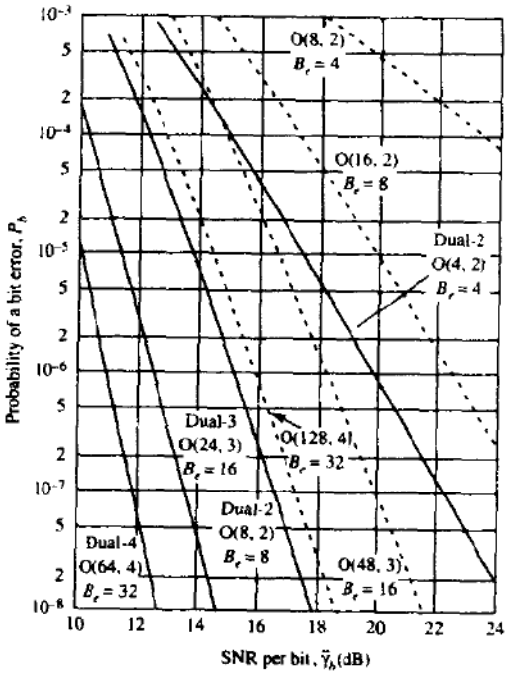

FIGURE 14-6-9 Comparison of performance between block orthogonal codes and dual-k with block orthogonal inner codes.

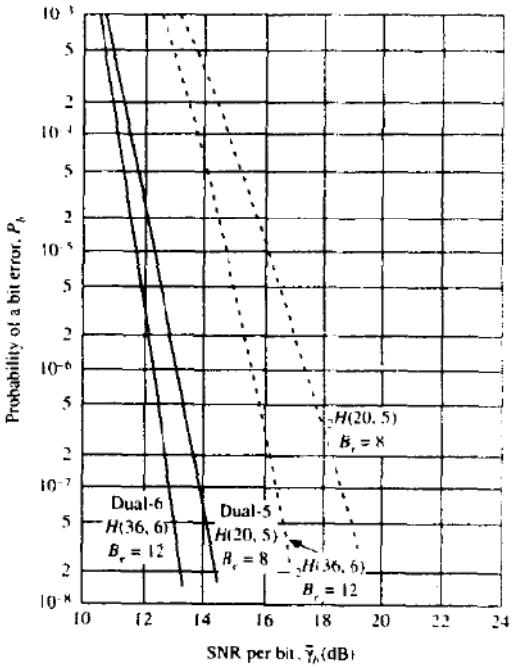

FIGURE 14-6-10 Comparison of performance between Hadamard codes and dual-k codes with Hadamard inner codes.

short, this gain may be attributed to the increased diversity (increase in minimum distance) obtained via code concatenation. Similarly, Fig. 14-6-10 illustrates the performance of two dual-k codes with Hadamard inner codes compared with the performance of the Hadamard codes alone for $B_e = 8$ and 12. It is observed that the performance gains due to code concatenation are still significant, but certainly not as impressive as those illustrated in Fig. 14-6-9. The reason is that the Hadamard codes alone yield a large diversity, so that the increased diversity arising from concatenation does not result in as large a gain in performance for the range of error rates covered in Fig. 14-6-10.

Next, we compare the performance for the two types of inner codes used with dual-k outer codes. Figure 14-6-11 shows the comparison for $B_e = 8$. Note that the $_2H(4, 2)$ inner code has $d_{\min} = 4$, and, hence, it has an effective order of diversity equal to 2. But this dual diversity is achieved by transmitting four frequencies per code word. On the other hand, the orthogonal code $O(8, 2)$ also gives dual diversity, but this is achieved by transmitting only two frequencies per code word. Consequently, the O(8, 2) code is 3 dB better than the $_2H(4, 2)$. This difference in performance is maintained when the two codes are used as inner codes in conjunction with dual-2 code. On the other hand, for $B_e = 8$, one can use the $H(20, 5)$ as the inner code of a dual-5 code, and its performance is significantly better than that of the dual-2 code at low error rates. This improvement in performance is achieved at the expense of an increase in decoding complexity. Similarly, in Fig. 14-6-12, we compare the

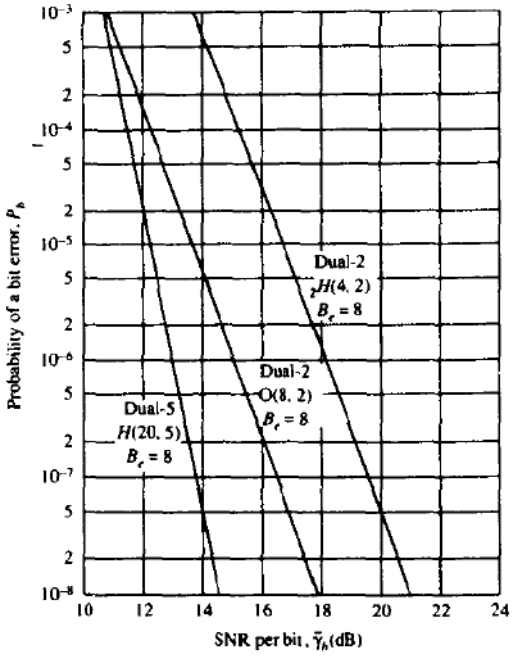

FIGURE 14-6-11 Performance of dual-k codes with either Hadamard or block orthogonal inner code for $B_c = 8$.

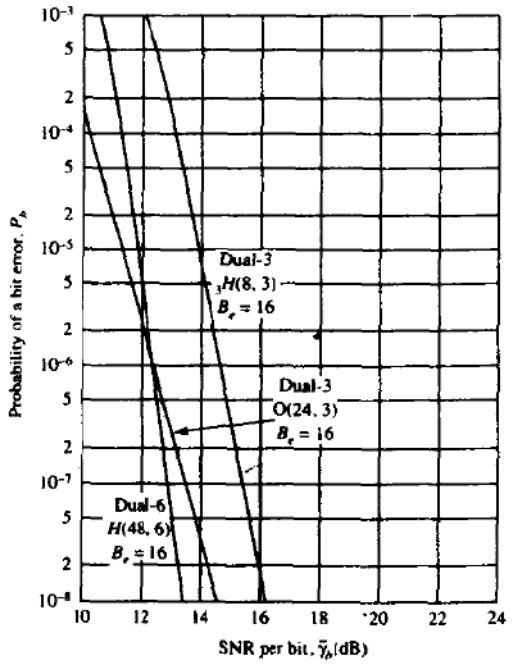

FIGURE 14-6-12 Performance of dual-k codes with either Hadamard or block orthogonal inner code for $B_c = 16$.

performance of the dual-k codes with two types of inner codes for $B_e = 16$. Note that the ${}_3H(8, 3)$ inner code has $d_{\min} = 12$, and, hence, it yields an effective diversity of 6. This diversity is achieved by transmitting 12 frequencies per code word. The orthogonal inner code O(24, 3) gives only third-order diversity, which is achieved by transmitting three frequencies per code word. Consequently the O(24, 3) inner code is more efficient at low SNR, that is, for the range of error rates covered in Fig. 14-6-12. At large SNR, the dual-3 code with the Hadamard ${}_3H(8, 3)$ inner code outperforms its counterpart with the O(24, 3) inner code due to the large diversity provided by the Hadamard code. For the same bandwidth expansion factor $B_e \approx 16$, one may use a dual-6 code with a $H(48, 6)$ code to achieve an improvement over the dual-3 code with the ${}_3H(8, 3)$ inner code. Again, this improvement in performance (which in this case is not as impressive as that shown in Fig. 14-6-11), must be weighed against the increased decoding complexity inherent in the dual-6 code.

The numerical results given above illustrate the performance advantages in using codes with good distance properties and soft-decision decoding on a Rayleigh fading channel as an alternative to conventional M-ary orthogonal signaling with diversity. In addition, the results illustrate the benefits of code concatenation on such a channel, using a dual-k convolutional code as the outer code and either a Hadamard code or a block orthogonal code as the inner code. Although dual-k codes were used for the outer code, similar results are obtained when a Reed-Solomon code is used for the outer code. There is an even greater choice in the selection of the inner code.

The important parameter in the selection of both the outer and the inner codes is the minimum distance of the resultant concatenated code required to achieve a specified level of performance. Since many codes will meet the performance requirements, the ultimate choice is made on the basis of decoding complexity and bandwidth requirements.

14-6-5 System Design Based on the Cutoff Rate

In the above treatment of coded waveforms, we have demonstrated the effectiveness of various codes for fading channels. In particular, we have observed the benefits of soft-decision decoding and code concatenation as a means for increasing the minimum distance and, hence, the amount of diversity in the coded waveforms. In this subsection, we consider randomly selected code words and derive an upper (union) bound on the error probability that depends on the cutoff rate parameter for the Rayleigh fading channel.

Let us consider the model for the communication system illustrated in Fig. 14-6-1. The modulator has a q-ary orthogonal FSK alphabet. Code words of block length n are mapped into waveforms by selecting n tones from the alphabet of q tones. The demodulation is performed by passing the signal through a bank of q matched filters followed by square-law detectors. The decoding is assumed to be soft-decision. Thus, the square-law detected outputs

from the demodulator are appropriately combined (added) with equal weighting to form M decision variables corresponding to the M possible transmitted code words.

To evaluate the union bound on the probability of error in a Rayleigh fading channel with AWGN, we first evaluate the binary error probability involving the decision variable U_1, which corresponds to the transmitted code word, and any of the other $M-1$ decision variables corresponding to the other code words. Let U_2 be the other decision variable and suppose that U_1 and U_2 have l tones in common. Hence, the contributions to U_1 and U_2 from these l tones are identical and, therefore, cancel out when we form the difference $U_1 - U_2$. Since the two decision variables differ in $n-l$ tones, the probability of error is simply that for a binary orthogonal FSK system with $n-l$ order diversity. The exact form for this probability of error is given by (14-6-4), where $p = 1/(2+\bar{\gamma}_c)$, and $\bar{\gamma}_c$ is the average SNR per tone. For simplicity, we choose to use the Chernoff bound for this binary event error probability, given by (14-6-7), i.e.,

$$P_2(U_1, U_2 \mid l) \leq [4p(1-p)]^{n-l} \tag{14-6-22}$$

Now, let us average over the ensemble of binary communication systems. There are q^n possible code words, from which we randomly select two code words. Thus, each code word is selected with equal probability. Then, the probability that two randomly selected code words have l tones in common is

$$P(l) = \binom{n}{l}\left(\frac{1}{q}\right)^l\left(1-\frac{1}{q}\right)^{n-l} \tag{14-6-23}$$

When we average (14-6-22) over the probability distribution of l given by (14-6-23), we obtain

$$\begin{aligned}\overline{P_2(U_1, U_2)} &= \sum_{l=0}^{n} P_2(U_1, U_2 \mid l)P(l) \\ &\leq \left\{\sum_{l=0}^{n}\binom{n}{l}\left(\frac{1}{q}\right)^l\left[4\left(1-\frac{1}{q}\right)p(1-p)\right]^{n-l}\right. \\ &\leq \left\{\frac{1}{q}[1+4(q-1)p(1-p)]\right\}^n \end{aligned} \tag{14-6-24}$$

Finally, the union bound for communication systems that use $M = 2^k$ randomly selected code words is simply

$$\bar{P}_M \leq (M-1)\overline{P_2(U_1, U_2)} < M\overline{P_2(U_1, U_2)} \tag{14-6-25}$$

By combining (14-6-24) with (14-6-25), we obtain the upper bound on the symbol error probability as

$$\bar{P}_M < 2^{-n(R_0 - R_c)} \tag{14-6-26}$$

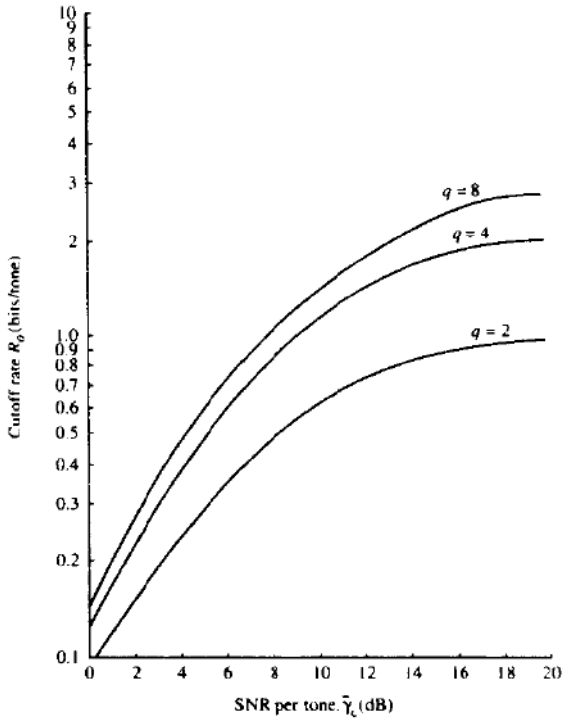

URE 14-6-13 Cutoff rate as a function of $\bar{\gamma}_c$ for Rayleigh fading channel.

where $R_c = k/n$ is the code rate and R_0 is the cutoff rate defined as

$$R_0 = \log_2 \frac{q}{1 + 4(q-1)p(1-p)} \tag{14-6-27}$$

with

$$p = \frac{1}{2 + \bar{\gamma}_c} \tag{14-6-28}$$

Graphs of R_0 as a function of $\bar{\gamma}_c$ are shown in Fig. 14-6-13 for $q = 2$, 4, and 8.

A more interesting form of (14-6-26) is obtained if we express $\bar{P}_M$ in terms of the SNR per bit. In particular, (14-6-26) may be expressed as

$$\bar{P}_M < 2^{-k[\bar{\gamma}_b g(q, \bar{\gamma}_c) - 1]} \tag{14-6-29}$$

where, by definition,

$$\begin{aligned} g(q, \bar{\gamma}_c) &= \frac{R_0}{\bar{\gamma}_c} \\ &= \frac{1}{\bar{\gamma}_c} \log_2 \left[\frac{q}{1 + 4(q-1)p(1-p)} \right] \end{aligned} \tag{14-6-30}$$

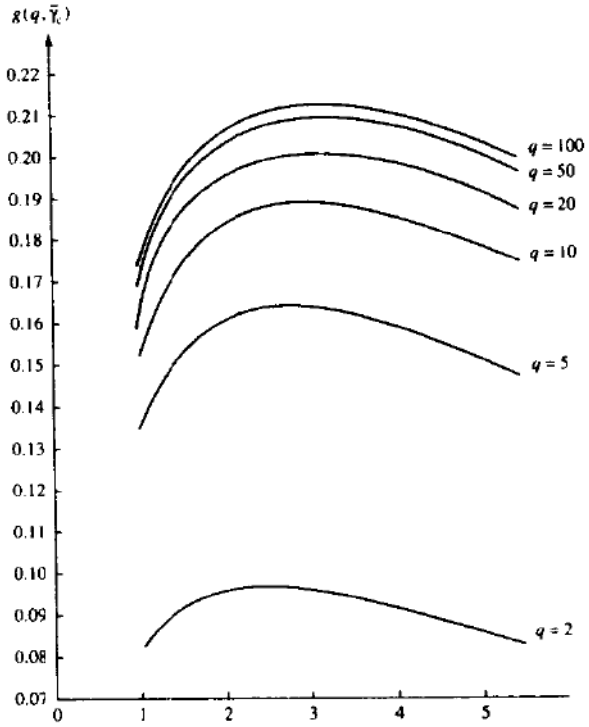

FIGURE 14-6-14 Graph of function $g(q, \bar{\gamma}_c)$.

Graphs of $g(q, \bar{\gamma}_c)$ as a function of $\bar{\gamma}_c$ are plotted in Fig. 14-6-14, with q as a parameter. First, we note thate is an optimum $\bar{\gamma}_c$ for each value of q that minimizes the probability of error. For large q, this value is approximately $\bar{\gamma}_c = 3$ (5 dB), which is consistent with our previous observation for ordinary square-law diversity combining. Furthermore, as $q \to \infty$, the function $g(q, \bar{\gamma}_c)$ approaches a limit, which is

$$\lim_{q\to\infty} g(q, \bar{\gamma}_c) = g_\infty(\bar{\gamma}_c) = \frac{1}{\bar{\gamma}_c} \log_2 \left[\frac{(2 + \bar{\gamma}_c)^2}{4(1 + \bar{\gamma}_c)}\right] \tag{14-6-31}$$

The value of $g_\infty(\bar{\gamma}_c)$ evaluated at $\bar{\gamma}_c = 3$ is

$$\begin{aligned} g_\infty(3) &= \max_{\bar{\gamma}_c} g_\infty(\bar{\gamma}_c) \\ &= 0.215 \end{aligned} \tag{14-6-32}$$

Therefore, the error probability in (14-6-29) for this optimum division of total SNR is

$$\bar{P}_M < 2^{-0.215k(\bar{\gamma}_b - 4.65)} \tag{14-6-33}$$

This result indicates that the probability of error can be made arbitrarily small with optimum SNR per code chip, if the average SNR per bit $\bar{\gamma}_b > 4.65$ (6.7 dB). Even a relatively modest value of $q = 20$ comes close to this minimum value. As seen from Fig. 14-6-14, $g(20, 3) = 0.2$, so that $P_M \to 0$, provided $\bar{\gamma}_b > 5$ (7 dB). On the other hand, if $q = 2$, the maximum value of $g(2, \bar{\gamma}_c) \approx 0.096$ and the corresponding minimum SNR per bit is 10.2 dB.

In the case of binary FSK waveforms ($q = 2$), we may easily compare the cutoff rate for the unquantized (soft-decision) demodulator output with the cutoff rate for binary quantization, for which

$$R_Q = 1 - \log[1 + \sqrt{4p(1-p)}], \qquad Q = 2$$

as was given in (8-1-104). Figure 14-6-15 illustrates the graphs for R_0 and R_Q. Note that the difference between R_0 and R_Q is approximately 3 dB for rates below 0.3 and the difference increases rapidly at high rates. This loss may be reduced significantly by increasing the number of quantization levels to $Q = 8$ (three bits).

Similar comparisons in the relative performance between unquantized soft-decision decoding and quantized decision decoding can also be made for $q > 2$.

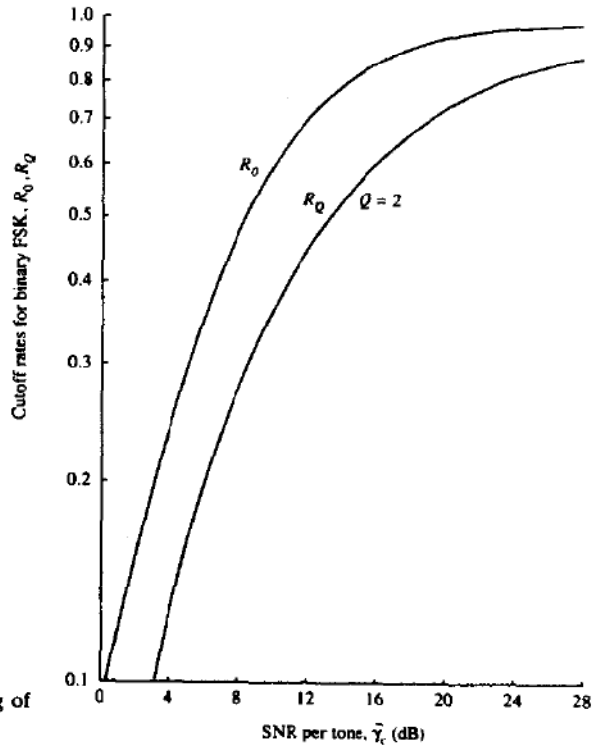

FIGURE 14-6-15 Cutoff rate for (unquantized) soft-decision and hard-decision decoding of coded binary FSK.

14-6-6 Trellis-Coded Modulation

Trellis-coded modulation was described in Section 8-3 as a means for achieving a coding gain on bandwidth-constrained channels, where we wish to transmit at a bit-rate-to-bandwidth ratio $R/W > 1$. For such channels, the digital communication system is designed to use bandwidth-efficient multilevel or multiphase modulation (PAM, PSK, DPSK, or QAM), which allows us to achieve an $R/W > 1$. When coding is applied in signal design for a bandwidth constrained channel, a coding gain is desired without expanding the signal bandwidth. This goal can be achieved, as described in Section 8-3, by increasing the number of signal points in the constellation over the corresponding uncoded system to compensate for the redundancy introduced by the code, and designing the trellis code so that the euclidean distance in a sequence of transmitted symbols corresponding to paths that merge at any node in the trellis is larger than the euclidean distance per symbol in an uncoded system.

In contrast, the coding schemes that we have described above in conjunction with FSK modulation expand the bandwidth of the modulated signal for the purpose of achieving signal diversity. Coupled with FSK modulation, which is not bandwidth-efficient, the coding schemes we have described are inappropriate for use on bandwidth-constrained channels.

In designing trellis-coded signal waveforms for fading channels, we may use the same basic principles that we have learned and applied in the design of conventional coding schemes. In particular, the most important objective in any coded signal design for fading channels is to achieve as large a signal diversity as possible. This implies that successive output symbols from the encoder must be interleaved or sufficiently separated in transmission, either in time or in frequency, so as to achieve independent fading in a sequence of symbols that equals or exceeds the minimum free distance of the trellis code. Therefore, we may represent such a trellis-coded modulation system by the block diagram in Fig. 14-6-16, where the interleaver is viewed broadly as a device that separates the successive coded symbols so as to provide independent fading on each symbol (through frequency or time separation of symbols) in the sequence. The receiver consists of a signal demodulator whose output is deinterleaved and fed to the trellis decoder.

FIGURE 14-6-16 Block diagram of trellis-coded modulation systems.

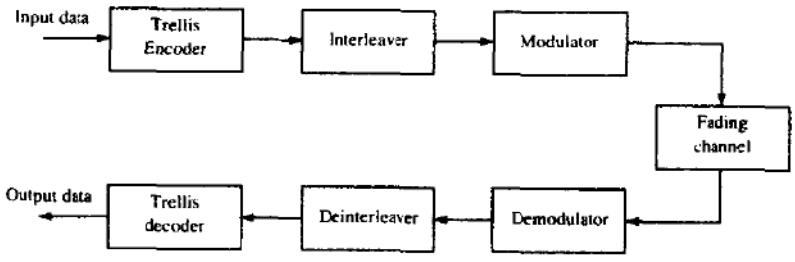

As indicated above, the candidate modulation methods that achieve high bandwidth efficiency are M-ary PSK, DPSK, QAM and PAM. The choice depends to a large extent on the channel characteristics. If there are rapid amplitude variations in the received signal, QAM and PAM may be particularly vulnerable, because a wideband automatic gain control (AGC) must be used to compensate for the channel variations. In such a case, PSK or DPSK are more suitable, since the information is conveyed by the signal phase and not by the signal amplitude. DPSK provides the additional benefit that carrier phase coherence is required only over two successive symbols. However, there is an SNR degradation in DPSK relative to PSK.

In the design of the trellis code, our objective is to achieve as large a free distance as possible, since this parameter is equivalent to the amount of diversity in the received signal. In conventional Ungerboeck trellis coding, each branch in the trellis corresponds to a single M-ary (PSK, DPSK, QAM) output channel symbol. Let us define the *shortest error event path* as the error event path with the smallest number of nonzero distances between itself and the correct path, and let L be its length. In other words, L is the Hamming distance between the M-ary symbols on the shortest error event path and those in the correct path. Hence, if we assume that the transmitted sequence corresponds to the all-zero path in the trellis, L is the number of branches in the shortest-length path with a nonzero M-ary symbol. In a trellis diagram with parallel paths, the paths are constrained to have a shortest error event length of one branch, so that $L = 1$. This means that such a trellis code provides no diversity in a fading channel and, hence, the probability of error is inversely proportional to the SNR per symbol. Therefore, in conventional trellis coding for a fading channel, it is undesirable to design a code that has parallel paths in its trellis, because such a code yields no diversity. This is the case in a conventional rate-$m/(m+1)$ trellis code, where we are forced to have parallel paths when the number of states is less than 2^m.

One possible way to increase the minimum free distance and, thus, the order of diversity in the code, is to introduce asymmetry in the signal point constellation. This approach appears to be somewhat effective, and has been investigated by Simon and Divsalar (1985), Divsalar and Yuen (1984), and Divsalar *et al.* (1987).

A more effective way to increase the distance L and, thus, the order of diversity is to employ multiple trellis-coded modulation (MTCM). In MTCM, illustrated in Fig. 14-6-17, b input bits to the encoder are coded into c output bits, which are then subdivided into k groups, each of m bits, such that $c = km$. Each m-bit group is mapped into an M-ary symbol. Thus, we obtain the M-ary output symbols. The special case $k = 1$ corresponds to the conventional Ungerboeck codes. With k M-ary output symbols, it is possible to design trellis codes with parallel paths having a distance $L = k$. Thus, we can achieve an error probability that decays inversely as $(\mathscr{E}/N_0)^k$.

An important consideration in the design of the decoder for the trellis code is the use of any side information regarding the channel attenuation for each

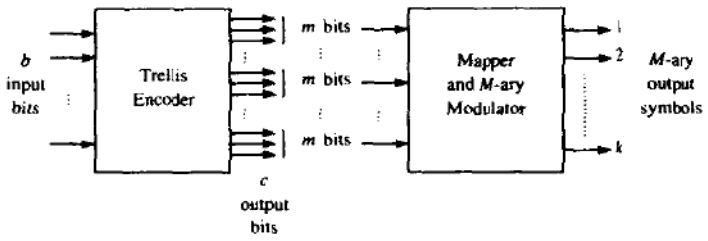

FIGURE 14-6-17 Block diagram of MTCM transmitter.

symbol. In the case of FSK modulation with square-law combination at the decoder to form the decision metrics, it is not necessary to know the channel attenuation for demodulated symbols. However, with coherent detection, the optimum euclidean distance metric for each demodulated symbol is of the form $|r_n - \alpha_n s_n|^2$, where α_n is the channel attenuation for the transmitted symbol s_n and r_n is the demodulation output. Hence, the sum of branch metrics for any given path through the trellis is of the form

$$D(\mathbf{r}, \mathbf{s}^{(i)}) = \sum_n |r_n - \alpha_n s_n^{(i)}|^2$$

where the superscript (i) indicates the ith path through the trellis. Therefore, the estimation of the channel attenuation must be performed in order to realize the optimum trellis decoder. The estimation of the channel attenuation and phase shift, is considered in Appendix C for the case of PSK modulation and demodulation. The effect of the quality of the attenuation and phase estimates on the performance of PSK (uncoded) modulation is also assessed in Appendix C.

14-7 BIBLIOGRAPHICAL NOTES AND REFERENCES

In this chapter, we have considered a number of topics concerned with digital communications over a fading multipath channel. We began with a statistical characterization of the channel and then described the ramifications of the channel characteristics on the design of digital signals and on their performance. We observed that the reliability of the communication system is enhanced by the use of diversity transmission and reception. Finally we demonstrated that channel encoding and soft-decision decoding provide a bandwidth-efficient means for obtaining diversity over such channels.

The pioneering work on the characterization of fading multipath channels and on signal and receiver design for reliable digital communications over such channels was done by Price (1954, 1956). This work was followed by additional significant contributions from Price and Green (1958, 1960), Kailath (1960, 1961), and Green (1962). Diversity transmission and diversity combining techniques under a variety of channel conditions have been considered in the papers by Pierce (1958), Brennan (1959), Turin (1961, 1962), Pierce and Stein

(1960), Barrow (1963), Bello and Nelin (1962a, b, 1963), Price (1962a, b), and Lindsey (1964).

Our treatment of coding for fading channels has relied on contributions from a number of researchers. In particular, the use of dual-k codes with M-ary orthogonal FSK was proposed in publications by Viterbi and Jacobs (1975) and Odenwalder (1976). The importance of coding for digital communications over a fading channel was also emphasized in a paper by Chase (1976). The benefits derived from concatenated coding with soft-decision decoding for a fading channel were demonstrated by Pieper *et al.* (1978). There, a Reed–Solomon code was used for the outer code and a Hadamard code was selected as the inner code. The performance of dual-k codes with either block orthogonal codes or Hadamard codes as inner code were investigated by Proakis and Rahman (1979). The error rate performance of maximal free distance binary convolutional codes was evaluated by Rahman (1981). Finally, the derivation of the cutoff rate for Rayleigh fading channels is due to Wozencraft and Jacobs (1965).

Trellis-coded modulation for fading channels has been investigated by many researchers, whose work was motivated to a large extent by applications to mobile and cellular communications. The book by Biglieri *et al.* (1991) gives a tutorial treatment of this topic and contains a large number of references to the technical literature.

Our treatment of digital communications over fading channels focused primarily on the Rayleigh fading channel model. For the most part, this is due to the wide acceptance of this model for describing the fading effects on many radio channels and to its mathematical tractability. Although other statistical models, such as a Ricean fading model or the Nakagami fading model may be more appropriate for characterizing fading on some real channels, the general approach in the design of reliable communications presented in this chapter carries over.

PROBLEMS

14-1 The scattering function $S(\tau; \lambda)$ for a fading multipath channel is nonzero for the range of values $0 \leq \tau \leq 1$ ms and -0.1 Hz $\leq \lambda \leq 0.1$ Hz. Assume that the scattering function is approximately uniform in the two variables.

a Give numerical values for the following parameters:

(i) the multipath spread of the channel;
(ii) the Doppler spread of the channel;
(iii) the coherence time of the channel;
(iv) the coherence bandwidth of the channel;
(v) the spread factor of the channel.

b Explain the meaning of the following, taking into consideration the answers given in (a):

(i) the channel is frequency-nonselective;
(ii) the channel is slowly fading;
(iii) the channel is frequency-selective.

c Suppose that we have a frequency allocation (bandwidth) of 10 kHz and we wish to transmit at a rate of 100 bits/s over this channel. Design a binary communications system with frequency diversity. In particular, specify (i) the type of modulation, (ii) the number of subchannels, (iii) the frequency separation between adjacent carriers, and (iv) the signaling interval used in your design. Justify your choice of parameters.

14-2 Consider a binary communications system for transmitting a binary sequence over a fading channel. The modulation is orthogonal FSK with third-order frequency diversity ($L = 3$). The demodulator consists of matched filters followed by square-law detectors. Assume that the FSK carriers fade independently and identically according to a Rayleigh envelope distribution. The additive noises on the diversity signals are zero-mean gaussian with autocorrelation functions $\frac{1}{2}E[z_k^*(t)z_k(t+\tau)] = N_0\delta(\tau)$. The noise processes are mutually statistically independent.

a The transmitted signal may be viewed as binary FSK with square-law detection, generated by a repetition code of the form

$$1 \rightarrow \mathbf{C}_1 = [1 \quad 1 \quad 1], \qquad 0 \rightarrow \mathbf{C}_0 = [0 \quad 0 \quad 0]$$

Determine the error rate performance P_{2h} for a hard-decision decoder following the square-law-detected signals.

b Evaluate P_{2h} for $\bar{\gamma}_c = 100$ and 1000.

c Evaluate the error rate P_{2s} for $\bar{\gamma}_c = 100$ and 1000 if the decoder employs soft-decision decoding.

d Consider the generalization of the result in (a). If a repetition code of block length L (L odd) is used, determine the error probability P_{2h} of the hard-decision decoder and compare that with P_{2s}, the error rate of the soft-decision decoder. Assume $\bar{\gamma} \gg 1$.

14-3 Suppose that the binary signal $s_i(t)$ is transmitted over a fading channel and the received signal is

$$r_i(t) = \pm a s_i(t) + z(t), \qquad 0 \leq t \leq T$$

where $z(t)$ is zero-mean white gaussian noise with autocorrelation function

$$\phi_{zz}(\tau) = N_0\delta(\tau)$$

The energy in the transmitted signal is $\mathcal{E} = \frac{1}{2}\int_0^T |s_i(t)|^2\,dt$. The channel gain a is specified by the probability density function

$$p(a) = 0.1\delta(a) + 0.9\delta(a-2)$$

a Determine the average probability of error P_2 for the demodulator that employs a filter matched to $s_i(t)$.

b What value does P_2 approach as $\mathcal{E}/N_0$ approaches infinity.

c Suppose that the same signal is transmitted on two statistically *independently fading* channels with gains a_1 and a_2, where

$$p(a_k) = 0.1\delta(a_k) + 0.9\delta(a_k - 2), \qquad k = 1, 2$$

The noises on the two channels are statistically independent and identically distributed. The demodulator employs a matched filter for each channel and

simply adds the two filter outputs to form the decision variable. Determine the average P_2.

d For the case in (c) what value does P_2 approach as $\mathcal{E}/N_0$ approaches infinity.

14-4 A multipath fading channel has a multipath spread of $T_m = 1$ s and a Doppler spread $B_d = 0.01$ Hz. The total channel bandwidth at bandpass available for signal transmission is $W = 5$ Hz. To reduce the effects of intersymbol interference, the signal designer selects a pulse duration $T = 10$ s.

a Determine the coherence bandwidth and the coherence time.

b Is the channel frequency selective? Explain.

c Is the channel fading slowly or rapidly? Explain.

d Suppose that the channel is used to transmit binary data via (antipodal) coherently detected PSK in a frequency diversity mode. Explain how you would use the available channel bandwidth to obtain frequency diversity and determine how much diversity is available.

e For the case in (d), what is the *approximate* SNR required per diversity to achieve an error probability of 10^{-6}?

f Suppose that a wideband signal is used for transmission and a RAKE-type receiver is used for demodulation. How many taps would you use in the RAKE receiver?

g Explain whether or not the RAKE receiver can be implemented as a coherent receiver with maximal ratio combining.

h If binary orthogonal signals are used for the wideband signal with square-law postdetection combining in the RAKE receiver, what is the *approximate* SNR required to achieve an error probability of 10^{-6}? (assume that all taps have the same SNR.)

14-5 In the binary communications system shown in Fig. P14-5, $z_1(t)$ and $z_2(t)$ are statistically independent white gaussian noise processes with zero mean and identical autocorrelation functions $\phi_{zz}(\tau) = N_0\delta(\tau)$. The sampled values U_1 and U_2 represent the *real parts* of the matched filter outputs. For example, if $s_i(t)$ is transmitted, then we have

$$U_1 = 2\mathcal{E} + N_1$$
$$U_2 = N_1 + N_2$$

where $\mathcal{E}$ is the transmitted signal energy and

$$N_k = \text{Re}\left[\int_0^T s_i^*(t) z_k(t)\, dt\right], \quad k = 1, 2$$

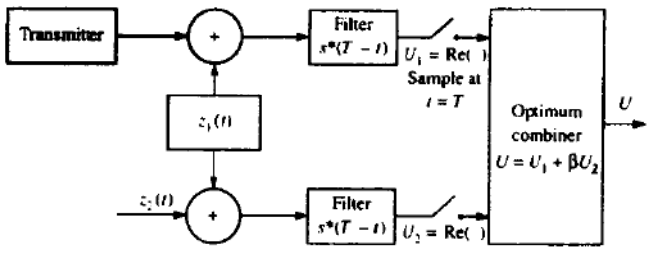

FIGURE P14-5

It is apparent that U_1 and U_2 are correlated gaussian variables while N_1 and N_2 are independent gaussian variables. Thus,

$$p(n_1) = \frac{1}{\sqrt{2\pi}\sigma} \exp\left(-\frac{n_1^2}{2\sigma^2}\right)$$

$$p(n_2) = \frac{1}{\sqrt{2\pi}\sigma} \exp\left(-\frac{n_2^2}{2\sigma^2}\right)$$

where the variance of N_k is $\sigma^2 = 2\mathscr{E}N_0$.

a Show that the joint probability density function for U_1 and U_2 is

$$p(U_1, U_2) = \frac{1}{2\pi\sigma^2} \exp\left\{-\frac{1}{2\sigma^2}\left[(U_1 - 2\mathscr{E})^2 - U_2(U_1 - 2\mathscr{E}) + \tfrac{1}{2}U_2^2\right]\right\}$$

if $s(t)$ is transmitted and

$$p(U_1, U_2) = \frac{1}{2\pi\sigma^2} \exp\left\{-\frac{1}{2\sigma^2}\left[(U_1 + 2\mathscr{E})^2 - U_2(U_1 + 2\mathscr{E}) + \tfrac{1}{2}U_2^2\right]\right\}$$

if $-s(t)$ is transmitted.

b Based on the likelihood ratio, show that the optimum combination of U_1 and U_2 results in the decision variable

$$U = U_1 + \beta U_2$$

where β is a constant. What is the optimum value of β?

c Suppose that $s(t)$ is transmitted. What is the probability density function of U?

d What is the probability of error assuming that $s(t)$ was transmitted? Express your answer as a function for the SNR $\mathscr{E}/N_0$.

e What is the loss in performance if only $U = U_1$ is the decision variable?

14-6 Consider the model for a binary communications system with diversity as shown in Fig. P14-6. The channels have fixed attenuations and phase shifts. The $\{z_k(t)\}$ are

FIGURE P14-6

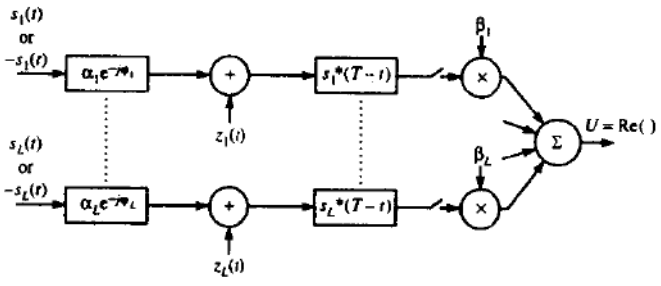

complex-valued white gaussian noise processes with zero mean and autocorrelation functions

$$\phi_{z_k z_k}(\tau) = \tfrac{1}{2}E[z_k^*(t)z_k(t+\tau)] = N_{0k}\delta(\tau)$$

(Note that the spectral densities $\{N_{0k}\}$ are all different.) Also, the noise processes $\{z_k(t)\}$ are mutually statistically independent. The $\{\beta_k\}$ are complex-valued weighting factors to be determined. The decision variable from the combiner is

$$U = \text{Re}\left(\sum_{k=1}^{L} \beta_k U_k\right) \gtrless_{-1}^{1} 0$$

a Determine the pdf $p(U)$ when $+1$ is transmitted.
b Determine the probability of error P_2 as a function of the weights $\{\beta_k\}$.
c Determine the values of $\{\beta_k\}$ that minimize P_2.

14-7 Determine the probability of error for binary orthogonal signaling with Lth-order diversity over a Rayleigh fading channel. The pdfs of the two decision variables are given by (14-4-31) and (14-4-32).

14-8 The rate-1/3, $L = 3$, binary convolutional code with transfer function given by (8-2-5) is used for transmitting data over a Rayleigh fading channel via binary PSK.
a Determine and plot the probability of error for hard-decision decoding. Assume that the transmitted waveforms corresponding to the coded bits fade independently.
b Determine and plot the probability of error for soft-decision decoding. Assume that the waveforms corresponding to the coded bits fade independently.

14-9 A binary sequence is transmitted via binary antipodal signaling over a Rayleigh fading channel with Lth-order diversity. When $s_i(t)$ is transmitted, the received equivalent lowpass signals are

$$r_k(t) = \alpha_k e^{-j\phi_k} s_i(t) + z_k(t), \quad k = 1, 2, \ldots, L$$

The fading among the L subchannels is statistically independent. The additive noise terms $\{z_k(t)\}$ are zero-mean, statistically independent and identically distributed white gaussian noise processes with autocorrelation function $\phi_{z_k z_k}(\tau) = N_0\delta(\tau)$. Each of the L signals is passed through a filter matched to $s_i(t)$ and the output is phase-corrected to yield

$$U_k = \text{Re}\left[e^{j\phi_k}\int_0^T r_k(t)s_i^*(t)\,dt\right], \quad k = 1, 2, \ldots, L$$

The $\{U_k\}$ are combined by a linear combiner to form the decision variable

$$U = \sum_{k=1}^{L} U_k$$

a Determine the pdf of U conditional on fixed values for the $\{a_k\}$.
b Determine the expression for the probability of error when the $\{\alpha_k\}$ are statistically independent and identically distributed Rayleigh random variables.

14-10 The Chernoff bound for the probability of error for binary FSK with diversity L in Rayleigh fading was shown to be

$$P_2(L) < [4p(1-p)]^L = \left[4\frac{1+\bar{\gamma}_c}{(2+\bar{\gamma}_c)^2}\right]^L$$
$$< 2^{-\bar{\gamma}_b g(\bar{\gamma}_c)}$$

where

$$g(\bar{\gamma}_c) = \frac{1}{\bar{\gamma}_c}\log_2\left[\frac{(2+\bar{\gamma}_c)^2}{4(1+\bar{\gamma}_c)}\right]$$

a Plot $g(\bar{\gamma}_c)$ and determine its approximate maximum value and the value of $\bar{\gamma}_c$ where the maximum occurs.

b For a given $\bar{\gamma}_b$, determine the optimal order of diversity.

c Compare $P_2(L)$, under the condition that $g(\bar{\gamma}_c)$ is maximized (optimal diversity), with the error probability for binary FSK in AWGN with no fading, which is

$$P_2 = \tfrac{1}{2}e^{-\gamma_b/2}$$

and determine the penalty in SNR due to fading and noncoherent (square-law) combining.

14-11 A DS spread-spectrum system is used to resolve the multipath signal components in a two-path radio signal propagation scenario. If the path length of the secondary path is 300 m longer than that of the direct path, determine the minimum chip rate necessary to resolve the multipath components.

14-12 A baseband digital communication system employs the signals shown in Fig. P14-12(*a*) for the transmission of two equiprobable messages. It is assumed that the communication problem studied here is a "one-shot" communication problem; that is, the above messages are transmitted just once and no transmission takes place afterward. The channel has no attenuation ($\alpha = 1$), and the noise is AWG with power spectral density $\frac{1}{2}N_0$.

a Find an appropriate orthonormal basis for the representation of the signals.

b In a block diagram, give the precise specifications of the optimum receiver using matched filters. Label the diagram carefully.

c Find the error probability of the optimum receiver.

d Show that the optimum receiver can be implemented by using just *one* filter

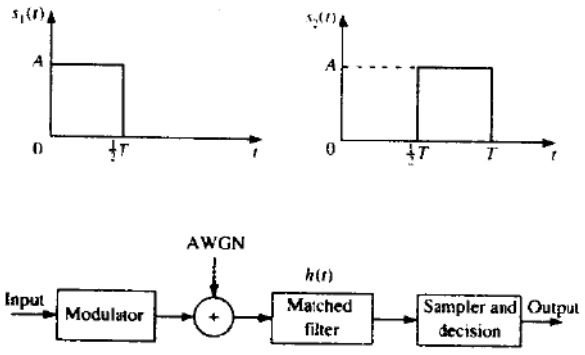

FIGURE P14-12

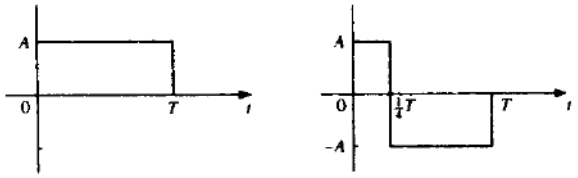

FIGURE P14-14

(see the block diagram in Fig. P14-12(*b*). What are the characteristics of the matched filter and the sampler and decision device?

e Now assume that the channel is not ideal but has an impulse response of $c(t) = \delta(t) + \frac{1}{2}\delta(t - \frac{1}{2}T)$. Using the same matched filter as (d), design an optimum reciever.

f Assuming that the channel impulse response is $c(t) = \delta(t) + a\delta(t - \frac{1}{2}T)$, where a is a random variable uniformly distributed on [0, 1], and using the same matched filter as in (d), design the optimum receiver.

14-13 A communication system employs dual antenna diversity and binary orthogonal FSK modulation. The received signals at the two antennas are

$$r_1(t) = \alpha_1 s(t) + n_1(t)$$
$$r_2(t) = \alpha_2 s(t) + n_2(t)$$

where α_1 and α_2 are statistically iid Rayleigh random variables, and $n_1(t)$ and $n_2(t)$ are statistically independent, zero-mean white gaussian random processes with power-spectral density $\frac{1}{2}N_0$. The two signals are demodulated, squared and then combined (summed) prior to detection.

a Sketch the functional block diagram of the entire receiver, including the demodulator, the combiner and the detector.

b Plot the probability of error for the detector and compare the result with the case of no diversity.

14-14 The two equivalent lowpass signals shown in Fig. P14-14 are used to transmit a binary sequence. The equivalent lowpass impulse response of the channel is $h(t) = 4\delta(t) - 2\delta(t - T)$. To avoid pulse overlap between successive transmissions, the transmission rate in bits/s is selected to be $R = 1/2T$. The transmitted signals are equally probable and are corrupted by additive zero-mean white gaussian noise having an equivalent lowpass representation $z(t)$ with an autocorrelation function

$$\phi_{zz}(\tau) = \tfrac{1}{2}E[z^*(t)z(t + \tau)] = N_0\delta(\tau)$$

a Sketch the two possible equivalent lowpass noise-free *received* waveforms.

b Specify the optimum receiver and sketch the equivalent lowpass impulse responses of all filters used in the optimum receiver. Assume *coherent detection* of the signals.

14-15 Verify the relation in (14-3-14) by making the change of variable $\gamma = \alpha^2\mathcal{E}_b/N_0$ in the Nakagami-m distribution.

15

MULTIUSER COMMUNICATIONS

Our treatment of communication systems up to this point has been focused on a single communication link involving a transmitter and a receiver. In this chapter, the focus shifts to multiple users and multiple communication links. We explore the various ways in which the multiple users access a common channel to transmit information. The multiple access methods that are described in this chapter form the basis for current and future wireline and wireless communication networks, such as satellite networks, cellular and mobile communication networks, and underwater acoustic networks.

15-1 INTRODUCTION TO MULTIPLE ACCESS TECHNIQUES

It is instructive to distinguish among several types of multiuser communication systems. One type is a multiple access system in which a large number of users share a common communication channel to transmit information to a receiver. Such a system is depicted in Fig. 15-1-1. The common channel may be the up-link in a satellite communication system, or a cable to which are connected a set of terminals that access a central computer, or some frequency band in the radio spectrum that is used by multiple users to communicate with a radio receiver. For example, in a mobile cellular communication system, the users are the mobile transmitters in any particular cell of the system and the receiver resides in the base station of the particular cell.

A second type of multiuser communication system is a broadcast network in which a single transmitter sends information to multiple receivers as depicted

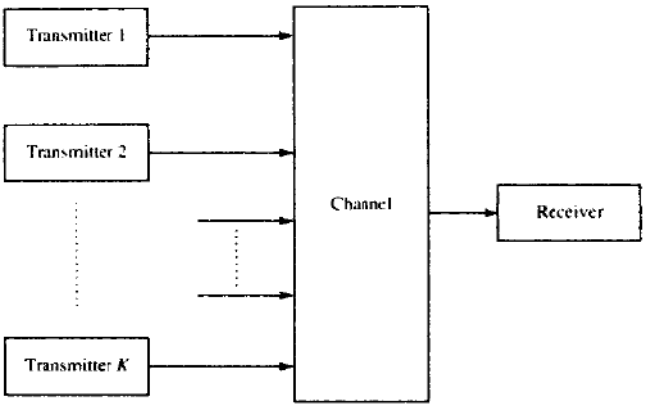

FIGURE 15-1-1 A multiple access system.

in Fig. 15-1-2. Examples of broadcast systems include the common radio and TV broadcast systems, as well as the down-links in a satellite system.

The multiple access and broadcast networks are probably the most common multiuser communication systems. A third type of multiuser system is a store-and-forward network, as depicted in Fig. 15-1-3. Yet a fourth type is the two-way communication system shown in Fig. 15-1-4.

In this chapter, we focus on multiple access methods for multiuser communications. In general, there are several different ways in which multiple users can send information through the communication channel to the receiver. One simple method is to subdivide the available channel bandwidth into a number, say N, of frequency nonoverlapping subchannels, as shown in Fig. 15-1-5, and to assign a subchannel to each user upon request by the users. This

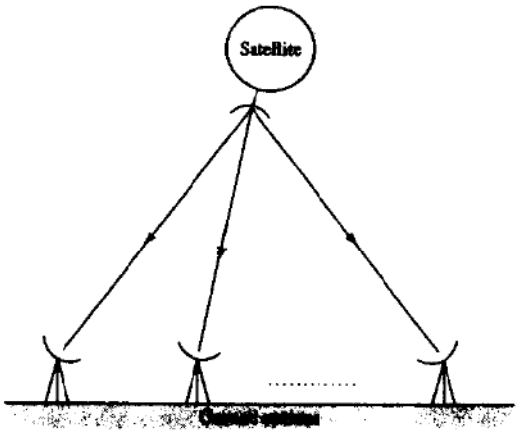

FIGURE 15-1-2 A broadcast network.

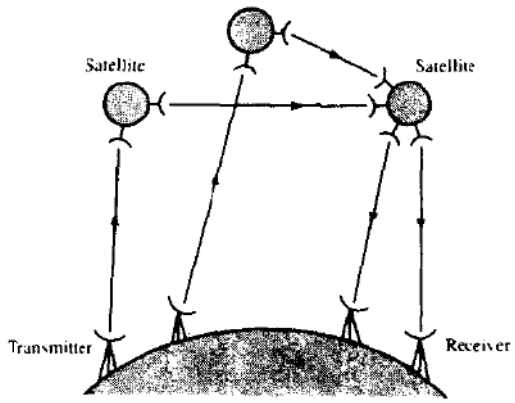

FIGURE 15-1-3 A store-and-forward communication network with satellite relays.

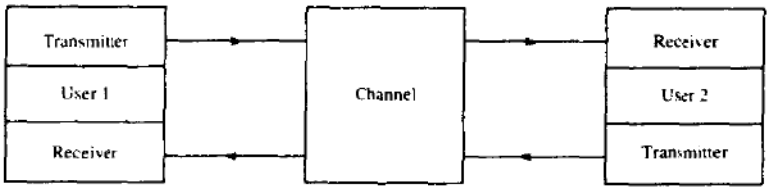

FIGURE 15-1-4 A two-way communication channel.

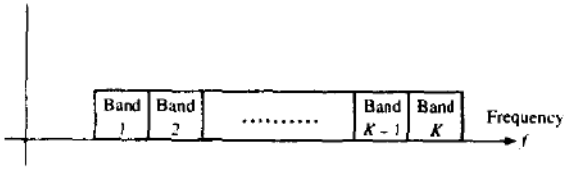

FIGURE 15-1-5 Subdivisions of the channel into nonoverlapping frequency bands.

method is generally called *frequency-division multiple access* (FDMA), and is commonly used in wireline channels to accommodate multiple users for voice and data transmission.

Another method for creating multiple subchannels for multiple access is to subdivide the duration T_f, called the *frame duration*, into, say, N nonoverlapping subintervals, each of duration T_f/N. Then each user who wishes to transmit information is assigned to a particular time slot within each frame. This multiple access method is called *time-division multiple access* (TDMA) and it is frequently used in data and digital voice transmission.

We observe that in FDMA and TDMA, the channel is basically partitioned into independent single-user subchannels. In this sense, the communication

system design methods that we have described for single-user communication are directly applicable and no new problems are encountered in a multiple access environment, except for the additional task of assigning users to available channels.

The interesting problems arise when the data from the users accessing the network is bursty in nature. In other words, the information transmissions from a single user are separated by periods of no transmission, where these periods of silence may be greater than the periods of transmission. Such is the case generally with users at various terminals in a computer communications network that contains a central computer. To some extent, this is also the case in mobile cellular communication systems carrying digitized voice, since speech signals typically contain long pauses.

In such an environment where the transmission from the various users is bursty and low-duty-cycle, FDMA and TDMA tend to be inefficient because a certain percentage of the available frequency slots or time slots assigned to users do not carry information. Ultimately, an inefficiently designed multiple access system limits the number of simultaneous users of the channel.

An alternative to FDMA and TDMA is to allow more than one user to share a channel or subchannel by use of direct-sequence spread spectrum signals. In this method, each user is assigned a unique code sequence or *signature sequence* that allows the user to spread the information signal across the assigned frequency band. Thus signals from the various users are separated at the receiver by cross-correlation of the received signal with each of the possible user signature sequences. By designing these code sequences to have relatively small cross-correlations, the crosstalk inherent in the demodulation of the signals received from multiple transmitters is minimized. This multiple access method is called *code-division multiple access* (CDMA).

In CDMA, the users access the channel in a random manner. Hence, the signal transmissions among the multiple users completely overlap both in time and in frequency. The demodulation and separation of these signals at the receiver is facilitated by the fact that each signal is spread in frequency by the pseudo-random code sequence. CDMA is sometimes called *spread-spectrum multiple access* (SSMA).

An alternative to CDMA is nonspread random access. In such a case, when two users attempt to use the common channel simultaneously, their transmissions collide and interfere with each other. When that happens, the information is lost and must be retransmitted. To handle collisions, one must establish protocols for retransmission of messages that have collided. Protocols for scheduling the retransmission of collided messages are described below.

15-2 CAPACITY OF MULTIPLE ACCESS METHODS

It is interesting to compare FDMA, TDMA, and CDMA in terms of the information rate that each multiple access method achieves in an ideal AWGN channel of bandwidth W. Let us compare the capacity of K users, where each

user has average power $P_i = P$, for all $1 \leq i \leq K$. Recall that in an ideal band-limited AWGN channel of bandwidth W, the capacity of a single user is

$$C = W \log_2 \left(1 + \frac{P}{WN_0}\right) \tag{15-2-1}$$

where $\frac{1}{2}N_0$ is the power spectral density of the additive noise.

In FDMA, each user is allocated a bandwidth W/K. Hence, the capacity of each user is

$$C_K = \frac{W}{K} \log_2 \left[1 + \frac{P}{(W/K)N_0}\right] \tag{15-2-2}$$

and the total capacity for the K users is

$$KC_K = W \log_2 \left(1 + \frac{KP}{WN_0}\right) \tag{15-2-3}$$

Therefore, the total capacity is equivalent to that of a single user with average power $P_{av} = KP$.

It is interesting to note that for a fixed bandwidth W, the total capacity goes to infinity as the number of users increases linearly with K. On the other hand, as K increases, each user is allocated a smaller bandwidth (W/K) and, consequently, the capacity per user decreases. Figure 15-2-1 illustrates the capacity C_K per user normalized by the channel bandwidth W, as a function of $\mathscr{E}_b/N_0$, with K as a parameter. This expression is given as

$$\frac{C_K}{W} = \frac{1}{K} \log_2 \left[1 + K \frac{C_K}{W} \left(\frac{\mathscr{E}_b}{N_0}\right)\right] \tag{15-2-4}$$

A more compact form of (15-2-4) is obtained by defining the normalized

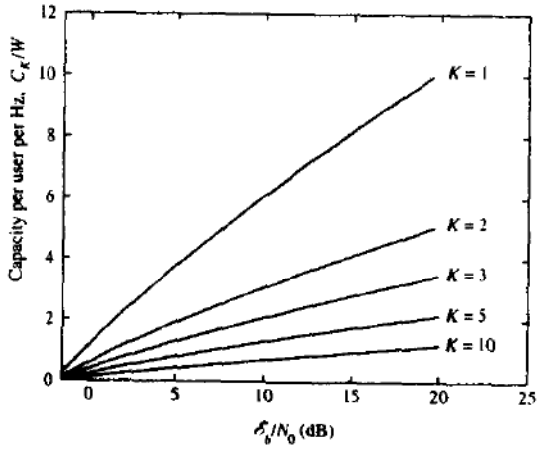

FIGURE 15-2-1 Normalized capacity as a function of $\mathscr{E}_b/N_0$ for FDMA.

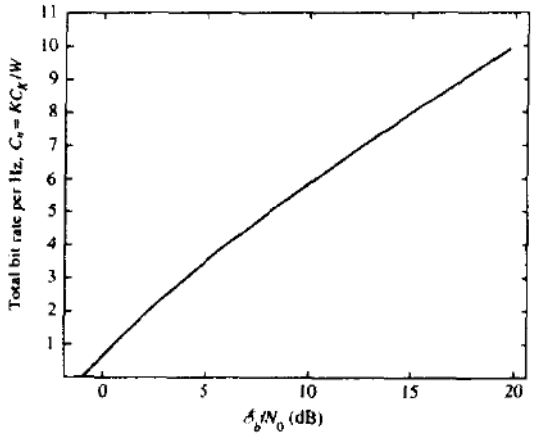

FIGURE 15-2-2 Total capacity per hertz as a function of $\mathscr{E}_b/N_0$ for FDMA.

total capacity $C_n = KC_K/W$, which is the total bit rate for all K users per unit of bandwidth. Thus, (15-2-4) may be expressed as

$$C_n = \log_2\left(1 + C_n\frac{\mathscr{E}_b}{N_0}\right) \tag{15-2-5}$$

or, equivalently,

$$\frac{\mathscr{E}_b}{N_0} = \frac{2^{C_n} - 1}{C_n} \tag{15-2-6}$$

The graph of C_n versus $\mathscr{E}_b/N_0$ is shown in Fig. 15-2-2. We observe that C_n increases as $\mathscr{E}_b/N_0$ increases above the minimum value of ln 2.

In a TDMA system, each user transmits for $1/K$ of the time through the channel of bandwidth W, with average power KP. Therefore, the capacity per user is

$$C_K = \left(\frac{1}{K}\right)W\log_2\left(1 + \frac{KP}{WN_0}\right) \tag{15-2-7}$$

which is identical to the capacity of an FDMA system. However, from a practical standpoint, we should emphasize that, in TDMA, it may not be possible for the transmitters to sustain a transmitter power of KP when K is very large. Hence, there is a practical limit beyond which the transmitter power cannot be increased as K is increased.

In a CDMA system, each user transmits a pseudo-random signal of a bandwidth W and average power P. The capacity of the system depends on the level of cooperation among the K users. At one extreme is noncooperative CDMA, in which the receiver for each user signal does not know the spreading waveforms of the other users, or chooses to ignore them in the demodulation process. Hence, the other users signals appear as interference at the receiver of each user. In this case, the multiuser receiver consists of a bank of K

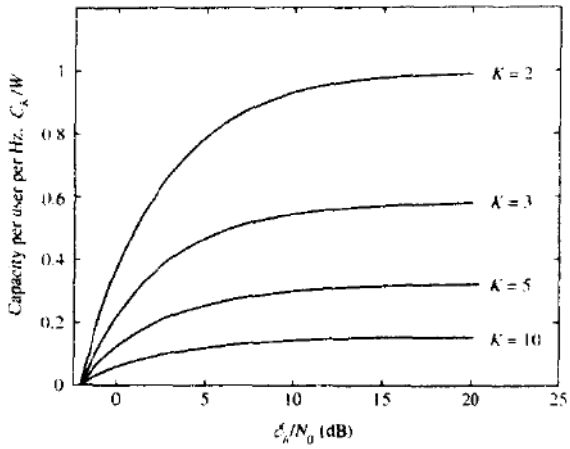

FIGURE 15-2-3 Normalized capacity as a function of $\mathscr{E}_b/N_0$ for noncooperative CDMA.

single-user receivers. If we assume that each user's pseudorandom signal waveform is gaussian then each user signal is corrupted by gaussian interference of power $(K-1)P$ and additive gaussian noise of power WN_0. Therefore, the capacity per user is

$$C_K = W \log_2\left[1 + \frac{P}{WN_0 + (K-1)P}\right] \tag{15-2-8}$$

or, equivalently,

$$\frac{C_K}{W} = \log_2\left[1 + \frac{C_K}{W}\frac{\mathscr{E}_b/N_0}{1 + (K-1)(C_K/W)\mathscr{E}_b/N_0}\right] \tag{15-2-9}$$

Figure 15-2-3 illustrates the graph of C_K/W versus $\mathscr{E}_b/N_0$, with K as a parameter.

For a large number of users, we may use the approximation $\ln(1+x) \leq x$. Hence,

$$\frac{C_K}{W} \leq \frac{C_K}{W}\frac{\mathscr{E}_b/N_0}{1 + K(C_K/W)(\mathscr{E}_b/N_0)}\log_2 e \tag{15-2-10}$$

or, equivalently,

$$\begin{aligned} C_n &\leq \log_2 e - \frac{1}{\mathscr{E}_b/N_0} \\ &\leq \frac{1}{\ln 2} - \frac{1}{\mathscr{E}_b/N_0} < \frac{1}{\ln 2} \end{aligned} \tag{15-2-11}$$

In this case, we observe that the total capacity does not increase with K as in TDMA and FDMA.

On the other hand, suppose that the K users cooperate by transmitting synchronously in time, and the multiuser receiver knows the spreading

waveforms of all users and jointly demodulates and detects all the users' signals. Thus, each user is assigned a rate R_i, $1 \leq i \leq K$, and a codebook containing a set of 2^{nR_i} codewords of power P. In each signal interval, each user selects an arbitrary codeword, say $\mathbf{X}_i$, from its own codebook and all users transmit their codewords simultaneously. Thus, the decoder at the receiver observes

$$\mathbf{Y} = \sum_{i=1}^{K} \mathbf{X}_i + \mathbf{Z} \tag{15-2-12}$$

where $\mathbf{Z}$ is an additive noise vector. The optimum decoder looks for the K codewords, one from each codebook, that have a vector sum closest to the received vector $\mathbf{Y}$ in euclidean distance.

The achievable K-dimensional rate region for the K users in an AWGN channel, assuming equal power for each user, is given by the following equations:

$$R_i < W \log_2 \left(1 + \frac{P}{WN_0}\right), \quad 1 \leq i \leq K \tag{15-2-13}$$

$$R_i + R_j < W \log_2 \left(1 + \frac{2P}{WN_0}\right), \quad 1 \leq i, j \leq K \tag{15-2-14}$$

$$\vdots$$

$$\sum_{i=1}^{K} R_i < W \log_2 \left(1 + \frac{KP}{WN_0}\right) \tag{15-2-15}$$

In the special case when all the rates are identical, the inequality (15-2-15) is dominant over the other $K-1$ inequalities. It follows that if the rates $\{R_i, 1 \leq i \leq K\}$ for the K cooperative synchronous users are selected to fall in the capacity region specified by the inequalities given above then the probabilities of error for the K users tend to zero as the code block length n tends to infinity.

From the above discussion, we conclude that the sum of the rates of the K users goes to infinity with K. Therefore, with cooperative synchronous users, the capacity of CDMA has a form similar to that of FDMA and TDMA. Note that if all the rates in the CDMA system are selected to be identical to R then (15-2-15) reduces to

$$R < \frac{W}{K} \log_2 \left(1 + \frac{KP}{WN_0}\right) \tag{15-2-16}$$

which is identical to the rate constraint in FDMA and TDMA. In this case, CDMA does not yield a higher rate than TDMA and FDMA. However, if the rates of the K users are selected to be unequal such that the inequalities (15-2-13)–(15-2-15) are satisfied then it is possible to find the points in the achievable rate region such that the sum of the rates for the K users in CDMA exceeds the capacity of FDMA and TDMA.

Example 15-2-1

Consider the case of two users in a CDMA system that employs coded signals as described above. The rates of the two users must satisfy the inequalities

$$R_1 < W \log_2 \left(1 + \frac{P}{WN_0}\right)$$

$$R_2 < W \log_2 \left(1 + \frac{P}{WN_0}\right)$$

$$R_1 + R_2 < W \log_2 \left(1 + \frac{2P}{WN_0}\right)$$

where P is the average transmitted power of each user and W is the signal bandwidth. Let us determine the capacity region for the two-user CDMA system.

The capacity region for the two-user CDMA system with coded signal waveforms has the form illustrated in Fig. 15-2-4, where

$$C_i = W \log_2 \left(1 + \frac{P_i}{WN_0}\right), \quad i = 1, 2$$

are the capacities corresponding to the two users with $P_1 = P_2 = P$. We note that if user 1 is transmitting at capacity C_1, user 2 can transmit up to a maximum rate

$$R_{2m} = W \log_2 \left(1 + \frac{2P}{WN_0}\right) - C_1$$

$$= W \log_2 \left(1 + \frac{P}{P + WN_0}\right) \tag{15-2-17}$$

which is illustrated in Fig. 15-2-4 as point A. This result has an interesting

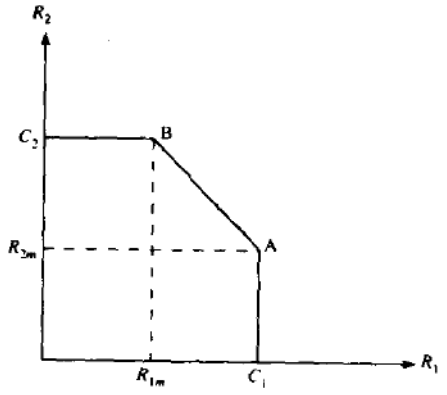

FIGURE 15-2-4 Capacity region of two-user CDMA multiple access gaussian channel.

interpretation. We note that rate R_{2m} corresponds to the case in which the signal from user 1 is considered as an equivalent additive noise in the detection of the signal of user 2. On the other hand, user 1 can transmit at capacity C_1, since the receiver knows the transmitted signal from user 2 and, hence, it can eliminate its effect in detecting the signal of user 1.

Due to symmetry, a similar situation exists if user 2 is transmitting at capacity C_2. Then, user 1 can transmit up to a maximum rate $R_{1m} = R_{2m}$, which is illustrated in Fig. 15.2.4 as point B. In this case, we have a similar interpretation as above, with an interchange in the roles of user 1 and user 2.

The points A and B are connected by a straight line. It is easily seen that this straight line is the boundary of the achievable rate region, since any point on the line corresponds to the maximum rate $W \log_2 (1 + 2P/WN_0)$, which can be obtained by simply time-sharing the channel between the two users.

In the next section, we consider the problem of signal detection for a multiuser CDMA system and assess the performance and the computational complexity of several receiver structures.

15-3 CODE-DIVISION MULTIPLE ACCESS

As we have observed, TDMA and FDMA are multiple access methods in which the channel is partitioned into independent, single-user subchannels, i.e., nonoverlapping time slots or frequency bands, respectively. In CDMA, each user is assigned a distinct signature sequence (or waveform), which the user employs to modulate and spread the information-bearing signal. The signature sequences also allow the receiver to demodulate the message transmitted by multiple users of the channel, who transmit simultaneously and, generally, asynchronously.

In this section, we treat the demodulation and detection of multiuser CDMA signals. We shall see that the optimum maximum-likelihood detector has a computational complexity that grows exponentially with the number of users. Such a high complexity serves as a motivation to devise suboptimum detectors having lower computational complexities. Finally, we consider the performance characteristics of the various detectors.

15-3-1 CDMA Signal and Channel Models

Let us consider a CDMA channel that is shared by K simultaneous users. Each user is assigned a signature waveform $g_k(t)$ of duration T, where T is the symbol interval. A signature waveform may be expressed as

$$g_k(t) = \sum_{n=0}^{L-1} a_k(n) p(t - nT_c), \qquad 0 \le t \le T \tag{15-3-1}$$

where $\{a_k(n), 0 \leq n \leq L-1\}$ is a pseudo-noise (PN) code sequence consisting of L chips that take values $\{\pm 1\}$, $p(t)$ is a pulse of duration T_c, and T_c is the chip interval. Thus, we have L chips per symbol and $T = LT_c$. Without loss of generality, we assume that all K signature waveforms have unit energy, i.e.,

$$\int_0^T g_k^2(t)\,dt = 1 \tag{15-3-2}$$

The cross-correlations between pairs of signature waveforms play an important role in the metrics for the signal detector and on its performance. We define the following cross-correlations:

$$\rho_{ij}(\tau) = \int_0^T g_i(t)g_j(t-\tau)\,dt, \qquad i \leq j \tag{15-3-3}$$

$$\rho_{ji}(\tau) = \int_0^T g_i(t)g_j(t+T-\tau)\,dt, \qquad i \leq j \tag{15-3-4}$$

For simplicity, we assume that binary antipodal signals are used to transmit the information from each user. Hence, let the information sequence of the kth user be denoted by $\{b_k(m)\}$, where the value of each information bit may be ± 1. It is convenient to consider the transmission of a block of bits of some arbitrary length, say N. Then, the data block from the kth user is

$$\mathbf{b}_k = [b_k(1) \quad \ldots \quad b_k(N)]' \tag{15-3-5}$$

and the corresponding equivalent lowpass, transmitted waveform may be expressed as

$$s_k(t) = \sqrt{\mathscr{E}_k} \sum_{i=1}^{N} b_k(i)g_k(t-iT) \tag{15-3-6}$$

where $\mathscr{E}_k$ is the signal energy per bit. The composite transmitted signal for the K users may be expressed as

$$\begin{aligned} s(t) &= \sum_{k=1}^{K} s_k(t-\tau_k) \\ &= \sum_{k=1}^{K} \sqrt{\mathscr{E}_k} \sum_{i=1}^{N} b_k(i)g_k(t-iT-\tau_k) \end{aligned} \tag{15-3-7}$$

where $\{\tau_k\}$ are the transmission delays, which satisfy the condition $0 \leq \tau_k < T$ for $1 \leq k \leq K$. Without loss of generality, we assume that $0 \leq \tau_1 \leq \tau_2 \leq \ldots \leq \tau_k < T$. This is the model for the multiuser transmitted signal in an asynchronous mode. In the special case of synchronous transmission, $\tau_k = 0$ for $1 \leq k \leq K$. The values of τ of interest in the cross-correlations given by (15-3-3) and (15-3-4) may also be restricted to $0 \leq \tau < T$, without loss of generality.

The transmitted signal is assumed to be corrupted by AWGN. Hence, the received signal may be expressed as

$$r(t) = s(t) + n(t) \tag{15-3-8}$$

where $s(t)$ is given by (15-3-7) and $n(t)$ is the noise, with power spectral density $\frac{1}{2}N_0$.

15-3-2 The Optimum Receiver

The optimum receiver is defined as the receiver that selects the most probable sequence of bits $\{b_k(n), 1 \leq n \leq N, 1 \leq k \leq K\}$ given the received signal $r(t)$ observed over the time interval $0 \leq t \leq NT + 2T$. First, let us consider the case of synchronous transmission; later, we shall consider asynchronous transmission.

Synchronous Transmission In synchronous transmission, each (user) interferer produces exactly one symbol which interferes with the desired symbol. In additive white gaussian noise, it is sufficient to consider the signal received in one signal interval, say $0 \leq t \leq T$, and determine the optimum receiver. Hence, $r(t)$ may be expressed as

$$r(t) = \sum_{k=1}^{K} \sqrt{\mathscr{E}_k} b_k(1) g_k(t) + n(t), \qquad 0 \leq t \leq T \tag{15-3-9}$$

The optimum maximum-likelihood receiver computes the log-likelihood function

$$\Lambda(\mathbf{b}) = \int_0^T \left[r(t) - \sum_{k=1}^{K} \sqrt{\mathscr{E}_k} b_k(1) g_k(t) \right]^2 dt \tag{15-3-10}$$

and selects the information sequence $\{b_k(1), 1 \leq k \leq K\}$ that minimizes $\Lambda(\mathbf{b})$. If we expand the integral in (15-3-10), we obtain

$$\Lambda(\mathbf{b}) = \int_0^T r^2(t)\, dt - 2 \sum_{k=1}^{K} \sqrt{\mathscr{E}_k} b_k(1) \int_0^T r(t) g_k(t)\, dt + \sum_{j=1}^{K} \sum_{k=1}^{K} \sqrt{\mathscr{E}_j \mathscr{E}_k} b_k(1) b_j(1) \int_0^T g_k(t) g_j(t)\, dt \tag{15-3-11}$$

We observe that the integral involving $r^2(t)$ is common to all possible sequences $\{b_k(1)\}$ and is of no relevance in determining which sequence was transmitted. Hence, it may be neglected. The term

$$r_k = \int_0^T r(t) g_k(t)\, dt, \qquad 1 \leq k \leq K \tag{15-3-12}$$

represents the cross-correlation of the received signal with each of the K signature sequences. Instead of cross-correlators, we may employ matched filters. Finally, the integral involving $g_k(t)$ and $g_j(t)$ is simply

$$\rho_{jk}(0) = \int_0^T g_j(t) g_k(t)\, dt \tag{15-3-13}$$

Therefore, (15-3-11) may be expressed in the form of correlation metrics

$$C(\mathbf{r}_K, \mathbf{b}_K) = 2 \sum_{k=1}^{K} \sqrt{\mathscr{E}_k} b_k(1) r_k - \sum_{j=1}^{K} \sum_{k=1}^{K} \sqrt{\mathscr{E}_j \mathscr{E}_k} b_k(1) b_j(1) \rho_{jk}(0) \tag{15-3-14}$$

These correlation metrics may also be expressed in vector inner product form as

$$C(\mathbf{r}_K, \mathbf{b}_K) = 2\mathbf{b}_K'\mathbf{r}_K - \mathbf{b}_K'\mathbf{R}_s\mathbf{b}_K \tag{15-3-15}$$

where

$$\mathbf{r}_K = [r_1 \quad r_2 \quad \cdots \quad r_K]', \qquad \mathbf{b}_K = [\sqrt{\mathscr{E}_1}b_1(1) \quad \cdots \quad \sqrt{\mathscr{E}_K}b_K(1)]$$

and $\mathbf{R}_s$ is the correlation matrix, with elements $\rho_{jk}(0)$. It is observed that the optimum detector must have knowledge of the received signal energies in order to compute the correlation metrics.

There are 2^K possible choices of the bits in the information sequence of the K users. The optimum detector computes the correlation metrics for each sequence and selects the sequence that yields the largest correlation metric. We observe that the optimum detector has a complexity that grows exponentially with the number of users, K.

In summary, the optimum receiver for symbol-synchronous transmission consists of a bank of K correlators or matched filters followed by a detector that computes the 2^K correlation metrics given by (15-3-15) corresponding to the 2^K possible transmitted information sequences. Then, the detector selects the sequence corresponding to the largest correlation metric.

Asynchronous Transmission In this case, there are exactly two consecutive symbols from each interferer that overlap a desired symbol. We assume that the receiver knows the received signal energies $\{\mathscr{E}_k\}$ for the K users and the transmission delays $\{\tau_k\}$. Clearly, these parameters must be measured at the receiver or provided to the receiver as side information by the users via some control channel.

The optimum maximum-likelihood receiver computes the log-likelihood function

$$\begin{aligned}\Lambda(\mathbf{b}) &= \int_0^{NT+2T}\left[r(t) - \sum_{k=1}^{K}\sqrt{\mathscr{E}_k}\sum_{i=1}^{N}b_k(i)g_k(t-iT-\tau_k)\right]^2 dt \\ &= \int_0^{NT+2T} r^2(t)\,dt - 2\sum_{k=1}^{K}\sqrt{\mathscr{E}_k}\sum_{i=1}^{N}b_k(i)\int_0^{NT+2T} r(t)g_k(t-iT-\tau_k)\,dt \\ &\quad + \sum_{k=1}^{K}\sum_{l=1}^{K}\sqrt{\mathscr{E}_k\mathscr{E}_l}\sum_{i=1}^{N}\sum_{j=1}^{N}b_k(i)b_l(j)\int_0^{NT+2T} g_k(t-iT-\tau_k)g_l(t-jT-\tau_l)\,dt\end{aligned} \tag{15-3-16}$$

where $\mathbf{b}$ represents the data sequences from the K users. The integral involving $r^2(t)$ may be ignored, since it is common to all possible information sequences. The integral

$$r_k(i) \equiv \int_{iT+\tau_k}^{(i+1)T+\tau_k} r(t)g_k(t-iT-\tau_k)\,dt, \qquad 1 \le i \le N \tag{15-3-17}$$

represents the outputs of the correlator or matched filter for the kth user in each of the signal intervals. Finally, the integral

$$\int_0^{NT+2T} g_k(t - iT - \tau_k) g_l(t - jT - \tau_l)\, dt = \int_{-iT-\tau_k}^{NT+2T-iT-\tau_k} g_k(t) g_l(t + iT - jT + \tau_k - \tau_l)\, dt \quad (15\text{-}3\text{-}18)$$

may be easily decomposed into terms involving the cross-correlation $\rho_{kl}(\tau) = \rho_{kl}(\tau_k - \tau_l)$ for $k \leq l$ and $\rho_{lk}(\tau)$ for $k > l$. Therefore, we observe that the log-likelihood function may be expressed in terms of a correlation metric that involves the outputs $\{r_k(i), 1 \leq k \leq K, 1 \leq i \leq N\}$ of K correlators or matched filters—one for each of the K signature sequences. Using vector notation, it can be shown that the NK correlator or matched filter outputs $\{r_k(i)\}$ can be expressed in the form

$$\mathbf{r} = \mathbf{R}_N \mathbf{b} + \mathbf{n} \quad (15\text{-}3\text{-}19)$$

where, by definition

$$\mathbf{r} = [\mathbf{r}'(1) \quad \mathbf{r}'(2) \quad \dots \quad \mathbf{r}'(N)]'$$
$$\mathbf{r}(i) = [r_1(i) \quad r_2(i) \quad \dots \quad r_K(i)]' \quad (15\text{-}3\text{-}20)$$

$$\mathbf{b} = [\mathbf{b}'(1) \quad \mathbf{b}'(2) \quad \dots \quad \mathbf{b}'(N)]'$$
$$\mathbf{b}(i) = [\sqrt{\mathscr{E}_1} b_1(i) \quad \sqrt{\mathscr{E}_2} b_2(i) \quad \dots \quad \sqrt{\mathscr{E}_K} b_K(i)]' \quad (15\text{-}3\text{-}21)$$

$$\mathbf{n} = [\mathbf{n}'(1) \quad \mathbf{n}'(2) \quad \dots \quad \mathbf{n}'(N)]'$$
$$\mathbf{n}(i) = [n_1(i) \quad n_2(i) \quad \dots \quad n_K(i)]' \quad (15\text{-}3\text{-}22)$$

$$\mathbf{R}_N = \begin{bmatrix} \mathbf{R}_a(0) & \mathbf{R}_a'(1) & \mathbf{0} & \dots & \dots & \mathbf{0} \\ \mathbf{R}_a(1) & \mathbf{R}_a(0) & \mathbf{R}_a'(1) & \mathbf{0} & \dots & \mathbf{0} \\ \vdots & \vdots & \vdots & \vdots & \vdots & \vdots \\ \mathbf{0} & \mathbf{0} & \mathbf{0} & \mathbf{R}_a(1) & \mathbf{R}_a(0) & \mathbf{R}_a'(1) \\ \mathbf{0} & \mathbf{0} & \mathbf{0} & \mathbf{0} & \mathbf{R}_a(1) & \mathbf{R}_a(0) \end{bmatrix} \quad (15\text{-}3\text{-}23)$$

and $\mathbf{R}_a(m)$ is a $K \times K$ matrix with elements

$$R_{kl}(m) = \int_{-\infty}^{\infty} g_k(t - \tau_k) g_l(t + mT - \tau_l)\, dt \quad (15\text{-}3\text{-}24)$$

The gaussian noise vectors $\mathbf{n}(i)$ have zero mean and autocorrelation matrix

$$E[\mathbf{n}(k)\mathbf{n}'(j)] = \tfrac{1}{2} N_0 \mathbf{R}_a(k - j) \quad (15\text{-}3\text{-}25)$$

Note that the vector $\mathbf{r}$ given by (15-3-19) constitutes a set of sufficient statistics for estimating the transmitted bits $b_k(i)$.

If we adopt a block processing approach, the optimum ML detector must compute 2^{NK} correlation metrics and select the K sequences of length N that correspond to the largest correlation metric. Clearly, such an approach is much too complex computationally to be implemented in practice, especially

when K and N are large. An alternative approach is ML sequence estimation employing the Viterbi algorithm. In order to construct a sequential-type detector, we make use of the fact that each transmitted symbol overlaps at most with $2K-2$ symbols. Thus, a significant reduction in computational complexity is obtained with respect to the block size parameter N, but the exponential dependence on K cannot be reduced.

It is apparent that the optimum ML receiver employing the Viterbi algorithm involves such a high computational complexity that its use in practice is limited to communication systems where the number of users is extremely small, e.g., $K < 10$. For larger values of K, one should consider a sequential-type detector that is akin to either the sequential decoding or the stack algorithms described in Chapter 8. Below, we consider a number of sub-optimums detectors whose complexity grows linearly with K.

15-3-3 Suboptimum Detectors

In the above discussion, we observed that the optimum detector for the K CDMA users has a computational complexity, measured in the number of arithmetic operations (additions and multiplications/divisions) per modulated symbol, that grows exponentially with K. In this subsection we describe suboptimum detectors with computational complexities that grow linearly with the number of users, K. We begin with the simplest suboptimum detector, which we call the conventional (single-user) detector.

Conventional Single-User Detector In conventional single-user detection, the receiver for each user consists of a demodulator that correlates (or match-filters) the received signal with the signature sequence of the user and passes the correlator output to the detector, which makes a decision based on the single correlator output. Thus, the conventional detector neglects the presence of the other users of the channel or, equivalently, assumes that the aggregate noise plus interference is white and gaussian.

Let us consider synchronous transmission. Then, the output of the correlator for the kth user for the signal in the interval $0 \leq t \leq T$ is

$$r_k = \int_0^T r(t)g_k(t)\,dt \tag{15-3-26}$$

$$= \sqrt{\mathscr{E}_k}b_k(1) + \sum_{\substack{j=1 \\ j\neq k}}^{K} \sqrt{\mathscr{E}_j}b_j(1)\rho_{jk}(0) + n_k(1) \tag{15-3-27}$$

where the noise component $n_k(1)$ is given as

$$n_k(1) = \int_0^T n(t)g_k(t)\,dt \tag{15-3-28}$$

Since $n(t)$ is white gaussian noise with power spectral density $\frac{1}{2}N_0$, the variance of $n_k(1)$ is

$$E[n_k^2(1)] = \tfrac{1}{2}N_0\int_0^T g_k^2(t)\,dt = \tfrac{1}{2}N_0 \tag{15-3-29}$$

Clearly, if the signature sequences are orthogonal, the interference from the other users given by the middle term in (15-3-27) vanishes and the conventional single-user detector is optimum. On the other hand, if one or more of the other signature sequences are not orthogonal to the user signature sequence, the interference from the other users can become excessive if the power levels of the signals (or the received signal energies) of one or more of the other users is sufficiently larger than the power level of the kth user. This situation is generally called the *near–far problem* in multiuser communications. and necessitates some type of power control for conventional detection.

· In asynchronous transmission, the conventional detector is more vulnerable to interference from other users. This is because it is not possible to design signature sequences for any pair of users that are orthogonal for all time offsets. Consequently, interference from other users is unavoidable in asynchronous transmission with the conventional single-user detection. In such a case, the near–far problem resulting from unequal power in the signals transmitted by the various users is particularly serious. The practical solution generally requires a power adjustment method that is controlled by the receiver via a separate communication channel that all users are continuously monitoring. Another option is to employ one of the multiuser detectors described below.

Decorrelating Detector We observe that the conventional detector has a complexity that grows linearly with the number of users, but its vulnerability to the near–far problem requires some type of power control. We shall now devise another type of detector that also has a linear computational complexity but does not exhibit the vulnerability to other-user interference.

Let us first consider the case of symbol-synchronous transmission. In this case, the received signal vector $\mathbf{r}_K$ that represents the output of the K matched filters is

$$\mathbf{r}_K = \mathbf{R}_s\mathbf{b}_K + \mathbf{n}_K \tag{15-3-30}$$

where $\mathbf{b}_K = [\sqrt{\mathscr{E}_1}b_1(1)\ \sqrt{\mathscr{E}_2}b_2(1)\ \ldots\ \sqrt{\mathscr{E}_K}b_K(1)]^t$ and the noise vector with elements $\mathbf{n}_K = [n_1(1)\ n_2(1)\ \ldots\ n_K(1)]^t$ has a covariance

$$E(\mathbf{n}_K\mathbf{n}_K') = \mathbf{R}_s \tag{15-3-31}$$

Since the noise is gaussian, $\mathbf{r}_K$ is described by a K-dimensional gaussian pdf with mean $\mathbf{R}_s\mathbf{b}_K$ and covariance $\mathbf{R}_s$. That is,

$$p(\mathbf{r}_K \mid \mathbf{b}_K) = \frac{1}{\sqrt{(2\pi)^K \det \mathbf{R}_s}} \exp\left[-\tfrac{1}{2}(\mathbf{r}_K - \mathbf{R}_s\mathbf{b}_K)'\mathbf{R}_s^{-1}(\mathbf{r}_K - \mathbf{R}_s\mathbf{b}_K)\right] \tag{15-3-32}$$

The best linear estimate of $\mathbf{b}_K$ is the value of $\mathbf{b}_K$ that minimizes the likelihood function

$$\Lambda(\mathbf{b}_K) = (\mathbf{r}_K - \mathbf{R}_s\mathbf{b}_K)'\mathbf{R}_s^{-1}(\mathbf{r}_K - \mathbf{R}_s\mathbf{b}_K) \tag{15-3-33}$$

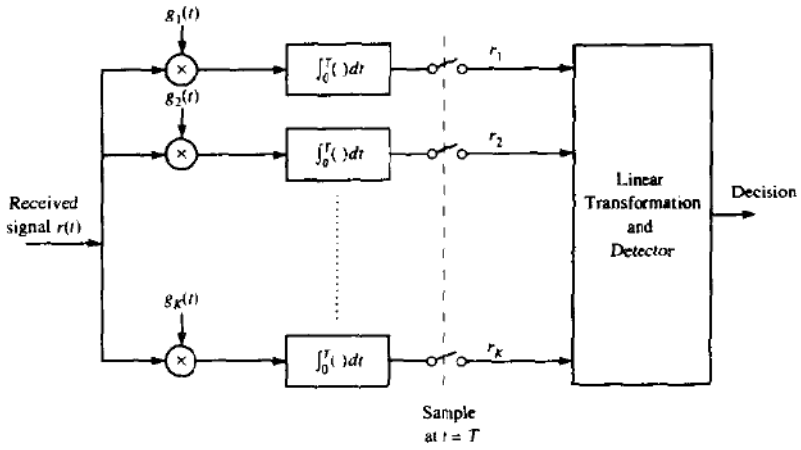

FIGURE 15-3-1 Receiver structure for decorrelation receiver.

The result of this minimization yields

$$\mathbf{b}_K^0 = \mathbf{R}_s^{-1}\mathbf{r}_K \tag{15-3-34}$$

Then, the detected symbols are obtained by taking the sign of each element of $\mathbf{b}_K^0$, i.e.

$$\hat{\mathbf{b}}_K = \text{sgn}\,(\mathbf{b}_K^0) \tag{15-3-35}$$

Figure 15-3-1 illustrates the receiver structure. Note from (15-3-34) and (15-3-35) that the decorrelator requires knowledge of the relative delays, in general, to form $\mathbf{R}_s$; no knowledge of the signal amplitudes is required.

Since the estimate $\mathbf{b}_K^0$ is obtained by performing a linear transformation on the vector of correlator outputs, the computational complexity is linear in K.

The reader should observe that the best (maximum-likelihood) linear estimate of $\mathbf{b}_K$ given by (15-3-34) is different from the optimum nonlinear ML sequence detector that finds the best discrete-valued $\{\pm 1\}$ sequence that maximizes the likelihood function. It is also interesting to note that the estimate $\mathbf{b}_K^0$ is the best linear estimate that maximizes the correlation metric given by (15-3-15).

An interesting interpretation of the detector that computes $\mathbf{b}_K^0$ as in (15-3-34) and makes decisions according to (15-3-35) is obtained by considering the case of $K = 2$ users. In this case,

$$\mathbf{R}_s = \begin{bmatrix} 1 & \rho \\ \rho & 1 \end{bmatrix} \tag{15-3-36}$$

$$\mathbf{R}_s^{-1} = \frac{1}{1-\rho^2}\begin{bmatrix} 1 & -\rho \\ -\rho & 1 \end{bmatrix} \tag{15-3-37}$$

where

$$\rho = \int_0^T g_1(t)g_2(t)\,dt \tag{15-3-38}$$

Then, if we correlate the received signal

$$r(t) = \sqrt{\mathscr{E}_1}b_1g_1(t) + \sqrt{\mathscr{E}_2}b_2g_2(t) + n(t) \tag{15-3-39}$$

with $g_1(t)$ and $g_2(t)$, we obtain

$$\mathbf{r}_2 = \begin{bmatrix} \sqrt{\mathscr{E}_1}b_1 + \rho\sqrt{\mathscr{E}_2}b_2 + n_1 \\ \rho\sqrt{\mathscr{E}_1}b_1 + \sqrt{\mathscr{E}_2}b_2 + n_2 \end{bmatrix} \tag{15-3-40}$$

where n_1 and n_2 are the noise components at the output of the correlators. Therefore,

$$\begin{aligned} \mathbf{b}_2^0 &= \mathbf{R}_s^{-1}\mathbf{r}_2 \\ &= \begin{bmatrix} \sqrt{\mathscr{E}_1}b_1 + (n_1 - \rho n_2)/(1-\rho^2) \\ \sqrt{\mathscr{E}_2}b_2 + (n_2 - \rho n_1)/(1-\rho^2) \end{bmatrix} \end{aligned} \tag{15-3-41}$$

This is a very interesting result, because the transformation $\mathbf{R}_s^{-1}$ has eliminated the interference components between the two users. Consequently, the near–far problem is eliminated and there is no need for power control.

It is interesting to note that a result similar to (15-3-41) is obtained if we correlate $r(t)$ given by (15-3-39) with the two modified signature waveforms

$$g_1'(t) = g_1(t) - \rho g_2(t) \tag{15-3-42}$$

$$g_2'(t) = g_2(t) - \rho g_1(t) \tag{15-3-43}$$

This means that, by correlating the received signal with the modified signature waveforms,[1] we have tuned out or *decorrelated* the multiuser interference. Hence, the detector based on (15-3-34) is called a *decorrelating detector.*

In asynchronous transmission, the received signal at the output of the correlators is given by (15-3-19). Hence, the log-likelihood function is given as

$$\Lambda(\mathbf{b}) = (\mathbf{r} - \mathbf{R}_N\mathbf{b})'\mathbf{R}_N^{-1}(\mathbf{r} - \mathbf{R}_N\mathbf{b}) \tag{15-3-44}$$

where $\mathbf{R}_N$ is defined by (15-3-23) and $\mathbf{b}$ is given by (15-3-21). It is relatively easy to show that the vector $\mathbf{b}$ that minimizes $\Lambda(\mathbf{b})$ is

$$\mathbf{b}^0 = \mathbf{R}_N^{-1}\mathbf{r} \tag{15-3-45}$$

This is the ML estimate of $\mathbf{b}$ and it is again obtained by performing a linear transformation of the outputs from the bank of correlators of matched filters.

Since $\mathbf{r} = \mathbf{R}_N\mathbf{b} + \mathbf{n}$, it follows from (15-3-45) that

$$\mathbf{b}^0 = \mathbf{b} + \mathbf{R}_N^{-1}\mathbf{n} \tag{15-3-46}$$

Therefore, $\mathbf{b}^0$ is an unbiased estimate of $\mathbf{b}$. This means that the multiuser

interference has been eliminated, as in the case of symbol-synchronous transmission. Hence, this detector for asynchronous transmission is also called a *decorrelating detector.*

A computationally efficient method for obtaining the solution given by (15-3-45) is the square-root factorization method described in Appendix D. Of course, there are many other methods that may be used to invert the matrix $\mathbf{R}_N$. Iterative methods to decorrelate the signals have also been explored.

Minimum Mean-Square-Error Detector In the above discussion, we showed that the linear ML estimate of $\mathbf{b}$ is obtained by minimizing the quadratic log-likelihood function in (15-3-44). Thus, we obtained the result given by (15-3-45), which is an estimate derived by performing a linear transformation on the outputs of the bank of correlators or matched filters.

Another, somewhat different, solution is obtained if we seek the linear transformation $\mathbf{b}^0 = \mathbf{Ar}$, where the matrix $\mathbf{A}$ is to be determined so as to minimize the mean square error (MSE)

$$\begin{aligned} J(\mathbf{b}) &= E[(\mathbf{b} - \mathbf{b}^0)'(\mathbf{b} - \mathbf{b}^0)] \\ &= E[(\mathbf{b} - \mathbf{Ar})'(\mathbf{b} - \mathbf{Ar})] \end{aligned} \tag{15-3-47}$$

It is easily shown that the optimum choice of $\mathbf{A}$ that minimizes $J(\mathbf{b})$ is

$$\mathbf{A}^0 = (\mathbf{R}_N + \tfrac{1}{2}N_0\mathbf{I})^{-1} \tag{15-3-48}$$

and, hence,

$$\mathbf{b}^0 = (\mathbf{R}_N + \tfrac{1}{2}N_0\mathbf{I})^{-1}\mathbf{r} \tag{15-3-49}$$

The output of the detector is then $\hat{\mathbf{b}} = \text{sgn}(\mathbf{b}^0)$.

The estimate given by (15-3-49) is called the *minimum MSE* (MMSE) estimate of $\mathbf{b}$. Note that when $\frac{1}{2}N_0$ is small compared with the diagonal elements of $\mathbf{R}_N$, the MMSE solution approaches the ML solution given by (15-3-45). On the other hand, when the noise level is large compared with the signal level in the diagonal elements of $\mathbf{R}_N$, $\mathbf{A}^0$ approaches the identity matrix (scaled by $\frac{1}{2}N_0$). In this low-SNR case, the detector basically ignores the interference from other users, because the additive noise is the dominant term. It should also be noted that the MMSE criterion produces a biased estimate of $\mathbf{b}$. Hence, there is some residual multiuser interference.

To perform the computations that lead to the values of $\mathbf{b}$, we solve the set of linear equations

$$(\mathbf{R}_N + \tfrac{1}{2}N_0\mathbf{I})\mathbf{b} = \mathbf{r} \tag{15-3-50}$$

This solution may be computed efficiently using a square-root factorization of the matrix $\mathbf{R}_N + \frac{1}{2}N_0\mathbf{I}$ as indicated above. Thus, to detect NK bits requires $3NK^2$ multiplications. Therefore, the computational complexity is $3K$ multiplications per bit, which is independent of the block length N and is linear in K.

Other Types of Detectors The decorrelating detector and the MMSE detector described above involve performing linear transformations on a block of data from a bank of K correlators or matched filters. The MMSE detector is akin to the linear MSE equalizer described in Chapter 10. Consequently, MMSE multiuser detection can be implemented by employing a tapped-delay-line filter with adjustable coefficients for each user and selecting the filter coefficients to minimize the MSE for each user signal. Thus, the received information bits are estimated sequentially with finite delay, instead of as a block.

The estimate $\mathbf{b}''$ given by (15-3-46), which is obtained by processing a block of N bits by a decorrelating detector, can also be computed sequentially. Xie *et al.* (1990) have demonstrated that the transmitted bits may be recovered sequentially from the received signal, by employing a form of a decision-feedback equalizer with finite delay. Thus, there is a similarity between the detection of signals corrupted by ISI in a single-user communication system and the detection of signals in a multiuser system with asynchronous transmission.

15-3-4 Performance Characteristics of Detectors

The bit error probability is generally the desirable performance measure in multiuser communications. In evaluating the effect of multiuser interference on the performance of the detector for a single user, we may use as a benchmark the probability of a bit error for a single-user receiver in the absence of other users of the channel, which is

$$P_k(\gamma_k) = Q(\sqrt{2\gamma_k}) \tag{15-3-51}$$

where $\gamma_k = \mathscr{E}_k/N_0$, $\mathscr{E}_k$ is the signal energy per bit and $\frac{1}{2}N_0$ is the power spectral density of the AWGN.

In the case of the optimum detector for either synchronous or asynchronous transmission, the probability of error is extremely difficult and tedious to evaluate. In this case, we may use (15-3-51) as a lower bound and the performance of a suboptimum detector as an upper bound.

Let us consider, first, the suboptimum, conventional single-user detector. For synchronous transmission, the output of the correlator for the kth user is given by (15-3-27). Therefore, the probability of error for the kth user, conditional on a sequence $\mathbf{b}_i$ of bits from other users, is

$$P_k(\mathbf{b}_i) = Q\left(\sqrt{2\left[\sqrt{\mathscr{E}_k} + \sum_{\substack{j=1 \\ j\neq k}}^{K} \sqrt{\mathscr{E}_j} b_j(1)\rho_{jk}(0)\right]^2 \Big/ N_0}\right) \tag{15-3-52}$$

Then, the average probability of error is simply

$$P_k = (\tfrac{1}{2})^{K-1} \sum_{\substack{i=1 \\ i\neq k}}^{K} P_k(\mathbf{b}_i) \tag{15-3-53}$$

The probability in (15-3-53) will be dominated by the term that has the smallest argument in the Q function. The smallest argument will result in an SNR of

$$(SNR)_{\min} = \frac{1}{N_0}\left[\sqrt{\mathscr{E}_k} - \sum_{\substack{j=1 \\ j\neq k}}^{K} \sqrt{\mathscr{E}_j}\,|\rho_{jk}(0)|\right]^2 \tag{15-3-54}$$

Therefore,

$$(\tfrac{1}{2})^{K-1} Q(\sqrt{2(SNR)_{\min}}) < P_k < (\tfrac{1}{2})^{K-1}(K-1)Q(\sqrt{2(SNR)_{\min}}) \tag{15-3-55}$$

A similar development can be used to obtain bounds on the performance for asynchronous transmission.

In the case of a decorrelating detector, the other-user interference is completely eliminated. Hence, the probability of error may be expressed as

$$P_k = Q(\mathscr{E}_k/\sigma_k^2) \tag{15-3-56}$$

where σ_k^2 is the variance of the noise in the kth element of the estimate $\mathbf{b}^0$.

Example 15-3-1

Consider the case of synchronous, two-user transmission, where $\mathbf{b}_2^0$ is given by (15-3-41). Let us determine the probability of error.

The signal component for the first term in (15-3-41) is $\sqrt{\mathscr{E}_1}$. The noise component is

$$n = \frac{n_1 - \rho n_2}{1-\rho^2}$$

where ρ is the correlation between the two signature signals. The variance of this noise is

$$\begin{aligned}\sigma_1^2 &= \frac{E[(n_1 - \rho n_2)]^2}{(1-\rho^2)^2} \\ &= \frac{1}{1-\rho^2}\frac{N_0}{2}\end{aligned} \tag{15-3-57}$$

and

$$P_1 = Q\left(\sqrt{\frac{2\mathscr{E}_1}{N_0}(1-\rho^2)}\right) \tag{15-3-58}$$

A similar result is obtained for the performance of the second user. Therefore, the noise variance has increased by the factor $(1-\rho^2)^{-1}$. This noise enhancement is the price paid for the elimination of the multiuser interference by the decorrelation detector.

The error rate performance of the MMSE detector is similar to that for the decorrelation detector when the noise level is low. For example, from

(15-3-49), we observe that when N_0 is small relative to the diagonal elements of the signal correlation matrix $\mathbf{R}_N$,

$$\mathbf{b}^0 \approx \mathbf{R}_N^{-1}\mathbf{r} \tag{15-3-59}$$

which is the solution for the decorrelation detector. For low multiuser interference, the MMSE detector results in a smaller noise enhancement compared with the decorrelation detector, but has some residual bias resulting from the other users. Thus, the MMSE detector attempts to strike a balance between the residual interference and the noise enhancement.

An alternative to the error probability as a figure of merit that has been used to characterize the performance of a multiuser communication system is the ratio of SNRs with and without the presence of interference. In particular, (15-3-51) gives the error probability of the kth user in the absence of other-user interference. In this case, the SNR is $\gamma_k = \mathscr{E}_k/N_0$. In the presence of multiuser interference, the user that transmits a signal with energy $\mathscr{E}_k$ will have an error probability P_k that exceeds $P_k(\gamma_k)$. The *effective SNR* γ_{ke} is defined as the SNR required to achieve the error probability

$$P_k = P_k(\gamma_{ke}) = Q(\sqrt{2\gamma_{ke}}) \tag{15-3-60}$$

The *efficiency* is defined as the ratio γ_{ke}/γ_k and represents the performance loss due to the multiuser interference. The desirable figure of merit is the *asymptotic efficiency*, defined as

$$\eta_k = \lim_{N_0 \to 0} \frac{\gamma_{ke}}{\gamma_k} \tag{15-3-61}$$

This figure of merit is often simpler to compute than the probability of error.

Example 15-3-2

Consider the case of two symbol-synchronous users with signal energies $\mathscr{E}_1$ and $\mathscr{E}_2$. Let us determine the asymptotic efficiency of the conventional detector.

In this case, the probability of error is easily obtained from (15-3-52) and (15-3-53) as

$$P_1 = \tfrac{1}{2}Q\left(\sqrt{2(\sqrt{\mathscr{E}_1} + \rho\sqrt{\mathscr{E}_2})^2/N_0}\right) + \tfrac{1}{2}Q\left(\sqrt{2(\sqrt{\mathscr{E}_1} - \rho\sqrt{\mathscr{E}_2})^2/N_0}\right)$$

However, the asymptotic efficiency is much easier to compute. It follows from the definition (15-3-61) and from (15-3-52) that

$$\eta_1 = \left[\max\left(0, 1 - \sqrt{\frac{\mathscr{E}_2}{\mathscr{E}_1}}|\rho|\right)\right]^2$$

A similar expression is obtained for η_2.

The asymptotic efficiency of the optimum and suboptimum detectors that we have described has been evaluated by Verdu (1986), Lupas and Verdu

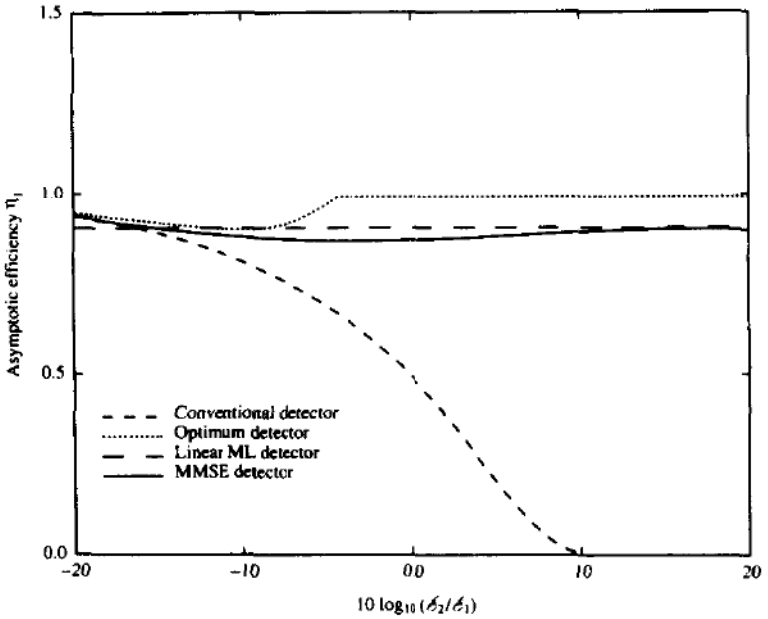

FIGURE 15-3-2 Asymptotic efficiencies of optimum (Viterbi) detector, conventional detector, MMSE detector, and linear ML detector in a two-user synchronous DS/SSMA system. [*From Xie* et al. *(1990),* ©*IEEE.*]

(1989), and Xie *et al.* (1990). Figure 15-3-2 illustrates the asymptotic efficiencies of these detectors when $K = 2$ users are transmitting synchronously. These graphs show that when the interference is small ($\mathscr{E}_2 \rightarrow 0$), the asymptotic efficiencies of these detectors are relatively large (near unity) and comparable. As $\mathscr{E}_2$ increases, the asymptotic efficiency of the conventional detector deteriorates rapidly. However, the other linear detectors perform relatively well compared with the optimum detector. Similar conclusions are reached by computing the error probabilities, but these computations are often more tedious.

15-4 RANDOM ACCESS METHODS

In this section, we consider a multiuser communication system in which users transmit information in packets over a common channel. In contrast to the CDMA method described in Section 15-3, the information signals of the users are not spread in frequency. As a consequence, simultaneous transmission of signals from multiple users cannot be separated at the receiver. The access methods described below are basically random, because packets are generated according to some statistical model. Users access the channel when they have one or more packets to transmit. When more than one user attempts to transmit packets simultaneously, the packets overlap in time, i.e., they collide,

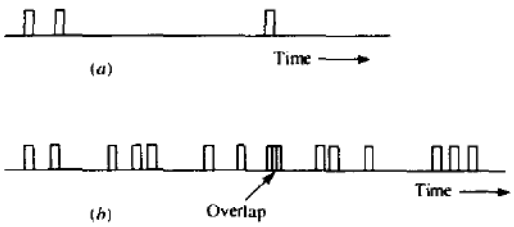

FIGURE 15-4-1 Random access packet transmission: (*a*) packets from a typical user; (*b*) packets from several users.

and, hence, a conflict results, which must be resolved by devising some channel protocol for retransmission of the packets. Below, we describe several random access channel protocols that resolve conflicts in packet transmission.

15-4-1 ALOHA Systems and Protocols

Suppose that a random access scheme is employed where each user transmits a packet as soon as it is generated. When a packet is transmitted by a user and no other user transmits a packet for the duration of the time interval then the packet is considered successfully transmitted. However, if one or more of the other users transmits a packet that overlaps in time with the packet from the first user, a collision occurs and the transmission is unsuccessful. Figure 15-4-1 illustrates this scenario. If the users know when their packets are transmitted successfully and when they have collided with other packets, it is possible to devise a scheme, which we may call a *channel access protocol*, for retransmission of collided packets.

Feedback to the users regarding the successful or unsuccessful transmission of packets is necessary and can be provided in a number of ways. In a radio broadcast system, such as one that employs a satellite relay as depicted in Fig. 15-4-2, the packets are broadcast to all the users on the down-link. Hence, all

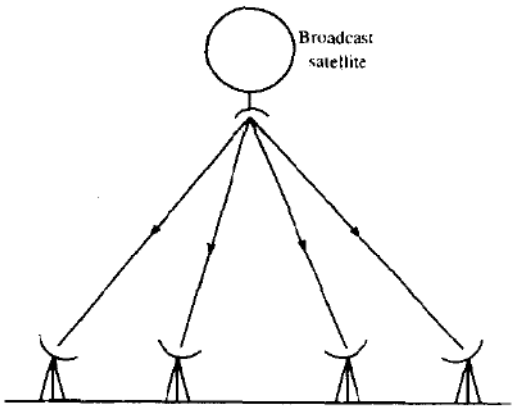

FIGURE 15-4-2 Broadcast system.

the transmitters can monitor their transmissions and, thus, obtain the following ternary information: no packet was transmitted, or a packet was transmitted successfully, or a collision occurred. This type of feedback to the transmitters is generally denoted as $(0, 1, c)$ feedback. In systems that employ wireline or filter-optic channels, the receiver may transmit the feedback signal on a separate channel.

The ALOHA system devised by Abramson (1973, 1977) and others at the University of Hawaii employs a satellite repeater that broadcasts the packets received from the various users who access the satellite. In this case, all the users can monitor the satellite transmissions and, thus, establish whether or not their packets have been transmitted successfully.

There are basically two types of ALOHA systems: *synchronized or slotted* and *unsynchronized or unslotted.* In an unslotted ALOHA system, a user may begin transmitting a packet at any arbitrary time. In a slotted ALOHA, the packets are transmitted in time slots that have specified beginning and ending times.

We assume that the start time of packets that are transmitted is a Poisson point process having an average rate of λ packets/s. Let T_p denote the time duration of a packet. Then, the normalized channel traffic G, also called the *offered channel traffic*, is defined as

$$G = \lambda T_p \tag{15-4-1}$$

There are many channel access protocols that can be used to handle collisions. Let us consider the one due to Abramson (1973). In Abramson's protocol, packets that have collided are retransmitted with some delay τ, where τ is randomly selected according to the pdf

$$p(\tau) = \alpha e^{-\alpha \tau} \tag{15-4-2}$$

where α is a design parameter. The random delay τ is added to the time of the initial transmission and the packet is retransmitted at the new time. If a collision occurs again, a new value of τ is randomly selected and the packet is retransmitted with a new delay from the time of the second transmission. This process is continued until the packet is transmitted successfully. The design parameter α determines the average delay between retransmissions. The smaller the value of α, the longer the delay between retransmissions.

Now, let λ', where $\lambda' < \lambda$, be the rate at which packets are transmitted successfully. Then, the normalized channel throughput is

$$S = \lambda' T_p \tag{15-4-3}$$

We can relate the channel throughput S to the offered channel traffic G by making use of the assumed start time distribution. The probability that a packet will not overlap a given packet is simply the probability that no packet

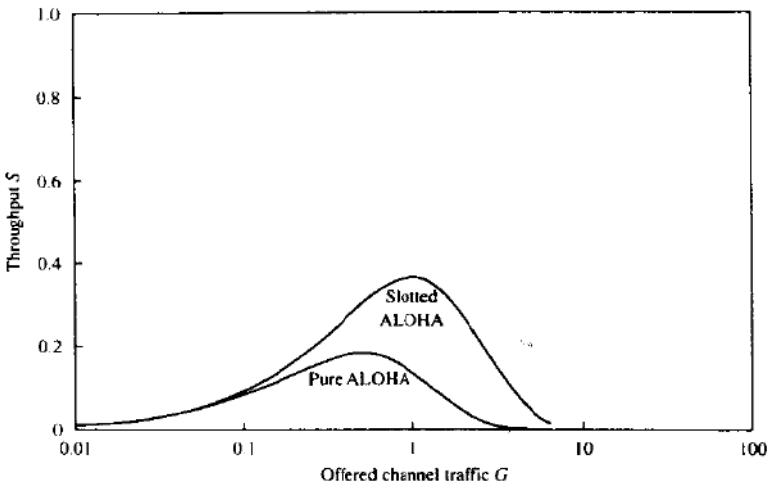

FIGURE 15-4-3 Throughput in ALOHA systems.

begins T_p s before or T_p s after the start time of the transmitted packet. Since the start time of all packets is Poisson-distributed, the probability that a packet will not overlap is $\exp(-2\lambda T_p) = \exp(-2G)$. Therefore,

$$S = Ge^{-2G} \tag{15-4-4}$$

This relationship is plotted in Fig. 15-4-3. We observe that the maximum throughput is $S_{max} = 1/2e = 0.184$ packets per slot, which occurs at $G = \frac{1}{2}$. When $G > \frac{1}{2}$, the throughput S decreases. The above development illustrates that an unsynchronized or unslotted random access method has a relatively small throughput and is inefficient.

Throughput for slotted ALOHA To determine the throughput in a slotted ALOHA system, let G_i be the probability that the ith user will transmit a packet in some slot. If all the K users operate independently and there is no statistical dependence between the transmission of the user's packet in the current slot and the transmission of the user's packet in previous time slots, the total (normalized) offered channel traffic is

$$G = \sum_{i=1}^{K} G_i \tag{15-4-5}$$

Note that, in this case, G may be greater than unity.

Now, let $S_i \leq G_i$ be the probability that a packet transmitted in a time slot is received without a collision. Then, the normalized channel throughput is

$$S = \sum_{i=1}^{K} S_i \tag{15-4-6}$$

The probability that a packet from the ith user will not have a collision with another packet is

$$Q_i = \prod_{\substack{j=1 \\ j \neq i}}^{K} (1 - G_j) \tag{15-4-7}$$

Therefore,

$$S_i = G_i Q_i \tag{15-4-8}$$

A simple expression for the channel throughput is obtained by considering K identical users. Then,

$$S_i = \frac{S}{K}, \qquad G_i = \frac{G}{K}$$

and

$$S = G\left(1 - \frac{G}{K}\right)^{K-1} \tag{15-4-9}$$

Then, if we let $K \to \infty$, we obtain the throughput

$$S = Ge^{-G} \tag{15-4-10}$$

This result is also plotted in Fig. 15-4-3. We observe that S reaches a maximum throughput of $S_{max} = 1/e = 0.368$ packets per slot at $G = 1$, which is twice the throughput of the unslotted ALOHA system.

The performance of the slotted ALOHA system given above is based on Abramson's protocol for handling collisions. A higher throughput is possible by devising a better protocol.

A basic weakness in Abramson's protocol is that it does not take into account the information on the amount of traffic on the channel that is available from observation of the collisions that occur. An improvement in throughput of the slotted ALOHA system can be obtained by using a tree-type protocol devised by Capetanakis (1979). In this algorithm, users are not allowed to transmit new packets that are generated until all earlier collisions are resolved. A user can transmit a new packet in a time slot immediately following its generation, provided that all previous packets that have collided have been transmitted successfully. If a new packet is generated while the channel is clearing the previous collisions, the packet is stored in a buffer. When a new packet collides with another, each user assigns its respective packet to one of two sets, say A or B, with equal probability (by flipping a coin). Then, if a packet is put in set A, the user transmits it in the next time slot. If it collides again, the user will again randomly assign the packet to one of two sets and the process of transmission is repeated. This process continues until all packets contained in set A are transmitted successfully. Then, all packets in set B are transmitted following the same procedure. All the users

monitor the state of the channel, and, hence, they know when all the collisions have been serviced.

When the channel becomes available for transmission of new packets, the earliest generated packets are transmitted first. To establish a queue, the time scale is subdivided into subintervals of sufficiently short duration such that, on average, approximately one packet is generated by a user in a subinterval. Thus, each packet has a "time tag" that is associated with the subinterval in which it was generated. Then, a new packet belonging to the first subinterval is transmitted in the first available time slot. If there is no collision then a packet from the second subinterval is transmitted, and so on. This procedure continues as new packets are generated and as long as any backlog of packets for transmission exists. Capetanakis has demonstrated that this channel access protocol achieves a maximum throughput of 0.43 packets per slot.

In addition to throughput, another important performance measure in a random access system is the average transmission delay in transmitting a packet. In an ALOHA system, the average number of transmissions per packet is G/S. To this number we may add the average waiting time between transmissions and, thus, obtain an average delay for a successful transmission. We recall from the above discussion that in the Abramson protocol, the parameter α determines the average delay between retransmissions. If we select α small, we obtain the desirable effect of smoothing out the channel load at times of peak loading, but the result is a long retransmission delay. This is the trade-off in the selection of α in (15-4-2). On the other hand, the Capetanakis protocol has been shown to have a smaller average delay in the transmission of packets. Hence, it outperforms Abramson's protocol in both average delay and throughput.

Another important issue in the design of random access protocols is the stability of the protocol. In our treatment of ALOHA-type channel access protocols, we implicitly assumed that for a given offered load, an equilibrium point is reached where the average number of packets entering the channel is equal to the average number of packets transmitted successfully. In fact, it can be demonstrated that any channel access protocol, such as the Abramson protocol, that does not take into account the number of previous unsuccessful transmissions in establishing a retransmission policy is inherently unstable. On the other hand, the Capetanakis algorithm differs from the Abramson protocol in this respect and has been proved to be stable. A thorough discussion of the stability issues of random access protocols is found in the paper by Massey (1988).

15-4-2 Carrier Sense Systems and Protocols

As we have observed, ALOHA-type (slotted and unslotted) random-access protocols yield relatively low throughput. Furthermore, a slotted ALOHA system requires that users transmit at synchronized time slots. In channels where transmission delays are relatively small, it is possible to design random

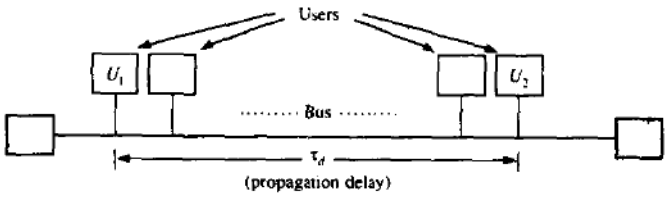

FIGURE 15-4-4 Local area network with bus architecture.

access protocols that yield higher throughput. An example of such a protocol is *carrier sensing* with collision detection, which is used as a standard Ethernet protocol in local area networks. This protocol is generally known as *carrier sense multiple access with collision detection* (CSMA/CD).

The CSMA/CD protocol is simple. All users listen for transmissions on the channel. A user who wishes to transmit a packet seizes the channel when it senses that the channel is idle. Collisions may occur when two or more users sense an idle channel and begin transmission. When the users that are transmitting simultaneously sense a collision, they transmit a special signal, called a *jam signal*, that serves to notify all users of the collision and abort their transmissions. Both the carrier sensing feature and the abortion of transmission when a collision occurs result in minimizing the channel down-time and, hence, yield a higher throughput.

To elaborate on the efficiency of CSMA/CD, let us consider a local area network having a bus architecture, as shown in Fig. 15-4-4. Consider two users U_1 and U_2 at the maximum separation, i.e., at the two ends of the bus, and let τ_d be the propagation delay for a signal to travel the length of the bus. Then, the (maximum) time required to sense an idle channel is τ_d. Suppose that U_1 transmits a packet of duration T_p. User U_2 may seize the channel τ_d s later by using carrier sensing, and begins to transmit. However, user U_1 would not know of this transmission until τ_d s after U_2 begins transmission. Hence, we may define the time interval $2\tau_d$ as the (maximum) time interval to detect a collision. If we assume that the time required to transmit the jam signal is negligible, the CSMA/CD protocol yields a high throughput when $2\tau_d \ll T_p$.

There are several possible protocols that may be used to reschedule transmissions when a collision occurs. One protocol is called *nonpersistent CSMA*, a second is called *1-persistent CSMA*, and a generalization of the latter is called p-persistant CSMA.

Nonpersistent CSMA In this protocol, a user that has a packet to transmit senses the channel and operates according to the following rule.

(a) If the channel is idle, the user transmits a packet.
(b) If the channel is sensed busy, the user schedules the packet

transmission at a later time according to some delay distribution. At the end of the delay interval, the user again senses the channel and repeats steps (a) and (b).

1-Persistent CSMA This protocol is designed to achieve high throughput by not allowing the channel to go idle if some user has a packet to transmit. Hence, the user senses the channel and operates according to the following rule.

(a) If the channel is sensed idle, the user transmits the packet with probability 1.

(b) If the channel is sensed busy, the user waits until the channel becomes idle and transmits a packet with probability one. Note that in this protocol, a collision will always occur when more than one user has a packet to transmit.

***p*-Persistent CSMA** To reduce the rate of collisions in 1-persistent CSMA and increase the throughput, we should randomize the starting time for transmission of packets. In particular, upon sensing that the channel is idle, a user with a packet to transmit sends it with probability p and delays it by τ with probability $1-p$. The probability p is chosen in a way that reduces the probability of collisions while the idle periods between consecutive (nonoverlapping) transmissions is kept small. This is accomplished by subdividing the time axis into minislots of duration τ and selecting the packet transmission at the beginning of a minislot. In summary, in the p-persistent protocol, a user with a packet to transmit proceeds as follows.

(a) If the channel is sensed idle, the packet is transmitted with probability p, and with probability $1-p$ the transmission is delayed by τ s.

(b) If at $t=\tau$, the channel is still sensed to be idle, step (a) is repeated. If a collision occurs, the users schedule retransmission of the packets according to some preselected transmission delay distribution.

(c) If at $t=\tau$, the channel is sensed busy, the user waits until it becomes idle, and then operates as in (a) and (b) above.

Slotted versions of the above protocol can also be constructed.

The throughput analysis for the nonpersistent and the p-persistent CSMA/CD protocols has been performed by Kleinrock and Tobagi (1975), based on the following assumptions:

1 the average retransmission delay is large compared with the packet duration T_p;

2 the interarrival times of the point process defined by the start times of all the packets plus retransmissions are independent and exponentially distributed.

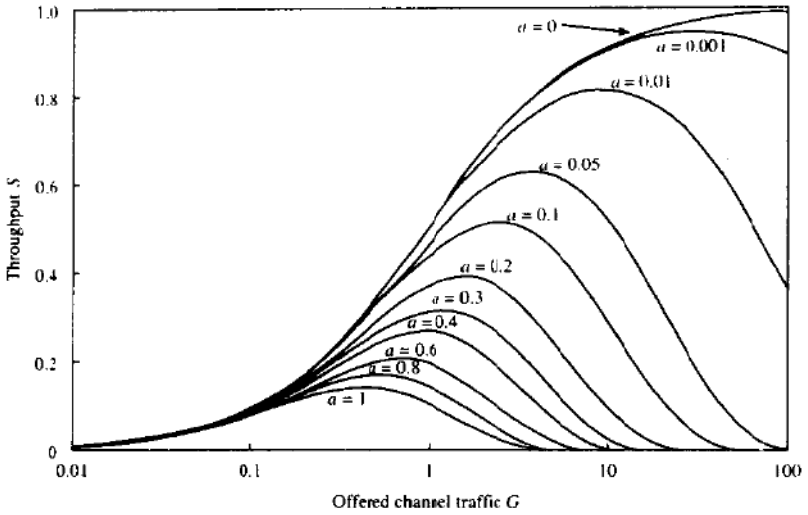

FIGURE 15-4-5 Throughput in nonpersistent CSMA. [*From Kleinrock and Tobagi (1975), © IEEE.*]

For the nonpersistent CSMA, the throughput is

$$S = \frac{Ge^{-aG}}{G(1+2a) + e^{-aG}} \tag{15-4-11}$$

where the parameter $a = \tau_d/T_p$. Note that as $a \to 0$, $S \to G/(1+G)$. Figure 15-4-5 illustrates the throughput versus the offered traffic G, with a as a parameter. We observe that $S \to 1$ as $G \to \infty$ for $a = 0$. For $a > 0$, the value of S_{max} decreases.

For the 1-persistent protocol, the throughput obtained by Kleinrock and Tobagi (1975) is

$$S = \frac{G[1+G+aG(1+G+\frac{1}{2}aG)]e^{-G(1+2a)}}{G(1+2a) - (1-e^{-aG}) + (1+aG)e^{-G(1+a)}} \tag{15-4-12}$$

In this case,

$$\lim_{a \to 0} S = \frac{G(1+G)e^{-G}}{G + e^{-G}} \tag{15-4-13}$$

which has a smaller peak value than the nonpersistent protocol.

By adopting the p-persistent protocol, it is possible to increase the throughput relative to the 1-persistent scheme. For example, Fig. 15-4-6 illustrates the throughput versus the offered traffic with $a = \tau_d/T_p$ fixed and with p as a parameter. We observe that as p increases toward unity, the maximum throughput decreases.

The transmission delay was also evaluated by Kleinrock and Tobagi (1975). Figure 15-4-7 illustrates the graphs of the delay (normalized by T_p) versus the

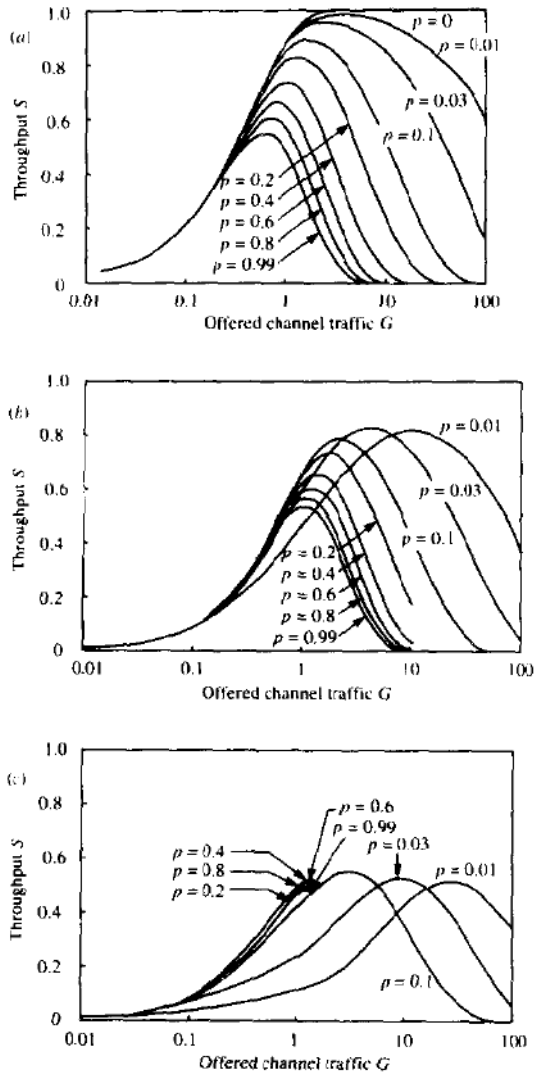

FIGURE 15-4-6 Channel throughput in p-persistent CSMA: (*a*) $a = 0$; (*b*) $a = 0.01$; (*c*) $a = 0.1$ [*From Kleinrock and Tobagi (1975). © IEEE.*]

throughput S for the slotted nonpersistent and p-persistent CSMA protocols. Also shown for comparison is the delay versus throughput characteristic of the ALOHA slotted and unslotted protocols. In this simulation, only the newly generated packets are derived independently from a Poisson distribution. Collisions and uniformly distributed random retransmissions are handled without further assumptions. These simulation results illustrate the superior performance of the p-persistent and the nonpersistent protocols relative to the ALOHA protocols. Note that the graph labeled "optimum p-persistent" is

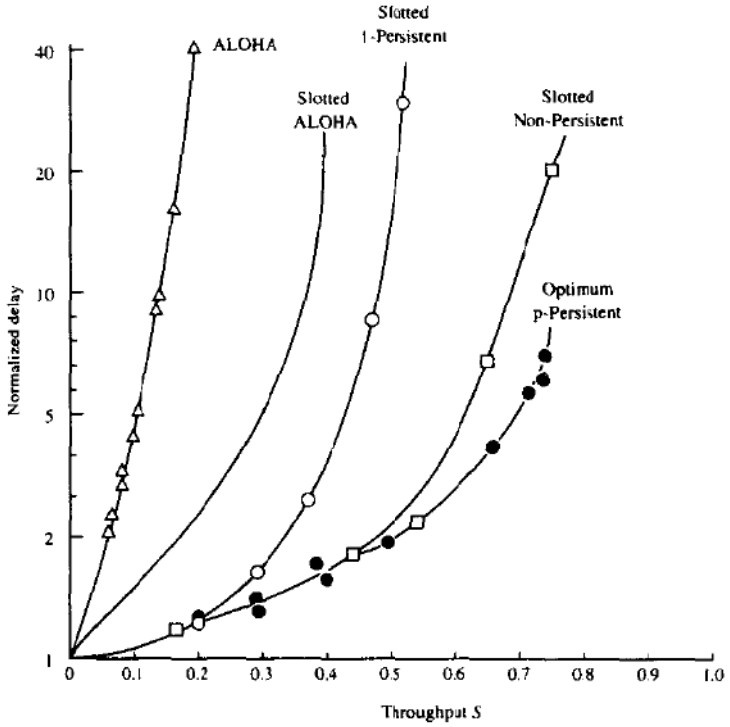

FIGURE 15-4-7 Throughput versus delay from simulation ($a = 0.01$). [*From Kleinrock and Tobagi (1975), © IEEE.*]

obtained by finding the optimum value of p for each value of the throughput. We observe that for small values of the throughput, the 1-persistent ($p = 1$) protocol is optimal.

15-5 BIBLIOGRAPHICAL NOTES AND REFERENCES

FDMA was the dominant multiple access scheme that has been used for decades in telephone communication systems for analog voice transmission. With the advent of digital speech transmission using PCM, DPCM, and other speech coding methods, TDMA has replaced FDMA as the dominant multiple access scheme in telecommunications. CDMA and random access methods, in general, have been developed over the past three decades, primarily for use in wireless signal transmission and in local area wireline networks.

Multiuser information theory deals with basic information-theoretic limits in source coding for multiple sources, and channel coding and modulation for multiple access channels. A large amount of literature exists on these topics. In the context of our treatment of multiple access methods, the reader will find

the papers by Cover (1972), El Gamal and Cover (1980) Bergmans and Cover (1974), and Hui (1984) particularly relevant. The capacity of a cellular CDMA system has been considered in the paper by Gilhousen *et al.* (1991).

Signal demodulation and detection for multiuser communications has received considerable attention in recent years. The reader is referred to the papers by Verdu (1986a–c, 1989), Lupas and Verdu (1990), Xie *et al.* (1990a, b), Poor and Verdu (1988), Zhang and Brady (1993), and Zvonar and Brady (1995). Earlier work on signal design and demodulation for multiuser communications is found in the papers by Van Etten (1975, 1976), Horwood and Gagliardi (1975), and Kaye and George (1970).

The ALOHA system, which was one of the earliest random access systems, is treated in the papers by Abramson (1970, 1977) and Roberts (1975). These papers contain the throughput analysis for unslotted and slotted systems. Stability issues regarding the ALOHA protocols may be found in the papers by Carleial and Hellman (1975), Ghez *et al.* (1988), and Massey (1988). Stable protocols based on tree algorithms for random access channels were first given by Capetanakis (1977). The carrier sense multiple access protocols that we described are due to Kleinrock and Tobagi (1975). Finally, we mention the IEEE Press book edited by Abramson (1993), which contains a collection of papers dealing with multiple access communications.

PROBLEMS

15-1 In the formulation of the CDMA signal and channel models described in Section 15-3-1, we assumed that the received signals are real. For $K > 1$, this assumption implies phase synchronism at all transmitters, which is not very realistic in a practical system. To accommodate the case where the carrier phases are not synchronous, we may simply alter the signature waveforms for the K users, given by (15-3-1), to be complex-valued, of the form

$$g_k(t) = e^{j\theta_k} \sum_{n=0}^{L-1} a_k(n) p(t - nT_c), \qquad 1 \leq k \leq K$$

where θ_k represents the constant phase offset of the kth transmitter as seen by the common receiver.

- **a** Given this complex-valued form for the signature waveforms, determine the form of the optimum ML receiver that computes the correlation metrics analogous to (15-3-15).
- **b** Repeat the derivation for the optimum ML detector for asynchronous transmission that is analogous to (15-3-19).

15-2 Consider a TDMA system where each user is limited to a transmitted power P, independent of the number of users. Determine the capacity per user, C_K, and the total capacity KC_K. Plot C_K and KC_K as functions of $\mathcal{E}_b/N_0$ and comment on the results as $K \to \infty$.

15-3 Consider an FDMA system with $K = 2$ users, in an AWGN channel, where user 1 is assigned a bandwidth $W_1 = \alpha W$ and user 2 is assigned a bandwidth $W_2 = (1 - \alpha)W$, where $0 \leq \alpha \leq 1$. Let P_1 and P_2 be the average powers of the two users.

a Determine the capacities C_1 and C_2 of the two users and their sum $C = C_1 + C_2$ as a function of α. On a two-dimensional graph of the rates R_2 versus R_1, plot the graph of the points (C_2, C_1) as α varies in the range $0 \leq \alpha \leq 1$.

b Recall that the rates of the two users must satisfy the conditions

$$R_1 < W_1 \log_2\left(1 + \frac{P_1}{W_1 N_0}\right)$$

$$R_2 < W_2 \log_2\left(1 + \frac{P_2}{W_2 N_0}\right)$$

$$R_1 + R_2 < W \log_2\left(1 + \frac{P_1 + P_2}{W N_0}\right)$$

Determine the total capacity C when $P_1/\alpha = P_2/(1-\alpha) = P_1 + P_2$, and, thus, show that the maximum rate is achieved when $\alpha/(1-\alpha) = P_1/P_2 = W_1/W_2$.

15-4 Consider a TDMA system with $K = 2$ users in an AWGN channel. Suppose that the two transmitters are peak-power-limited to P_1 and P_2, and let user 1 transmit for $100\alpha\%$ of the available time and user 2 transmit $100(1-\alpha)\%$ of the time. The available bandwidth is W.

a Determine the capacities C_1, C_2, and $C = C_1 + C_2$ as functions of α.

b Plot the graph of the points (C_2, C_1) as α varies in the range $0 \leq \alpha \leq 1$.

15-5 Consider a TDMA system with $K = 2$ users in an AWGN channel. Suppose that the two transmitters are average-power-limited, with powers P_1 and P_2. User 1 transmits $100\alpha\%$ of the time and user 2 transmits $100(1-\alpha)\%$ of the time. The channel bandwidth is W.

a Determine the capacities C_1, C_2, and $C = C_1 + C_2$ as functions of α.

b Plot the graph of the points (C_2, C_1) as α varies in the range $0 \leq \alpha \leq 1$.

c What is the similarity between this solution and the FDMA system in Problem 15-3.

15-6 Consider the two-user, *synchronous*, multiple-access channel and the signature sequences shown in Fig. P15-6. The parameter $A \geq 0$ describes the relative strength between the two users, and $0 \leq B \leq 1$ describes the degree of correlation between the waveforms. Let

$$r(t) = \sum_{k=1}^{2} \sum_{i=-\infty}^{\infty} b_k(i) s_k(t-i) + n(t)$$

FIGURE P15-6

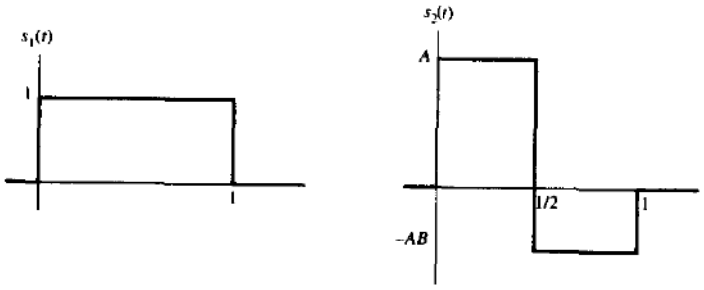

denote the received waveform at time t, where $n(t)$ is white gaussian noise with power spectral density σ^2, and $b_k(i) \in \{-1, +1\}$. In the following problems, you will compare the structure of the conventional multiuser detector to optimimum receiver structures for various values of A, $0 \leq B \leq 1$, and σ^2.

a Show that, given the observation $\{r(t), -\infty < t \leq 1\}$, a sufficient statistic for the data $b_1(0)$ and $b_2(0)$ is the observation during $t \in [0, 1]$.

b Conventional (suboptimum) multiuser detection chooses the data $b_k(0)$ according to the following rule:

$$b_k(0) = \text{sgn}\,(y_k)$$

where

$$y_k = \int_0^1 r(t)s_k(t)\,dt$$

Determine an expression for the probability of bit error for user 1, using the notation

$$w_k = \int_0^1 s_k^2(t)\,dt$$

$$\rho_{12} = \int_0^1 s_1(t)s_2(t)\,dt.$$

c What is the form of this expression for $A \to 0$, $B < 1$, and arbitrary σ^2?

d What is the form of this expression for arbitrarily large A, $B < 1$, and arbitrary σ^2? What does this say about conventional detection?

e What is the form of this expression for $B = 1$, and arbitrary σ^2 and A? Why does this differ from the result in (d)?

f Determine the form of this expression for arbitrarily large σ^2, arbitrary A, and $B < 1$.

g Determine the form of this expression for $\sigma^2 \to 0$, arbitrary A, and $B < 1$.

15-7 Refer to Problem 15-6. The maximum-likelihood sequence receiver for this channel selects the data $b_1(0)$ and $b_2(0)$ transmitted during the interval $[0, 1]$ according to the rule

$$(\widehat{b_1(0)}, \widehat{b_2(0)}) = \underset{b_1, b_2}{\text{argmax}}\, \Lambda[\{r(t), 0 < t < 1\} \mid b_1, b_2]$$

where $\Lambda[\{r(t), 0 < t < 1\} \mid b_1, b_2]$ is the likelihood function of b_1 and b_2 given an observation of $\{r(t), 0 < t < 1\}$. It will be helpful to write this maximization as

$$(\widehat{b_1(0)}, \widehat{b_2(0)}) = \underset{b_1}{\text{argmax}}\, \underset{b_2}{\text{argmax}}\, \Lambda[\{r(t), 0 < t < 1\} \mid b_1, b_2]$$

where the value b_2^* that satisfies the inner maximization may depend on b_1. Note that the need for "sequence detection" is obviated.

a Express this maximization in the *simplest* possible terms, using the same notation as in Problem 15-6(b). Reduce this maximization to simplest form, using facts like

$$\underset{x}{\text{argmax}}\, Ke^{f_1(x)} = \underset{x}{\text{argmax}}\, f_1(x)$$

if, say, K is independent of x.

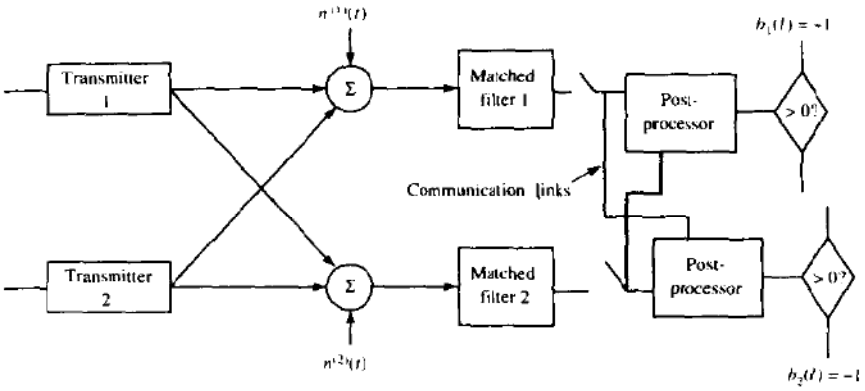

FIGURE P15-8

b What is the simplest structure of the MLS receiver as the relative strength of the interferer vanishes, $A \to 0$? How does it compare with conventional detection?

c What is the simplest structure of the MLS receiver for $B = 1$ and arbitrary A and σ^2? How does it compare with conventional detection? Why?

d What is the simplest structure of the MLS receiver for arbitrarily large σ^2 and arbitrary A and B? How does it compare with conventional detection? Determine the error rate for user 1 in this case. [*Hint:* Use the fact that $\text{sgn}(y_2) = \text{sgn}(y_2 \pm \rho_{12})$ with high probability in this case.]

e Determine the error probability of user 1 of the MLS receiver for $\sigma^2 \to 0$, and arbitrarily large A and $B < 1$? How does it compare with conventional detection?

f What is the structure of the MLS receiver for arbitrarily large A, and $B < 1$, and arbitrary σ_2? How does it compare with conventional detection? What does this say about conventional detection in this case? [*Hint:* Use the fact that $E|y_2|$ is roughly A times greater than $E|y_1|$.]

15-8 Consider the asynchronous communication system shown in Fig. P15-8. The two receivers are not colocated, and the white noise processes $n^{(1)}(t)$ and $n^{(2)}(t)$ may be considered to be independent. The noise processes are identically distributed, with power spectral density σ^2 and zero mean. Since the receivers are not colocated, the relative delays between the users are not the same—denote the relative delay of user k at receiver i by $\tau_k^{(i)}$. All other signal parameters coincide for the receivers, and the received signal at receiver i is

$$r^{(i)}(t) = \sum_{k=1}^{2} \sum_{l=-\infty}^{\infty} b_k(l) s_k(t - lT - \tau_k^{(i)}) + n^{(i)}(t)$$

where s_k has support on $[0, T]$. You may assume that the receiver i has full knowledge of the waveforms, energies, and relative delays $\tau_1^{(i)}$ and $\tau_2^{(i)}$. Although receiver i is eventually interested only in the data from transmitter i, note that there is a free communication link between the sampler of one receiver, and the postprocessing circuitry of the other. Following each postprocessor, the decision is attained by threshold detection. In this problem, you will consider options for postprocessing and for the communication link in order to improve performance.

a What is the bit error probability for users 1 and 2 of a receiver pair that does not utilize the communication link, and does not perform postprocessing. Use the following notation:

$$y_k(l) = \int s_k(t - lT - \tau_k^{(k)}) r^{(k)}(t)\, dt$$

$$\rho_{12}^{(l)} = \int s_1(t - \tau_1^{(l)}) s_2(t - \tau_2^{(l)})\, dt$$

$$\rho_{21}^{(l)} = \int s_1(t - \tau_1^{(l)}) s_2(t + T - \tau_2^{(l)})\, dt$$

$$w_k = \int s_k^2(t - \tau_k^{(1)})\, dt = \int s_k^2(t - \tau_k^{(2)})\, dt$$

b Consider a postprocessor for receiver 1 that accepts $y_2(l-1)$ and $y_2(l)$ from the communication link, and implements the following postprocessing on $y_1(l)$

$$z_l(l) = y_1(l) - \rho_{21}^{(l)} \operatorname{sgn}[y_2(l-1)] - \rho_{12}^{(l)} \operatorname{sgn}[y_2(l)].$$

Determine an exact expression for the bit error rate for user 1.

c Determine the asymptotic multiuser efficiency of the receiver proposed in (b), and compare with that in (a). Does this receiver always perform better than that proposed in (a)?

15-9 The baseband waveforms shown in Fig. P15-6 are assigned to two users who share the same *asynchronous*, narrowband channel. Assume that $B = 1$ and $A = 4$. We should like to compare the performance of several receivers, with a criterion of $\mathcal{P}_1(0)$. Since this expression is too complicated in some cases, we shall also be interested in comparing the asymptotic multiuser efficiency η_1 of each receiver. Assume that $\tau_1 = 0$ but that $0 < \tau_2 < T$ is fixed and known at the receiver, and assume that we have *infinite horizon transmission*, $2M + 1 \to \infty$.

a For the conventional, multiuser detector:

(i) Find the exact bit probability of error for user 1. Express this result in terms of w_1, ρ_{12}, ρ_{21}, and σ^2. [*Hint:* Conditioning on $b_2(-1)$ and $b_2(0)$ will help.]

(ii) Plot the asymptotic multiuser efficiency η_1 as a function of τ_2. Indicate and explain the maximum and minimum values of η_1 in this plot.

b For the MLS receiver:

(i) Plot η_1 as a function of τ_2. Explain maximum and minimum values, and compare with (a)(ii).

(ii) Which error sequences are most likely for each value of τ_2?

c For the limiting decorrelating detector:

(i) Find an exact expression for the probability of error for user 1, with similar parameters as in (a)(i) [*Hint:* Don't forget to normalize ρ_{12} and ρ_{21}.]

(ii) Plot η_1 as a function of τ_2. Explain the minimum value of η_1 in this case, and compare with (a)(ii).

15-10 The symbol-by-symbol detector that minimizes the probability of a symbol error differs from the maximum-likelihood sequence detector. The former is more completely described as the detector that selects each $b_k(0)$ according to the rule

$$\widehat{b_k(0)} = \underset{b_k(0)}{\operatorname{argmax}} \Lambda[\{r(t), 0 < t < 1\} \mid b_k(0)]$$

a Show that this decision rule minimizes $\Lambda[b_k(0) \neq \widehat{b_k(0)}]$ among all decision rules with observation $\{r(t), 0 < t < 1\}$. Subject to this criteria, it is superior to the MLS receiver.

b Show that the simplest structure of the minimum-probability-of-error receiver for user 1 is given by

$$\widehat{b_1(0)} = \underset{b_1}{\operatorname{argmax}} \left[\exp\left(\frac{b_1 y_1}{\sigma^2}\right) \cosh\left(\frac{y_2 - b_1 \rho_{12}}{\sigma^2}\right) \right] .$$

c Find the simplest form of the minimum-probability-of-error receiver for $B = 1$ and arbitrary A and σ^2. How does this compare with the above receivers?

d Find the limiting form of the minimum-probability-of-error receiver for arbitrarily large σ^2 and arbitrary A and B. Compare with the above receivers.

e Find the limiting form of the minimum-probability-of-error receiver for $A \gg 1$ and arbitrary σ^2 and B. Compare with the above receivers.

f Find the limiting form of the minimum-probability-of-error receiver for $A \gg 1$ $\sigma^2 \to 0$ and arbitrary B. Compare with the above receivers.

15-11 In a pure ALOHA system, the channel bit rate is 2400 bits/s. Suppose that each terminal transmits a 100 bit message every minute on the average.

a Determine the maximum number of terminals that can use the channel.

b Repeat (a) if slotted ALOHA is used.

15-12 Determine the maximum input traffic for the pure ALOHA and slotted ALOHA protocols.

15-13 For a Poisson process, the probability of k arrivals in a time interval T is

$$P(k) = \frac{e^{-\lambda T}(\lambda T)^k}{k!}, \qquad k = 0, 1, 2, \ldots$$

a Determine the average number or arrivals in the interval T.

b Determine the variance σ^2 in the number of arrivals in the interval T.

c What is the probability of at least one arrival in the interval T?

d What is the probability of exactly one arrival in the interval T?

15-14 Refer to Problem 15-13. The average arrival rate is $\lambda = 10$ packets/s. Determine

a the average time between arrivals;

b the probability that another packet will arrive within 1 s; within 100 ms.

15-15 Consider a pure ALOHA system that is operating with a throughput $G = 0.1$ and packets are generated with a Poisson arrival rate λ. Determine

a the value of λ;

b the average number of attempted transmissions to send a packet.

15-16 Consider a CSMA/CD system in which the transmission rate on the bus is 10 Mbits/s. The bus is 2 km and the propagation delay is 5 μs/km. Packets are 1000 bits long. Determine

a the end-to-end delay τ_d;

b the packet duration T_p;

c the ratio τ_d / T_p;

d the maximum utilization of the bus and the maximum bit rate.

APPENDIX A

THE LEVINSON–DURBIN ALGORITHM

The Levinson–Durbin algorithm is an order-recursive method for determining the solution to the set of linear equations

$$\mathbf{\Phi}_p \mathbf{a}_p = \mathbf{\phi}_p \tag{A-1}$$

where $\mathbf{\Phi}_p$ is a $p \times p$ Toeplitz matrix, $\mathbf{a}_p$ is the vector of predictor coefficients expressed as

$$\mathbf{a}_p' = [a_{p1} \quad a_{p2} \quad \cdots \quad a_{pp}]$$

and $\mathbf{\phi}_p$ is a p-dimensional vector with elements

$$\mathbf{\phi}_p' = [\phi(1) \quad \phi(2) \quad \cdots \quad \phi(p)]$$

For a first-order ($p = 1$) predictor, we have the solution

$$\begin{aligned} \phi(0)a_{11} &= \phi(1) \\ a_{11} &= \phi(1)/\phi(0) \end{aligned} \tag{A-2}$$

The residual mean square error (MSE) for the first-order predictor is

$$\begin{aligned} \mathscr{E}_1 &= \phi(0) - a_{11}\phi(1) \\ &= \phi(0) - a_{11}^2\phi(0) \\ &= \phi(0)(1 - a_{11}^2) \end{aligned} \tag{A-3}$$

In general, we may express the solution for the coefficients of an mth-order

predictor in terms of the coefficients of the $(m-1)$th-order predictor. Thus, we express $\mathbf{a}_m$ as the sum of two vectors, namely,

$$\mathbf{a}_m = \begin{bmatrix} a_{m1} \\ a_{m2} \\ \vdots \\ a_{mm} \end{bmatrix} = \begin{bmatrix} \mathbf{a}_{m-1} \\ 0 \end{bmatrix} + \begin{bmatrix} \mathbf{d}_{m-1} \\ k_m \end{bmatrix} \tag{A-4}$$

where the vector $\mathbf{d}_{m-1}$ and the scalar k_m are to be determined. Also, $\mathbf{\Phi}_m$ may be expressed as

$$\mathbf{\Phi}_m = \begin{bmatrix} \mathbf{\Phi}_{m-1} & \boldsymbol{\phi}'_{m-1} \\ \boldsymbol{\phi}'_{m-1} & \phi(0) \end{bmatrix} \tag{A-5}$$

where $\boldsymbol{\phi}'_{m-1}$ is just the vector $\boldsymbol{\phi}_{m-1}$ in reverse order.

Now

$$\begin{bmatrix} \mathbf{\Phi}_{m-1} & \boldsymbol{\phi}'_{m-1} \\ \boldsymbol{\phi}'_{m-1} & \phi(0) \end{bmatrix} \left(\begin{bmatrix} \mathbf{a}_{m-1} \\ 0 \end{bmatrix} + \begin{bmatrix} \mathbf{d}_{m-1} \\ k_m \end{bmatrix} \right) = \begin{bmatrix} \boldsymbol{\phi}_{m-1} \\ \phi(m) \end{bmatrix} \tag{A-6}$$

From (A-6), we obtain two equations. The first is the matrix equation

$$\mathbf{\Phi}_{m-1}\mathbf{a}_{m-1} + \mathbf{\Phi}_{m-1}\mathbf{d}_{m-1} + k_m\boldsymbol{\phi}'_{m-1} = \boldsymbol{\phi}_{m-1} \tag{A-7}$$

But $\mathbf{\Phi}_{m-1}\mathbf{a}_{m-1} = \boldsymbol{\phi}_{m-1}$. Hence, (A-7) simplifies to

$$\mathbf{\Phi}_{m-1}\mathbf{d}_{m-1} + k_m\boldsymbol{\phi}'_{m-1} = \mathbf{0} \tag{A-8}$$

This equation has the solution

$$\mathbf{d}_{m-1} = -k_m\mathbf{\Phi}_{m-1}^{-1}\boldsymbol{\phi}'_{m-1} \tag{A-9}$$

But $\boldsymbol{\phi}'_{m-1}$ is just $\boldsymbol{\phi}_{m-1}$ in reverse order. Hence, the solution in (A-9) is simply $\mathbf{a}_{m-1}$ in reverse order multiplied by $-k_m$. That is,

$$\mathbf{d}_{m-1} = -k_m \begin{bmatrix} a_{m-1,m-1} \\ a_{m-1,m-2} \\ \vdots \\ a_{m-1,1} \end{bmatrix} \tag{A-10}$$

The second equation obtained from (A-6) is the scalar equation

$$\boldsymbol{\phi}'_{m-1}\mathbf{a}_{m-1} + \boldsymbol{\phi}'_{m-1}\mathbf{d}_{m-1} + \phi(0)k_m = \phi(m) \tag{A-11}$$

We eliminate $\mathbf{d}_{m-1}$ from (A-11) by use of (A-10). The resulting equation gives us k_m. That is,

$$\begin{aligned} k_m &= \frac{\phi(m) - \boldsymbol{\phi}'_{m-1}\mathbf{a}_{m-1}}{\phi(0) - \boldsymbol{\phi}'_{m-1}\mathbf{\Phi}_{m-1}^{-1}\boldsymbol{\phi}'_{m-1}} \\ &= \frac{\phi(m) - \boldsymbol{\phi}'_{m-1}\mathbf{a}_{m-1}}{\phi(0) - \mathbf{a}'_{m-1}\boldsymbol{\phi}_{m-1}} \\ &= \frac{\phi(m) - \boldsymbol{\phi}'_{m-1}\mathbf{a}_{m-1}}{\mathcal{E}_{m-1}} \end{aligned} \tag{A-12}$$

where $\mathscr{E}_{m-1}$ is the residual MSE given as

$$\mathscr{E}_{m-1} = \phi(0) - \mathbf{a}'_{m-1}\boldsymbol{\phi}_{m-1} \tag{A-13}$$

By substituting (A-10) for $\mathbf{d}_{m-1}$ in (A-4), we obtain the order-recursive relation

$$a_{mk} = a_{m-1,k} - k_m a_{m-1,m-k}, \quad k = 1, 2, \ldots, m-1, \quad m = 1, 2, \ldots, p \tag{A-14}$$

and

$$a_{mm} = k_m$$

The minimum MSE may also be computed recursively. We have

$$\mathscr{E}_m = \phi(0) - \sum_{k=1}^{m} a_{mk}\phi(k) \tag{A-15}$$

Using (A-14) in (A-15), we obtain

$$\mathscr{E}_m = \phi(0) - \sum_{k=1}^{m-1} a_{m-1,k}\phi(k) - a_{mm}\left[\phi(m) - \sum_{k=1}^{m-1} a_{m-1,m-k}\phi(k)\right] \tag{A-16}$$

But the term in square brackets in (A-16) is just the numerator of k_m in (A-12). Hence,

$$\begin{aligned}\mathscr{E}_m &= \mathscr{E}_{m-1} - a_{mm}^2\mathscr{E}_{m-1} \\ &= \mathscr{E}_{m-1}(1 - a_{mm}^2)\end{aligned} \tag{A-17}$$

APPENDIX **B**

ERROR PROBABILITY FOR MULTICHANNEL BINARY SIGNALS

In multichannel communication systems that employ binary signaling for transmitting information over the AWGN channel, the decision variable at the detector can be expressed as a special case of the general quadratic form

$$D = \sum_{k=1}^{L} (A|X_k|^2 + B|Y_k|^2 + CX_kY_k^* + C^*X_k^*Y_k) \tag{B-1}$$

in complex-valued gaussian random variables. A, B, and C are constants; X_k and Y_k are a pair of correlated complex-valued gaussian random variables. For the channels considered, the L pairs $\{X_k, Y_k\}$ are mutually statistically independent and identically distributed.

The probability of error is the probability that $D < 0$. This probability is evaluated below.

The computation begins with the characteristic function, denoted by $\psi_D(jv)$, of the general quadratic form. The probability that $D < 0$, denoted here as the probability of error P_b, is

$$P_b = P(D < 0) = \int_{-\infty}^{0} p(D)\,dD \tag{B-2}$$

where $p(D)$, the probability density function of D, is related to $\psi_D(jv)$ by the Fourier transform, i.e.,

$$p(D) = \frac{1}{2\pi}\int_{-\infty}^{\infty} \psi_D(jv)e^{-jvD}\,dv$$

Hence,

$$P_b = \int_{-\infty}^{0} dD \frac{1}{2\pi} \int_{-\infty}^{\infty} \psi_D(jv) e^{-jvD} dv \tag{B-3}$$

Let us interchange the order of integration and carry out first the integration with respect to D. The result is

$$P_b = -\frac{1}{2\pi j} \int_{-\infty-j\varepsilon}^{\infty+j\varepsilon} \frac{\psi_D(jv)}{v} dv \tag{B-4}$$

where a small positive number ε has been inserted in order to move the path of integration away from the singularity at $v = 0$ and which must be positive in order to allow for the interchange in the order of integration.

Since D is the sum of statistically independent random variables, the characteristic function of D factors into a product of L characteristic functions, with each function corresponding to the individual random variables d_k, where

$$d_k = A|X_k|^2 + B|Y_k|^2 + CX_kY_k^* + C^*X_k^*Y_k$$

The characteristic function of d_k is

$$\phi_{d_k}(jv) = \frac{v_1 v_2}{(v + jv_1)(v - jv_2)} \exp\left[\frac{v_1 v_2(-v^2\alpha_{1k} + jv\alpha_{2k})}{(v + jv_1)(v - jv_2)}\right] \tag{B-5}$$

where the parameters v_1, v_2, α_{1k}, and α_{2k} depend on the means $\bar{X}_k$ and $\bar{Y}_k$ and the second (central) moments μ_{xx}, μ_{yy}, and μ_{xy} of the complex-vlaued gaussian variables X_k and Y_k through the following definitions ($|C|^2 - AB > 0$):

$$\begin{aligned}
v_1 &= \sqrt{w^2 + \frac{1}{4(\mu_{xx}\mu_{yy} - |\mu_{xy}|^2)(|C|^2 - AB)}} - w \\
v_2 &= \sqrt{w^2 + \frac{1}{4(\mu_{xx}\mu_{yy} - |\mu_{xy}|^2)(|C|^2 - AB)}} + w \\
w &= \frac{A\mu_{xx} + B\mu_{yy} + C\mu_{xy}^* + C^*\mu_{xy}}{4(\mu_{xx}\mu_{yy} - |\mu_{xy}|^2)(|C|^2 - AB)} \\
\alpha_{1k} &= 2(|C|^2 - AB)(|\bar{X}_k|^2\mu_{yy} + |\bar{Y}_k|^2\mu_{xx} - \bar{X}_k^*\bar{Y}_k\mu_{xy} - \bar{X}_k\bar{Y}_k^*\mu_{xy}^*) \\
\alpha_{2k} &= A|\bar{X}_k|^2 + B|\bar{Y}_k|^2 + C\bar{X}_k^*\bar{Y}_k + C^*\bar{X}_k\bar{Y}_k^* \\
\mu_{xy} &= \tfrac{1}{2}E[(X_k - \bar{X}_k)(Y_k - \bar{Y}_k)^*]
\end{aligned} \tag{B-6}$$

Now, as a result of the independence of the random variables d_k, the characteristic function of D is

$$\begin{aligned}
\psi_D(jv) &= \prod_{k=1}^{L} \psi_{d_k}(jv) \\
\psi_D(jv) &= \frac{(v_1 v_2)^L}{(v + jv_1)^L(v - jv_2)^L} \exp\left[\frac{v_1 v_2(jv\alpha_2 - v^2\alpha_1)}{(v + jv_1)(v - jv_2)}\right]
\end{aligned} \tag{B-7}$$

where

$$\alpha_1 = \sum_{k=1}^{L} \alpha_{1k}, \qquad \alpha_2 = \sum_{k=1}^{L} \alpha_{2k} \tag{B-8}$$

The result (B-7) is substituted for $\psi_D(jv)$ in (B-4), and we obtain

$$P_b = -\frac{(v_1 v_2)^L}{2\pi j}\int_{-\infty+j\mu}^{\infty+j\mu} \frac{dv}{v(v+jv_1)^L(v-jv_2)^L}\exp\left[\frac{v_1 v_2(jv\alpha_2 - v^2\alpha_1)}{(v+jv_1)(v-jv_2)}\right] \tag{B-9}$$

This integral is evaluated as follows.

The first step is to express the exponential function in the form

$$\exp\left(-A_1 + \frac{jA_2}{v+jv_1} - \frac{jA_3}{v-jv_2}\right)$$

where one can easily verify that the constants A_1, A_2, and A_3 are given as

$$\begin{aligned} A_1 &= \alpha_1 v_1 v_2 \\ A_2 &= \frac{v_1^2 v_2}{v_1+v_2}(\alpha_1 v_1 + \alpha_2) \\ A_3 &= \frac{v_1 v_2^2}{v_1+v_2}(\alpha_1 v_2 - \alpha_2) \end{aligned} \tag{B-10}$$

Second, a conformal transformation is made from the v plane onto the p plane via the change in variable

$$p = -\frac{v_1}{v_2}\frac{v-jv_2}{v+jv_1} \tag{B-11}$$

In the p plane, the integral given by (B-9) becomes

$$P_b = \frac{\exp\left[v_1 v_2(-2\alpha v_1 v_2 + \alpha_2 v_1 - \alpha_2 v_2)/(v_1+v_2)^2\right]}{(1+v_2/v_1)^{2L-1}}\frac{1}{2\pi j}\int_\Gamma f(p)\,dp \tag{B-12}$$

where

$$f(p) = \frac{[1+(v_2/v_1)p]^{2L-1}}{p^L(1-p)}\exp\left[\frac{A_2(v_2/v_1)}{v_1+v_2}p + \frac{A_3(v_1/v_2)}{v_1+v_2}\frac{1}{p}\right] \tag{B-13}$$

and Γ is a circular contour of radius less than unity that encloses the origin.

The third step is to evaluate the integral

$$\begin{aligned} \frac{1}{2\pi j}\int_\Gamma f(p)\,dp = \frac{1}{2\pi j}\int_\Gamma &\frac{(1+(v_2/v_1)p)^{2L-1}}{p^L(1-p)} \\ &\times \exp\left[\frac{A_2(v_2/v_1)}{v_1+v_2}p + \frac{A_3(v_1/v_2)}{v_1+v_2}\frac{1}{p}\right]dp \end{aligned} \tag{B-14}$$

In order to facilitate subsequent manipulations, the constants $a \geq 0$ and $b \geq 0$ are introduced and defined as follows:

$$\tfrac{1}{2}a^2 = \frac{A_3(v_1/v_2)}{v_1+v_2}, \qquad \tfrac{1}{2}b^2 = \frac{A_2(v_2/v_1)}{v_1+v_2} \tag{B-15}$$

Let us also expand the function $[1 + (v_2/v_1)p]^{2L-1}$ as a binomial series. As a result, we obtain

$$\frac{1}{2\pi j}\int_\Gamma f(p)\,dp = \sum_{k=0}^{2L-1}\binom{2L-1}{k}\left(\frac{v_2}{v_1}\right)^k \times \frac{1}{2\pi j}\int_\Gamma \frac{p^k}{p^L(1-p)}\exp\left(\frac{\frac{1}{2}a^2}{p} + \tfrac{1}{2}b^2p\right)dp \qquad \text{(B-16)}$$

The contour integral given in (B-16) is one representation of the Bessel function. It can be solved by making use of the relations

$$I_n(ab) = \begin{cases} \dfrac{1}{2\pi j}\left(\dfrac{a}{b}\right)^n \displaystyle\int_\Gamma \frac{1}{p^{n+1}}\exp\left(\frac{\frac{1}{2}a^2}{p} + \tfrac{1}{2}b^2p\right)dp \\ \dfrac{1}{2\pi j}\left(\dfrac{b}{a}\right)^n \displaystyle\int_\Gamma p^{n-1}\exp\left(\frac{\frac{1}{2}a^2}{p} + \tfrac{1}{2}b^2p\right)dp \end{cases}$$

where $I_n(x)$ is the nth order modified Bessel function of the first kind and the series representation of Marcum's Q function in terms of Bessel functions, i.e.,

$$Q_1(a,b) = \exp\left[-\tfrac{1}{2}(a^2+b^2)\right] + \sum_{n=0}^{\infty}\left(\frac{a}{b}\right)^n I_n(ab)$$

First, consider the case $0 \leq k \leq L-2$ in (B-16). In this case, the resulting contour integral can be written in the form†

$$\frac{1}{2\pi j}\int_\Gamma \frac{1}{p^{L-k}(1-p)}\exp\left(\frac{\frac{1}{2}a^2}{p} + \tfrac{1}{2}b^2p\right)dp = Q_1(a,b)\exp\left[\tfrac{1}{2}(a^2+b^2)\right] + \sum_{n=1}^{L-1-k}\left(\frac{b}{a}\right)^n I_n(ab) \qquad \text{(B-17)}$$

Next, consider the term $k = L-1$. The resulting contour integral can be expressed in terms of the Q function as follows:

$$\frac{1}{2\pi j}\int_\Gamma \frac{1}{p(1-p)}\exp\left(\frac{\frac{1}{2}a^2}{p} + \tfrac{1}{2}b^2p\right)dp = Q_1(a,b)\exp\left[\tfrac{1}{2}(a^2+b^2)\right] \qquad \text{(B-18)}$$

Finally, consider the case $L \leq k \leq 2L-1$. We have

$$\begin{aligned}\frac{1}{2\pi j}\int_\Gamma \frac{p^{k-L}}{1-p}\exp\left(\frac{\frac{1}{2}a^2}{p} + \tfrac{1}{2}b^2p\right)dp &= \sum_{n=0}^{\infty}\frac{1}{2\pi j}\int_\Gamma p^{k-L+n}\exp\left(\frac{\frac{1}{2}a^2}{p} + \tfrac{1}{2}b^2p\right)dp \\ &= \sum_{n=k+1-L}^{\infty}\left(\frac{a}{b}\right)^n I_n(ab) = Q_1(a,b)\exp\left[\tfrac{1}{2}(a^2+b^2)\right] - \sum_{n=0}^{k-L}\left(\frac{a}{b}\right)^n I_n(ab) \qquad \text{(B-19)}\end{aligned}$$

Collecting the terms that are indicated on the right-hand side of (B-16) and using

† This contour integral is related to the generalized Marcum Q function, defined as

$$Q_m(a,b) = \int_b^\infty x(x/a)^{m-1}\exp\left[-\tfrac{1}{2}(x^2+a^2)\right]I_{m-1}(ax)\,dx, \quad m \geq 1$$

in the following manner:

$$Q_m(a,b)\exp\left[\tfrac{1}{2}(a^2+b^2)\right] = \frac{1}{2\pi j}\int_\Gamma \frac{1}{p^m(1-p)}\exp\left(\frac{\frac{1}{2}a^2}{p} + \tfrac{1}{2}b^2p\right)dp$$

the results given in (B-17)–(B-19), the following expression for the contour integral is obtained after some algebra:

$$\frac{1}{2\pi j}\int_{\Gamma} f(p)\,dp = \left(1+\frac{v_2}{v_1}\right)^{2L-1}\left[\exp\left[\tfrac{1}{2}(a^2+b^2)\right]Q_1(a,b) - I_0(ab)\right] + I_0(ab)\sum_{k=0}^{L-1}\binom{2L-1}{k}\left(\frac{v_2}{v_1}\right)^k + \sum_{n=1}^{L-1} I_n(ab)\sum_{k=0}^{L-1-n}\binom{2L-1}{k}\left[\left(\frac{b}{a}\right)^n\left(\frac{v_2}{v_1}\right)^k - \left(\frac{a}{b}\right)^n\left(\frac{v_2}{v_1}\right)^{2L-1-k}\right] \tag{B-20}$$

Equation (B-20) in conjunction with (B-12) gives the result for the probability of error. A further simplification results when one uses the following identity, which can easily be proved:

$$\exp\left[\frac{v_1 v_2}{(v_1+v_2)^2}(-2\alpha_1 v_1 v_2 + \alpha_2 v_1 - \alpha_2 v_2)\right] = \exp\left[-\tfrac{1}{2}(a^2+b^2)\right]$$

Therefore, it follows that

$$\begin{aligned} P_b &= Q_1(a,b) - I_0(ab)\exp\left[-\tfrac{1}{2}(a^2+b^2)\right] \\ &\quad + \frac{I_0(ab)\exp\left[-\tfrac{1}{2}(a^2+b^2)\right]}{(1+v_2/v_1)^{2L-1}}\sum_{k=0}^{L-1}\binom{2L-1}{k}\left(\frac{v_2}{v_1}\right)^k + \frac{\exp\left[-\tfrac{1}{2}(a^2+b^2)\right]}{(1+v_2/v_1)^{2L-1}} \\ &\quad \times \sum_{n=1}^{L-1} I_n(ab)\sum_{k=0}^{L-1-n}\binom{2L-1}{k} \\ &\quad \times \left[\left(\frac{b}{a}\right)^n\left(\frac{v_2}{v_1}\right)^k - \left(\frac{a}{b}\right)^n\left(\frac{v_2}{v_1}\right)^{2L-1-k}\right] \quad (L>1) \end{aligned} \tag{B-21}$$

$$P_b = Q_1(a,b) - \frac{v_2/v_1}{1+v_2/v_1} I_0(ab)\exp\left[-\tfrac{1}{2}(a^2+b^2)\right] \quad (L=1)$$

This is the desired expression for the probability of error. It is now a simple matter to relate the parameters a and b to the moments of the pairs $\{X_k, Y_k\}$. Substituting for A_2 and A_3 from (B-10) into (B-15), we obtain

$$\begin{aligned} a &= \left[\frac{2v_1^2 v_2(\alpha_1 v_2 - \alpha_2)}{(v_1+v_2)^2}\right]^{1/2} \\ b &= \left[\frac{2v_1 v_2^2(\alpha_1 v_1 + \alpha_2)}{(v_1+v_2)^2}\right]^{1/2} \end{aligned} \tag{B-22}$$

Since v_1, v_2, α_1, and α_2 have been given in (B-6) and (B-8) directly in terms of the moments of the pairs X_k and Y_k, our task is completed.

APPENDIX C

ERROR PROBABILITIES FOR ADAPTIVE RECEPTION OF M-PHASE SIGNALS

In this appendix, we derive probabilities of error for two- and four-phase signaling over an L-diversity-branch time-invariant additive guassian noise channel and for M-phase signaling over an L-diversity-branch Rayleigh fading additive gaussian noise channel. Both channels corrupt the signaling waveforms transmitted through them by introducing additive white gaussian noise and an unknown or random multiplicative gain and phase shift in the transmitted signal. The receiver processing consists of cross-correlating the signal plus noise received over each diversity branch by a noisy reference signal, which is derived either from the previously received information-bearing signals or from the transmission and reception of a pilot signal, and adding the outputs from all L-diversity branches to form the decision variable.

C-1 MATHEMATICAL MODEL FOR AN M-PHASE SIGNALING COMMUNICATIONS SYSTEM

In the general case of M-phase signaling, the signaling waveforms at the transmitter are†

$$s_n(t) = \text{Re}\left[s_{l_n}(t)e^{j2\pi f_c t}\right]$$

† The complex representation of real signals is used throughout. Complex conjugation is denoted by an asterisk.

where

$$s_{ln}(t) = g(t) \exp\left[j\frac{2\pi}{M}(n-1)\right], \quad n = 1, 2, \ldots, M, \quad 0 \leq t \leq T \tag{C-1}$$

and T is the time duration of the signaling interval.

Consider the case in which one of these M waveforms is transmitted, for the duration of the signaling interval, over L channels. Assume that each of the channels corrupts the signaling waveform transmitted through it by introducing a multiplicative gain and phase shift, represented by the complex-valued number g_k, and an additive noise $z_k(t)$. Thus, when the transmitted waveform is $s_{ln}(t)$, the waveform received over the kth channel is

$$r_{lk}(t) = g_k s_{ln}(t) + z_k(t), \quad 0 \leq t \leq T, \quad k = 1, 2, \ldots, L \tag{C-2}$$

The noises $\{z_k(t)\}$ are assumed to be sample functions of a stationary white gaussian random process with zero mean and autocorrleation function $\phi_z(\tau) = N_0\delta(\tau)$, where N_0 is the value of the spectral density. These sample functions are assumed to be mutually statistically independent.

At the demodulator, $r_{lk}(t)$ is passed through a filter whose impulse response is matched to the waveform $g(t)$. The output of this filter, sampled at time $t = T$, is denoted as

$$X_k = 2\mathscr{E}g_k \exp\left[j\frac{2\pi}{M}(n-1)\right] + N_k \tag{C-3}$$

where $\mathscr{E}$ is the transmitted signal energy per channel and N_k is the noise sample from the kth filter. In order for the demodulator to decide which of the M phases was transmitted in the signaling interval $0 \leq t \leq T$, it attempts to undo the phase shift introduced by each channel. In practice, this is accomplished by multiplying the matched filter output X_k by the complex conjugate of an estimate $\hat{g}_k$ of the channel gain and phase shift. The result is a weighted and phase-shifted sampled output from the kth-channel filter, which is then added to the weighted and phase-shifted sampled outputs from the other $L - 1$ channel filters.

The estimate $\hat{g}_k$ of the gain and phase shift of the kth channel is assumed to be derived either from the transmission of a pilot signal or by undoing the modulation on the information-bearing signals received in previous signaling intervals. As an example of the former, suppose that a pilot signal, denoted by $s_{pk}(t)$, $0 \leq t \leq T$, is transmitted over the kth channel for the purpose of measuring the channel gain and phase shift. The received waveform is

$$g_k s_{pk}(t) + z_{pk}(t), \quad 0 \leq t \leq T$$

where $z_{pk}(t)$ is a sample function of a stationary white gaussian random process with zero mean and autocorrelation function $\phi_p(\tau) = N_0\delta(\tau)$. This signal plus noise is passed through a filter matched to $s_{pk}(t)$. The filter output is sampled at time $t = T$ to yield the random variable $X_{pk} = 2\mathscr{E}_p g_k + N_{pk}$, where $\mathscr{E}_p$ is the energy in the pilot signal, which is assumed to be identical for all channels, and N_{pk} is the additive noise sample. An estimate of g_k is obtained by properly normalizing X_{pk}, i.e., $\hat{g}_k = g_k + N_{pk}/2\mathscr{E}_p$.

On the other hand, an estimate of g_k can be obtained from the information-bearing signal as follows. If one knew the information component contained in the matched filter output then an estimate of g_k could be obtained by properly normalizing this

output. For example, the information component in the filter output given by (C-3) is $2\mathscr{E}g_k \exp[j(2\pi/M)(n-1)]$, and hence, the estimate is

$$\hat{g}_k = \frac{X_k}{2\mathscr{E}} \exp\left[-j\frac{2\pi}{M}(n-1)\right] = g_k + \frac{N_k'}{2\mathscr{E}}$$

where $N_k' = N_k \exp[-j(2\pi/M)(n-1)]$ and the pdf of N_k' is identical to the pdf of N_k. An estimate that is obtained from the information-bearing signal in this manner is called a *clairvoyant estimate*. Although a physically realizable receiver does not possess such clairvoyance, it can approximate this estimate by employing a time delay of one signaling interval and by feeding back the estimate of the transmitted phase in the *previous signaling interval*.

Whether the estimate of g_k is obtained from a pilot signal or from the information-bearing signal, the estimate can be improved by extending the time interval over which it is formed to include several prior signaling intervals in a way that has been described by Price (1962a, b). As a result of extending the measurement interval, the signal-to-noise ratio in the estimate of g_k is increased. In the general case where the estimation interval is the infinite past, the normalized *pilot signal estimate* is

$$\hat{g}_k = g_k + \sum_{i=1}^{\infty} c_i N_{pki} \Big/ 2\mathscr{E}_p \sum_{i=1}^{\infty} c_i \tag{C-4}$$

where c_i is the weighting coefficient on the subestimate of g_k derived from the ith prior signal interval and N_{pki} is the sample of additive gaussian noise at the output of the filter matched to $s_{pk}(t)$ in the ith prior signaling interval. Similarly, the clairvoyant estimate that is obtained from the information-bearing signal by undoing the modulation over the infinite past is

$$\hat{g}_k = g_k + \sum_{i=1}^{\infty} c_i N_{ki} \Big/ 2\mathscr{E} \sum_{i=1}^{\infty} c_i \tag{C-5}$$

As indicated, the demodulator forms the product between $\hat{g}_k^*$ and X_k and adds this to the products of the other $L-1$ channels. The random variable that results is

$$\begin{aligned} z &= \sum_{k=1}^{L} X_k \hat{g}_k^* = \sum_{k=1}^{L} X_k Y_k^* \\ &= z_r + jz_i \end{aligned} \tag{C-6}$$

where, by definition, $Y_k = \hat{g}_k$, $z_r = \mathrm{Re}(z)$, and $z_i = \mathrm{Im}(z)$. The phase of z is the decision variable. This is simply

$$\theta = \tan^{-1}\left(\frac{z_i}{z_r}\right) = \tan^{-1}\left[\mathrm{Im}\left(\sum_{k=1}^{L} X_k Y_k^*\right) \Big/ \mathrm{Re}\left(\sum_{k=1}^{L} X_k Y_k^*\right)\right] \tag{C-7}$$

C-2 CHARACTERISTIC FUNCTION AND PROBABILITY DENSITY FUNCTION OF THE PHASE θ

The following derivation is based on the assumption that the transmitted signal phase is zero, i.e., $n = 1$. If desired, the pdf of θ conditional on any other transmitted signal phase can be obtained by translating $p(\theta)$ by the angle $2\pi(n-1)/M$. We also assume

that the complex-valued numbers $\{g_k\}$, which characterize the L channels, are mutually statistically independent and identically distributed zero-mean gaussian random variables. This characterization is appropriate for slowly Rayleigh fading channels. As a consequence, the rrandom variables (X_k, Y_k) are correlated, complex-valued, zero-mean, gaussian, and statistically independent, but identically distributed with any other pair (X_i, Y_i).

The method that has been used in evaluating the probability density $p(\theta)$ in the general case of diversity reception is as follows. First, the characteristic function of the joint probability distribution function of z_r and z_i, where z_r and z_i are two components that make up the decision variable θ, is obtained. Second, the double Fourier transform of the characteristic function is performed and yields the density $p(z_r, z_i)$. Then the transformation

$$r = \sqrt{z_r^2 + z_i^2}, \qquad \theta = \tan^{-1}\left(\frac{z_i}{z_r}\right) \tag{C-8}$$

yields the joint pdf of the envelope r and the phase θ. Finally, integration of this joint pdf over the random variable r yields the pdf of θ.

The joint characteristic function of the random variables z_r and z_i can be expressed in the form

$$\psi(jv_1, jv_2) = \left[\frac{4}{m_{xx}m_{yy}(1-|\mu|^2)\left(v_1 - j\dfrac{2|\mu|\cos\varepsilon}{\sqrt{m_{xx}m_{yy}(1-|\mu|^2)}}\right)^2 + \left(v_2 - j\dfrac{2|\mu|\sin\varepsilon}{\sqrt{m_{xx}m_{yy}(1-|\mu|^2)}}\right)^2 + \dfrac{4}{m_{xx}m_{yy}(1-|\mu|^2)^2}} \right]^L \tag{C-9}$$

where, by definition,

$$\begin{aligned} m_{xx} &= E(|X_k|^2) \qquad \text{identical for all } k \\ m_{yy} &= E(|Y_k|^2) \qquad \text{identical for all } k \\ m_{xy} &= E(X_k Y_k^*) \qquad \text{identical for all } k \\ \mu &= \frac{m_{xy}}{\sqrt{m_{xx}m_{yy}}} = |\mu| e^{-j\varepsilon} \end{aligned} \tag{C-10}$$

The result of Fourier-transforming the function $\psi(jv_1, jv_2)$ with respect to the variables v_1 and v_2 is

$$p(z_r, z_i) = \frac{(1-|\mu|^2)^L}{(L-1)!\pi 2^L}(\sqrt{z_r^2 + z_i^2})^{L-1} \times \exp[|\mu|(z_r\cos\varepsilon + z_i\sin\varepsilon)]K_{L-1}(\sqrt{z_r^2 + z_i^2}) \tag{C-11}$$

where $K_n(x)$ is the modified Hankel function of order n. Then the transformation of random variables, as indicated in (C-8) yields the joint pdf of the envelope r and the phase θ in the form

$$p(r, \theta) = \frac{(1-|\mu|^2)^L}{(L-1)!\pi 2^L} r^L \exp[|\mu| r\cos(\theta - \varepsilon)]K_{L-1}(r) \tag{C-12}$$

Now, integration over the variable r yields the marginal pdf of the phase θ. We have evaluated the integral to obtain $p(\theta)$ in the form

$$p(\theta) = \frac{(-1)^{L-1}(1-|\mu|^2)^L}{2\pi(L-1)!}\left\{\frac{\partial^{L-1}}{\partial b^{L-1}}\left[\frac{1}{b-|\mu|^2\cos^2(\theta-\varepsilon)} + \frac{|\mu|\cos(\theta-\varepsilon)}{[b-|\mu|^2\cos^2(\theta-\varepsilon)]^{3/2}}\cos^{-1}\left(-\frac{|\mu|\cos(\theta-\varepsilon)}{b^{1/2}}\right)\right]\right\}\Bigg|_{b=1} \tag{C-13}$$

In this equation, the notation

$$\frac{\partial^L}{\partial b^L} f(b,\mu)\Big|_{b=1}$$

denotes the Lth partial derivative of the function $f(b, \mu)$ evaluated at $b = 1$.

C-3 ERROR PROBABILITIES FOR SLOWLY RAYLEIGH FADING CHANNELS

In this section, the probability of a character error and the probability of a binary digit error are derived for M-phase signaling. The probabilities are evaluated via the probability density function and the probability distribution function of θ.

The Probability Distribution Function of the Phase In order to evaluate the probability of error, we need to evaluate the definite integral

$$P(\theta_1 \le \theta \le \theta_2) = \int_{\theta_1}^{\theta_2} p(\theta)\, d\theta$$

where θ_1 and θ_2 are limits of integration and $p(\theta)$ is given by (C-13). All subsequent calculations are made for a real cross-correlation coefficient μ. A real-valued μ implies that the signals have symmetric spectra. This is the usual situation encountered. Since a complex-valued μ causes a shift of ε in the pdf of θ, i.e., ε is simply a bias term, the results that are given for real μ can be altered in a trivial way to cover the more general case of complex-valued μ.

In the integration of $p(\theta)$, only the range $0 \le \theta \le \pi$ is considered, because $p(\theta)$ is an even function. Furthermore, the continuity of the integrand and its derivatives and the fact that the limits θ_1 and θ_2 are independent of b allow for the interchange of integration and differentiation. When this is done, the resulting integral can be evaluated quite readily and can be expressed as follows:

$$\int_{\theta_1}^{\theta_2} p(\theta)\, d\theta = \frac{(-1)^{L-1}(1-\mu^2)^L}{2\pi(L-1)!} \times \frac{\partial^{L-1}}{\partial b^{L-1}}\left\{\frac{1}{b-\mu^2}\left[\frac{\mu\sqrt{1-(b/\mu^2-1)x^2}}{b^{1/2}}\cot^{-1}x - \cot^{-1}\left(\frac{xb^{1/2}\mu}{\sqrt{1-(b/\mu^2-1)x^2}}\right)\right]\right\}_{x_1}^{x_2}\Bigg|_{b=1} \tag{C-14}$$

where, by definition,

$$x_i = \frac{-\mu\cos\theta_i}{\sqrt{b-\mu^2\cos\theta_i}}, \quad i = 1, 2 \tag{C-15}$$

Probability of a Symbol Error The probability of a symbol error for any M-phase signaling system is

$$P_M = 2\int_{\pi/M}^{\pi} p(\theta)\, d\theta$$

When (C-14) is evaluated at these two limits, the result is

$$P_M = \frac{(-1)^{L-1}(1-\mu^2)^L}{\pi(L-1)!}\frac{\partial^{L-1}}{\partial b^{L-1}}\left\{\frac{1}{b-\mu^2}\left[\frac{\pi}{M}(M-1) - \frac{\mu\sin(\pi/M)}{\sqrt{b-\mu^2\cos^2(\pi/M)}}\cot^{-1}\left(\frac{-\mu\cos(\pi/M)}{\sqrt{b-\mu^2\cos^2(\pi/M)}}\right)\right]\right\}\Bigg|_{b=1} \tag{C-16}$$

Probability of a Binary Digit Error First, let us consider two-phase signaling. In this case, the probability of a binary digit error is obtained by integrating the pdf $p(\theta)$ over the range $\frac{1}{2}\pi < \theta < 3\pi$. Since $p(\theta)$ is an even function and the signals are a priori equally likely, this probability can be written as

$$P_2 = 2\int_{\pi/2}^{\pi} p(\theta)\, d\theta$$

It is easily verified that $\theta_1 = \frac{1}{2}\pi$ implies $x_1 = 0$ and $\theta_2 = \pi$ implies $x_2 = \mu/\sqrt{b-\mu^2}$. Thus,

$$P_2 = \frac{(-1)^{L-1}(1-\mu^2)^L}{2(L-1)!}\frac{\partial^{L-1}}{\partial b^{L-1}}\left[\frac{1}{b-\mu^2} - \frac{\mu}{b^{1/2}(b-\mu^2)}\right]\Bigg|_{b=1} \tag{C-17}$$

After performing the differentiation indicated in (C-17) and evaluating the resulting function at $b = 1$, the probability of a binary digit error is obtained in the form

$$P_2 = \frac{1}{2}\left[1 - \mu\sum_{k=0}^{L-1}\binom{2k}{k}\left(\frac{1-\mu^2}{4}\right)^k\right] \tag{C-18}$$

Next, we consider the case of four-phase signaling in which a Gray code is used to map pairs of bits into phases. Assuming again that the transmitted signal is $s_{i1}(t)$, it is clear that a single error is committed when the received phase is $\frac{1}{4}\pi < \theta < \frac{3}{4}\pi$, and a double error is committed when the received phase is $\frac{3}{4}\pi < \theta < \pi$. That is, the probability of a binary digit error is

$$P_{4b} = \int_{\pi/4}^{3\pi/4} p(\theta)\, d\theta + 2\int_{3\pi/4}^{\pi} p(\theta)\, d\theta \tag{C-19}$$

It is easily established from (C-14) and (C-19) that

$$P_{4b} = \frac{(-1)^{L-1}(1-\mu^2)^L}{2(L-1)!}\frac{\partial^{L-1}}{\partial b^{L-1}}\left[\frac{1}{b-\mu^2} - \frac{\mu}{(b-\mu^2)(2b-\mu^2)^{1/2}}\right]\Bigg|_{b=1}$$

Hence, the probability of a binary digit error for four-phase signaling is

$$P_{4b} = \frac{1}{2}\left[1 - \frac{\mu}{\sqrt{2-\mu^2}}\sum_{k=0}^{L-1}\binom{2k}{k}\left(\frac{1+\mu^2}{4-2\mu^2}\right)^k\right] \tag{C-20}$$

Note that if one defines the quantity $\rho = \mu/\sqrt{2-\mu^2}$, the expression for P_{4b} in terms of ρ is

$$P_{4b} = \frac{1}{2}\left[1 - \rho\sum_{k=0}^{L-1}\binom{2k}{k}\left(\frac{1-\rho^2}{4}\right)^k\right] \tag{C-21}$$

In other words, P_{4b} has the same form as P_2 given in (C-18). Furthermore, note that ρ, just like μ, can be interpreted as a cross-correlation coefficient, since the range of ρ is $0 \leq \rho \leq 1$ for $0 \leq \mu \leq 1$. This simple fact will be used in Section C-4.

The above procedure for obtaining the bit error probability for an M-phase signal with a Gray code can be used to generate results for $M = 8$, 16, etc., as shown by Proakis (1968).

Evaluation of the Cross-Correlation Coefficient The expressions for the probabilities of error given above depend on a single parameter, namely, the cross-correlation coefficient μ. The clairvoyant estimate is given by (C-5), and the matched filter output, when signal waveform $s_{i1}(t)$ is transmitted, is $X_k = 2\mathcal{E}g_k + N_k$. Hence, the cross-correlation coefficient is

$$\mu = \frac{\sqrt{\nu}}{\sqrt{(\bar{\gamma}_c^{-1} + 1)(\bar{\gamma}_c^{-1} + \nu)}} \tag{C-22}$$

where, by definition,

$$\begin{aligned} \nu &= \left|\sum_{i=1}^{\infty} c_i\right|^2 \Big/ \sum_{i=1}^{\infty} |c_i|^2 \\ \bar{\gamma}_c &= \frac{\mathcal{E}}{N_0} E(|g_k|^2), \quad k = 1, 2, \ldots, L \end{aligned} \tag{C-23}$$

The parameter ν represents the effective number of signaling intervals over which the estimate is formed, and $\bar{\gamma}_c$ is the average SNR per channel.

In the case of differential phase signaling, the weighting coefficients are $c_1 = 1$, $c_i = 0$ for $i \neq 1$. Hence, $\nu = 1$ and $\mu = \bar{\gamma}_c/(1 + \bar{\gamma}_c)$.

When $\nu = \infty$, the estimate is perfect and

$$\lim_{\nu \to \infty} \mu = \sqrt{\frac{\bar{\gamma}_c}{\bar{\gamma}_c + 1}}$$

Finally, in the case of a pilot signal estimate, given by (C-4) the cross-correlation coefficient is

$$\mu = \left[\left(1 + \frac{r+1}{r\bar{\gamma}_t}\right)\left(1 + \frac{r+1}{\nu\bar{\gamma}_t}\right)\right]^{-1/2} \tag{C-24}$$

where, by definition,

$$\begin{aligned} \bar{\gamma}_t &= \frac{\mathcal{E}_t}{N_0} E(|g_k|^2) \\ \mathcal{E}_t &= \mathcal{E} + \mathcal{E}_p \\ r &= \mathcal{E}/\mathcal{E}_p \end{aligned}$$

The values of μ given above are summarized in Table C-1.

C-4 ERROR PROBABILITIES FOR TIME-INVARIANT AND RICEAN FADING CHANNELS

In Section C-2, the complex-valued channel gains $\{g_k\}$ were characterized as zero-mean gaussian random variables, which is appropriate for Rayleigh fading channels. In this section, the channel gains $\{g_k\}$ are assumed to be nonzero-mean gaussian random variables. Estimates of the channel gains are formed by the demodulator and are used

TABLE C-1 RAYLEIGH FADING CHANNEL

Type of estimate	Cross-correlation coefficient μ
Clairvoyant estimate	$\dfrac{\sqrt{\nu}}{\sqrt{(\bar{\gamma}_c^{-1}+1)(\bar{\gamma}_c^{-1}+\nu)}}$
Pilot signal estimate	$\dfrac{\sqrt{r\nu}}{(r+1)\sqrt{\left(\dfrac{1}{\bar{\gamma}_c}+\dfrac{r}{r+1}\right)\left(\dfrac{1}{\bar{\gamma}_c}+\dfrac{\nu}{r+1}\right)}}$
Differential phase signaling	$\dfrac{\bar{\gamma}_c}{\bar{\gamma}_c+1}$
Perfect estimate	$\sqrt{\dfrac{\bar{\gamma}_c}{\bar{\gamma}_c+1}}$

as described in Section C-1. Moreover, the decision variable θ is defined again by (C-7). However, in this case, the gaussian random variables X_k and Y_k, which denote the matched filter output and the estimate, respectively, for the kth channel, have nonzero means, which are denoted by $\bar{X}_k$ and $\bar{Y}_k$. Furthermore, the second moments are

$$m_{xx} = E(|X_k - \bar{X}_k|^2) \qquad \text{identical for all channels}$$
$$m_{yy} = E(|Y_k - \bar{Y}_k|^2) \qquad \text{identical for all channels}$$
$$m_{xy} = E[(X_k - \bar{X}_k)(Y_k^* - \bar{Y}_k^*)] \qquad \text{identical for all channels}$$

and the normalized covariance is defined as

$$\mu = \frac{m_{xy}}{\sqrt{m_{xx}m_{yy}}}$$

Error probabilities are given below only for two- and four-phase signaling with this channel model. We are interested in the special case in which the fluctuating component of each of the channel gains $\{g_k\}$ is zero, so that the channels are time-invariant. If, in addition to this time invariance, the noises between the estimate and the matched filter output are uncorrelated then $\mu = 0$.

In the general case, the probability of error for two-phase signaling over L statistically independent channels characterized in the manner described above can be obtained from the results in Appendix B. In its most general form, the expresssion for the binary error rate is

$$\begin{aligned} P_2 &= Q_1(a,b) - I_0(a)\exp\left[-\tfrac{1}{2}(a^2+b^2)\right] \\ &\quad + \frac{I_0(ab)\exp\left[-\frac{1}{2}(a^2+b^2)\right]}{[2/(1-\mu)]^{2L-1}}\sum_{k=0}^{L-1}\binom{2L-1}{k}\left(\frac{1+\mu}{1-\mu}\right)^k \\ &\quad + \frac{\exp\left[-\frac{1}{2}(a^2+b^2)\right]}{[2/(1-\mu)]^{2L-1}} \\ &\quad \times \sum_{k=1}^{L-1} I_n(ab)\sum_{k=0}^{L-1-n}\binom{2L-1}{k}\left[\left(\frac{b}{a}\right)^n\left(\frac{1+\mu}{1-\mu}\right)^k - \left(\frac{a}{b}\right)^n\left(\frac{1+\mu}{1-\mu}\right)^{2L-1-k}\right] \quad (L \geq 2) \end{aligned} \tag{C-25}$$

$$P_2 = Q_1(a,b) - \tfrac{1}{2}(1+\mu)I_0(ab)\exp\left[-\tfrac{1}{2}(a^2+b^2)\right] \quad (L=1)$$

where, by definition,

$$a = \left(\tfrac{1}{2} \sum_{k=1}^{L} \left| \frac{\bar{X}_k}{\sqrt{m_{xx}}} - \frac{\bar{Y}_k}{\sqrt{m_{yy}}} \right|^2 \right)^{1/2}$$

$$b = \left(\tfrac{1}{2} \sum_{k=1}^{L} \left| \frac{\bar{X}_k}{\sqrt{m_{xx}}} + \frac{\bar{Y}_k}{\sqrt{m_{yy}}} \right|^2 \right)^{1/2} \tag{C-26}$$

$$Q_1(a, b) = \int_b^\infty x \exp\left[-\tfrac{1}{2}(a^2 + x^2)\right] I_0(ax)\, dx$$

$I_n(x)$ is the modified Bessel function of the first kind and of order n.

Let us evaluate the constants a and b when the channel is time-invariant, $\mu = 0$, and the channel gain and phase estimates are those given in Section C-1. Recall that when signal $s_1(t)$ is transmitted, the matched filter output is $X_k = 2\mathscr{E}g_k + N_k$. The clairvoyant estimate is given by (C-5). Hence, for this estimate, the moments are $\bar{X}_k = 2\mathscr{E}g_k$, $\bar{Y}_k = g_k$, $m_{xx} = 4\mathscr{E}N_0$, and $m_{yy} = N_0/\mathscr{E}v$, where $\mathscr{E}$ is the signal energy, N_0 is the value of the noise spectral density, and v is defined in (C-23). Substitution of these moments into (C-26) results in the following expressions for a and b:

$$a = \sqrt{\tfrac{1}{2}\gamma_b}\,|\sqrt{v} - 1|$$

$$b = \sqrt{\tfrac{1}{2}\gamma_b}\,|\sqrt{v} + 1| \tag{C-27}$$

$$\gamma_b = \frac{\mathscr{E}}{N_0} \sum_{k=1}^{L} |g_k|^2$$

This is a result originally derived by Price (1962).

The probability of error for differential phase signaling can be obtained by setting $v = 1$ in (C-27).

Next, consider a pilot signal estimate. In this case, the estimate is given by (C-4) and the matched filter output is again $X_k = 2\mathscr{E}g_k + N_k$. When the moments are calculated and these are substituted into (C-26), the following expressions for a and b are obtained:

$$a = \sqrt{\frac{\gamma_t}{2}} \left| \sqrt{\frac{v}{r+1}} - \sqrt{\frac{r}{r+1}} \right|$$

$$b = \sqrt{\frac{\gamma_t}{2}} \left(\sqrt{\frac{v}{r+1}} + \sqrt{\frac{r}{r+1}} \right) \tag{C-28}$$

where

$$\gamma_t = \frac{\mathscr{E}_t}{N_0} \sum_{k=1}^{L} |g_k|^2$$

$$\mathscr{E}_t = \mathscr{E} + \mathscr{E}_p$$

$$r = \mathscr{E}/\mathscr{E}_p$$

Finally, we consider the probability of a binary digit error for four-phase signaling over a time-invariant channel for which the condition $\mu = 0$ obtains. One approach that can be used to derive this error probability is to determine the pdf of θ and then to integrate this over the appropriate range of values of θ. Unfortunately, this approach proves to be intractable mathematically. Instead, a simpler, albeit roundabout, method may be used that involves the Laplace transform. In short, the integral in (14-4-14) of the text that relates the error probability $P_2(\gamma_b)$ in an AWGN channel to the error

TABLE C-2 TIME-INVARIANT CHANNEL

Type of estimate	a	b
	Two-phase signaling	
Clairvoyant estimate	$\sqrt{\frac{1}{2}\gamma_b}\lvert\sqrt{\nu}-1\rvert$	$\sqrt{\frac{1}{2}\gamma_b}(\sqrt{\nu}+1)$
Differential phase signaling	0	$\sqrt{2\gamma_b}$
Pilot signal estimate	$\sqrt{\frac{\gamma_t}{2}}\left\lvert\sqrt{\frac{\nu}{r+1}}-\sqrt{\frac{r}{r+1}}\right\rvert$	$\sqrt{\frac{\gamma_t}{2}}\left(\sqrt{\frac{\nu}{r+1}}+\sqrt{\frac{r}{r+1}}\right)$
	Four-phase signaling	
Clairvoyant estimate	$\sqrt{\frac{1}{2}\gamma_b}\lvert\sqrt{\nu+1+\sqrt{\nu^2+1}}$ $-\sqrt{\nu+1-\sqrt{\nu^2+1}}\rvert$	$\sqrt{\frac{1}{2}\gamma_b}\left(\sqrt{\nu+1-\sqrt{\nu^2+1}}\right.$ $\left.+\sqrt{\nu+1-\sqrt{\nu^2+1}}\right)$
Differential phase signaling	$\sqrt{\frac{1}{2}\gamma_b}\left(\sqrt{2+\sqrt{2}}-\sqrt{2-\sqrt{2}}\right)$	$\sqrt{\frac{1}{2}\gamma_b}\left(\sqrt{2+\sqrt{2}}+\sqrt{2-\sqrt{2}}\right)$
Pilot signal estimate	$\sqrt{\frac{\gamma_t}{4(r+1)}}\lvert\sqrt{\nu+r+\sqrt{\nu^2+r^2}}$ $-\sqrt{\nu+r-\sqrt{\nu^2+r^2}}\rvert$	$\sqrt{\frac{\gamma_t}{4(r+1)}}\left(\sqrt{\nu+r+\sqrt{\nu^2+r^2}}\right.$ $\left.+\sqrt{\nu+r-\sqrt{\nu^2+r^2}}\right)$

probability P_2 in a Rayleigh fading channel is a Laplace transform. Since the bit error probabilities P_2 and P_{4b} for a Rayleigh fading channel, given by (C-18) and (C-21), respectively, have the same form but differ only in the correlation coefficient, it follows that the bit error probabilities for the time-invariant channel also have the same form. That is, (C-25) with $\mu = 0$ is also the expression for the bit error probability of a four-phase signaling system with the parameters a and b modified to reflect the difference in the correlation coefficient. The detailed derivation may be found in the paper by Proakis (1968). The expressions for a and b are given in Table C-2.

APPENDIX **D**

SQUARE-ROOT FACTORIZATION

Consider the solution of the set of linear equations

$$\mathbf{R}_N\mathbf{C}_N = \mathbf{U}_N \tag{D-1}$$

where $\mathbf{R}_N$ is an $N \times N$ positive-definite symmetric matrix, $\mathbf{C}_N$ is an N-dimensional vector of coefficients to be determined, and $\mathbf{U}_N$ is an arbitrary N-dimensional vector. The equations in (D-1) can be solved efficiently by expressing $\mathbf{R}_N$ in the factored form

$$\mathbf{R}_N = \mathbf{S}_N\mathbf{D}_N\mathbf{S}_N' \tag{D-2}$$

where $\mathbf{S}_N$ is a lower triangular matrix with elements $\{s_{ik}\}$ and $\mathbf{D}_N$ is a diagonal matrix with diagonal elements $\{d_k\}$. The diagonal elements of $\mathbf{S}_N$ are set to unity, i.e., $s_{ii} = 1$. Then we have

$$\begin{aligned} r_{ij} &= \sum_{k=1}^{j} s_{ik}d_k s_{jk}, \qquad 1 \leq j \leq i-1, \quad i \geq 2 \\ r_{11} &= d_1 \end{aligned} \tag{D-3}$$

where $\{r_{ij}\}$ arte the elements of $\mathbf{R}_N$. Consequently, the elements $\{s_{ik}\}$ and $\{d_k\}$ are determined from (D-3) according to the equations

$$\begin{aligned} d_1 &= r_{11} \\ s_{ij}d_j &= r_{ij} - \sum_{k=1}^{j-1} s_{ik}d_k s_{jk}, \qquad 1 \leq j \leq i-1, \quad 2 \leq i \leq N \\ d_i &= r_{ii} - \sum_{k=1}^{i-1} s_{ik}^2 d_k, \qquad 2 \leq i \leq N \end{aligned} \tag{D-4}$$

Thus, (D-4) define $\mathbf{S}_N$ and $\mathbf{D}_N$ in terms of the elements of $\mathbf{R}_N$.

The solution to (D-1) is performed in two steps. With (D-2) substituted into (D-1) we have

$$\mathbf{S}_N\mathbf{D}_N\mathbf{S}_N'\mathbf{C}_N = \mathbf{U}_N$$

Let

$$\mathbf{Y}_N = \mathbf{D}_N\mathbf{S}_N'\mathbf{C}_N \tag{D-5}$$

Then

$$\mathbf{S}_N\mathbf{Y}_N = \mathbf{U}_N \tag{D-6}$$

First we solve (D-6) for $\mathbf{Y}_N$. Because of the triangular form of $\mathbf{S}_N$, we have

$$\begin{aligned} y_1 &= u_1 \\ y_i &= u_i - \sum_{j=1}^{i-1} s_{ij}y_j, \qquad 2 \le i \le N \end{aligned} \tag{D-7}$$

Having obtained $\mathbf{Y}_N$, the second step is to compute $\mathbf{C}_N$. That is,

$$\begin{aligned} \mathbf{D}_N\mathbf{S}_N'\mathbf{C}_N &= \mathbf{Y}_N \\ \mathbf{S}_N'\mathbf{C}_N &= \mathbf{D}_N^{-1}\mathbf{Y}_N \end{aligned}$$

Beginning with

$$c_N = y_N/d_N \tag{D-8}$$

the remaining coefficients of $\mathbf{C}_N$ are obtained recursively as follows:

$$c_i = \frac{y_i}{d_i} - \sum_{j=i+1}^{N} s_{ij}c_j, \qquad 1 \le i \le N-1 \tag{D-9}$$

The number of multiplications and divisions required to perform the factorization of $\mathbf{R}_N$ is proportional to N^3. The number of multiplications and divisions required to compute $\mathbf{C}_N$, once $\mathbf{S}_N$ is determined, is proportional to N^2. In contrast, when $\mathbf{R}_N$ is Toeplitz the Levinson–Durbin algorithm should be used to determine the solution of (D-1), since the number of multiplications and divisions is proportional to N^2. On the other hand, in a recursive least-squares formulation, $\mathbf{S}_N$ and $\mathbf{D}_N$ are not computed as in (D-3), but they are updated recursively. The update is accomplished with N^2 operations (multiplications and divisions). Then the solution for the vector $\mathbf{C}_N$ follows the steps (D-5)–(D-9). Consequently, the computational burden of the recursive least-squares formulation is proportional to N^2.

REFERENCES AND BIBLIOGRAPHY

Abend, K. and Fritchman, B. D. (1970). "Statistical Detection for Communication Channels with Intersymbol Interference," *Proc. IEEE*, pp. 779–785, May.

Abramson, N. (1963). *Information Theory and Coding*, McGraw-Hill, New York.

Abramson, N. (1970). "The ALOHA System—Another Alternative for Computer Communications," *1970 Fall Joint Comput. Conf., AFIDS Conf. Proc.*, vol. 37, pp. 281–285, AFIPS Press, Montvale, N.J.

Abramson, N. (1977). "The Throughput of Packet Broadcasting Channels," *IEEE Trans. Commun.*, vol. COM-25, pp. 117–128, January.

Abramson, N. (1993). *Multiple Access Communications*, IEEE Press, New York.

Adler, R. L., Coppersmith, D., and Hassner, M. (1983). "Algorithms for Sliding Block Codes," *IEEE Trans. Inform. Theory*, vol. IT-29, pp. 5–22, January.

Al-Hussaini, E. and Al-Bassiouni (1985). "Performance of MRC Diversity Systems for the Detection of Signals with Nakagami Fading," *IEEE Trans. Commun.*, vol. COM-33, pp. 1315–1319, December.

Altekar, S. A. and Beaulieu, N. C. (1993). "Upper Bounds on the Error Probability of Decision Feedback Equalization," *IEEE Trans. Inform. Theory*, vol. IT-39, pp. 145–156, January.

Anderberg, M. R. (1973). *Cluster Analysis for Applications*, Academic, New York.

Anderson, J. B., Aulin, T., and Sundberg, C. W. (1986). *Digital Phase Modulation*, Plenum, New York.

Anderson, R. R. and Salz, J. (1965). "Spectra of Digital FM," *Bell Syst. Tech. J.*, vol. 44 pp. 1165–1189, July–August.

Ash, R. B. (1965). *Information Theory*, Interscience, New York.

Aulin, T. (1980). "Viterbi Detection of Continuous Phase Modulated Signals," *Nat. Telecommun. Conf. Record*, pp. 14.2.1–14.2.7, Houston, Texas, November.

Aulin, T., Rydbeck, N., and Sundberg, C. W. (1981). "Continuous Phase Modulation—Part II: Partial Response Signaling," *IEEE Trans. Commun.*, vol. COM-29, pp. 210–225, March.

Aulin, T. and Sundberg, C. W. (1981). "Continuous Phase Modulation—Part I: Full Response Signaling," *IEEE Trans. Commun.*, vol. COM-29, pp. 196–209, March.

Aulin, T. and Sundberg, C. W. (1982a). "On the Minimum Euclidean Distance for a Class of Signal Space Codes," *IEEE Trans. Inform. Theory*, vol. IT-28, pp. 43–55, January.

Aulin, T. and Sundberg, C. W. (1982b). "Minimum Euclidean Distance and Power Spectrum for a Class of Smoothed Phase Modulation Codes with Constant Envelope," *IEEE Trans. Commun.*, vol. COM-30, pp. 1721–1729, July.

Aulin, T. and Sundberg, C. W. (1984). "CPM—An Efficient Constant Amplitude Modulation Scheme," *Int. J. Satellite Commun.*, vol. 2, pp. 161–186.

Austin, M. E. (1967). "Decision-Feedback Equalization for Digital Communication Over Dispersive Channels," *MIT Lincoln Laboratory, Lexington, Mass., Tech. Report No. 437*, August

Barrow, B. (1963). "Diversity Combining of Fading Signals with Unequal Mean Strengths," *IEEE Trans. Commun., Syst.*, vol. CS-11, pp. 73–78, March.

Beaulieu, N. C. (1990). "An Infinite Series for the Computation of the Complementary Probability Distribution Function of a Sum of Independent Random Variables and Its Application to the Sum of Rayleigh Random Variables," *IEEE Trans. Commun.*, vol. COM-38, pp. 1463–1474, September.

Beaulieu, N. C. and Abu-Dayya, A. A. (1991). "Analysis of Equal Gain Diversity on Nakagami Fading Channels," *IEEE Trans. Commun.*, vol. COM-39, pp. 225–234, February.

Bekir, N. E., Scholtz, R. A., and Welch, L. R. (1978). "Partial-Period Correlation Properties of PN Sequences," *1978 Nat. Telecommun. Conf. Record*, pp. 35.1.1–25.1.4, Birmingham, Alabama, November.

Belfiore, C. A. and Park, J. H., Jr. (1979). "Decision-Feedback Equalization," *Proc. IEEE*, vol. 67, pp. 1143–1156, August.

Bellini, J. (1986). "Bussgang Techniques for Blind Equalization," *Proc. GLOBECOM'86*, pp. 46.1.1–46.1.7, Houston, Texas, December.

Bello, P. A. and Nelin, B. D. (1962a). "Predetection Diversity Combining with Selectivity Fading Channels," *IRE Trans. Commun. Syst.*, vol. CS-10, pp. 32–42, March.

Bello, P. A. and Nelin, B. D. (1962b). "The Influence of Fading Spectrum on the Binary Error Probabilities of Incoherent and Differentially Coherent Matched Filter Receivers," *IRE Trans. Commun. Syst.*, vol. CS-10, pp. 160–168, June.

Bello, P. A. and Nelin, B. D. (1963). "The Effect of Frequency Selective Fading on the Binary Error Probabilities of Incoherent and Differentially Coherent Matched Filter Receivers," *IEEE Trans. Commun. Syst.*, vol. CS-11, pp. 170–186, June.

Bennett, W. R. and Davey, J. R. (1965). *Data Transmission*, McGraw-Hill, New York.

Bennett, W. R. and Rice, S. O. (1963). "Spectral Density and Autocorrelation Functions Associated with Binary Frequency-Shift Keying," *Bell Syst. Tech. J.*, vol. 42, pp. 2355–2385, September.

Benveniste, A. and Goursat, M. (1984). "Blind Equalizers," *IEEE Trans. Commun.*, vol. COM-32, pp. 871–883, August.

Berger, T. (1971). *Rate Distortion Theory*, Prentice-Hall, Englewood Cliffs, N.J.

Berger, T. and Tufts, D. W. (1967). "Optimum Pulse Amplitude Modulation, Part I: Transmitter-Receiver Design and Bounds from Information Theory," *IEEE Trans. Inform. Theory*, vol. IT-13, pp. 196–208.

Bergmans, P. P. and Cover, T. M. (1974). "Cooperative Broadcasting," *IEEE Trans. Inform. Theory*, vol. IT-20, pp. 317–324, May.

Berlekamp, E. R. (1968). *Algebraic Coding Theory*, McGraw-Hill, New York.

Berlekamp, E. R. (1973). "Goppa Codes," *IEEE Trans. Inform. Theory*, vol. IT-19, pp. 590–592.

Berlekamp, E. R. (1974). *Key Papers in the Development of Coding Theory*, IEEE Press, New York.

Bierman, G. J. (1977). *Factorization Methods for Discrete Sequential Estimation*, Academic, New York.

Biglieri, E., Divsalar, D., McLane, P. J., and Simon, M. K. (1991). *Introduction to Trellis-Coded Modulation with Applications*, Macmillan, New York.

Bingham, J. A. C. (1990). "Multicarrier Modulation for Data Transmission: An Idea Whose Time Has Come," *IEEE Commun. Mag.*, vol. 28, pp. 5–14, May.

Blahut, R. E. (1983). *Theory and Practice of Error Control Codes*, Addison-Wesley, Reading, Mass.

Blahut, R. E. (1987). *Principles and Practice of Information Theory*, Addison-Wesley, Reading, Mass.

Bose, R. C. and Ray-Chaudhuri, D. K. (1960a). "On a Class of Error Correcting Binary Group Codes," *Inform. Control*, vol. 3, pp. 68–79, March.

Bose, R. C. and Ray-Chaudhuri, D. K. (1960b). "Further Results in Error Correcting Binary Group Codes," *Inform. Control*, vol. 3, pp. 279–290, September.

Brennan, D. G. (1959). "Linear Diversity Combining Techniques," *Proc. IRE.*, vol. 47, pp. 1075–1102.

Busgang, J. J. (1952). "Crosscorrelation Functions of Amplitude-Distored Gaussian Signals," MIT RLE Tech. Report 216.

Bucher, E. A. (1980). "Coding Options for Efficient Communications on Non-Stationary Channels," *Rec. IEEE Int. Conf. Commun.*, pp. 4.1.1–4.1.7.

Burton, H. O. (1969). "A Class of Asymptotically Optimal Burst Correcting Block Codes," *Proc. ICCC*, Boulder, Col., June.

Buzo, A., Gray, A. H., Jr., Gray, R. M., and Markel, J. D. (1980). "Speech Coding Based Upon Vector Quantization," *IEEE Trans. Acoust., Speech, Signal Processing*, Vol. ASSP-28 pp. 562–574, October.

Cahn, C. R. (1960). "Combined Digital Phase and Amplitude Modulation Communication Systems," *IRE Trans. Commun. Syst.*, vol. CS-8, pp. 150–155, September.

Calderbank, A. R. and Sloane, N. J. A. (1987). "New Trellis Codes Based on Lattices and Cosets," *IEEE Trans. Inform. Theory*, vol. IT-33, pp. 177–195, March.

Campanella, S. J. and Robinson, G. S. (1971). "A Comparison of Orthogonal Transformations for Digital Speech Processing," *IEEE Trans. Commun.*, vol. COM-19, pp. 1045–1049, December.

Campopiano, C. N. and Glazer, B. G. (1962). "A Coherent Digital Amplitude and Phase Modulation Scheme," *IRE Trans. Commun. Syst.*, vol. CS-10, pp. 90–95, June.

Capetanakis, J. I. (1979). "Tree Algorithms for Packet Broadcast Channels," *IEEE Trans. Inform. Theory*, vol. IT-25, pp. 505–515, September.

Caraiscos, C. and Liu, B. (1984). "A Roundoff Error Analysis of the LMS Adaptive Algorithm," *IEEE Trans. Acoust., Speech, Signal Processing*, Vol. ASSP-32, pp. 34–41, January.

Carayannis, G., Manolakis, D. G., and Kalouptsidis, N. (1983). "A Fast Sequential Algorithm for Least-Squares Filtering and Prediction," *IEEE Trans. Acoust., Speech, Signal Processing*, Vol. ASSP-31, pp. 1394–1402, December.

Carayannis, G. Manolakis, D. G., and Kalouptsidis, N. (1986). "A Unified View of Parametric Processing Algorithms for Prewindowed Signals," *Signal Processing*, vol. 10, pp. 335–368, June.

Carleial, A. B. and Hellman, M. E. (1975). "Bistable Behavior of ALOHA-Type Systems," *IEEE Trans. Commun.*, vol. COM-23, pp. 401–410, April 1975.

Carlson, A. B. (1975). *Communication Systems*, McGraw-Hill, New York.

Chang, D. Y., Gersho, A., Ramamurthi, B., and Shohan, Y. (1984). "Fast Search Algorithms for Vector Quantization and Pattern Matching," *Proc. IEEE Int. Conf. Acoust., Speech, Signal Processing*, paper 9.11, San Diego, Calif., March.

Chang, R. W. (1966). "Synthesis of Band-Limited Orthogonal Signals for Multichannel Data Transmission," *Bell Syst. Tech. J.*, vol. 45, pp. 1775–1796, December.

Charash, U. (1979). "Reception Through Nakagami Fading Multipath Channels with Random Delays," *IEEE Trans. Commun.*, vol. COM-27, pp. 657–670, April.

Chase, D. (1972). "A Class of Algorithms for Decoding Block Codes With Channel Measurement Information," *IEEE Trans. Inform. Theory*, vol. IT-18, pp. 170–182, January.

Chase, D. (1976). "Digital Signal Design Concepts for a Time-Varying Ricean Channel," *IEEE Trans. Commun.*, vol. COM-24, pp. 164–172, February.

Chien, R. T. (1964). "Cyclic Decoding Procedures for BCH Codes," *IEEE Trans. Inform. Theory*, vol. IT-10, pp. 357–363, October.

Chow, J. S., Tu, J. C., and Cioffi, J. M. (1991). "A Discrete Multitone Transceiver System for HDSL Applications," *IEEE J. Selected Areas Commun.*, vol. SAC-9, pp. 895–908, August.

Chyi, G. T., Proakis, J. G., and Keller, C. M. (1988). "Diversity Selection/Combining Schemes with Excess Noise-Only Diversity Receptions Over a Rayleigh-Fading Multipath Channel." *Proc. Conf. Inform. Sci. Syst.*, Princeton University, Princeton, N.J. March.

Cioffi, J. M. and Kailath, T. (1984). "Fast Recursive-Least Squares Transversal Filters for Adaptive Filtering," *IEEE Trans. Acoust., Speech, Signal Processing*, vol. ASSP-32, pp. 304–337, April.

Cook, C. E., Ellersick, F. W., Milstein, L. B., and Schilling, D. L. (1983). *Spread Spectrum Communcations*, IEEE Press, New York.

Costas, J. P. (1956). "Synchronous Communications," *Proc. IRE*, vol. 44, pp. 1713–1718, December.

Cover, T. M. (1972). "Broadcast Channels," *IEEE Trans. Inform. Theory*, vol. IT-18, pp. 2–14, January.

Cramér, H. (1946). *Mathematical Methods of Statistics*, Princeton University Press, Princeton, N.J.

Daut, D. G., Modestino, J. W., and Wismer, L. D. (1982). "New Short Constraint Length Convolutional Code Construction for Selected Rational Rates," *IEEE Trans. Inform. Theory*, vol. IT-28, pp. 793–799, September.

Davenport, W. B., Jr. (1970). *Probability and Random Processes*, McGraw-Hill, New York.

Davenport, W. B. Jr. and Root, W. L. (1958). *Random Signals and Noise*, McGraw-Hill, New York.

Davisson, L. D. (1973). "Universal Noiseless Coding," *IEEE Trans. Inform. Theory*, vol. IT-19, pp. 783–795.

Davisson, L. D., McEliece, R. J., Pursley, M. B., and Wallace, M. S. (1981). "Efficient Universal Noiselss Source Codes," *IEEE Trans. Inform. Theory*, vol. IT-27, pp. 269–279.

deBuda, R. (1972). "Coherent Demodulation of Frequency Shift Keying with Low Deviation Ratio," *IEEE Trans. Commun.*, vol. COM-20, pp. 429–435, June.

Deller, J. P., Proakis, J. G., and Hansen, H. L. (1993). *Discrete-Time Processing of Speech Signals*, MacMillan, New York.

Ding, Z. (1990). *Application Aspects of Blind Adaptive Equalizers in QAM Data Communications*, Ph.D. Thesis, Department of Electrical Engineering, Cornell University.

Ding, Z., Kennedy, R. A., Anderson, B. D. O., and Johnson, C. R. (1989). "Existence and Avoidance of Ill-Convergence of Godard Blind Equalizers in Data Communication Systems," *Proc. 23rd Conf. on Inform. Sci. Systems*, Baltimore, Md.

Divsalar, D., Simon, M. K., and Yuen, J. H. (1987). "Trellis Coding with Asymmetric Modulation," *IEEE Trans. Commun.*, vol. COM-35, pp. 130–141, February.

Divsalar, D. and Yuen, J. H. (1984). "Asymmetric MPSK for Trellis Codes," *Proc. GLOBECOM'84*, pp. 20.6.1–20.6.8, Atlanta, Georgia, November.

Dixon, R. C. (1976). *Spread Spectrum Techniques*, IEEE Press, New York.

Doetz, M. L., Heald, E. T., and Martin, D. L. (1957). "Binary Data Transmission Techniques for Linear Systems," *Proc. IRE*, vol. 45, pp. 656–661, May.

Drouilhet, P. R., Jr. and Bernstein, S. L. (1969). "TATS—A Bandspread Modulation-Demodulation System for Multiple Access Tactical Satellite Communication," *1969 IEEE Electronics and Aersopace Systems (EASCON) Conv. Record*, Washington, D.C., pp. 126–132, October 27–29.

Duffy, F. P. and Tratcher, T. W. (1971). "Analog Transmission Performance on the Switched Telecommunications Network," *Bell Syst. Tech. J.*, vol. 50, pp. 1311–1347, April.

Durbin, J. (1959). "Efficient Estimation of Parameters in Moving-Average Models," *Biometrika*, vol. 46, parts 1 and 2, pp. 306–316.

Duttweiler, D. L., Mazo, J. E., and Messerschmitt, D. G. (1974). "Error Propagation in Decision-Feedback Equalizers," *IEEE Trans. Inform. Theory*, vol. IT-20, pp. 490–497, July.

Eleftheriou, E. and Falconer, D. D. (1987). "Adaptive Equalization Techniques for HF Channels," *IEEE J. Selected Areas Commun.*, vol. SAC-5 pp. 238–247, February.

El Gamal, A. and Cover, T. M. (1980). "Multiple User Information Theory," *Proc. IEEE*, vol. 68, pp. 1466–1483, December.

Elias, P. (1954). "Error-Free Coding," *IRE Trans. Inform. Theory*, vol. IT-4, pp. 29–37, September.

Elias, P. (1955). "Coding for Noisy Channels," *IRE Convention Record*, vol. 3, part 4, 37–46.

Esposito, R. (1967). "Error Probabilities for the Nakagami Channel," *IEEE Trans. Inform. Theory*, vol. IT-13, pp. 145–148, January.

Eyuboglu, V. M. (1988). "Detection of Coded Modulation Signals on Linear, Severely Distorted Channels Using Decision-Feedback Noise Prediction with Interleaving," *IEEE Trans. Commun.*, vol. COM-36, pp. 401–409, April.

Falconer, D. D. (1976). "Jointly Adaptive Equalization and Carrier Recovery in Two-Dimensional Digital Communication Systems," *Bell Syst. Tech. J.*, vol. 55, pp. 317–334, March.

Falconer, D. D. and Ljung, L. (1978). "Application of Fast Kalman Estimation to Adaptive Equalization," *IEEE Trans. Commun.*, vol. COM-26, pp. 1439–1446, October.

Falconer, D. D. and Salz, J. (1977). "Optimal Reception of Digital Data Over the Gaussian Channel with Unknown Delay and Phase Jitter," *IEEE Trans. Inform. Theory*, vol. IT-23, pp. 117–126, January.

Fano, R. M. (1961). *Transmission of Information*, MIT Press, Cambridge, Mass.

Fano, R. M. (1963). "A Heuristic Discussion of Probabilistic Coding," *IEEE Trans. Inform. Theory*, vol. IT-9, pp. 64–74, April.

Feinstein, A. (1958). *Foundations of Information Theory*, McGraw-Hill, New York.

Fire, P. (1959). "A Class of Multiple-Error-Correcting Binary Codes for Non-Independent Errors." Sylvania Report No. RSL-E-32, Sylvania Electronic Defense Laboratory, Mountain View, Calif., March.

Flanagan, J. L., et al. (1979). "Speech Coding," *IEEE Trans. Commun.*, vol. COM-27, pp. 710–736, April.

Forney, G. D., Jr. (1965). "One Decoding BCH Codes," *IEEE Trans. Inform. Theory*, vol. IT-11, pp. 549–557, October.

Forney, G. D., Jr. (1966a). *Concatenated Codes*, MIT Press, Cambridge, Mass.

Forney, G. D., Jr. (1966b). "Generalized Minimum Distance Decoding," *IEEE Trans. Inform. Theory*, vol. IT-12, pp. 125–131, April.

Forney, G. D., Jr. (1968). "Exponential Error Bounds for Erasure, List, and Decision-Feedback Schemes," *IEEE Trans. Inform. Theory*, vol. IT-14, pp. 206–220, March.

Forney, G. D., Jr. (1970a). "Coding and Its Application in Space Communications," *IEEE Spectrum*, vol. 7, pp. 47–58, June.

Forney, G. D., Jr. (1970b). "Convolutional Codes I: Algebraic Structure," *IEEE Trans. Inform. Theory*, vol. IT-16, pp. 720–738, November.

Forney, G. D., Jr. (1971). "Burst Correcting Codes for the Classic Bursty Channel," *IEEE Trans. Commun. Tech.*, vol. COM-19, pp. 772–781, October.

Forney, G. D., Jr. (1972). "Maximum-Likelihood Sequence Estimation of Digital Sequences in the Presence of Intersymbol Interference," *IEEE Trans. Inform. Theory*, vol. IT-18, pp. 363–378, May.

Forney, G. D., Jr. (1974). "Convolutional Codes III: Sequential Decoding," *Inform. Control*, vol. 25, pp. 267–297, July.

Forney, G. D., Jr. (1988). "Coset Codes I: Introduction and Geometrical Classification," *IEEE Trans. Inform. Theory*, vol. IT-34, pp. 671–680, September.

Forney, G. D., Jr., Gallager, R. G., Lang, G. R., Longstaff, F. M., and Qureshi, S. U. (1984). "Efficient Modulation for Band-Limited Channels," *IEEE J. Selected Areas Commun.*, vol. SAC-2, pp. 632–647, September.

Foschini, G. J. (1984). "Contrasting Performance of Faster-Binary Signaling with QAM," *Bell Syst. Tech. J.*, vol. 63, pp. 1419–1445, October.

Foschini, G. J. (1985). "Equalizing Without Altering or Detecting Data, *Bell Syst. Tech. J.*, vol. 64, pp. 1885–1911, October.

Foschini, G. J., Gitlin, R. D., and Weinstein, S. B. (1974). "Optimization of Two-Dimensional Signal Constellations in the Presence of Gaussian Noise," *IEEE Trans. Commun.*, vol. COM-22, pp. 28–38, January.

Franaszek, P. A. (1968). "Sequence-State Coding for Digital Transmission," *Bell Syst. Tech. J.*, vol. 27, p. 143.

Franaszek, P. A. (1969). "On Synchronous Variable Length Coding for Discrete Noiseless Channels," *Inform. Control*, vol. 15, pp. 155–164.

Franaszek, P. A. (1970). "Sequence-State Methods for Run-Length-Limited Coding," *IBM J. Res. Dev.*, pp. 376–383, July.

Franks, L. E. (1969). *Signal Theory*, Prentice-Hall, Englewood Cliff, N.J.

Franks, L. E. (1983). "Carrier and Bit Synchronization in Data Communication—A Tutorial Review," *IEEE Trans. Commun.*, vol. COM-28, pp. 1107–1121, August.

Franks, L. E. (1981). "Synchronization Subsystems: Analysis and Design," in *Digital Communications, Satellite/Earth Station Engineering*, K. Feher (ed.), Prentice-Hall, Englewood Cliffs, N.J.

Fredricsson, S. (1975). "Pseudo-Randomness Properties of Binary Shift Register Sequences," *IEEE Trans. Inform. Theory*, vol. IT-21, pp. 115–120, January.

Freiman, C. E. and Wyner, A. D. (1964). "Optimum Block Codes for Noiseless Input Restricted Channels," *Inform. Control*, vol. 7, pp. 398–415.

Gaarder, N. T. (1971). "Signal Design for Fast-Fading Gaussian Channels," *IEEE Trans. Inform. Theory*, vol. IT-17, pp. 247–256, May.

Gabor, A. (1967). "Adaptive Coding for Self Clocking Recording," *IEEE Trans. Electronic Comp.* vol. EC-16, p. 866.

Gallager, R. G. (1965). "Simple Derivation of the Coding Theorem and Some Applications," *IEEE Trans. Inform. Theory*, vol. IT-11, pp. 3–18, January.

Gallager, R. G. (1968). *Information Theory and Reliable Communication*, Wiley, New York.

Gardner, F. M. (1979). *Phaselock Techniques*, Wiley, New York.

Gardner, W. A. (1984). "Learning Characteristics of Stochastic-Gradient Descent Algorithms: A General Study, Analysis, and Critique," *Signal Processing*, vol. 6, pp. 113–133, April.

George, D. A., Bowen, R. R., and Storey, J. R. (1971). "An Adaptive Decision-Feedback Equalizer," *IEEE Trans. Commun. Tech.*, vol. COM-19, pp. 281–293, June.

Gersho, A. (1982). "On the Structure of Vector Quantizers," *IEEE Trans. Inform. Theory*, vol. IT-28, pp. 157–166, March.

Gersho, A. and Gray, R. M. (1992). *Vector Quantization and Signal Compression*, Kluwer Academic Publishers, Boston.

Gersho, A. and Lawerence, V. B. (1984). "Multidimensional Signal Constellations for Voiceband Data Transmission," *IEEE J. Selected Areas Commun.*, vol. SAC-2, pp. 687–702, September.

Gerst, I. and Diamond, J. (1961). "The Elimination of Intersymbol Interference by Input Pulse Shaping," *Proc. IRE*, vol. 53, July.

Ghez, S., Verdu, S., and Schwartz, S. C. (1988). "Stability Properties of Slotted Aloha with Multipacket Reception Capability," *IEEE Trans. Autom. Control*, vol. 33, pp. 640–649, July.

Ghosh, M. and Weber, C. L. (1991). "Maximum likelihood Blind Equalization," *Proc. 1991 SPIE Conf.*, San Diego, Calif. July.

Gilbert, E. N. (1952). "A Comparison of Signaling Alphabets," *Bell Syst. Tech. J.*, vol. 31, pp. 504–522, May.

Gilhousen, K. S., Jacobs, I. M., Podovani, R., Viterbi, A. J., Weaver, L. A., and Wheatley, G. E. III (1991). "On the Capacity of a Cellular CDMA System," *IEEE Trans. Vehicular Tech.*, vol. 40, pp. 303–312, May.

Gitlin, R. D. Meadors, H. C., and Weinstein, S. B. (1982). "The Tap Leakage Algorithm: An Algorithm for the Stable Operation of a Digitally Implemented Fractionally Spaced, Adaptive Equalizer," *Bell Syst. Tech. J.*, vol. 61, pp. 1817–1839, October.

Gitlin, R. D. and Weinstein, S. B. (1979). "On the Required Tap-Weight Precision for Digitally Implemented Mean-Squared Equalizers," *Bell Syst. Tech. J.*, vol. 58, pp. 301–321, February.

Gitlin, R. D. and Weinstein, S. B. (1981). "Fractionally-Spaced Equalization: An Improved Digital Transversal Equalizer," *Bell Syst. Tech. J.*, vol. 60, pp. 275–296, February.

Glave, F. E. (1972). "An Upper Bound on the Probability of Error due to Intersymbol Interference for Correlated Digital Signals," *IEEE Trans. Inform. Theory*, vol. IT-18, pp. 356–362, May.

Goblick, T. J., Jr. and Holsinger, J. L. (1967). "Analog Source Digitization: A Comparison of Theory and Practice," *IEEE Trans. Inform. Theory*, vol. IT-13, pp. 323–326, April.

Godard, D. N. (1974). "Channel Equalization Using a Kalman Filter for Fast Data Transmission," *IBM J. Res. Dev.*, vol. 18, pp. 267–273, May.

Godard, D. N. (1980). "Self-Recovering Equalization and Carrier Tracking in Two-Dimensional Data Communications Systems," *IEEE Trans. Commun.*, vol. COM-28, pp. 1867–1875, November.

Golay, M. J. E. (1949). "Note on Digital Coding," *Proc. IRE*, vol. 37, p. 657, June.

Gold, R. (1967). "Optimal Binary Sequences for Spread Spectrum Multiplexing," *IEEE Trans. Inform. Theory*, vol. IT-13, pp. 619–621, October.

Gold, R. (1968). "Maximal Recursive Sequences with 3-Valued Recursive Cross Correlation Functions," *IEEE Trans. Inform. Theory*, vol. IT-14, pp. 154–156, January.

Golomb, S. W. (1967). *Shift Register Sequences*, Holden-Day, San Francisco, Calif.

Goppa, V. D. (1970). "New Class of Linear Correcting Codes," *Probl. Peredach. Inform.*, vol. 6, pp. 24–30.

Goppa, V. D. (1971). "Rational Presentation of Codes and (L, g)-Codes," *Probl. Peredach. Inform.*, vol 7, pp. 41–49.

Gray, R. M. (1975). "Sliding Block Source Coding," *IEEE Trans. Inform. Theory*, vol. IT 21, pp. 357–368, July.

Gray, R. M. (1990). *Source Coding Theory*, Kluwer Academic Publishers, Boston.

Greefkes, J. A. (1970). "A Digitally Companded Delta Modulation Modem for Speech Transmission," *Proc. IEEE Int. Conf. on Commun.* pp. 7.33–7.48, June.

Green, P. E., Jr. (1962). "Radar Astronomy Measurement Techniques," MIT Lincoln Laboratory, Lexington, Mass., Tech. Report No. 282, December.

Gronemeyer, S. A. and McBride, A. L. (1976). "MSK and Offset QPSK Modulation," *IEEE Trans. Commun.*, vol. COM-24, pp. 809–820, August.

Gupta, S. C. (1975). "Phase-Locked Loops," *Proc. IEEE*, vol. 63, pp. 291–306, February.

Hahn, P. M. (1962). "Theoretical Diversity Improvement in Multiple Frequency Shift Keying," *IRE Trans. Commun. Syst.*, vol. CS-10, pp. 177–184, June.

Hamming, R. W. (1950). "Error Detecting and Error Correcting Codes," *Bell Syst. Tech. J.*, vol. 29, pp. 147–160, April.

Hamming, R. W. (1986). *Coding and Information Theory*, Prentice-Hall, Englewood Cliffs, N.J.

Hancock, J. C. and Lucky, R. W. (1960). "Performance of Combined Amplitude and Phase-Modulated Communication Systems," *IRE Trans. Commun. Syst.*, vol. CS-8, pp. 232–237, December.

Hartley, R. V. (1928). "Transmission of Information," *Bell Syst. Tech. J.*, vol. 7, p. 535.

Hatzinakos, D. and Nikias, C. L. (1991). "Blind Equalization Using a Tricepstrum-Based Algorithm," *IEEE Trans. Commun.*, vol. COM-39, pp. 669–682, May.

Hecht, M. and Guida, A. (1969). "Delay Modulation," *Proc. IEEE*, vol. 57, pp. 1314–1316, July.

Heller, J. A. (1968). "Short Constraint Length Convolutional Codes," Jet Propulsion Laboratory, California Institue of Technology, Pasadena, Calif., *Space Program Summary* 37–54, vol. 3, pp. 171–174, December.

Heller, J. A. (1975). "Feedback Decoding of Convolutional Codes," in *Advances in Communication Systems*, vol. 4, A. J. Viterbi (ed.), Academic, New York.

Heller, J. A. and Jacobs, I. M. (1971). "Viterbi Decoding for Satellite and Space Commmunication," *IEEE Trans. Commun. Tech.*, vol. COM-19, pp. 835–848, October.

Helstrom, C. W. (1955). "The Resolution of Signals in White Gaussian Noise," *Proc. IRE*, vol. 43, pp. 1111–1118, September.

Helstrom, C. W. (1968). *Statistical Theory of Signal Detection*, Pergamon, London.
Helstrom, C. W. (1991). *Probability and Stochastic Processes for Engineers*, Macmillan, New York.
Hildebrand, F. B. (1960). *Methods of Applied Mathematics*, Prentice-Hall, Englewood Cliffs, N.J.
Hirosaki, B. (1981). "An Orthogonality Multiplexed QAM System Using the Discrete Fourier Transform," *IEEE Trans. Commun.*, vol. COM-29, pp. 982–989, July.
Hirosaki, B., Hasegawa, S., and Sabato, A. (1986). "Advanced Group-Band Modem Using Orthogonally Multiplexed QAM Techniques," *IEEE Trans. Commun.*, vol. COM-34, pp. 587–592, June.
Ho, E. Y. and Yeh, Y. S. (1970). "A New Approach for Evaluating the Error Probability in the Presence of Intersymbol Interference and Additive Gaussian Noise," *Bell Syst. Tech. J.*, vol. 49, pp. 2249–2265, November.
Hocquenghem, A. (1959). "Codes Correcteurs d'Erreurs," *Chiffres*, vol. 2, pp. 147–156.
Holmes, J. K. (1982). *Coherent Spread Spectrum Systems*, Wiley-Interscience, New York.
Horwood, D. and Gagliardi, R. (1975). "Signal Design for Digital Multiple Access Communications," *IEEE Trans. Commun.*, vol. COM-23, pp. 378–383, March.
Hsu, F. M. (1982). "Square-Root Kalman Filtering for High-Speed Data Received over Fading Dispersive HF Channels," *IEEE Trans. Inform. Theory*, vol. IT-28, pp. 753–763, September.
Huffman, D. A. (1952). "A Method for the Construction of Minimum Redundancy Codes," *Proc. IRE*, vol. 40, pp. 1098–1101, September.
Hui, J. Y. N. (1984). "Throughput Analysis for Code Division Multiple Accessing of the Spread Spectrum Channel," *IEEE J. Selected Areas Commun.*, vol. SAC-2, pp. 482–486, July.
Immink, K. A. S. (1990). "Runlength-Limited Sequences," *Proc. IEEE*, vol. 78, pp. 1745–1759, November.
Itakura, F. (1975). "Minimum Prediction Residual Principle Applied to Speech Recognition," *IEEE Trans. Acoust., Speech, Signal Processing*, vol. ASSP-23, pp. 67–72, February.
Itakura, F. and Saito, S. (1968). "Analysis Synthesis Telephony Based on the Maximum-Likelihood Methods," *Proc. 6th Int. Congr. Acoust.*, Tokyo, Japan, pp. C17–C20.
Jacobs, I. M. (1974). "Practial Applications of Coding," *IEEE Trans. Inform. Theory*, vol. IT-20, pp. 305–310, May.
Jacoby, G. V. (1977). "A New Look-Ahead Code for Increased Data Density," *IEEE Trans. Magnetics*, vol. MAG-13, 1202–1204.
Jayant, N. S. (1970). "Adaptive Delta Modulation with a One-Bit Memory," *Bell Syst. Tech. J.*, pp. 321–342, March.
Jayant, N. S. (1974). "Digital Coding of Speech Waveforms: PCM, DPCM, and DM Quantizers," *Proc. IEEE*, vol. 62, pp. 611–632, May.
Jayant, N. S. (1976). *Waveform Quantization and Coding*, IEEE Press, New York.
Jayant, N. S. and Noll, P. (1984). *Digital Coding of Waveforms*, Prentice-Hall, Englewood Cliffs, N.J.
Jelinek, F. (1968). *Probabilistic Information Theory*, McGraw-Hill, New York.
Jelinek, F. (1969). "Fast Sequential Decoding Algorithm Using a Stack," *IBM J. Res. Dev.*, vol. 13, pp. 675–685, November.
Johnson, C. R. (1991). "Admissibility in Blind Adaptive Channel Equalization," *IEEE Control Syst. Mag.*, pp. 3–15, January.
Jones, S. K., Cavin, R. K. and Reed, W. M. (1982). "Analysis of Error-Gradient Adaptive Linear Equalizers for a Class of Stationary-Dependent Processes," *IEEE Trans. Inform. Theory*, vol. IT-28, pp. 318–329, March.
Jordan, K. L., Jr. (1966). "The Performance of Sequential Decoding in Conjunction with Efficient Modulation," *IEEE Trans. Commun. Syst.*, vol. CS-14, pp. 283–287, June.
Justesen, J. (1972). "A Class of Constructive Asymptotically Good Algebraic Codes," *IEEE Trans. Inform. Theory*, vol. IT-18, pp. 652–656, September.
Kailath, T. (1960). "Correlation Detection of Signals Perturbed by a Random Channel," *IRE Trans. Inform. Theory*, vol. IT-6, pp. 361–366, June.

Kailath, T. (1961). "Channel Characterization: Time-Variant Dispersive Channels, In *Lectures on Communication System Theory*, Chap. 6, E. Baghdady (ed.), McGraw-Hill, New York.

Kalet, I. (1989). "The Multitone Channel," *IEEE Trans. Commun.*, vol. COM-37, pp. 119–124, February.

Karabed, R. and Siegel, P. H. (1991). "Matched-Spectral Null Codes for Partial-Response Channels," *IEEE Trans. Inform. Theory*, vol. IT-37, pp. 818–855, May.

Kasami, T. (1966). "Weight Distribution Formula for Some Class of Cyclic Codes," Coordinated Science Laboratory, University of Illinois, Urbana, Ill., Tech. Report No. R-285, April.

Kaye, A. R. and George, D. A. (1970). "Transmission of Multiplexed PAM Signals over Multiple Channel and Diversity Systems," *IEEE Trans. Commun.*, vol. COM-18, pp. 520–525, October.

Kelly, E. J., Reed, I. S., and Root, W. L. (1960). "The Detection of Radar Echoes in Noise, Pt. I," *J. SIAM*, vol. 8, pp. 309–341, September.

Kleinrock, L. and Tobagi, F. A. (1975). "Packet Switching in Radio Channels: Part I—Carrier Sense Multiple-Access Modes and Their Throughput-Delay Characteristics," *IEEE Trans. Commun.*, vol. COM-23, pp. 1400–1416, December.

Kobayashi, H. (1971). "Simultaneous Adaptive Estimation and Decision Algorithm for Carrier Modulated Data Transmission Systems," *IEEE Trans. Commun. Tech.*, vol. COM-19, pp. 268–280, June.

Kotelnikov, V. A. (1947). "The Theory of Optimum Noise Immunity," Ph.D. Dissertation, Molotov Energy Institute, Moscow. [Translated by R. A. Silverman, McGraw-Hill, New York.]

Kretzmer, E. R. (1966). "Generalization of a Technique for Binary Data Communication," *IEEE Trans. Commun. Tech.*, vol. COM-14, pp. 67–68, February.

Larsen, K. J. (1973). "Short Convolutional Codes with Maximal Free Distance for Rates 1/2, 1/3, and 1/4," *IEEE Trans. Inform. Theory*, vol. IT-19, pp. 371–372, May.

Lender, A. (1963). "The Duobinary Technique for High Speed Data Transmission," *AIEE Trans. Commun. Electronics*, vol. 82, pp. 214–218.

Leon-Garcia, A. (1994). *Probability and Random Processes for Electrical Engineering*, Addison-Wesley, Reading, Mass.

Levinson, N. (1947). "The Wiener RMS (Root Mean Square) Error Criterion in Filter Design and Prediction," *J. Math. and Phys.*, vol. 25, pp. 261–278.

Lin, S. and Costello, D. J., Jr. (1983). *Error Control Coding: Fundamentals and Applications*, Prentice-Hall, Englewood Cliffs, N.J.

Linde, Y., Buzo, A., and Gray, R. M. (1980). "An Algorithm for Vector Quantizer Design," *IEEE Trans. Commun. vol. COM-28*, pp. 84–95, January.

Lindell, G. (1985). "On Coded Continuous Phase Modulation," Ph.D. Dissertation, Telecommunication Theory, University of Lund, Lund, Sweden, May.

Lindholm, J. H. (1968). "An Analysis of the Pseudo-Randomness Properties of Subsequences of Long *m*-Sequences," *IEEE Trans. Inform. Theory*, vol. IT-14, pp. 569–576, July.

Lindsey, W. C. (1964). "Error Probabilities for Ricean Fading Multichannel Reception of Binary and *N*-Ary Signals," *IEEE Trans. Inform. Theory*, vol. IT-10, pp. 339–350, October.

Lindsey, W. C. (1972). *Synchronization Systems in Communications*, Prentice-Hall, Englewood Cliffs, N.J.

Lindsey, W. C. and Chie, C. M. (1981). "A Survey of Digital Phase-Locked Loops," *Proc. IEEE*, vol. 69, pp. 410–432.

Lindsey, W. C. and Simon, M. K. (1973). *Telecommunication Systems Engineering*, Prentice-Hall, Englewood Cliffs, N.J.

Ling, F. (1988). "Convergence Characteristics of LMS and LS Adaptive Algorithms for Signals with Rank-Deficient Correlation Matrices," *Proc. Int. Conf. Acoust., Speech, Signal Processing*, New York, 25.D.4.7, April.

Ling, F., Manolakis, D. G., and Proakis, J. G. (1986a). "Finite Word-Length Effects in Recursive Least Squares Algorithms with Application to Adaptive Equalization," *Annales des Telecommunications*, vol. 41, pp. 1–9, May–June.

Ling, F., Manolakis, D. G., and Proakis, J. G. (1986b). "Numerically Robust Least-Squares Lattice-Ladder Alghorithms with Direct Updating of the Reflection Coefficients," *IEEE Trans. Acoust., Speech, Signal Processing*, vol. ASSP-34, pp. 837–845, August.

Ling, F. and Proakis, J. G. (1982). "Generalized Least Squares Lattice and Its Applications to DFE," *Proc. 1982, IEEE Int. Conf. on Acoustics, Speech, Signal Processing*, Paris, France, May.

Ling, F. and Proakis, J. G. (1984a), "Numerical Accuracy and Stability: Two Problems of Adaptive Estimation Algorithms Caused by Round-Off Error," *Proc. Int. Conf. Acoust., Speech, Signal Processing*, pp. 30.3.1–30.3.4, San Diego, Calif., March.

Ling, F. and Proakis, J. G. (1984b). "Nonstationary Learning Characteristics of Least Squares Adaptive Estimation Algorithms," *Proc. Int. Conf. Acoust., Speech, Signal Processing*, pp. 3.7.1–3.7.4, San Diego, Calif., March.

Ling, F. and Proakis, J. G. (1984c). "A Generalized Multichannel Least-Squares Lattice Algorithm with Sequential Processing Stages," *IEEE Trans. Acoust., Speech, Signal Processing*, vol. ASSP-32, pp. 381–389, April.

Ling, F. and Proakis, J. G. (1985). "Adaptive Lattice Decision-Feedback Equalizers—Their Performance and Application to Time-Variant Multipath Channels," *IEEE Trans. Commun.*, vol. COM-33, pp. 348–356, April.

Ling, F. and Proakis, J. G. (1986). "A Recursive Modified Gram–Schmidt Algorithm," *IEEE Trans. Acoust., Speech, Signal Processing*, vol. ASSP-34, pp. 829–836, August.

Ling, F. and Quershi, S. U. H. (1986). "Lattice Predictive Decision-Feedback Equalizer for Digital Communication Over Fading Multipath Channels," *Proc. GLOBECOM '86*, Houston, Texas, December.

Ljung, S. and Ljung, L. (1985). "Error Propagation Properties of Recursive Least-Squares Adaptation Algorithms," *Automatica*, vol. 21, pp. 159–167.

Lloyd, S. P. (1982). "Least Squares Quantization in PCM," *IEEE Trans. Inform. Theory*, vol. IT-28, pp. 129–137, March.

Loeve, M. (1955). *Probability Theory*, Van Nostrand, Princeton, N.J.

Long, G., Ling, F., and Proakis, J. G. (1987). "Adaptive Transversal Filters with Delayed Coefficient Adaptation," *Proc. Int. Conf. Acoust., Speech, Signal Processing*, Dallas, Texas, March.

Long, G., Ling, F., and Proakis, J. G. (1988a). "Fractionally-Spaced Equalizers Based on Singular-Value Decomposition," *Proc. Int. Conf. Acoust., Speech, Signal Processing*, New York, 25.D.4.10, April.

Long, G., Ling, F., and Proakis, J. G. (1988b). "Applications of Fractionally-Spaced Decision-Feedback Equalizers to HF Fading Channels," *Proc. MILCOM*, San Diego, Calif., October.

Long, G., Ling, F., and Proakis, J. G. (1989). "The LMS Algorithm with Delayed Coefficient Adaptation, "*IEEE Trans. Acoust., Speech, Signal Processing*, vol. ASSP-37, October.

Lucky, R. W. (1965). "Automatic Equalization for Digital Communications, *Bell Syst. Tech. J.*, vol. 44, pp. 547–588, April.

Lucky, R. W. (1966). "Techniques for Adaptive Equalization of Digital Communication," *Bell Syst. Tech. J.*, vol. 45, pp. 255–286.

Lucky, R. W. and Hancock, J. C. (1962). "On the Optimum Performance of N-ary Systems Having Two Degrees of Freedom," *IRE Trans. Commun. Syst.*, vol. CS-10, pp. 185–192, June.

Lucky, R. W., Salz, J., and Weldon, E. J., Jr. (1968). *Principles of Data Communication*, McGraw-Hill, New York.

Lugannani, R. (1969). "Intersymbol Interference and Probability of Error in Digital Systems," *IEEE Trans. Inform. Theory*, vol. IT-15, pp. 682–688, November.

Lundgren, C. W. and Rummler, W. D. (1979). "Digital Radio Outage Due to Selective Fading—Observation vs. Prediction from Laboratory Simulation," *Bell Syst. Tech. J.*, vol. 58, pp. 1074–1100, May–June.

Lupas, R. and Verdu, S. (1989). "Linear Multiuser Detectors for Synchronous Code-Division Multiple-Access Channels," *IEEE Trans. Inform. Theory*, vol. IT-35, pp. 123–136, January.

Lupas, R. and Verdu, S. (1990). "Near–Far Resistance of Multiuser Detectors in Asynchronous Channels," *IEEE Trans. Commun.*, vol. COM-38, pp. 496–508, April.

MacKenchnie, L. R. (1973). "Maximum Likelihood Receivers for Channels Having Memory," Ph.D. Dissertation, Department of Electrical Engineering, University of Notre Dame, Notre Dame, Ind., January.

MacWilliams, F. J. and Sloane, J. J. (1977). *The Theory of Error Correcting Codes,* North Holland, New York.

Magee, F. R. and Proakis, J. G. (1973). "Adaptive Maximum-Likelihood Sequence Estimation for Digital Signaling in the Presence of Intersymbol Interference," *IEEE Trans. Inform. Theory*, vol. IT-19, pp. 120–124, January.

Makhoul, J. (1978). "A Class of All-Zero Lattice Digital Filters: Properties and Applications," *IEEE Trans. Acoust., Speech, Signal Processing*, vol. ASSP-26, pp. 304–314, August.

Makhoul, J., Roucos, S., and Gish, H. (1985). "Vector Quantization in Speech Coding," *Proc. IEEE*, vol. 73, pp. 1551–1587, November.

Martin, D. R. and McAdam, P. L. (1980). "Convolutional Code Performance with Optimal Jamming," *Conf. Rec. Int. Conf. Commun.*, pp. 4.3.1–4.3.7, May.

Massey, J. L. (1963). *Threshold Decoding*, MIT Press, Cambridge, Mass.

Massey, J. L. (1965). "Step-by-Step Decoding of the BCH Codes," *IEEE Trans. Inform. Theory*, vol. IT-11, pp. 580–585, October.

Massey, J. L. (1988). "Some New Approaches to Random Access Communications," *Performance '87*, pp. 551–569. [Reprinted 1993 in *Multiple Access Communications*, N. Abramson (ed.), IEEE Press, New York.]

Massey, J. L. and Sain, M. (1968). "Inverses of Linear Sequential Circuits," *IEEE Trans. Comput.*, vol. C-17, pp. 330–337, April.

Matis, K. R. and Modestino, J. W. (1982). "Reduced-State Soft-Decision Trellis Decoding of Linear Block Codes," *IEEE Trans. Inform. Theory*, vol. IT-28, pp. 61–68, January.

Max, J. (1960). "Quantizing for Minimum Distortion," *IRE Trans. Inform. Theory*, vol. IT-6, pp. 7–12, March.

Mazo, J. E. (1975). "Faster-Than-Nyquist Signaling," *Bell Syst. Tech. J.*, vol. 54, pp. 1451–1462, October.

Mazo, J. E. (1979). "On the Independence Theory of Equalizer Convergence," *Bell Syst. Tech. J.*, vol. 58, pp. 963–993, May.

McMahon, M. A. (1984). *The Making of a Profession—A Century of Electrical Engineering in America*, IEEE Press, New York.

Mengali, U. (1977). "Joint Phase and Timing Acquisition in Data Transmission," *IEEE Trans. Commun.*, vol. COM-25, pp. 1174–1185, October.

Meyers, M. H. and Franks, L. E. (1980). "Joint Carrier Phase and Symbol Timing for PAM Systems," *IEEE Trans. Commun.*, vol. COM-28, pp. 1121–1129, August.

Meyr, H. and Ascheid, G. (1990). *Synchronization in Digital Communications*, Wiley Interscience, New York.

Miller, K. S. (1964). *Multidimensional Gaussian Distributions*, Wiley, New York.

Millman, S. (ed.) (1984). *A History of Engineering and Science in the Bell System—Communication Sciences (1925–1980)*, AT&T Bell Laboratoreis.

Miyagaki, Y., Morinaga, N., and Namekawa, T. (1978). "Error Probability Characteristics for CPSK Signal Through m-Distributed Fading Channel," *IEEE Trans. Commun.*, vol. COM-26, pp. 88–100, January.

Monsen, P. (1971). "Feedback Equalization for Fading Dispersive Channels," *IEEE Trans. Inform. Theory*, vol. IT-17, pp. 56–64, January.

Morf, M. (1977). "Ladder Forms in Estimation and System Identification," *Proc. 11th Annual Asilomar Conf. on Circuits, Systems and Computers*, Monterey, Calif., Nov. 7–9.

Morf, M., Dickinson, B., Kailath, T., and Vieira, A. (1977). "Efficient Solution of Covariance Equations for Linear Prediction," *IEEE Trans. Acoust., Speech, Signal Processing*, vol. ASSP-25, pp. 429–433, October.

Morf, M. and Lee, D. (1979). "Recursive Lest Squares Ladder Forms for Fast Parameter

Tracking," *Proc. 1978 IEEE Conf. on Decision and Control*, San Diego, Calif., pp. 1362–1367, January 12.

Morf, M., Lee, D., Nickolls, J. and Vieira, A. (1977). "A Classification of Algorithms for ARMA Models and Ladder Realizations," *Proc. 1977 IEEE Int. Conf on Acoustics, Speech, Signal Processing*, Hartford, Conn., pp. 13–19, May.

Morf, M., Vieira, A., and Lee, D. (1977). "Ladder Forms for Identification and Speech Processing," *Proc. 1977 IEEE Conf. on Decision and Control*, New Orleans, La, pp. 1074–1078, December.

Mueller, K. H. and Muller, M. S. (1976). "Timing Recovery in Digital Synchronous Data Receivers," *IEEE Trans. Commun.*, vol. COM-24, pp. 516–531, May.

Muller, D. E. (1954). "Application of Boolean Algebra to Switching Circuit Design and to Error Detection," *IRE Trans. Electronic Comput.*, vol. EC-3, pp. 6–12, September.

Mulligan, M. G. (1988). "Multi-Amplitude Continuous Phase Modulation with Convolutional Coding," Ph.D. Dissertation, Department of Electrical and Computer Engineering, Northeastern University, June.

Nakagami, M. (1960). "The m-Distribution—A General Formula of Intensity Distribution of Rapid Fading," in *Statistical Methods of Radio Wave Propagation*, W. C. Hoffman (ed.), pp. 3–36, Pergamon Press, New York.

Natali, F. D. and Walbesser, W. J. (1969). "Phase-Locked Loop Detection of Binary PSK Signals Utilizing Decision Feedback," *IEEE Trans. Aerospace Electronic Syst.*, vol. AES-5, pp. 83–90, January.

Neyman, J. and Pearson, E. S. (1933). "On the Problem of the Most Efficient Tests of Statistical Hypotheses," *Phil. Trans. Roy. Soc. London, Series A*, vol. 231, 289–337.

North, D. O. (1943). "An Analysis of the Factors Which Determine Signal/Noise Discrimination in Pulse-Carrier Systems," RCA Tech. Report No. 6 PTR-6C.

Nyquist, H. (1924). "Certain Factors Affecting Telegraph Speed," *Bell Syst. Tech. J.*, vol. 3, pp. 324.

Nyquist, H. (1928). "Certain Topics in Telegraph Transmission Theory," *AIEE Trans.*, vol. 47, pp. 617–644.

Odenwalder, J. P. (1970). "Optimal Decoding of Convolutional Codes," Ph.D. Dissertation, Department of Systems Sciences, School of Engineering and Applied Sciences, University of California, Los Angeles.

Odenwalder, J. P. (1976). "Dual-k Convolutional Codes for Noncoherently Demodulated Channels," *Proc. Int. Telemetering Conf.* vol. 12, pp. 165–174, September.

Olsen, J. D. (1977). "Nonlinear Binary Sequences with Asymptotically Optimum Periodic Cross Correlation," Ph.D. Dissertation, University of Southern California, December.

Omura, J. (1971). "Optimal Receiver Design for Convolutional Codes and Channels with Memory Via Control Theoretical Concepts," *Inform. Sci.*, vol, 3, pp. 243–266.

Omura, J. K. and Levitt, B. K. (1982). "Code Error Probability Evaluation for Antijam Communication Systems," *IEEE Trans. Commun.*, vol. COM-30, pp. 896–903, May.

Osborne, W. P. and Luntz, M. B. (1974). "Coherent and Noncoherent Detection of CPFSK," *IEEE Trans. Commun.*, vol. COM-22, pp. 1023–1036, August.

Paaske, E. (1974). "Short Binary Convolutional Codes with Maximal Free Distance for Rates 2/3 and 3/4," *IEEE Trans. Inform. Theory*, vol. IT-20, pp. 683–689, September.

Paez, M. D. and Glisson, T. H. (1972). "Minimum Mean Squared Error Quantization in Speech PCM and DPCM Systems," *IEEE Trans. Commun.*, vol. COM-20, pp. 225–230, April.

Pahlavan, K. (1985). "Wireless Communications for Office Information Networks," *IEEE Commun. Mag.*, vol. 23, pp. 18–27, June.

Papoulis, A. (1984). *Probability, Random Variables, and Stochastic Processes*, McGraw-Hill, New York.

Paul, D. B. (1983). "An 800 bps Adaptive Vector Quantization Vocoder Using a Preceptual Distance Measure," *Proc. IEEE Int. Conf. Acoust., Speech, Signal Processing*, Boston, Mass, pp. 73–76, April.

Pearson, K., (1965). *Tables of the Incomplete Γ-Function*, Cambridge University Press, London.

Peebles, P. Z. (1987). *Probability, Random Variables, and Random Signal Principles*, McGraw-Hill, New York.

Peterson, W. W. (1960). "Encoding and Error-Correction Procedures for Bose-Chaudhuri Codes," *IRE Trans. Inform. Theory*, vol. IT-6, pp. 459–470, September.

Peterson, W. W. and Weldon, E. J., Jr. (1972). *Error-Correcting Codes*, 2d ed., MIT Press, Cambrdige, Mass.

Picci, G. and Prati, G. (1987). "Blind Equalization and Carrier Recovery Using a Stop-and-Go Decision Directed Algorithm," *IEEE Trans. Commun.*, vol. COM-35, pp. 877–887, September.

Picinbono, B. (1978). "Adaptive Signal Processing for Detection and Communication," in *Communication Systems and Random Process Theory*, J. K. Skwirzynski (ed.), Sijthoff & Nordhoff, Alphen aan den Rijn, The Netherlands.

Pickholtz, R. L., Schilling, D. L., and Milstein, L. B. (1982). "Theory of Spread Spectrum Communications—A Tutorial," *IEEE Trans. Commun.*, vol. COM-30, pp. 855–884, May.

Pieper, J. F., Proakis, J. G., Reed, R. R., and Wolf, J. K. (1978). "Design of Efficient Coding and Modulation for a Rayleigh Fading Channel," *IEEE Trans. Inform. Theory*, vol. IT-24, pp. 457–468, July.

Pierce, J. N. (1958). "Theoretical Diversity Improvement in Frequency-Shift Keying," *Proc. IRE*, vol. 46, pp. 903–910, May.

Pierce, J. N. and Stein, S. (1960). "Multiple Diversity with Non-Independent Fading," *Proc. IRE*, vol. 48, pp. 89–104, January.

Plotkin, M. (1960). "Binary Codes with Specified Minimum Distance," *IRE Trans. Inform. Theory*, vol. IT-6, pp. 445–450, September.

Poor, H. V. and Verdu, S. (1988). "Single-User Detectors for Multiuser Channels," *IEEE Trans. Commun.*, vol. 36, pp. 50–60, January.

Price, R. (1954). "The Detection of Signals Perturbed by Scatter and Noise," *IRE Trans. Inform. Theory*, vol. PGIT-4, pp. 163–170, September.

Price, R. (1956). "Optimum Detection of Random Signals in Noise, with Application to Scatter-Multipath Communicaton," *IRE Trans. Inform. Theory*, vol. IT-2, pp. 125–135, December.

Price, R. (1962a). "Error Probabalities for Adaptive Multichannel Reception of Binary Signals," MIT Lincoln Laboratory, Lexington, Mass., Tech. Report No. 258, July.

Price, R. (1962b). "Error Probabilities for Adaptive Multichannel Reception of Binary Signals," *IRE Trans. Inform. Theory*, vol. IT-8, pp. 305–316, September.

Price, R. (1972). "Nonlinearly Feedback-Equalized PAM vs. Capacity," *Proc. 1972 IEEE Int. Conf. on Commun.* Philadelphia, Penn., pp. 22.12–22.17, June.

Price, R. and Green, P. E., Jr. (1958). "A Communication Technique for Multipath Channels," *Proc. IRE*, vol. 46, pp. 555–570, March.

Price, R. and Green, P. E., Jr. (1960). "Signal Processing in Radar Astronomy—Communication via Fluctuating Multipath Media," MIT Lincoln Laboratory, Lexington, Mass., Tech. Report No. 234, October.

Proakis, J. G. (1968). "Probabilities of Error for Adaptive Reception of M-Phase Signals," *IEEE Trans. Commun. Tech.*, vol. COM-16, pp. 71–81, February.

Proakis, J. G. (1975). "Advances in Equalization for Intersymbol Interference," in *Advances in Communication Systems*, vol. 4, A. J. Viterbi (ed.), Academic, New York.

Proakis, J. G., Drouilhet, P. R., Jr., and Price, R. (1964). "Performance of Coherent Detection Systems Using Decision-Directed Channel Measurement," *IEEE Trans. Commun. Syst.*, vol. CS-12, pp. 54–63, March.

Proakis, J. G. and Ling, F. (1984). "Recursive Least Squares Algorithms for Adaptive Equalization of Time-Variant Multipath Channels," *Proc. Int. Conf. Commun.* Amsterdam, The Netherlands, May.

Proakis, J. G. and Manolakis, D. G. (1988). *Introduction to Digital Processing*, Macmillan, New York.

Proakis, J. G. and Miller, J. H. (1969). "Adaptive Receiver for Digital Signaling through

Channels with Intersymbol Interference," *IEEE Trans. Inform. Theory*, vol. IT-15, pp. 484–497, July.

Proakis, J. G. and Rahman, I. (1979). "Performance of Concatenated Dual-*k* Codes on a Rayleigh Fading Channel with a Bandwidth Constraint," *IEEE Trans. Commun.*, vol. COM-27, pp. 801–806, May.

Pursley, M. B. (1979). "On the Mean-Square Partial Correlation of Periodic Sequences," *Proc. 1979 Conf. Inform. Science and Systems*, Johns Hopkins University, Baltimore, Md., pp. 377–379, March.

Qureshi, S. U. H. (1976). "Timing Recovery for Equalized Partial Response Systems," *IEEE Trans. Commun.*, vol. COM-24, pp. 1326–1331, December.

Qureshi, S. U. H. (1985). "Adaptive Equalization," *Proc. IEEE*, vol. 53, pp. 1349–1387, September.

Qureshi, S. U. H. and Forney, G. D., Jr. (1977). "Performance and Properties of a $T/2$ Equalizer," *Natl. Telecom. Conf. Record*, pp. 11.1.1–11.1.14, Los Angeles, Calif., December.

Rabiner, L. R. and Schafer, R. W. (1978). *Digital Processing of Speech Signals*, Prentice-Hall, Englewood Cliffs, N.J.

Raheli, R., Polydoros, A., and Tzou, C.-K. (1995). "The Principle of Per-Survivor Processing: A General Approach to Approximate and Adaptive MLSE," *IEEE Trans. Commun.*, vol. COM-43 (to appear).

Rahman, I. (1981). "Bandwidth Constrained Signal Design for Digital Communication over Rayleigh Fading Channels and Partial Band Interference Channels," Ph.D. Dissertation, Department of Electrical Engineering, Northeastern University, Boston, Mass.

Ramsey, J. L. (1970). "Realization of Optimum Interleavers," *IEEE Trans. Inform. Theory*, vol. IT-16, pp. 338–345.

Reed, I. S. (1954). "A Class of Multiple-Error Correcting Codes and the Decoding Scheme," *IRE Trans. Inform.*, vol. IT-4, pp. 38–49, September.

Reed, I. S. and Solomon, G. (1960). "Polynomial Codes Over Certain Finite Fields," *SIAM J.*, vol. 8, pp. 300–304, June.

Rizos, A. D., Proakis, J. G., and Nguyen, T. Q. (1994). "Comparison of DFT and Cosine Modulated Filter Banks in Multicarrier Modulation," *Proc. Globecom '94*, pp. 687–691, San Francisco. Calif., November.

Roberts, L. G. (1975). "Aloha Packet System with and without Slots and Capture," *Comp. Commun. Rev.*, vol. 5, pp. 28–42, April.

Roucos, S., Schwartz, R., and Makhoul, J. (1982). "Segment Quantization for Very-Low-Rate Speech Coding," *Proc. Int. Conf. Acoust., Speech, Signal Processing*, Paris, France, pp. 1565–569, May.

Rowe, H. E. and Prabhu, V. K. (1975). "Power Spectrum of a Digital Frequency Modulation Signal," *Bell Syst. Tech. J.*, vol. 54, pp. 1095–1125, July–August.

Rummler, W. D. (1979). "A New Selective Fading Model: Application to Propagation Data," *Bell Syst. Tech. J.*, vol. 58, pp. 1037–1071, May–June.

Ryder, J. D. and Fink, D. G. (1984). *Engineers and Electronics*, IEEE Press, New York.

Saltzberg, B. R. (1967). "Performance of an Efficient Parallel Data Transmission System," *IEEE Trans. Commun.*, vol. COM-15, pp. 805–811, December.

Saltzberg, B. R. (1968). "Intersymbol Interference Error Bounds with Application to Ideal Bandlimited Signaling," *IEEE Trans. Inform. Theory*, vol. IT-14, pp. 563–568, July.

Salz, J. (1973). "Optimum Mean-Square Decision Feedback Equalization," *Bell Syst. Tech. J.*, vol. 52, pp. 1341–1373, October.

Salz, J., Sheehan, J. R., and Paris, D. J. (1971). "Data Transmission by Cominbed AM and PM," *Bell Syst. Tech. J.*, vol. 50, pp. 2399–2419, September.

Sarwate, D. V. and Pursley, M. B. (1980). "Crosscorrelation Properties of Pseudorandom and Related Sequences," *Proc. IEEE*, vol. 68, pp. 593–619, May.

Sato, Y. (1975). "A Method of Self-Recovering Equalization for Multilevel Amplitude-Modulation Systems," *IEEE Trans. Commun.*, vol. COM-23, pp. 679–682, June.

Sato, Y. *et al.* (1986). "Blind Suppression of Time Dependency and its Extension to Multi-Dimensional Equalization," *Proc. ICC'86*, pp. 46.4.1–46.4.5.

Satorius, E. H. and Alexander, S. T. (1979). "Channel Equalization Using Adaptive Lattice Algorithms," *IEEE Trans. Commun.*, vol. COM-27, pp. 899–905, June.

Satorius, E. H. and Pack, J. D. (1981). "Application of Least Squares Lattice Algorithms to Adaptive Equalization," *IEEE Trans. Commun.*, vol. COM-29, pp. 136–142, February.

Savage, J. E. (1966). "Sequential Decoding—The Computation Problem," *Bell Syst. Tech. J.*, vol. 45, pp. 149–176, January.

Scholtz, R. A. (1977). "The Spread Spectrum Concept," *IEEE Trans. Commun.*, vol. COM-25, pp. 748–755, August.

Scholtz, R. A. (1979). "Optimal CDMA Codes," *1979 Nat. Telecommun. Conf. Rec.*, Washington, D.C., pp. 54.2.1–54.2.4, November.

Scholtz, R. A. (1982). "The Origins of Spread Spectrum," *IEEE Trans. Commun.*, vol. COM-30, pp. 822–854, May.

Schonhoff, T. A. (1976). "Symbol Error Probabilities for M-ary CPFSK: Coherent and Noncoherent Detection," *IEEE Trans. Commun.*, vol. COM-24, pp. 644–652, June.

Seshadri, N. (1994). "Joint Data and Channel Estimation Using Fast Blind Trellis Search Techniques," *IEEE Trans. Commun.*, vol. COM-42, pp. 1000–1011, March.

Shalvi, O. and Weinstein, E. (1990). "New Criteria for Blind Equalization of Nonminimum Phase Systems Channels," *IEEE Trans. Inform. Theory*, vol. IT-36, pp. 312–321, March.

Shannon, C. E. (1948a). "A Mathematical Theory of Communication," *Bell Syst. Tech. J.*, vol. 27, pp. 379–423, July.

Shannon, C. E. (1948b). "A Mathematical Theory of Communication," *Bell Syst. Tech. J.*, vol. 27, pp. 623–656, October.

Shannon, C. E. (1949). "Communication in the Presence of Noise," *Proc. IRE*, vol. 37, pp. 10–21, January.

Shannon, C. E. (1959a). "Coding Theorems for a Discrete Source with a Fidelity Criterion," *IRE Nat. Conv. Rec.*, pt. 4, pp. 142–163, March.

Shannon, C. E. (1959b). "Probability of Error for Optimal Codes in a Gaussian Channel," *Bell Syst. Tech. J.*, vol. 38, pp. 611–656, May.

Shannon, C. E., Gallager, R. G., and Berlekamp, E. R. (1967). "Lower Bounds to Error Probability for Coding on Discrete Memoryless Channels, I and II," *Inform. Control.*, vol. 10, pp. 65–103, January; pp. 527–552, May.

Shimbo, O. and Celebiler, M. (1971). "The Probability of Error due to Intersymbol Interference and Gaussian Noise in Digital Communication Systems," *IEEE Trans. Commun. Tech.*, vol. COM-19, pp. 113–119, April.

Simon, M. K. and Divsalar, D. (1985). "Combined Trellis Coding with Asymmetric MPSK Modulation," *JPL Publ. 85-24*, Pasadena, Calif, May.

Simon, M. K., Omura, J. K., Scholtz, R. A., and Levitt, B. K. (1985). *Spread Spectrum Communications Vol. I, II, III*, Computer Science Press, Rockville, Md.

Simon, M. K. and Smith, J. G. (1973). "Hexagonal Multiple Phase-and-Amplitude-Shift Keyed Signal Sets," *IEEE Trans. Commun.*, vol. COM-21, pp. 1108–1115, October.

Slepian, D. (1956). "A Class of Binary Signaling Alphabets," *Bell Syst. Tech. J.*, vol. 35, pp. 203–234, January.

Slepian, D. (1974). *Key Papers in the Development of Information Theory*, IEEE Press, New York.

Slepian, D. and Wolf, J. K. (1973). "A Coding Theorem for Multiple Access Channels with Correlated Sources," *Bell Syst. Tech. J.*, vol. 52, pp. 1037–1076.

Sloane, N. J. A. and Wyner, A. D. (1993). *The Collected Papers of Shannon*, IEEE Press, New York.

Slock, D. T. M. and Kailath, T. (1988). "Numerically Stable Fast Recursive Least-Squares Transversal Filters," *Proc. Int. Conf. Acoust., Speech, Signal Processing*, pp. 1365–1368, New York, April.

Smith, J. W. (1965). "The Joint Optimization of Transmitted Signal and Receiving Filter for Data Transmission Systems," *Bell Syst. Tech. J.*, vol. 44, pp. 1921–1942, December.

Stenbit, J. P. (1964). "Table of Generators for BCH Codes," *IEEE Trans. Inform. Theory*, vol. IT-10, pp. 390–391, October.

Stiffler, J. J. (1971). *Theory of Synchronous Communications*, Prentice-Hall, Englewood Cliffs, N.J.

Sundberg, C. E. (1986). "Continuous Phase Modulation," *IEEE Commun. Mag.*, vol. 24, pp. 25–38, April.

Suzuki, H. (1977). "A Statistical Model for Urban Multipath Channels with Random Delay," *IEEE Trans. Commun.*, vol. COM-25, pp. 673–680, July.

Tang, D. L. and Bahl, L. R. (1970). "Block Codes for a Class of Constrained Noiseless Channels," *Inform. Control*, vol. 17, pp. 436–461.

Titsworth, R. C. and Welch, L. R. (1961). "Power Spectra of Signals Modulated by Random and Pseudorandom Sequences," *JPL Tech. Rep. 32-140*, October 10.

Thomas, C. M., Weidner, M. Y., and Durrani, S. H. (1974). "Digital Amplitude-Phase-Keying with *M*-ary Alphabets," *IEEE Trans. Commun.*, vol. COM-22, pp. 168–180, February.

Tong, L. Xu, G., and Kailath, T. (1994). "Blind Identification and Equalization Based on Second-Order Statistics," *IEEE Trans. Inform. Theory*, vol. IT-40, pp. 340–349, March.

Tufts, D. W. (1965). "Nyquist's Problem—The Joint Optimization of Transmitter and Receiver in Pulse Amplitude Modulation," *Proc. IEEE*, vol. 53, pp. 248–259, March.

Turin, G. L. (1961). "On Optimal Diversity Reception," *IRE Trans. Inform. Theory*, vol. IT-7, pp. 154–166, July.

Turin, G. L. (1962). "On Optimal Diversity Reception II," *IRE Trans. Commun. Syst.*, vol. CS-12, pp. 22–31, March.

Turin, G. L. *et al.* (1972). "Simulation of Urban Vehicle Monitoring Systems," *IEEE Trans. Vehicular Tech.*, pp. 9–16, February.

Tzannes, M. A., Tzannes, M. C., Proakis, J. G., and Heller, P. N. (1994). "DMT Systems, DWMT Systems and Digital Filter Banks," *Proc. Int. Conf. Commun.*, pp. 311–315, New Orleans, Louisiana, May 1–5.

Ungerboeck, G. (1972). "Theory on the Speed of Convergence in Adaptive Equalizers for Digital Communication," *IBM J. Res. Dev.*, vol. 16, pp. 546–555, November.

Ungerboeck, G. (1974). "Adaptive Maximum-Likelihood Receiver for Carrier-Modulated Data-Transmission Systems," *IEEE Trans. Commun.*, vol. COM-22, pp. 624–636, May.

Ungerboeck, G. (1976). "Fractional Tap-Spacing Equalizer and Consequences for Clock Recovery in Data Modems," *IEEE Trans. Commun.*, vol. COM-24, pp. 856–864, August.

Ungerboeck, G. (1982). "Channel Coding with Multilevel/Phase Signals," *IEEE Trans. Inform. Theory*, vol. IT-28, pp. 55–67, January.

Ungerboeck, G. (1987). "Trellis-Coded Modulation with Redundant Signal Sets, Parts I and II," *IEEE Commun. Mag.*, vol. 25, pp. 5–21, February.

Ungerboeck, G. and Csajka, I. (1976). "On Improving Data-Link Performance by Increasing the Channel Alphabet and Introducing Sequence Coding, *1976 Int. Conf. Inform. Theory, Ronneby, Sweden*, June.

Vaidyanathan, P. P. (1993). *Multirate Systems and Filter Banks*, Prentice-Hall, Englewood Cliffs, N.J.

Van Etten, W. (1975). "An Optimum Linear Receiver for Multiple Channel Digital Transmission Systems," *IEEE Trans. Commun.*, vol. COM-23, pp. 828–834, August.

Van Etten, W. (1976). "Maximum Likelihood Receiver for Multiple Channel Transmission Systems," *IEEE Trans. Commun.*, vol. COM-24, pp. 276–283, February.

Van Trees, H. L. (1968). *Detection, Estimation, and Modulation Theory, Part I*, Wiley, New York.

Varsharmov, R. R. (1957). "Estimate of the Number of Signals in Error Correcting Codes," *Doklady Akad. Nauk, S.S.S.R.*, vol. 117, pp. 739–741.

Verdu, S. (1986a). "Minimum Probability of Error for Asynchronous Gaussian Multiple-Access Channels," *IEEE Trans. Inform. Theory*, vol. IT-32, pp. 85–96, January.

Verdu, S. (1986b). "Multiple-Access Channels with Point-Process Observation: Optimum Demodulation," *IEEE Trans. Inform. Theory*, vol. IT-32, pp. 642–651, September.

Verdu, S. (1986c). "Optimum Multiuser Asymptotic Efficiency," *IEEE Trans. Commun.*, vol. COM-34, pp. 890–897, September.

Verdu, S. (1989). "Recent Progress in Multiuser Detection," *Advances in Communications and Signal Processing*, Springer-Verlag, Berlin. [Reprinted in *Multiple Access Communications*, N. Abramson (ed.), IEEE Press, New York.]

Viterbi, A. J. (1966). *Principles of Coherent Communication*, McGraw-Hill, New York.

Viterbi, A. J. (1967). "Error Bounds for Convolutional Codes and an Asymptotically Optimum Decoding Algorithm," *IEEE Trans. Inform. Theory*, vol. IT-13, pp. 260–269, April.

Viterbi, A. J. (1969). "Error Bounds for White Gaussian and Other Very Noisy Memoryless Channels with Generalized Decision Regions," *IEEE Trans. Inform. Theory*, vol. IT-15, pp. 279–287, March.

Viterbi, A. J. (1971). "Convolutional Codes and Their Performance in Communication Systems," *IEEE Trans. Commun. Tech.*, vol. COM-19, pp. 751–772, October.

Viterbi, A. J. (1978). "A Processing Satellite Transponder for Multiple Access by Low-Rate Mobile Users," *Proc. Fourth Int. Conf. on Digital Satellite Communications*, Montreal, Canada, pp. 166–174, October.

Viterbi, A. J. (1979). "Spread Spectrum Communication—Myths and Realities," *IEEE Commun. Mag.*, vol. 17, pp. 11–18, May.

Viterbi, A. J. (1985). "When Not to Spread Spectrum—A Sequel," *IEEE Commun. Mag.*, vol. 23, pp. 12–17, April.

Viterbi, A. J. and Jacobs, I. M. (1975). "Advances in Coding and Modulation for Noncoherent Channels Affected by Fading, Partial Band, and Multiple-Access Interference," in *Advances in Communication Systems*, vol. 4, A. J. Viterbi (ed.), Academic, New York.

Viterbi, A. J. and Omura, J. K. (1979). *Principles of Digital Communication and Coding*, McGraw-Hill, New York.

Wainberg, S. and Wolf, J. K. (1970). "Subsequences of Pseudo-Random Sequences," *IEEE Trans. Commun. Tech.*, vol. COM-18, pp. 606–612, October.

Wainberg, S. and Wolf, J. K. (1973). "Algebraic Decoding of Block Codes Over a q-ary Input, Q-ary Output Channel, $Q > q$," *Inform. Control*, vol. 22, pp. 232–247, April.

Wald, A. (1947). *Sequential Analysis*, Wiley, New York.

Ward, R. B. (1965). "Acquisition of Pseudonoise Signals by Sequential Estimation," *IEEE Trans. Commun. Tech.*, vol. COM-13, pp. 474–483, December.

Ward, R. B. and Yiu, K. P. (1977). "Acquisition of Pseudonoise Signals by Recursion-Aided Sequential Estimation," *IEEE Trans. Commun.*, vol. COM-25, pp. 784–794, August.

Weber, W. J., III, Stanton, P. H., and Sumida, J. T. (1978). "A Bandwidth Compressive Modulation System Using Multi-Amplitude Minimum-Shift Keying (MAMSK)," *IEEE Trans. Commun.*, vol. COM-26, pp. 543–551, May.

Wei, L. F. (1984a). "Rotationally Invariant Convolutional Channel Coding with Expanded Signal Space, Part I: 180°," *IEEE J. Selected Areas Commun.*, vol. SAC-2, pp. 659–671, September.

Wei, L. F. (1984b). "Rotationally Invariant Convolutional Channel Coding with Expanded Signal Space, Part II: Nonlinear Codes," *IEEE J. Selected Areas Commun.*, vol. SAC-2, pp. 672–686, September.

Wei, L. F. (1987). "Trellis-Coded Modulation with Multi-Dimensional Constellations," *IEEE Trans. Inform. Theory*, vol. IT-33, pp. 483–501, July.

Weinstein, S. B. and Ebert, P. M. (1971). "Data Transmission by Frequency-Division Multiplexing Using the Discrete Fourier Transform," *IEEE Trans. Commun.*, vol. COM-19, pp. 628–634, October.

Welch, L. R. (1974). "Lower Bounds on the Maximum Cross Correlation of Signals," *IEEE Trans. Inform. Theory*, vol. IT-20, pp. 397–399, May.

Weldon, E. J., Jr. (1971). "Decoding Binary Block Codes on Q-ary Output Channels," *IEEE Trans. Inform. Theory*, vol. IT-17, pp. 713–718, November.

Widrow, B. (1966). "Adaptive Filters, I: Fundamentals," Stanford Electronics Laboratory, Stanford University, Stanford, Calif., Tech Report No. 6764-6, December.

Widrow, B. (1970). "Adaptive Filters," *Aspects of Network and System Theory*, R. E. Kalman and N. DeClaris (eds.), Holt, Rinehart and Winston, New York.

Widrow, B. and Hoff, M. E., Jr. (1960). "Adaptive Switching Circuits," *IRE WESCON Conv. Rec.*, pt. 4, pp. 96–104.

Widrow, B. *et al.* (1975). "Adaptive Noise Cancelling: Principles and Applications," *Proc. IEEE*, vol. 63, pp. 1692–1716, December.

Wiener, N. (1949). *The Extrapolation, Interpolation, and Smoothing of Stationary Time Series with Engineering Applications*, Wiley, New York (reprint of original work published as an MIT Radiation Laboratory Report in 1942).

Wintz, P. A. (1972). "Transform Picture Coding," *Proc. IEEE*, vol. 60, pp. 880–920, July.

Wolf, J. K. (1978). "Efficient Maximum Likelihood Decoding of Linear Block Codes Using a Trellis," *IEEE Trans. Inform. Theory*, vol. IT-24, pp. 76–81, January.

Wozencraft, J. M. (1957). "Sequential Decoding for Reliable Communication," *IRE Nat. Conv. Rec.*, vol. 5, pt. 2, pp. 11–25.

Wozencraft, J. M. and Jacobs, I. M. (1965). *Principles of Communication Engineering*, Wiley, New York.

Wozencraft, J. M. and Kennedy, R. S. (1966). "Modulation and Demodulation for Probabilistic Decoding," *IEEE Trans. Inform. Theory*, vol. IT-12, pp. 291–297, July.

Wozencraft, J. M. and Rieffen, B. (1961). *Sequential Decoding*, MIT Press, Cambridge, Mass.

Wyner, A. D. (1965). "Capacity of the Band-Limited Gaussian Channel," *Bull. Syst. Tech. J.*, vol. 45, pp. 359–371, March.

Xie, Z., Rushforth, C. K., and Short, R. T. (1990a). "Multiuser Signal Detection Using Sequential Decoding," *IEEE Trans. Commun.*, vol. COM-38, pp. 578–583, May.

Xie, Z., Short, R. T., and Rushforth, C. K. (1990b). "A Family of Suboptimum Detectors for Coherent Multiuser Communications," *IEEE J. Selected Areas Commun.*, vol. SAC-8, pp. 683–690, May.

Yao, K. (1972). "On Minimum Average Probability of Error Expression for Binary Pulse-Communication System with Intersymbol Interference," *IEEE Trans. Inform. Theory*, vol. IT-18, pp. 528–531, July.

Yao, K. and Tobin, R. M. (1976). "Moment Space Upper and Lower Error Bounds for Digital Systems with Intersymbol Interference," *IEEE Trans. Inform. Theory*, vol. IT-22, pp. 65–74, January.

Yue, O. (1983). "Spread Spectrum Mobile Radio 1977–1982," *IEEE Trans. Vehicular Tech.*, vol. VT-32, pp. 98–105, February.

Zelinski, P. and Noll, P. (1977). "Adaptive Transform Coding of Speech Signals," *IEEE Trans. Acoustics, Speech, Signal Processing*, vol. ASSP-25, pp. 299–309, August.

Zervas, E., Proakis, J. G., and Eyuboglu, V. (1991). "A Quantized Channel Approach to Blind Equalization," *Proc. ICC'91*, Chicago, Il, June.

Zhang, X. and Brady, D. (1993). "Soft-Decision Multistage Detection of Asynchronous AWGN Channels," *Proc. 31st Allerton Conf. on Commun., Contr., Comp.* Allerton, IL, October.

Zhou, K. and Proakis, J. G. (1988). "Coded Reduced-Bandwidth QAM with Decision-Feedback Equalization," *Conf. Rec. IEEE Int. Conf. Commun.*, Philadelphia, Penn., pp. 12.6.1–12.6.5, June.

Zhou, K., Proakis, J. G., and Ling, F. (1987). "Decision-Feedback Equalization of Fading Dispersive Channels with Trellis-Coded Modulation," *Int. Conf. Commun. Tech.*, Nanjing, China, November.

Zhou, K., Proakis, J. G., and Ling, F. (1990). "Decision-Feedback Equalization of Time-Dispersive Channels with Coded Modulation," *IEEE Trans. Commun.*, vol. COM-38, pp. 18–24, January.

Ziemer, R. E. and Peterson, R. L. (1985). *Digital Communications and Spread Spectrum Systems*, Macmillan, New York.

Zigangirov, K. S. (1966). "Some Sequential Decoding Procedures," *Probl. Peredach. Inform.*, vol. 2, pp. 13–25.

Ziv, J. (1985). "Universal Quantization," *IEEE Trans. Inform. Theory*, vol. 31, pp. 344–347.

Ziv, J. and Lempel, A. (1977). "A Universal Algorithm for Sequential Data Compression," *IEEE Trans. Inform. Theory*, vol. IT-23, pp. 337–343.

Ziv, J. and Lempel, A. (1978). "Compression of Individual Sequences via Variable-Rate Coding," *IEEE Trans. Inform. Theory*, vol. IT-24, pp. 530–536.

Zvonar, Z. and Brady, D. (1995). "Differentially Coherent Multiuser Detection in Asynchronous CDMA Flat Rayleigh Fading Channels," *IEEE Trans. Commun.*, vol. COM-43, to appear.

INDEX